1971

Compensation of synchronous machines for stability

Darrell Charles Schroder
Iowa State University

Compensation of synchronous machines for stability

by

Darrell Charles Schroder

A Dissertation Submitted to the
Graduate Faculty in Partial Fulfillment of
The Requirements for the Degree of
DOCTOR OF PHILOSOPHY

Major Subject: Electrical Engineering

Approved:

Signature was redacted for privacy.

In Charge of Major Work

Signature was redacted for privacy.

For the Major Department

Signature was redacted for privacy.

For the Graduate College

Iowa State University
Ames, Iowa
1971

TABLE OF CONTENTS

LIST OF TABLES

LIST OF FIGURES

I. INTRODUCTION

A power system has two basic functions. It converts energy from one form to another and transmits it from one place to another. Fundamental emphasis in both the design of power system components and in their operation is placed upon maintaining a continuous, orderly flow of energy. On occasion, however, a power system is subjected to disturbances which disrupt this orderly flow and which result in excesses or deficiencies of energy in various system components. One of the more critical components is the synchronous machine because it has the ability to store energy, in addition to providing for the conversion process from mechanical energy to electrical energy. Deficiencies or excesses of energy in the system are compensated for initially by changes in the kinetic energy of the machine rotors. The energy storage capability of the synchronous machine is limited, however, and if the disturbance is sufficiently large, an unstable condition will result causing the generator to lose synchronism.

Classically the question of power system stability has been divided into two distinct areas of study, transient stability and steady-state stability. Transient stability concerns itself with answering the following question. Given a specified operating condition and impact, will the generators remain in synchronism? The basic concern is to provide sufficient restoring forces to cancel out relative machine accelerating energies.

Steady-state stability implies that a generator will remain in synchronism after being perturbed by some small random unspecified disturbance.

Dynamic stability implies both transient and steady-state stability and, in addition, adequate damping of oscillations (58).

One or more of the following approaches are generally used to increase power system stability (58).

1. Reduction of disturbance both in magnitude and time.
2. Increasing natural restoring forces through strengthening of the transmission system.
3. Injection of braking energy through fast prime-mover energy control.
4. Cross field excitation.
5. Injection of braking energy through temporary switching of resistors or other network parameters.
6. Increasing restoring synchronizing forces through transient forcing of excitation and consequent boost of internal machine flux levels.

Economic considerations dictate which of the above approaches will be implemented in solving a particular problem. Certain generalizations may be made concerning each of the above approaches as follows.

The effects of system disturbances may be reduced considerably by using high-speed circuit breakers and associated relaying allowing faults to be cleared in shorter time intervals. Development in this area appears to have reached a plateau, however, with small improvements in fault clearing time requiring relatively large additional costs.

The relative strength of a transmission system is determined largely by economic rather than by technical considerations.

Presently the last four approaches offer the greatest potential for economically improving system performance.

Modern steam turbine speed control systems have the capability of fast control valve and intercept valve closure to prevent turbine overspeed under load rejection conditions. Either or both of these valves may also be closed upon the detection of a loss of load and then reopened, the close-open cycle being referred to as "fast valving" or "early valving". This process minimizes the excess kinetic energy acquired by the turbine and generator rotor.

If "fast valving" is to be used, the boiler and turbine control systems must be designed accordingly, and the logic controlling the fast valving must prevent excessive operation which would result in severe maintenance problems.

With single field machines the effectiveness of damping through excitation control is related to the load angle of the machine. At no load, changing flux levels does not change power output.

It has been shown that if a second field winding is added and the two windings are properly controlled, positive system damping can be obtained even during light or no load conditions (69). This approach appears especially desirable for machines feeding cable networks because it provides stable operation under low leading power factor conditions. An additional field winding must be added to the rotor, however, resulting in an increase in the cost of the generator.

The use of braking resistors of suitable size, switched at the appropriate times, will theoretically eliminate transient stability problems (58), but because of the cost of resistors capable of dissipating the required energy and the associated switching apparatus, there have been few applications of this approach. Braking resistors could be particularly

desirable when used on hydrosystems where hydraulic turbine gates and water inertia do not allow measures analogous to fast valving as in the case of steam turbines (41). Switching of series capacitors in the transmission system to decrease line impedance has also been shown to be effective in increasing transient stability. The cost of the capacitors and switching apparatus is high, and the logic necessary to determine the optimum time for insertion is complicated.

Transient stability may also be improved by excitation system forcing. The benefits that can be derived by this technique depend upon how fast and how high the excitation system can boost machine flux linkages. Higher response ratio exciters increase synchronizing torques thus helping the transient stability problem, but at the same time decrease damping torques, thus contributing to the dynamic stability problem. In the limit an ideal excitation system, one with no time delay and infinite gain, would hold the terminal voltage constant and destroy all natural damping of the machine (58).

When high-speed excitation systems are adjusted to utilize their small time lags, there is often a need to increase system damping. This may be done by deriving a stabilizing signal from speed or some other machine-related variable and, after appropriate phase compensation, feeding this signal back into the excitation system which provides increased damping torques.

Networks to accomplish the above are available commercially and are called power system stabilizers. In recent years they have found wide application in areas with dynamic stability problems which are generally those areas with appreciable hydrogeneration (31, 46, 64).

Power system stabilizers provide a good way of combating dynamic stability problems because they are relatively inexpensive and they may be installed on existing equipment with little modification.

The stability problems of synchronous machines result from the inability to control their energy input and output quickly and accurately enough. The energy input is controlled by the turbine governor system which is mechanical and has appreciable time lags. The instantaneous power output of the machine may be modified by the excitation system which is electrical in nature, and, compared to the governor, it is very fast. Thus considerable effort has been directed to improvements in the excitation system and auxiliary control systems associated with it. In this dissertation several possible improved control systems are developed and their effectiveness is compared with that of presently used systems.

II. REVIEW OF LITERATURE

A. System Modeling

Studies concerning various aspects of power system stability are intimately related to the problem of determining an appropriate mathematical model to represent the system and measuring or calculating the various parameters which are used in the representation.

A significant simplification in synchronous machine modeling was achieved by Park in his development of a two-reaction theory of synchronous machines (90, 91, 92). A Park-type transformation in its orthogonalized form transforms a set of differential equations containing time dependent inductances into a set containing asymmetric speed voltage terms which considerably reduces the mathematical complexity of the representation (7).

Prentice (97) carefully studied the various aspects of determining synchronous machine reactances and Rankin (99, 100) and later Lewis (75) developed techniques for normalizing the equations describing a synchronous machine. Synchronous machines have been extensively analyzed and the literature on this subject is quite extensive (1, 24, 27, 35, 45, 73, 76).

B. Analog Computer Simulation

The differential equations developed in studying a particular problem may be solved either by digital or analog computer, but for studies involving detailed representations of the synchronous machine, the analog simulations have distinct advantages. Nonlinearities are more easily represented and parameter optimization is generally more easily and cheaply accomplished.

Riaz (101) proposed an analog computer simulation of a synchronous machine suitable for voltage regulator studies; and, in a discussion of this paper, Thomas suggested a model based on the flux linkage form of the synchronous machine equations. Krause (68) developed this form further and Nandi (86) converted the representation to conform to proposed IEEE definitions (59). Numerous other studies using analog computer representations are to be found in the literature (2, 3, 8, 10, 15, 109).

C. Linear Studies

Linear modeling has been extremely popular because of the relative ease in testing for stability by use of such techniques as eigenvalue tests or the Routh-Hurwitz criterion, and has been used by many authors in studying various aspects of the stability problem (23, 31, 83, 120).

Other linear methods of analysis and synthesis such as root-locus plots and Bode plots, which have been extensively used in control systems engineering for many years, have found little application in the solution of power system control problems as evidenced by the small number of articles found which have used these techniques (94, 113).

D. Synchronous Machine Control Systems

The first control loop to be added to a synchronous machine was the voltage regulator. Its inclusion made it possible to maintain much tighter control of the machine terminal voltage and markedly increased the available synchronizing torques, thus increasing the steady-state stability of the synchronous machine (23).

Stability first became important about 1930 with the development of hydrogeneration sites located some distance from the metropolitan load centers. The power systems were well damped, however, and voltage regulators were slow acting so the negative damping contributed by the voltage regulator presented no problems. In fact, stability studies were conducted in two parts. If the machine exhibited transient stability and steady-state stability, it was assumed that adequate damping was present to insure that the machine would settle down to a steady state after the disturbance (58).

Higher capacity generators with larger per-unit reactances and lower inertia constants, longer transmission lines, more numerous interconnections, and voltage regulators with shorter time constants all contributed to the dynamic stability problem and made it desirable to develop improved excitation systems for the synchronous machine.

One of the first researchers to recognize the desirability of improved control systems and to develop them was Gabriel Kron (70). The basic system which Kron patented is shown in Figure 1.

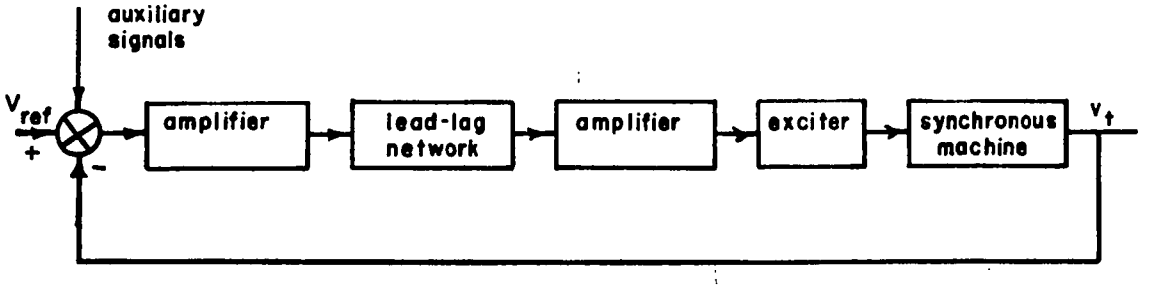

Figure 1. Excitation system patented by Kron in 1954

Kron recognized that the phase lag caused by the excitation system decreased system stability limits and he introduced a phase lead network in the forward loop to counteract this effect. Kron indicated that it may be desirable, although not essential, to overcompensate with the phase lead network. For example, he indicated that typically the phase lag introduced by a system employing an electronic pilot exciter and rotating main exciter was approximately 45°, and the phase lead network should introduce approximately 65° phase lead at the natural frequency of the machine for this condition, thus providing an anticipatory effect.

Kron also recognized that machine excitation should be controlled jointly in response to variations in terminal voltage and in accordance with rotational transient movements of the machine rotor produced by changes in the electrical load of the machine. He developed several circuits to generate the necessary auxiliary signals.

In the preferred form of the invention, an auxiliary signal was produced by adding voltages proportional to the rate of change of both synchronous machine field voltage and field current. The signal proportional to field voltage was degenerative, that is, an increase in field voltage generated an auxiliary signal which tended to decrease field voltage, and the signal proportional to field current was regenerative, that is, an increase in field current caused a signal which tended to increase field current further.

A slight modification of the above scheme allowed the generation of a signal which was proportional to the rate of change of flux linkages and was fed back degeneratively along with a regenerative signal proportional to field current.

Kron also developed circuitry to generate a stabilizing signal derived from such sources as the component of armature current in phase with armature voltage, synchronous machine power output, rotor speed, and load angle, and he suggested more complicated sources for the stabilizing signal, such as making it responsive to the difference in momentary speed changes between the generator and its load.

E. Development of Auxiliary Control Systems

Interconnection of both public and private utilities west of the Rocky Mountains in the mid 1960's and subsequent power and frequency oscillations on the interconnected systems generated intense interest in the development of auxiliary control systems for synchronous machines.

Initially, oscillations occurred at a frequency of about 5 cycles/minute and auxiliary control systems applied to the governors of selected machines were capable of controlling the power swings, although continued movement of hydraulic oil, servo pistons, and wicket gates caused severe maintenance problems (67).

Closure of two 500 KV lines interconnecting the Pacific Northwest and Southwest increased the oscillation frequency to approximately 25 cycles/minute and it was agreed that turbine controls and amortisseur windings would be ineffective in damping intertie oscillations at these frequencies. It was known that the instantaneous power output of a synchronous machine could be altered by excitation control, so various control loops were developed to feed an auxiliary signal into the synchronous machine excitation system to improve system damping (17, 19, 41, 50, 52, 107, 109, 113, 126).

The problem of generating an appropriate stabilizing signal was explored analytically by deMello and Concordia (31) in some detail. The authors represented a synchronous machine connected to an infinite bus with a fourth order linear model, and, by varying tie line impedance and machine parameters over a normal range of values, they were able to make scatter plots of the gain and phase angle of the stabilizing function necessary to satisfy a given damping criterion. From these scatter plots the authors were able to deduce the form of a stabilizing network which they contend is almost universally applicable.

The cumulation of the previously mentioned research efforts has been the development of commercial power system stabilizers by both Westinghouse and General Electric (46, 64). Both power system stabilizers have a transfer function of the following form:

$$\frac{KT_1s}{(1+T_1s)} \frac{(1+T_2s)}{(1+T_3s)} \frac{(1+T_4s)}{(1+T_5s)}$$

where range of parameter adjustment is as follows:

Parameter	Westinghouse	General Electric
Lead time constants T_2, T_4	.2 - 2 sec.	.2 - 1.5 sec.
Lag time constants T_3, T_5	.02 - .15 sec.	.02 - .1 sec.
Signal reset time constant T_1	.05 - 55 sec.	.1 - 50 sec.
Stabilizer gain K	.1 - 100 p.u.	2 - 100 p.u.
Limit of stabilizing signals effect on terminal voltage	.02 - .25 p.u.	.02 - .1 p.u.
Speed input signal	solid state	tachometer

Both stabilizers are equipped with limiting to prevent excessive excursions of terminal voltage. Should the supplementary signal go to the limit and remain there for a time interval from 2 to 60 seconds, a failure of the stabilizer is assumed and its output is disconnected from the voltage regulator.

The Westinghouse system obtains the frequency deviation signal from solid-state circuitry driven from the secondary of one of the machine potential transformers. The General Electric system uses a turbine-mounted tachometer to generate the input to the supplementary control or, in the case of hydrogeneration, an appropriate signal is obtained from the 3-phase potential transformer secondary.

Many power system stabilizers are presently installed and, if they are properly adjusted, they are capable of adding sufficient damping to the system to cancel the negative damping resulting from the high-speed exciters.

The trend toward larger machines, higher system reactances and faster excitation systems will, in all probability, continue to necessitate further improvements in synchronous machine excitation systems.

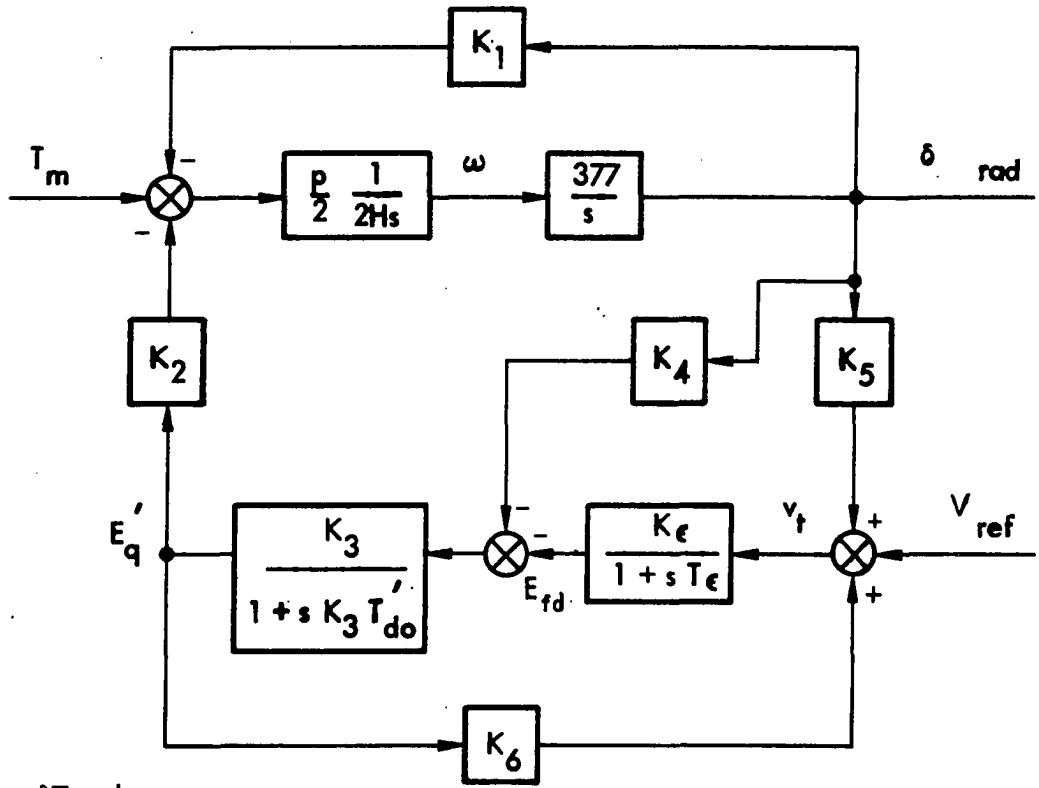

$K_1 = \frac{\partial T_e}{\partial \delta} \Big|_{E'_q}$ change in electrical torque for a change in rotor angle with constant flux linkages in the d-axis

$K_2 = \frac{\partial T_e}{\partial E'_q} \Big|_{\delta}$ change in electrical torque for a change in d-axis flux linkages with constant rotor angle

$K_3 =$ impedance factor

$K_4 = \frac{\partial E'_q}{\partial K_3 \delta}$ demagnetizing effect of a change in rotor angle

$K_5 = \frac{\partial v_t}{\partial \delta} \Big|_{E'_q}$ change in terminal voltage with change in rotor angle for constant E'_q

$K_6 = \frac{\partial v_t}{\partial E'_q} \Big|_{\delta}$ change in terminal voltage with change in E'_q for constant rotor angle

$T'_{do} =$ field open circuit time constant

$K_3 T'_{do} =$ effective field time constant under load

Figure 2. Block diagram of linearized synchronous machine

III. DEVELOPMENT OF BASIC CONCEPTS

Insight into various aspects of the stability problem can be developed by considering a linearized model of a synchronous machine connected to a large system through a transmission line (31, 111). The model may be developed from more complicated representations by neglecting amortisseur windings, armature resistance, derivatives of armature flux linkages, and saturation (see Appendix B). The model and definitions of various parameters are shown in Figure 2. For simplicity the entire excitation system is represented by a first order system having gain K_ε and time constant T_ε.

The torque-angle loop of the model is shown in Figure 3. Although nonexistent in the linearized model, the feedback path through block D has been added to facilitate comparison with the standard form of the characteristic equation for a second order system and to develop the concepts of synchronizing and damping torques.

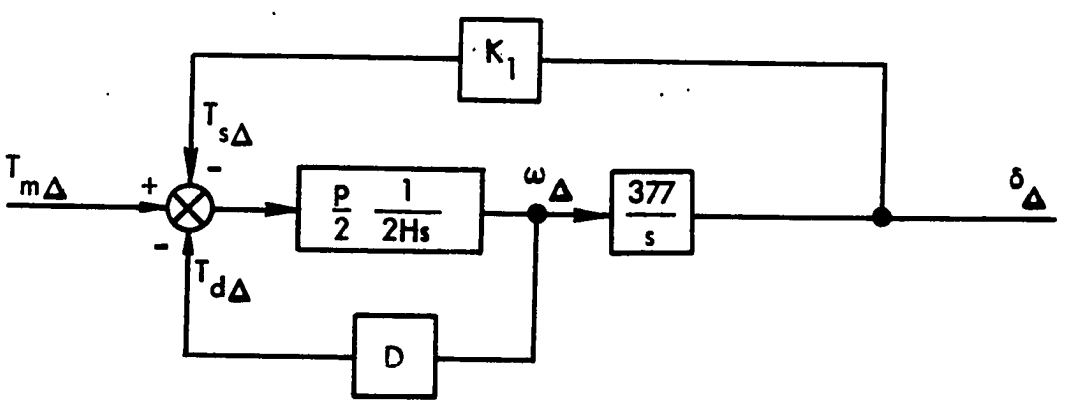

Figure 3. Torque-angle loop of linearized synchronous machine model

The closed-loop transfer function for the system of Figure 3 is

$$\frac{\delta\Delta}{T_{m\Delta}} = \frac{\frac{377}{2H}}{s^2 + \frac{p}{2}\frac{D}{2H}s + \frac{p}{2}\frac{K_1 377}{2H}} \qquad [1]$$

Comparison of the denominator of this transfer function with the characteristic equation of a second order system

$$s^2 + 2\xi\omega_n s + \omega_n^2 = 0 \qquad [2]$$

shows that the natural frequency of the system is

$$\omega_n = \sqrt{\frac{p}{2}\frac{K_1 377}{2H}} \qquad [3]$$

which for a typical machine has a value between 0.5 and 2.5 Hz.

The damping ratio is

$$\xi = \frac{D}{2}\sqrt{\frac{p}{2}\frac{1}{2HK_1 377}} \qquad [4]$$

which is very small, normally between 0.03 and 0.05.

Figure 3 also serves to illustrate the concepts of synchronizing and damping torques. An increase in mechanical torque, $T_{m\Delta}$, results in an increase in ω_Δ which is fed back through block D and results in a retarding torque at the summing junction. Such a torque which is in phase with speed will be defined to be a damping torque. Another component of retarding torque is fed back through block K_1 from δ_Δ. Such torques which are in phase with δ_Δ are defined to be synchronizing torques. Stability

can be endangered by a lack of either, or both, synchronizing or damping torques.

In Figure 4, the effect of armature reaction is expressed as a demagnetizing influence resulting from increased rotor angle feeding back through K_4. The effect of this component of torque can be seen from the transfer function relating change in torque to change in angle.

$$\frac{T_\Delta}{\delta_\Delta} = \frac{-K_2 K_3 K_4}{1 + s\, T'_{do}\, K_3} \qquad [5]$$

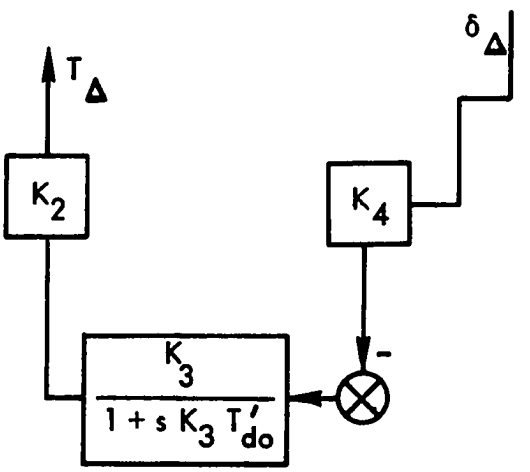

Figure 4. Block diagram showing torque developed as a result of armature reaction

The coefficients are always positive, so at steady state this feedback loop produces a synchronizing torque which is opposite in sign to that produced through K_1. The familiar steady-state stability criterion with constant field voltage defines the stability limit as the condition for which the steady-state synchronizing power coefficient $K_1 - K_2K_3K_4$ is zero.

At frequencies where $\omega >> 1/K_3T'_{do}$, the phase angle of the above

expression is +90°, which means that at these frequencies the torque due to this loop is almost entirely damping torque. A typical value of $1/K_3T'_{do}$ might be 1/.3410(6) = .486 radians. If $\omega = 10/K_3T'_{do}$, for example, this would correspond to a frequency of .745 Hz. Thus, this loop contributes some damping in the range of frequencies near the natural frequency of the synchronous machine.

Figure 5 shows the block diagram after adding a simple voltage regulator. Typical values for K_ε and T_ε might be 25 and 0.05, respectively, where K_ε is the transient regulator gain, and is considerably lower than the steady-state gain. The transfer function for this figure, neglecting effects through K_5, is

$$\frac{T_\Delta}{\delta_\Delta} \simeq - \frac{K_2K_4}{K_\varepsilon K_6(1 + s\ T'_{do}/K_\varepsilon K_6)} \qquad [6]$$

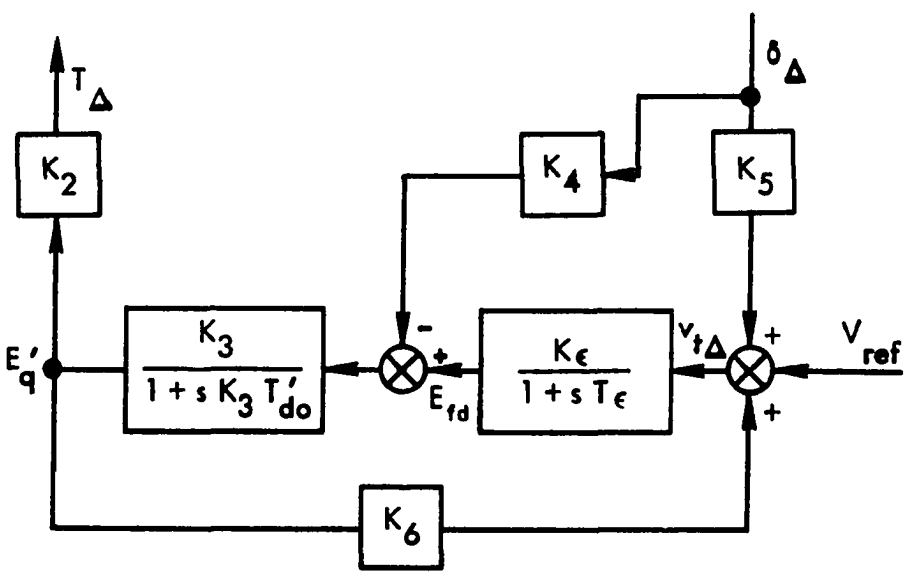

Figure 5. Block diagram after adding voltage regulator

Comparison of Equations 5 and 6 shows that at low frequencies, Equation 6 is smaller than 5 by a factor of $1/K_\varepsilon K_3 K_6$, while at high frequencies the two expressions become nearly equal. The net effect of adding the voltage regulator is to reduce the component of damping torque coming through K_4 to a level where it is negligible.

The component of torque resulting from a change in angle with voltage regulator effects included may be analyzed by developing the transfer function of the block diagram shown in Figure 5. The resulting transfer function, neglecting K_4, is

$$\frac{T_\Delta}{\delta_\Delta} = - \frac{K_\varepsilon K_2 K_5}{(1/K_3 + K_\varepsilon K_6) + s(T_\varepsilon/K_3 + T'_{do}) + s^2 T'_{do} T_\varepsilon} \qquad [7]$$

which at low frequencies reduces to

$$\frac{T_\Delta}{\delta_\Delta} \simeq - \frac{K_2 K_5}{K_6} \qquad [8]$$

for large K_ε, and this loop produces synchronizing torque. The total synchronizing torque may be found by adding the signals through K_1 and the regulator loop

$$T_{s\Delta} = K_1 - K_2 K_5 / K_6 \qquad [9]$$

For normal loadings K_1 is high and $T_{s\Delta}$ is significantly greater than zero. At high system transfer impedances and heavy loadings, K_5 may approach zero or even become negative, and for cases where K_1 is small, a negative value of K_5 increases synchronizing torque producing a beneficial effect. The damping component of torque due to regulator action is

$$\frac{T_{d\Delta}}{\delta_{\Delta}} = \frac{K_{\varepsilon} K_2 K_5 (T_{\varepsilon}/K_3 + T'_{do})\omega}{(1/K_3 + K_{\varepsilon}K_6 - \omega^2 T'_{do}\, T_{\varepsilon})^2 + (T_{\varepsilon}/K_3 + T'_{do})^2\, \omega^2} \qquad [10]$$

When K_5 becomes negative, the damping torque also becomes negative which may lead to an unstable condition.

Thus, we have conflicting requirements. In the cases when K_5 is negative, which are the ones generally involving stability problems, the voltage regulator is of great help in producing synchronizing torques, but in so doing it may add negative damping, causing the system to oscillate.

A satisfactory solution to the problem can normally be found by adding just enough regulator gain to provide adequate synchronizing power coefficient without cancelling all of the inherent machine damping.

A. Increased Damping Resulting From Auxiliary Signals

It has been recognized for some time that damping torques can be increased by feeding an auxiliary signal into the excitation system of a synchronous machine (70). This signal may be derived from a number of sources, but because rotor speed is relatively easy to measure with sufficient accuracy and has been found to be a suitable signal, it has most often been used.

In order to cancel phase lag introduced by the regulating circuit, the speed signal must be fed through a stabilizing function G(s) as shown in Figure 6. The transfer function associated with this figure is

$$\frac{T_{sig\Delta}}{\omega_{\Delta}} = \frac{G(s)\, K_2 K_{\varepsilon}}{(1/K_3 + K_{\varepsilon}K_6) + s(T_{\varepsilon}/K_3 + T'_{do}) + s^2 T'_{do} T_{\varepsilon}} \qquad [11]$$

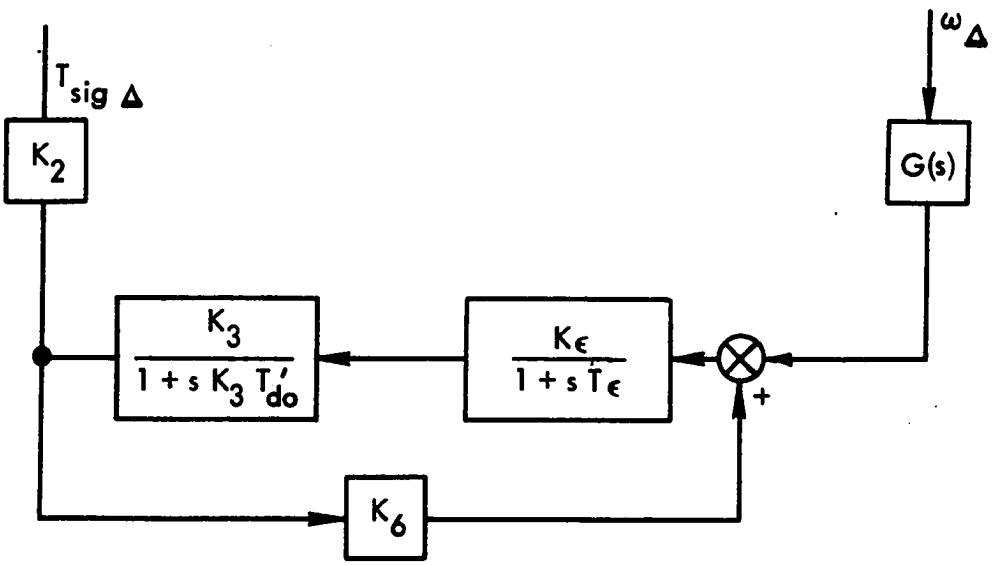

Figure 6. Component of torque produced from speed-derived signal as a result of voltage regulator action

If $T_{sig\Delta}$ is to provide pure damping, G(s) should be a function having phase lead equal to the phase lag of Equation 11. Ideally it would be of the following form:

$$G(s) = \frac{C(1/K_3 + K_\varepsilon K_6 + s(T_\varepsilon/K_3 + T'_{do}) + s^2 T'_{do} T_\varepsilon)}{K_2 K_\varepsilon} \qquad [12]$$

Such a function is not physically realizable; therefore, some compromise function must be developed which provides damping over the spectrum of expected frequencies of oscillation. There are an almost infinite number of functions which may be used for G(s) which provide increased system damping. One form that has been suggested (31) is

$$G(s) = \frac{k\, s(1 + sT_1)^2}{(1 + sT)(1 + sT_2)^2} \qquad [13]$$

where typical values of parameters might be

T	2 to 4
T_1	0.1 to 0.2
T_2	.05
k/T	10 to 40

Since the machine and exciter K's enter into the expression for an ideal G(s), it is instructive to observe how they vary as tie line impedance and machine loading are changed. Appropriate equations for the various K's are developed during the linearization process (see Appendix B) and are listed in Table 1. A simplified phasor diagram is also necessary to define the machine operating point, and is shown in Figure 7.

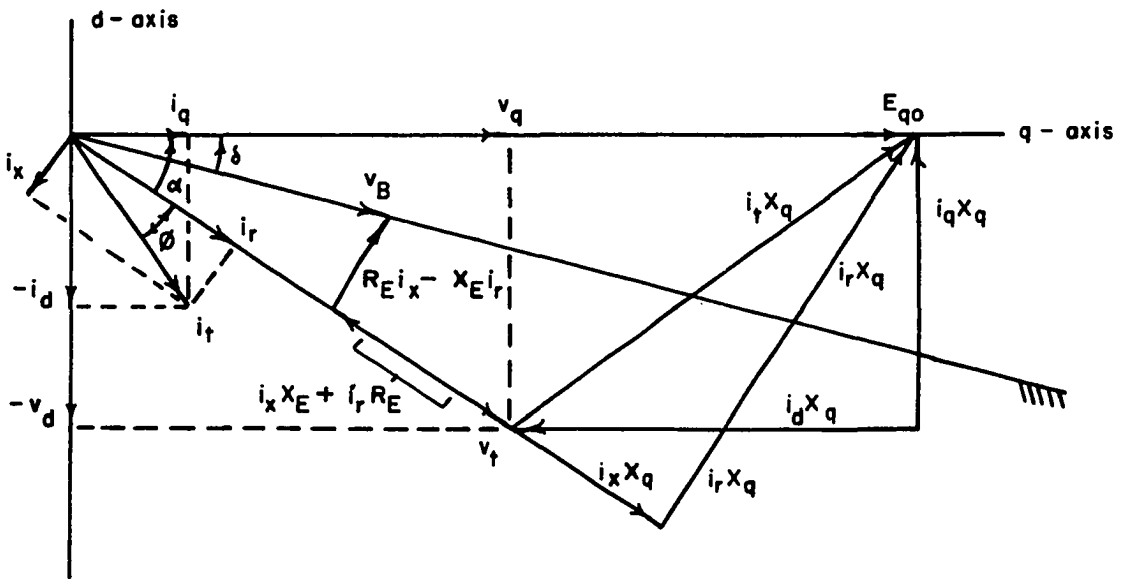

Figure 7. Phasor diagram used to specify initial conditions of machine

Table 1. Parameters of linearized synchronous machine model

$$K_1 = \frac{E_{qo}\sqrt{3}\,V_B}{A}\left[R_E \sin\delta_o + (\omega_o L_E + \omega_o \ell_d)\cos\delta_o\right]$$

$$+ \frac{i_{qo}\sqrt{3}\,V_B}{A}\left[\omega_o(L_q-\ell_d)(\omega_o L_E + \omega_o L_q)\sin\delta_o - \omega_o(L_q-\ell_d)R_E\cos\delta_o\right]$$

$$K_2 = \frac{R_E E_{qo}}{A} + i_{qo}\left[1 + \frac{\omega_o(L_q-\ell_d)(\omega_o L_E + \omega_o L_q)}{A}\right]$$

$$K_3 = \left[1 + \frac{(X_d - X_d')(X_q + X_E)}{A}\right]^{-1}$$

$$K_4 = \frac{\sqrt{3}\,V_B\,(X_d - X_d')}{A}\left[-R_E\cos\delta_o + (X_q + X_E)\sin\delta_o\right]$$

$$K_5 = \frac{v_{do}\omega_o L_q}{Av_{to}}\left[\sqrt{3}\,V_B \sin\delta_o\, R_E + \sqrt{3}\,V_B\cos\delta_o\,(\omega_o L_E + \omega_o \ell_d)\right]$$

$$+ \frac{v_{qo}\omega_o \ell_d}{Av_{to}}\left[\sqrt{3}\,V_B\cos\delta_o\,R_E - \sqrt{3}\,V_B\sin\delta_o\,(\omega_o L_E + \omega_o L_q)\right]$$

$$K_6 = \frac{v_{do}\omega_o L_q R_E}{v_{to}\,A} + \frac{v_{qo}}{v_{to}}\left[1 - \frac{\omega_o \ell_d(\omega_o L_E + \omega_o L_q)}{A}\right]$$

where

$$A = R_E^2 + (\omega_o L_E + \omega_o \ell_d)(\omega_o L_E + \omega_o L_q)$$

In order to reduce the amount of labor involved in investigating a large number of conditions, a short computer program was written to calculate the K's for a given set of system parameters and the generator loading

(see Appendix C). The system parameters and various machine power outputs which were used to calculate the following curves are shown in Table 2.

Table 2. System parameters and machine power outputs used to calculate K's

Machine parameters	X_d	= 1.159 per unit
	X_q	= 1.136
	X'_d	= .133
	H	= 6.7 sec.
	T'_{do}	= 6.0
Tie line parameters	$R_E + jX_E$	= 0.02 + j0.4 per unit
		0.0 + j1.0
		0.2 + j0.4
		1.0 + j1.0
		1.0 + j5.0
Machine loading per phase	P + jQ	= 0.33 + j0.0 per unit
		+ j0.25
		- j0.25
		0.66 + j0.0
		+ j0.5
		- j0.5
		1.00 + j0.0
		+ j0.75
		- j0.75

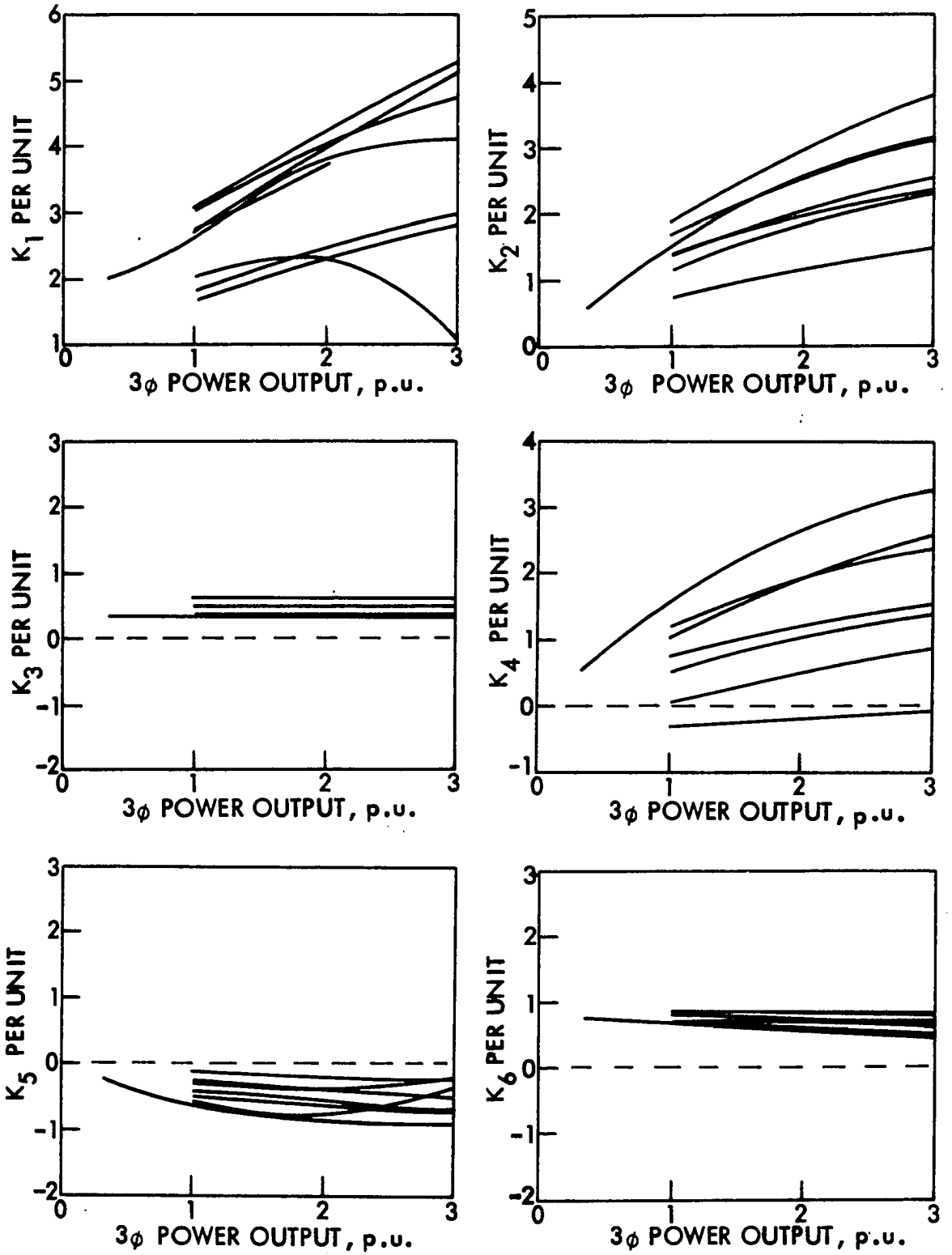

Figure 8. Linearized model parameters as a function of power output for various var loadings and tie line impedances

The resulting curves are shown in Figure 8. From these curves it is noted that K_1, K_2, and K_4 vary over a rather large range, but, in general, increase with increased machine loading. K_3 and K_6 are not greatly affected by system loading or changes in tie line impedance, and K_5, the parameter whose sign determines whether damping is positive or negative, is, for this particular system, always negative.

B. Generation of Auxiliary Stabilizing Signals with an Analog Computer

Although the linear model presented provides an excellent means to define the problem and to develop concepts which may be used to increase system damping, it is recognized that it neglects amortisseur windings and other effects which may well be important. This fact, coupled with the observation that the problem will involve optimization of various parameters, suggests that actual solutions be attempted using the analog computer.

We may conceptualize the problem as follows. The synchronous machine may be represented as a black box with mechanical torque, T_m, and the terminal voltage reference, V_{ref}, as inputs, and rotor position, δ, and some auxiliary signal not yet defined as the outputs (see Figure 9).

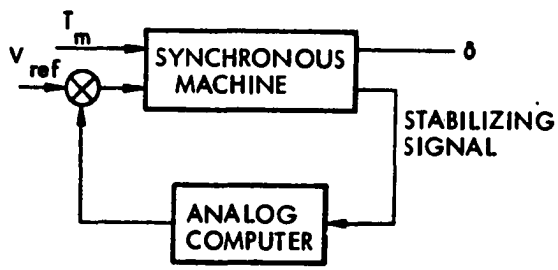

Figure 9. Analog computer used to increase damping

A stabilizing signal from the synchronous machine is fed into the analog computer where it is processed in some manner to generate an auxiliary signal which is fed into the excitation system of the synchronous machine. It was noted earlier that the main cause of decreased damping was the phase lag in the voltage regulator loop of the linear model, and, in order to increase stability, some sort of phase lead must be introduced, e.g., by an appropriate G(s).

Time scaling is readily accomplished on the analog computer. That is, solutions may be calculated at speeds faster, equal to, or slower than a system operating in real time. The above observations suggest that an appropriate stabilizing signal might be generated by running an analog computer simulation of a synchronous machine in parallel with the actual system, but at a speed greater than real time. This idea is represented in Figure 10. To determine if this scheme is an appropriate technique, the transfer function of Figure 10 may be determined if the linearized model of Figure 2 is inserted into the block labeled "synchronous machine" and some unspecified transfer function $G_1(s)$ is put into the analog computer simulation block.

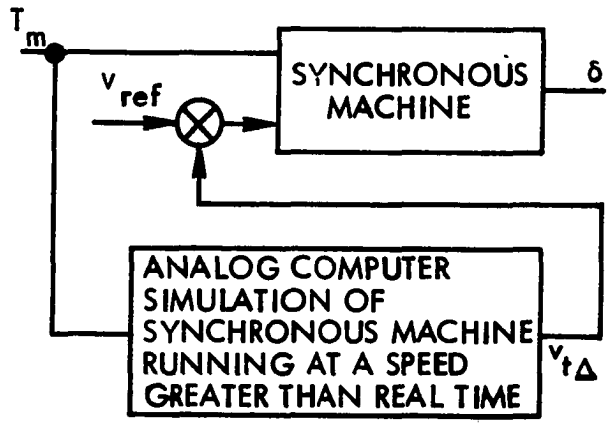

Figure 10. Analog computer operating in parallel with synchronous machine

Block diagram algebra is used to simplify the representations, and the result is shown in Figure 11, where A and B represent rather complicated transfer functions formed in the reduction process. The block diagram of Figure 11 clearly shows that $G_1(s)$ is not contained in the open-loop transfer function of the system and thus it cannot be used to modify poles and zeros of the synchronous machine.

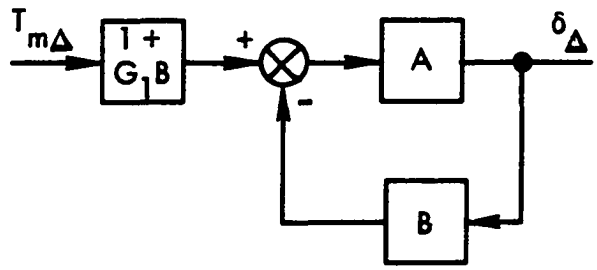

Figure 11. Block diagram indicating parallel operation of synchronous machine and analog computer after reduction

It was noted previously that ω_Δ was an appropriate source of compensating signals, so the approach to the problem is modified as shown in Figure 12. To simplify analysis, the fourth order linear model of Figure 2 is again inserted directly into the box of Figure 12 marked "synchronous machine". The box marked "analog computer simulation" is replaced by the system shown in Figure 13. This is essentially the same diagram as Figure 2, but it has been redrawn to show ω_Δ as an input and v_t as the output. In addition, a damping term, D, has been included, and a parameter, K, has been added to represent the ability to change time scaling in the analog computer model.

Using block diagram algebra, it is again possible to reduce the system suggested by Figure 12 to a form suitable for analysis. The

resulting open-loop transfer function has a numerator of fourth order and a denominator of eighth order. The complexity of this system makes it desirable to explore the system stability by root-locus techniques using a computer program to plot the root-locus and calculate polynomial coefficients.

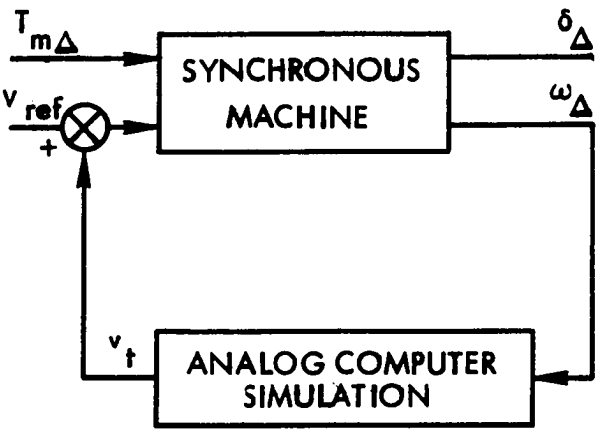

Figure 12. Analog computer producing stabilizing signal from speed

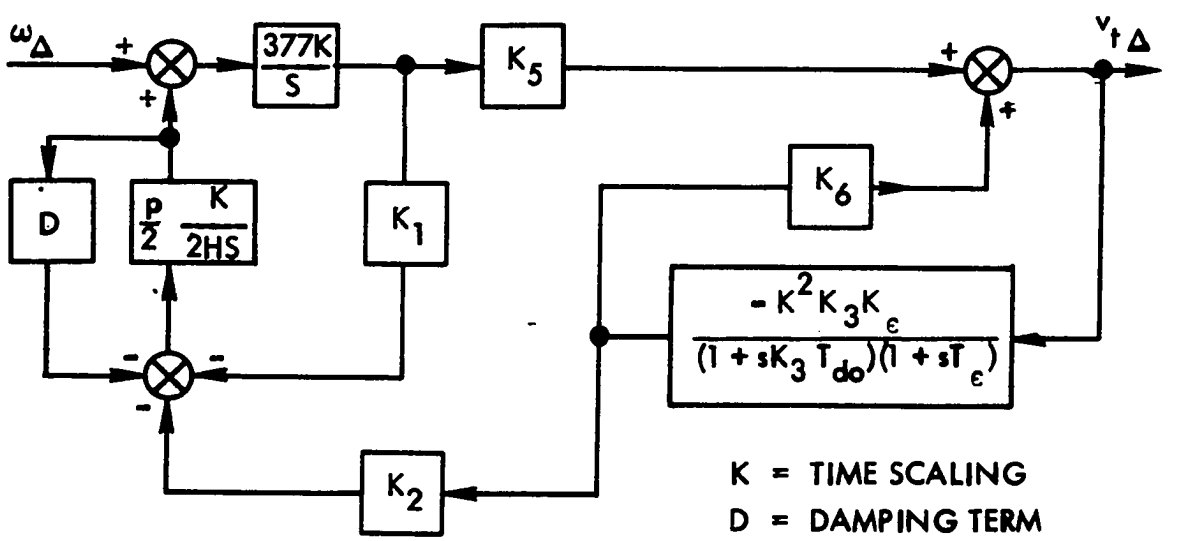

Figure 13. Analog computer model of synchronous machine with input ω_Δ and output $v_{t\Delta}$

A root-locus plot of the system of Figure 2 is shown in Figure 14. System parameters and generator loading have been chosen so as to provide an almost oscillatory condition as evidenced by complex poles very near the jω-axis.

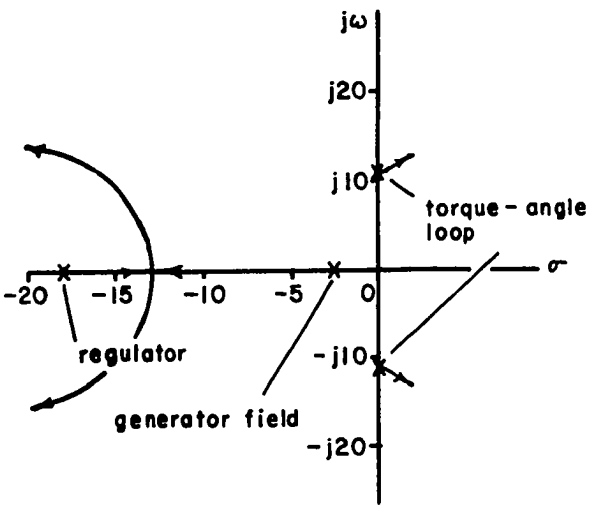

Figure 14. Root-locus of system shown in Figure 2 with parameters chosen to make system almost oscillatory

A pole-zero plot of the system suggested by Figure 12 is shown in Figure 15. Comparison with Figure 14 readily identifies which poles and zeros have been added as a result of adding the analog computer representation. In Figure 15, sufficient damping was added to the analog computer representation to move the complex poles of that representation to a favorable position. Then K, the time parameter, was varied until the complex pair of zeros was produced. The root-locus resulting from the parameter choices mentioned above is shown in Figure 16. It is to be noted that the poles associated with the torque-angle loop of the generator make an excursion into the left half plane before they cross the jω-axis. Thus damping is improved for certain values of regulator gain.

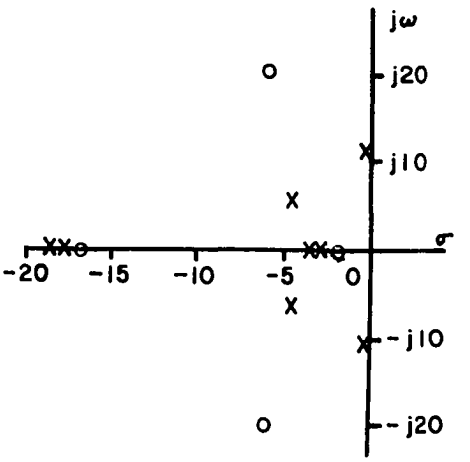

Figure 15. Pole-zero plot of Figure 12

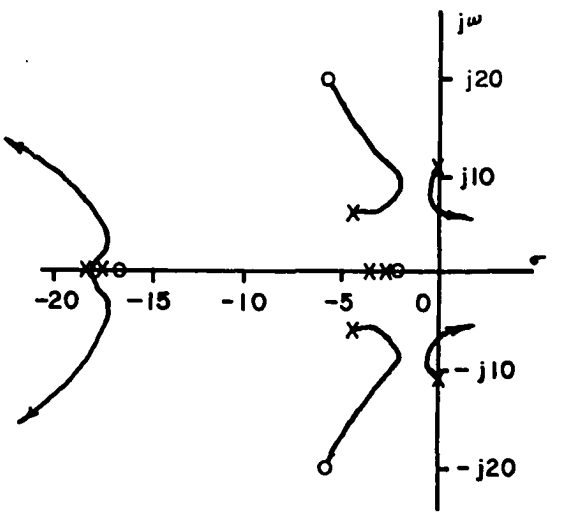

Figure 16. Root-locus resulting from varying voltage regulator gain for compensation scheme of Figure 12

Inspection of Figure 15 reveals that adding a feedback path through an analog computer simulation adds four additional poles and four zeros. The two additional poles on the negative real axes are located near two of the zeros and comparison of Figures 14 and 16 shows that the introduction of these pole-zero pairs has little overall effect on the root-locus.

The complex poles and zeros which have been added are, however, able to pull the torque-angle loop poles into the left half plane before they cross the $j\omega$-axis, thus increasing the stability of the system. It is also noted that the complex pole-zero pairs which resulted from feedback through the analog computer representation could equally well have been added by a bridged-T filter with appropriately chosen parameters.

IV. ROOT-LOCUS ANALYSIS OF A LINEARIZED SYNCHRONOUS MACHINE AND EXCITATION SYSTEM

In order to study various control systems which may be applied to the excitation system of a synchronous machine it is necessary to develop a more detailed representation of the system.

The linear model of the synchronous machine analyzed in the previous chapter may be combined with a linearized model of the excitation system (see Appendix D) as shown in Figure 17. The model includes provision for adding various types of compensation networks. L_N and L_D are the numerator and denominator, respectively, of a series compensation network inserted in the feedforward loop of the exciter. Similarly, R_N and R_D result from a rate feedback loop deriving its input from speed deviation, and F_N and F_D are the numerator and denominator, respectively, of a transfer function representing rate feedback from the excitation system.

Block diagram algebra may be used to simplify the block diagram of Figure 17. Initially the takeoff point from ω_Δ is moved to δ and the torque-angle loop of the synchronous machine is closed as shown in Figure 18. The takeoff point for the feedforward loop through K_6 may now also be moved to δ, and, since signals through the K_5 and K_6 loops are then in parallel, these may be combined. The feedback loop composed of K_4 can now also be eliminated as shown in Figure 19. Finally, the takeoff point for the excitation system rate feedback may be moved to v_t as shown in Figure 20.

Further reduction is possible but the particular steps to be followed depend upon which compensation networks and parameters are to be studied.

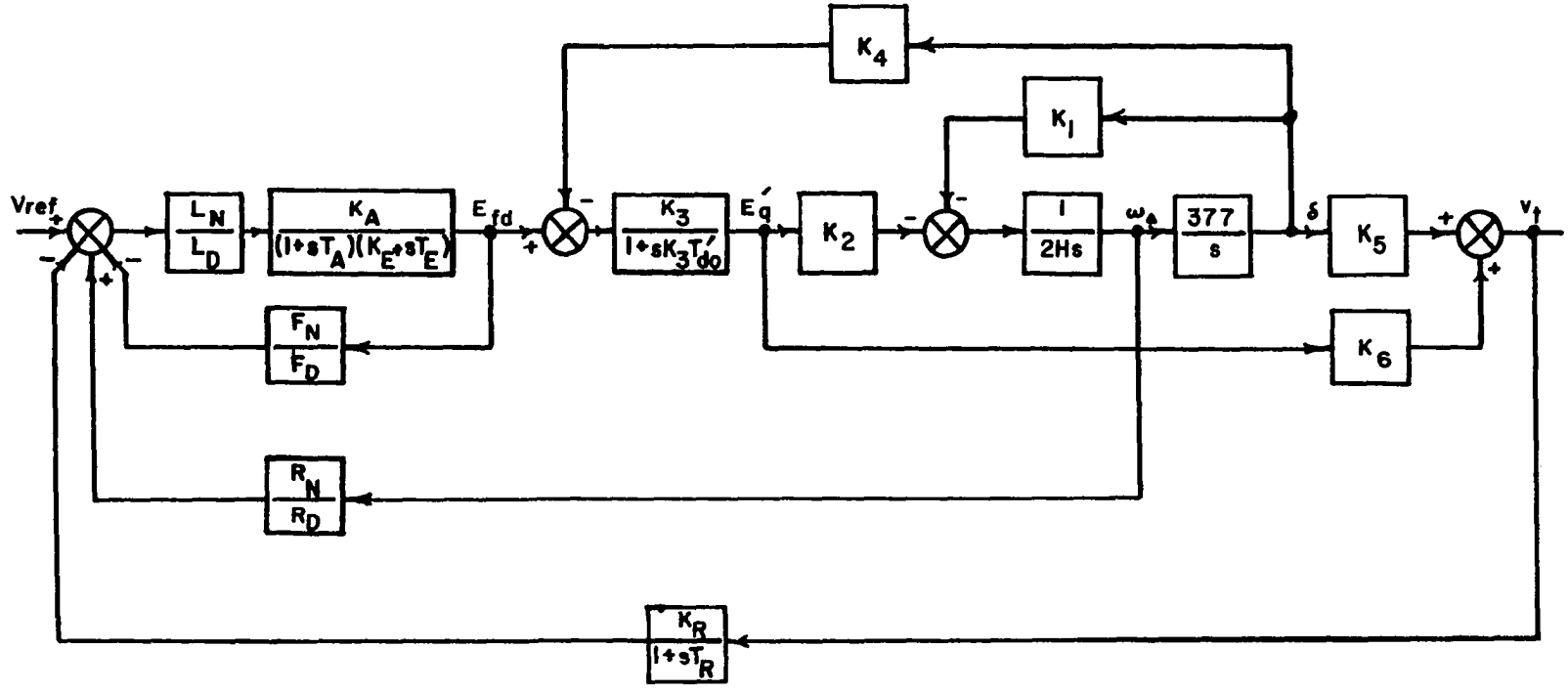

Figure 17. Block diagram of synchronous machine and exciter

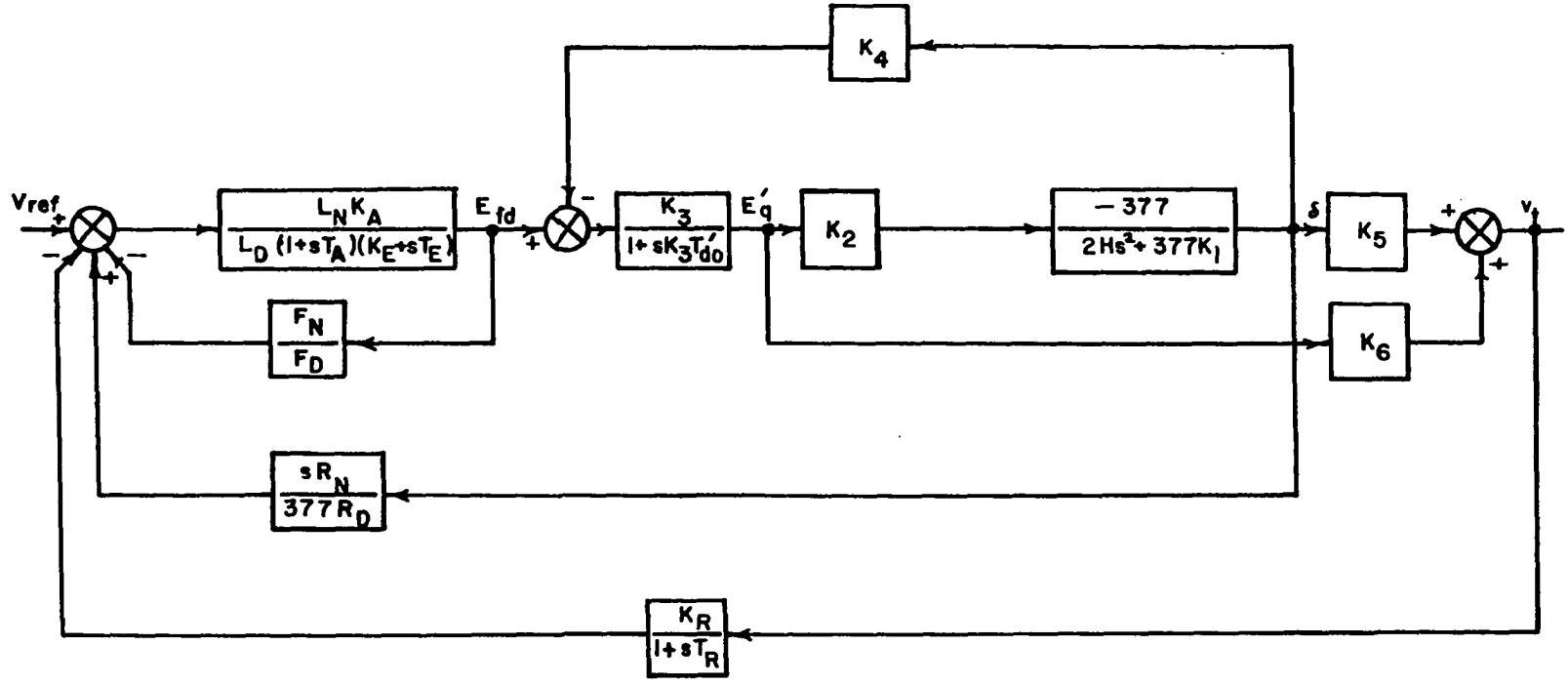

Figure 18. Block diagram after moving takeoff point and closing torque-angle loop

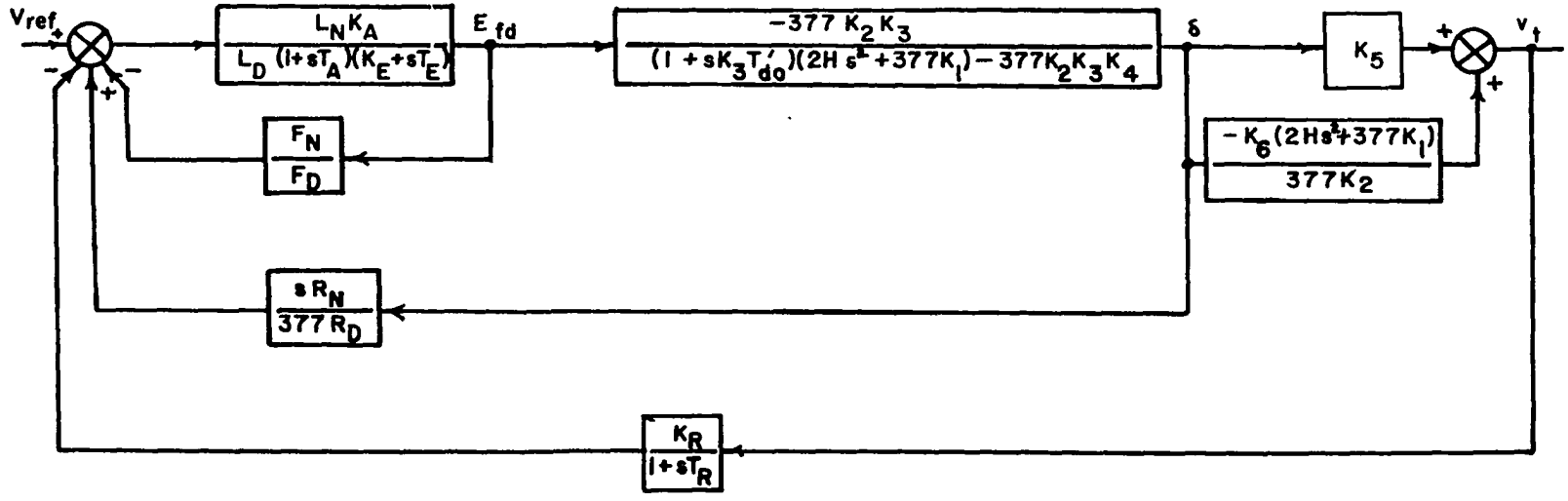

Figure 19. Elimination of feedback path through K_4

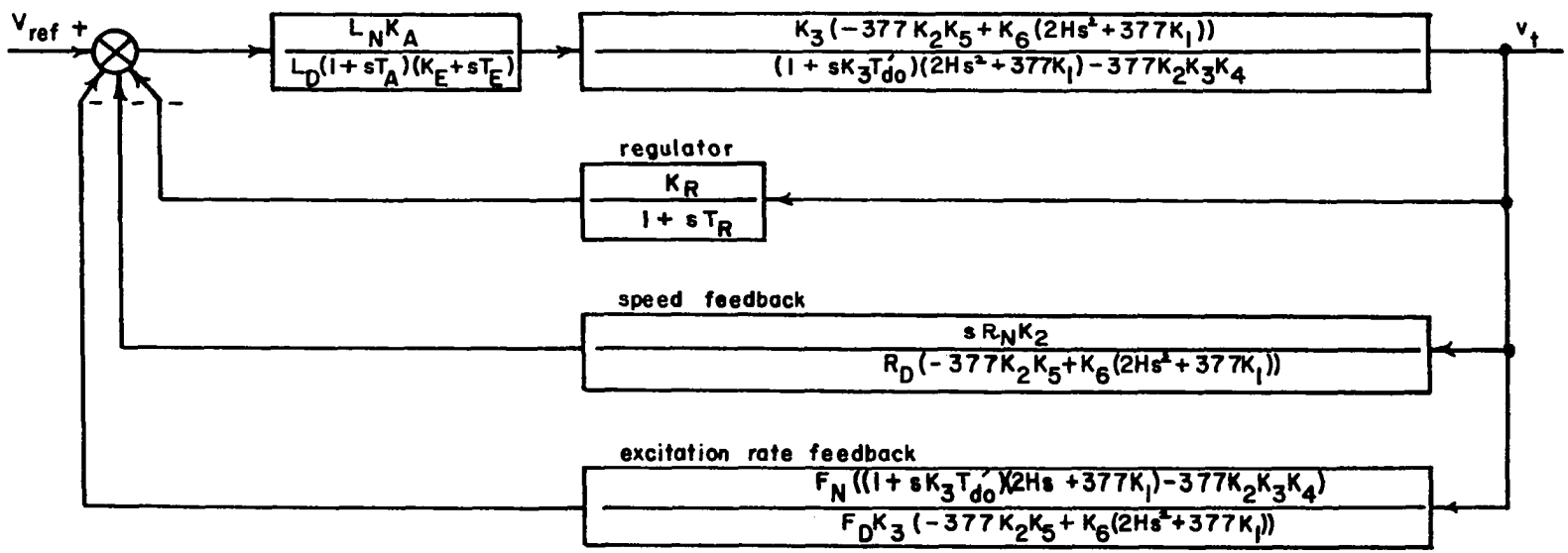

Figure 20. Block diagram of synchronous machine and exciter after reduction

A. Development of the Open-loop Transfer Function to Study Effect of Varying Amplifier Gain, K_A

The transfer functions in the feedback loops of Figure 20 are put over a common denominator, Figure 21, and the three feedback loops are then combined. The open-loop transfer function which results is

voltage regulator

complex zeros — speed feedback

excitation system rate feedback

$$\frac{L_N K_A \left[K_R\{2HK_6 s^2 + 377(K_1K_6 - K_2K_5)\}R_D F_D K_3 + sR_N F_D K_3(1+T_R s)K_2 + F_N R_D(1+T_R s)\{(1+sK_3T'_{do})(2Hs^2+377K_1) - 377K_2K_3K_4\}\right]}{L_D\,(1+T_A s)(K_E+T_E s)\,\{(1+sK_3T'_{do})(2Hs^2+377K_1) - 377K_2K_3K_4\}\,R_D F_D(1+T_R s)} \qquad [14]$$

amplifier — exciter — generator — voltage regulator

complex torque-angle loop poles and field pole

The accuracy of this transfer function may be checked by reducing the generator model to a first order system as follows.

Set $K_1=0$ $K_2=0$ $K_4=0$ $K_5=0$ $K_6=1$

$L_N=1$ $L_D=1$ $F_D=(1+T_F s)$ $F_N=sK_F$ $R_N=0$ $R_D=1$

$K_3=K_G$ $K_3T'_{do}=T_G$

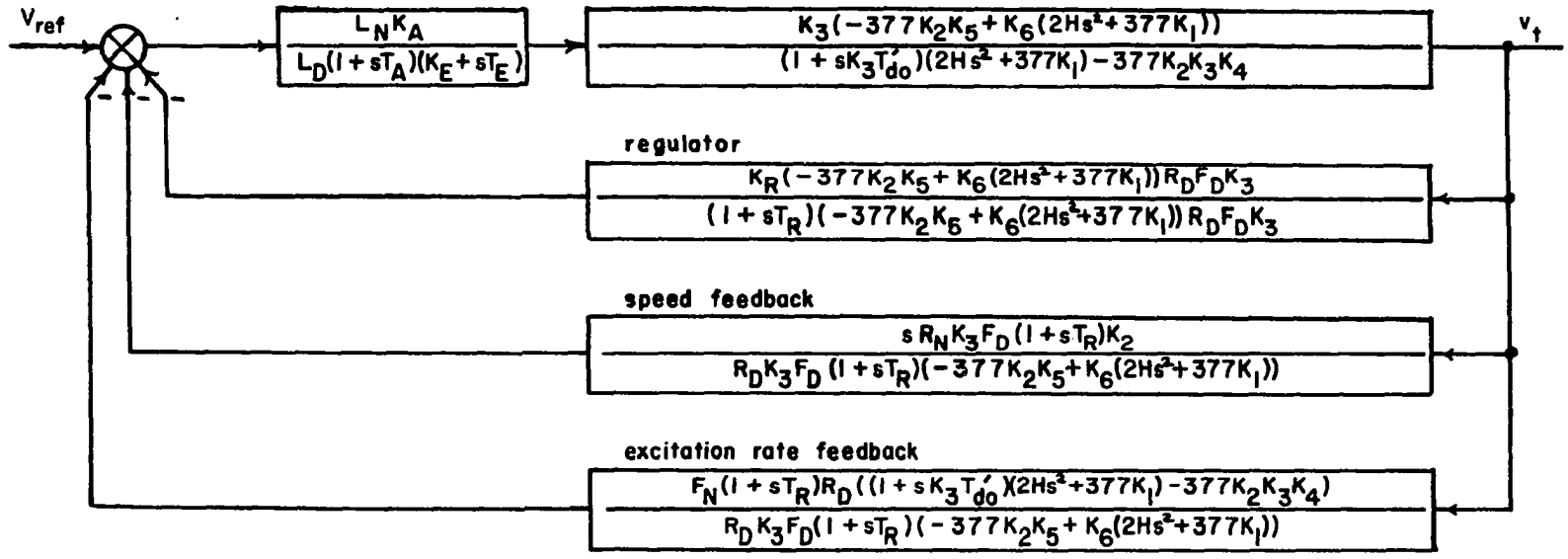

Figure 21. Block diagram of synchronous machine and exciter after putting feedback loop over a common denominator

$$OLTF = \frac{K_A\,[(1+T_F s)\{2HK_R K_3 s^2\} + 0 + sK_F\,(1+sT_R s)(1+sK_3 T'_{do})(2Hs^2)]}{(1+T_A s)(K_E+T_E s)(1+sK_3 T'_{do})(2Hs^2)(1+T_F s)(1+T_R s)}$$

$$= \frac{K_A\,[K_R K_3(1+T_F s) + sK_F\,(1+T_R s)(1+sK_3 T'_{do})]}{(1+T_A s)(K_E+T_E s)(1+T_R s)(1+sK_3 T'_{do})(1+T_F s)}$$

Replace $K_3 T'_{do}$ with T_G and K_3 with K_G.

$$OLTF = \frac{K_A K_R K_G(1+T_F s) + sK_A K_F(1+T_R s)(1+T_G s)}{(1+T_A s)(K_E+T_E s)(1+T_R s)(1+sT_G)(1+T_F s)}$$

$$= \frac{K_A K_F T_R T_G s(1/T_R+s)(1/T_G+s) + K_A K_R K_G T_F(1/T_F+s)}{T_A T_E T_R T_G T_F(1/T_A+s)(K_E/T_E+s)(1/T_R+s)(1/T_G+s)(1/T_F+s)}$$

$$= \frac{\frac{K_A K_6}{T_A T_E T_G}\left[\frac{K_F T_G}{T_F K_G}\, s(1/T_R+s)(1/T_G+s) + K_R/T_R(1/T_F+s)\right]}{(1/T_A+s)(K_E/T_E+s)(1/T_R+s)(1/T_G+s)(1/T_F+s)}$$

This is the same expression for the first order model derived in reference (7).

The open-loop transfer function of Equation 14 has the denominator in factored form except for the third order polynomial arising from the machine torque-angle loop and field poles. This loop has been closed because arbitrary compensation networks cannot be inserted into it and its closure simplifies the numerator of the open-loop transfer function. The parameters of this loop are fixed for a given machine design and loading condition, and thus once the polynomial is factored the pole positions resulting from it are known and constant irrespective of

various compensation networks placed in other loops. The numerator is not in factored form, however, and zero locations are found by multiplying out expressions, combining terms, and then factoring.

B. Uncompensated System

If all compensation is neglected by setting $L_N=L_D=F_D=R_D=1$, and $F_N=R_N=T_R=0$ the resulting root-locus is shown in Figure 22 where the poles and zeros resulting from various terms are readily identified. This root-locus clearly shows the basic problem. The system response is dominated by a pair of complex poles arising from the torque-angle loop of the synchronous machine and a pole near the origin resulting from the field winding. Small increases in amplifier gain K_A drive the complex poles into the right half plane making the system unstable.

Note that if all feedback loops are removed by setting K_R, the voltage regulator gain, equal to zero in Equation 14 and $F_D=R_D=L_N=L_D=F_N=1$ and $T_R=R_N=0$, a third order polynomial occurs in the numerator which will cancel the one in the denominator of Equation 14 leaving an open-loop transfer function of the form

$$\frac{K}{(1 + T_A s)(K_E + T_E s)}$$

having root-locus asymptotes of 90° and 270°, which is a stable configuration for all gains.

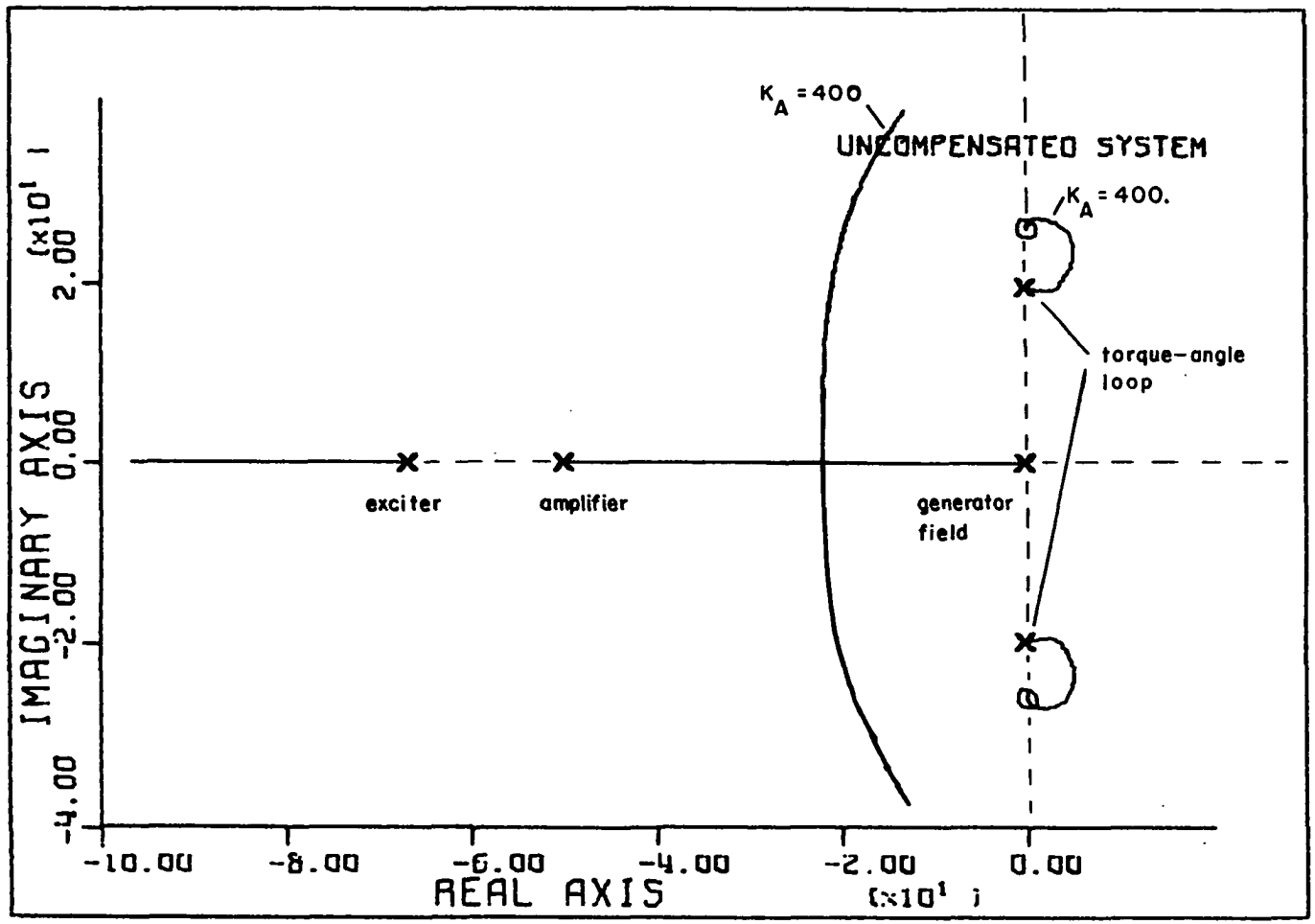

Figure 22. Root-locus of uncompensated synchronous machine and exciter with $K=K_A$

C. Rate Feedback

Consider adding rate feedback in the excitation system. The field voltage is measured and fed back through F_N/F_D to the voltage summing junction. One form of transfer function which has been used for this feedback loop is

$$F_N/F_D = sK_F/1+T_Fs \qquad [15]$$

The open-loop transfer function is found by inserting Equation 15 into Equation 14 and setting $R_N=0$, $R_D=L_N=L_D=1$. The resulting expression is

$$\frac{K_A\,[K_R\{2HK_6s^2 + 377(K_1K_6-K_2K_5)\}(1+T_Rs)K_3 + sK_F(1+T_Rs)\{(1+sK_3T'_{do})(2Hs^2 + 377K_1) - 377K_2K_3K_4\}]}{(1+T_As)(K_E+T_Es)\{(1+sK_3T'_{do})(2Hs^2 + 377K_1) - 377K_2K_3K_4\}(1+T_Rs)(1+T_Fs)} \qquad [16]$$

This form is not appropriate for a root-locus plot using gain K_F because K_F does not appear as a product of all terms in the numerator. An appropriate open-loop transfer function which contains K_F multiplying all terms in the numerator is developed as follows. The regulator loop of Figure 21 is first closed, resulting in the block diagram of Figure 23, and the resulting open-loop transfer function after combining the parallel feedback branches is

$$\frac{K_3L_NK_A(1+T_Rs)\{R_DF_N[(1+sK_3T'_{do})(2Hs^2 + 377K_1) - 377K_2K_3K_4] + F_DR_NK_2K_3s\}}{R_DF_DK_3\{L_D(1+T_As)(K_E+T_Es)(1+T_Rs)[(1+sK_3T'_{do})(2Hs^2 + 377K_1) - 377K_2K_3K_4] + K_RL_NK_AK_3[2HK_6s^2 + 377(K_1K_6-K_2K_5)]\}} \qquad [17]$$

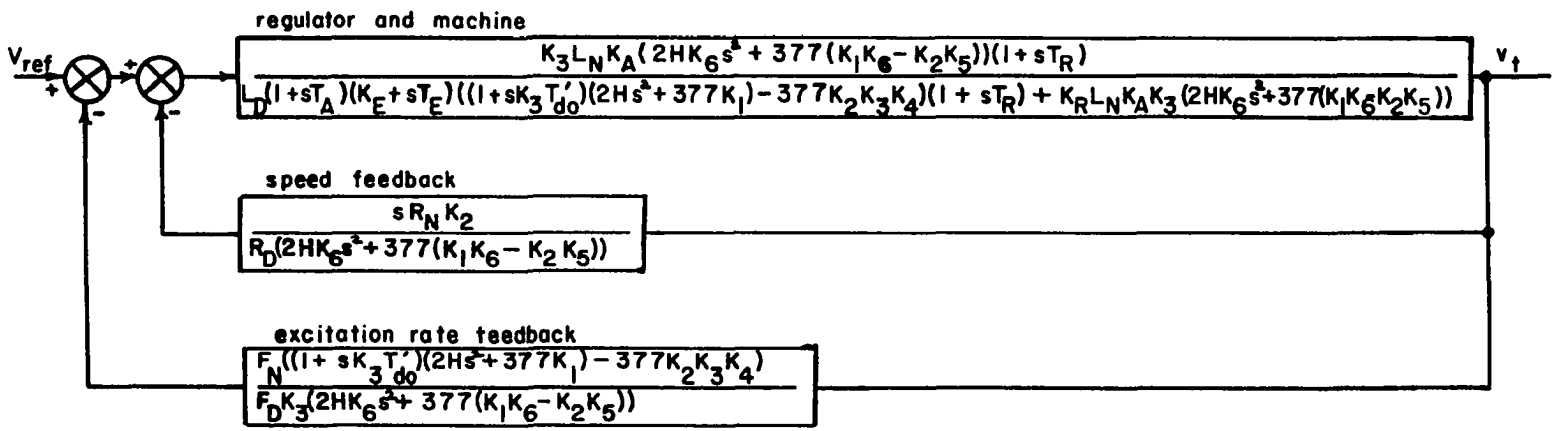

Figure 23. Block diagram after closing regulator loop

The transfer function is again checked by reducing the generator representation to a first order system as follows.

Set $K_1=0$	$L_N=1$
$K_2=0$	$L_D=1$
$K_3=K_G$	$F_N=sK_F$
$K_4=0$	$F_D=1+T_Fs$
$K_5=0$	$R_N=0$
$K_3T'_{do}=T_G$	$R_D=1$

Equation 17 becomes

$$\frac{K_GK_A(1+T_Rs)\{sK_F\ (1+sT_G)(2Hs^2)\ +\ 0\}}{K_G(1+T_Fs)\{(1+T_As)(K_E+T_Es)(1+T_Rs)(1+sT_G)(2Hs^2)\ +\ K_RK_AK_6 2Hs^2\}}$$

$$= \frac{sK_F(1+T_Gs)}{K_G(1+T_Fs)}\frac{K_GK_A(1+T_Rs)}{\{(1+T_As)(K_E+T_Es)(1+T_Rs)(1+T_Gs)\ +\ K_RK_AK_G\}} = HG$$

Find the closed-loop transfer function.

$$CLTF = \frac{K_AK_G(1+T_Rs)(1+T_Fs)\ K_G}{K_G(1+T_Fs)\{(1+T_As)(K_E+T_Es)(1+T_Rs)(1+T_Gs)+K_RK_AK_G\}+K_AK_GK_Fs(1+T_Rs)(1+T_Gs)}$$

$$= \frac{K_AK_GT_RT_F(1/T_R+s)(1/T_F+s)}{T_AT_ET_RT_GT_F\{(1/T_A+s)(K_E/T_E+s)(1/T_R+s)(1/T_G+s)(1/T_F+s)}$$

$$+\ K_RK_AK_GT_F(1/T_F+s)\} + K_AK_FT_RT_Gs(1/T_R+s)(1/T_G+s)$$

$$= \frac{K_A K_G T_R T_F (1/T_R+s)(1/T_F+s)}{T_A T_E T_R T_G T_F \{(1/T_A+s)(K_E/T_E+s)(1/T_R+s)(1/T_G+s)(1/T_F+s)}$$

$$+ \frac{K_A K_G}{T_A T_E T_R T_G T_F} [K_R T_F (1/T_F+s) + \frac{K_F T_R T_G}{K_G} s (1/T_R+s)(1/T_G+s)]\}$$

$$= \frac{\frac{K_A K_G}{T_A T_E T_F} (1/T_R+s)(1/T_F+s)}{(1/T_A+s)(K_E/T_E+s)(1/T_R+s)(1/T_G+s)(1/T_F+s)}$$

$$+ \frac{K_A K_G}{T_A T_E T_G} \left[\frac{K_R}{T_R} \frac{K_F}{T_F} (1/T+s) + \frac{K_F T_R T_G}{T_R T_F K_G} s (1/T_R+s)(1/T_G+s)\right]$$

$$= \frac{\frac{K_A K_G}{T_A T_F T_E} (1/T_R+s)(1/T_F+s)}{(1/T_A+s)(K_E/T_E+s)(1/T_R+s)(1/T_G+s)(1/T_F+s)}$$

$$+ \frac{K_A K_G}{T_A T_E T_G} \left[\frac{K_F}{T_F} \frac{T_G}{K_G} s (1/T_R+s)(1/T_G+s) + \frac{K_R}{T_R} (1/T_F+s)\right]$$

This is the same expression derived for a first order model in reference (7).

If the following substitutions are made in Equation 17, $L_N=L_D=R_D=1$, $R_N=T_R=0$, $F_N=sK_F$, $F_D=(1+T_F s)$, $T_F=.05$, the resulting root-locus is shown in Figure 24. K_F must be increased until the RHP poles move very near the complex zeros at about ± j19.6 to make the system stable, but at this gain level the root-locus branches from the complex poles in the LHP have already arrived near the second order zeros at the origin producing a poorly damped response.

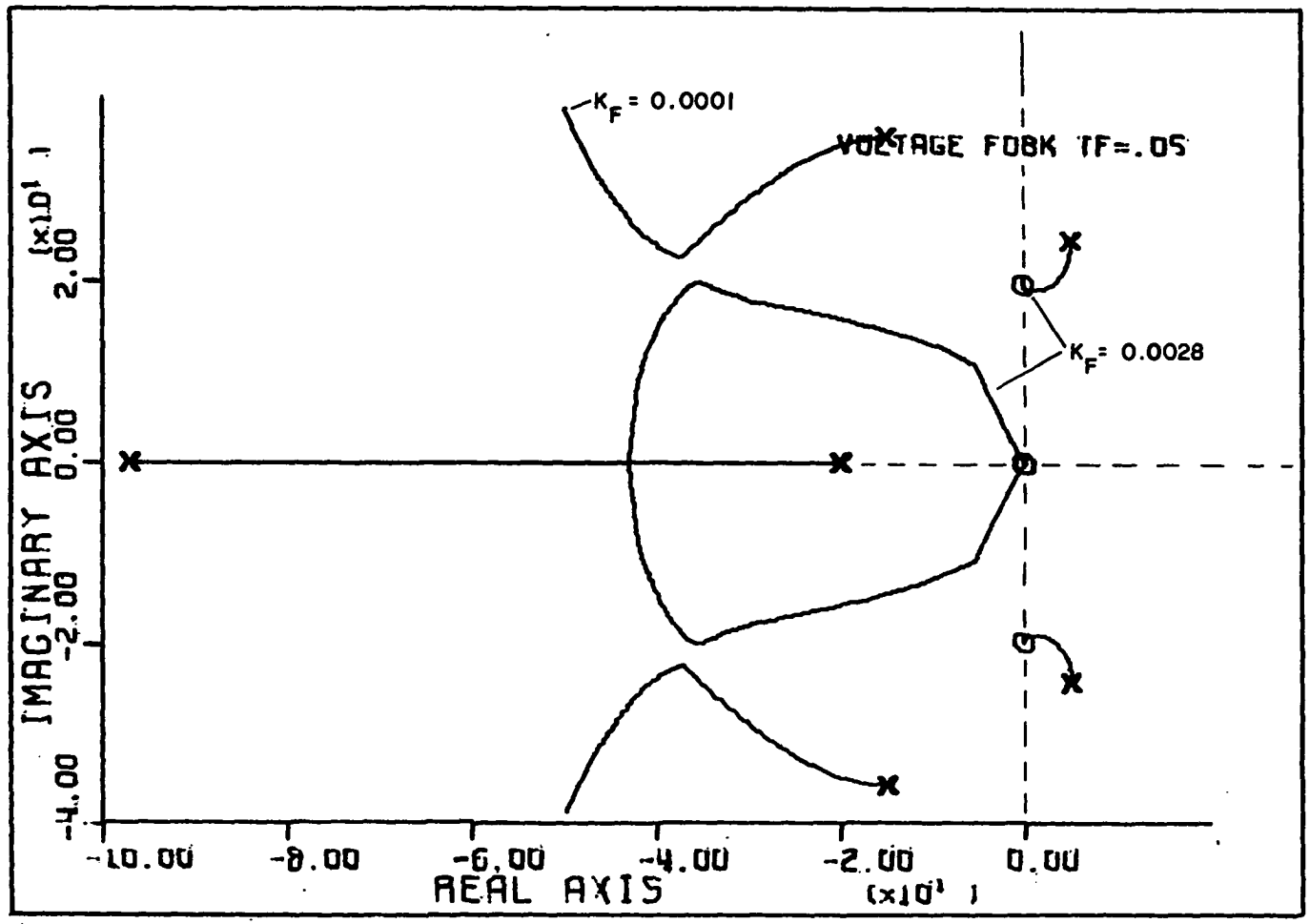

Figure 24. Root-locus of synchronous machine and exciter with excitation rate feedback and $K=K_F$, T_F=0.05 sec

For T_F=10 (see Figure 25) the pole added by the denominator of the excitation system rate feedback term lies between the two zeros near the origin and a root-locus with different characteristics is obtained. The generator torque-angle poles will move to the complex zeros, but the poles on the real axis now move to the zeros near the origin and dominate the response of the system.

D. Power System Stabilizer

Recently an auxiliary control system called a power system stabilizer has been developed to combat dynamic stability problems occurring in regions with significant amounts of hydrogeneration, or resulting from high-speed excitation systems. This device is a rate feedback control loop operating from a speed deviation signal. Lead-lag networks in the feedback loop are adjusted to cancel phase lags of the excitation system. One form of the transfer function often used is as follows,

$$\frac{R_N}{R_D} = \frac{GRN\ s(1+sT_1)^2}{(1+sT)(1+sT_2)^2}$$

where appropriate parameter values are suggested by deMello and Concordia (31).

$$T_1 = 0.20$$
$$T_2 = 0.05 \quad \text{sec}$$
$$T = 3.00$$

The open-loop transfer function with the above speed feedback is developed from Equation 17 so that the effects of changing GRN may be observed.

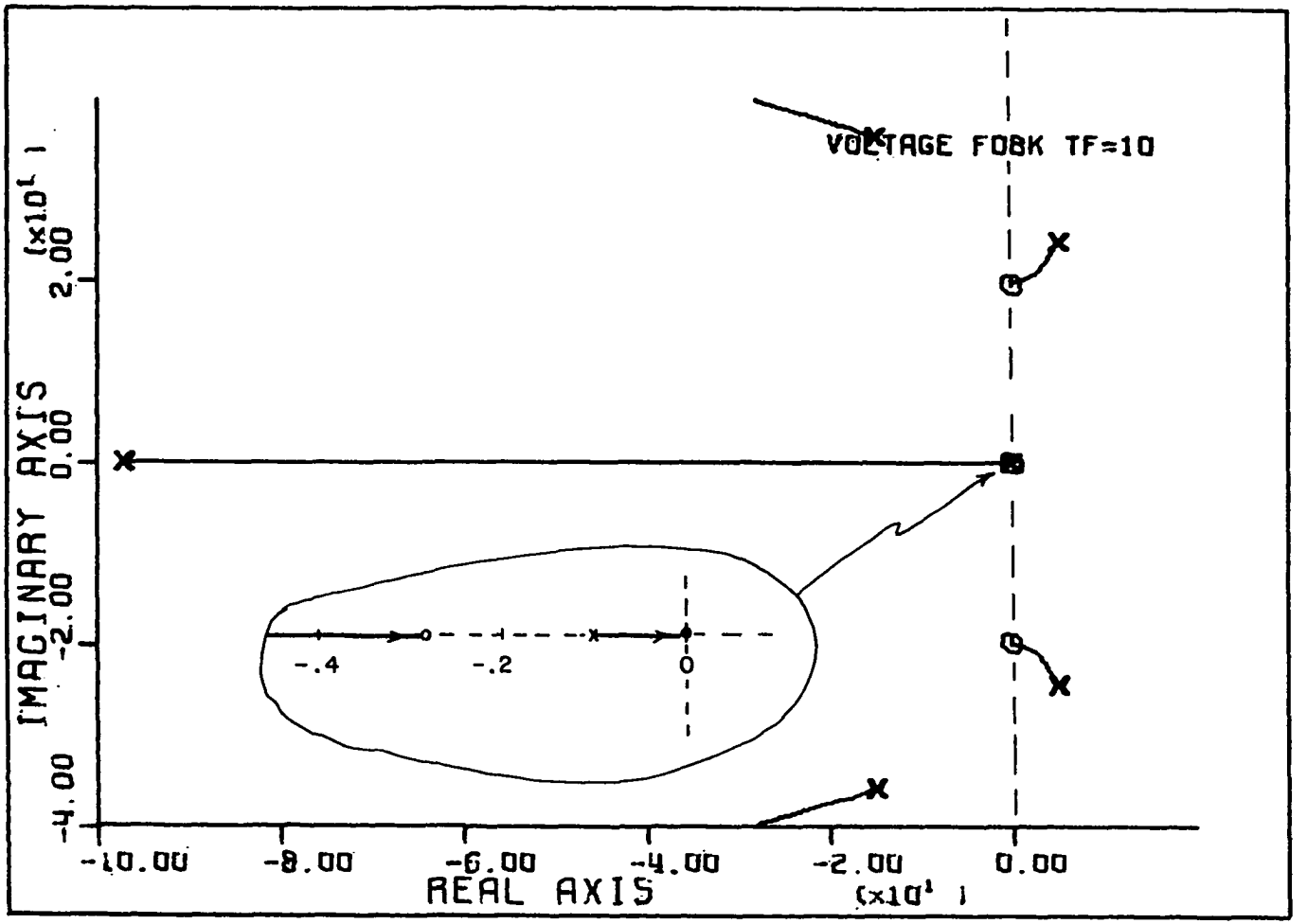

Figure 25. Root-locus of synchronous machine and exciter with excitation rate feedback and $K=K_F$, $T_F=10$ sec

If $L_N=L_D=F_D=1$, $F_N=T_R=0$ the resulting transfer function is

$$\frac{K_A GRN\, s^2(1+sT_1)^2K_2K_3}{(1+sT)(1+sT_2)^2\{(1+T_As)(K_E+T_Es)[(1+sK_3T'_{do})(2Hs^2+377K_1)-377K_2K_3K_4]}$$

$$+ K_RK_AK_3[sHK_6s^2+377(K_1K_6-K_2K_5)]\}$$

and the resulting root-locus is shown in Figure 26 for positive GRN and Figure 27 for negative GRN.

The system response is again dominated by a pole very near the origin in Figure 26. Figure 27 would lead to an unstable configuration because of the movement of the complex pole pair farther into the right half plane.

E. Bridged-T Network

As mentioned previously, the basic problem of the generator excitation system is the dominant second order poles resulting from the torque-angle loop of the machine as shown in Figure 22. Inspection of this figure also reveals that if the complex zeros occurred below the complex poles then the root-locus from the poles would break away into the left half plane (LHP), a very desirable situation. The complex zeros result, however, from the term

$$[2HK_6s^2 + 377(K_1K_6-K_2K_5)]$$

of Equation 14 and are functions of machine and transmission line parameters and machine loading and thus are not easily varied.

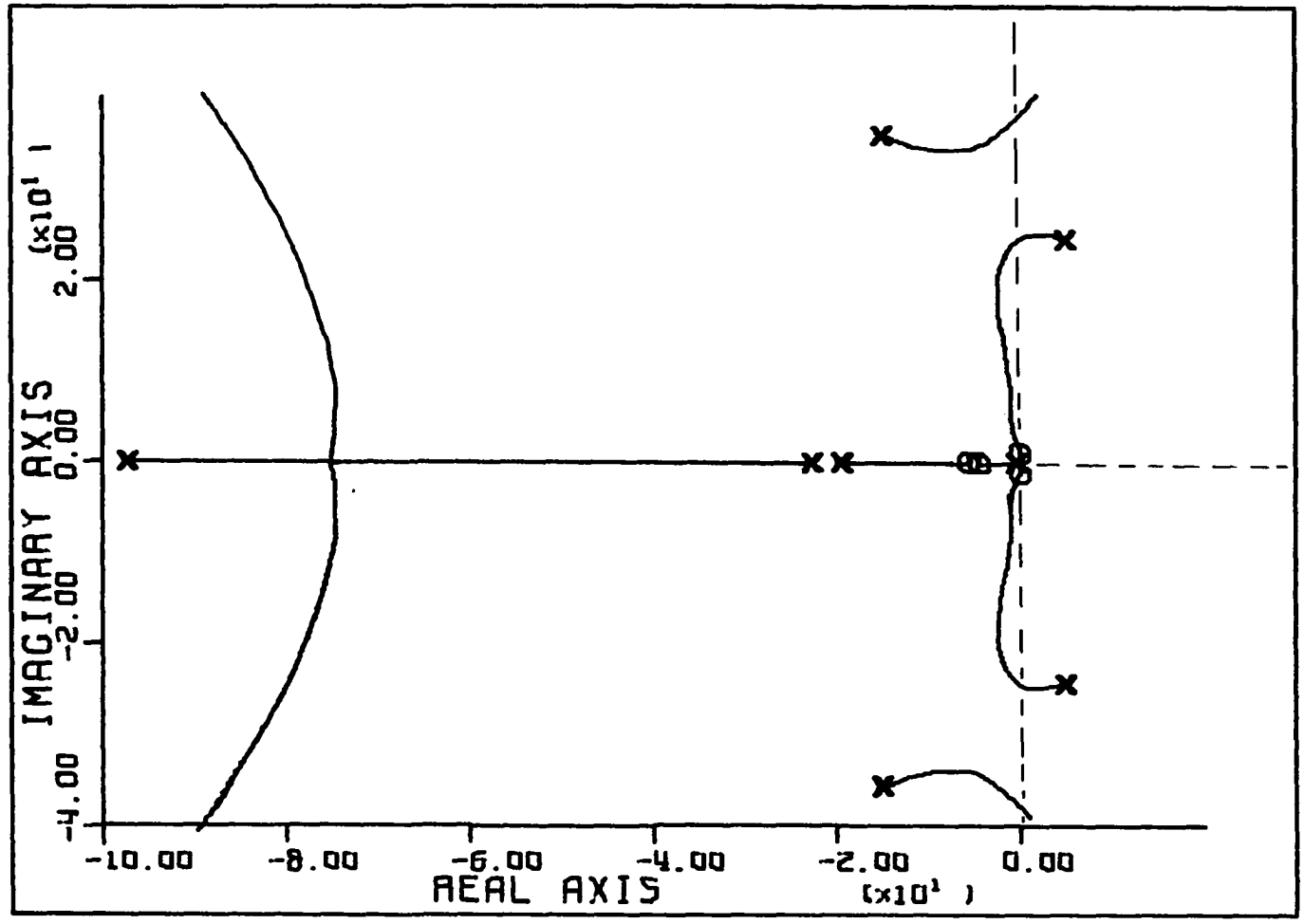

Figure 26. Root-locus of synchronous machine and exciter with power system stabilizer and K=GRN=+3.3 pu, T_1=0.2 sec, T_2=.05 sec and T=3 sec

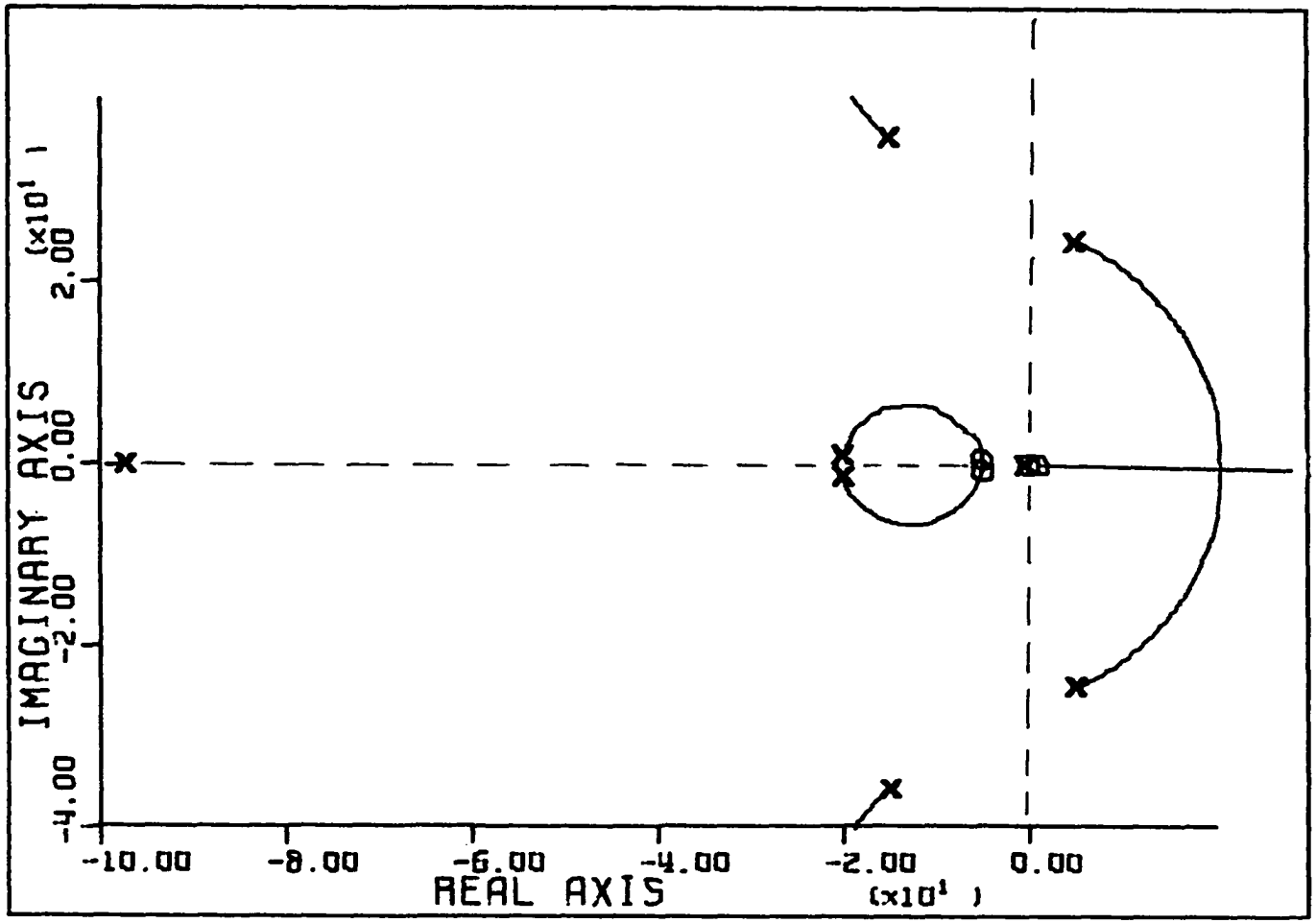

Figure 27. Root-locus of synchronous machine and exciter with power system stabilizer and K=GRN=-3.3 pu, T_1=0.2 sec, T_2=.05 sec and T=3 sec

The root-locus of Figure 22 and the analysis of the previous section suggest that a bridged-T network in the forward loop with judiciously placed zeros might cause the torque-angle loop poles to break away into the LHP.

The appropriate open-loop transfer function is developed from Equation 14 by setting $R_D=F_D=1$, $R_N=F_N=0$ and $L_N=s^2 + rn\omega_o s + \omega_o^2$ and $L_D=s^2 + n\omega_o s + \omega_o^2$ and letting r=.1, n=2 and ω_o=23. The resulting root-locus obtained by varying K_A is shown in Figure 28. The torque-angle loop breaks into the LHP as desired but the system becomes unstable at relatively low values of K_A ($K_A \simeq 152$).

The location of the complex zero pair of the bridged-T is also fairly critical. For example, if ω_o of the bridged-T = 19.7 rad/sec with the same r and n as above, the root-locus of Figure 29 results and the torque-angle loop poles again break into the RHP. Somewhat similar results occur for the bridged-T tuned for a higher frequency ω_o=26 rad/sec and r=.4 and n=2. chosen to move the zeros farther into the LHP as shown in Figure 30.

Intuitively, the effectiveness of the bridged-T may be explained as follows. If damping were to be represented in the block diagram of Figure 17 there would be a feedback path from ω_Δ to the torque summing junction with the gain of this path determining the amount of damping. Pure damping could also be obtained through the feedback path R_N/R_D if the phase lag introduced by excitation system and generator field were zero. This possibility will be explored later. The other possible path for damping is through the voltage regulator loop. The takeoff point for this loop is δ which lags ω_Δ by 90°, and additional phase lag introduced by the excitation system and field produces a signal at the torque summing

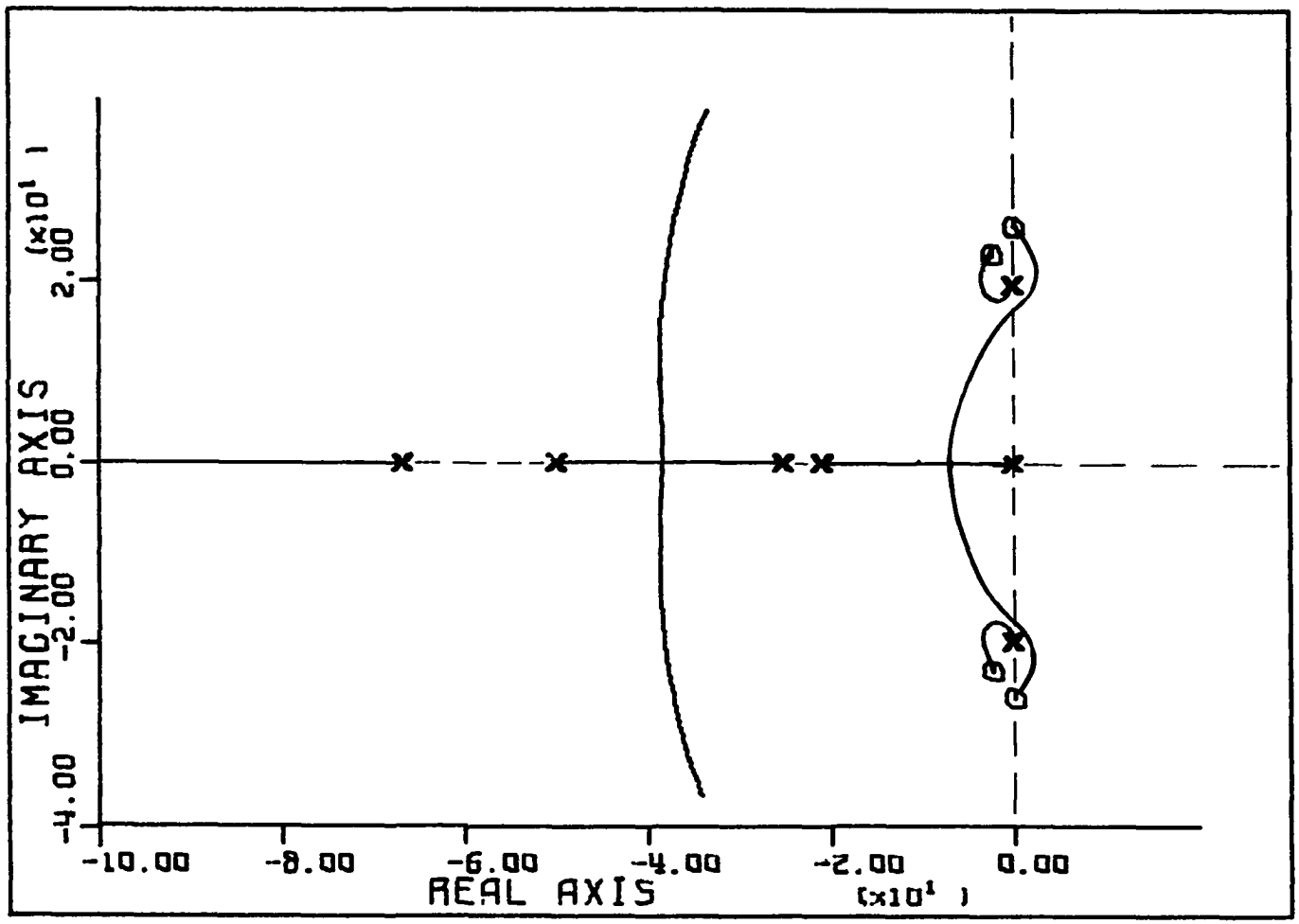

Figure 28. Root-locus diagram of synchronous machine and exciter with bridged-T network placed in exciter forward loop and $K=K_A$, $\omega_o=23$ rad/sec, $r=.1$ and $n=2$

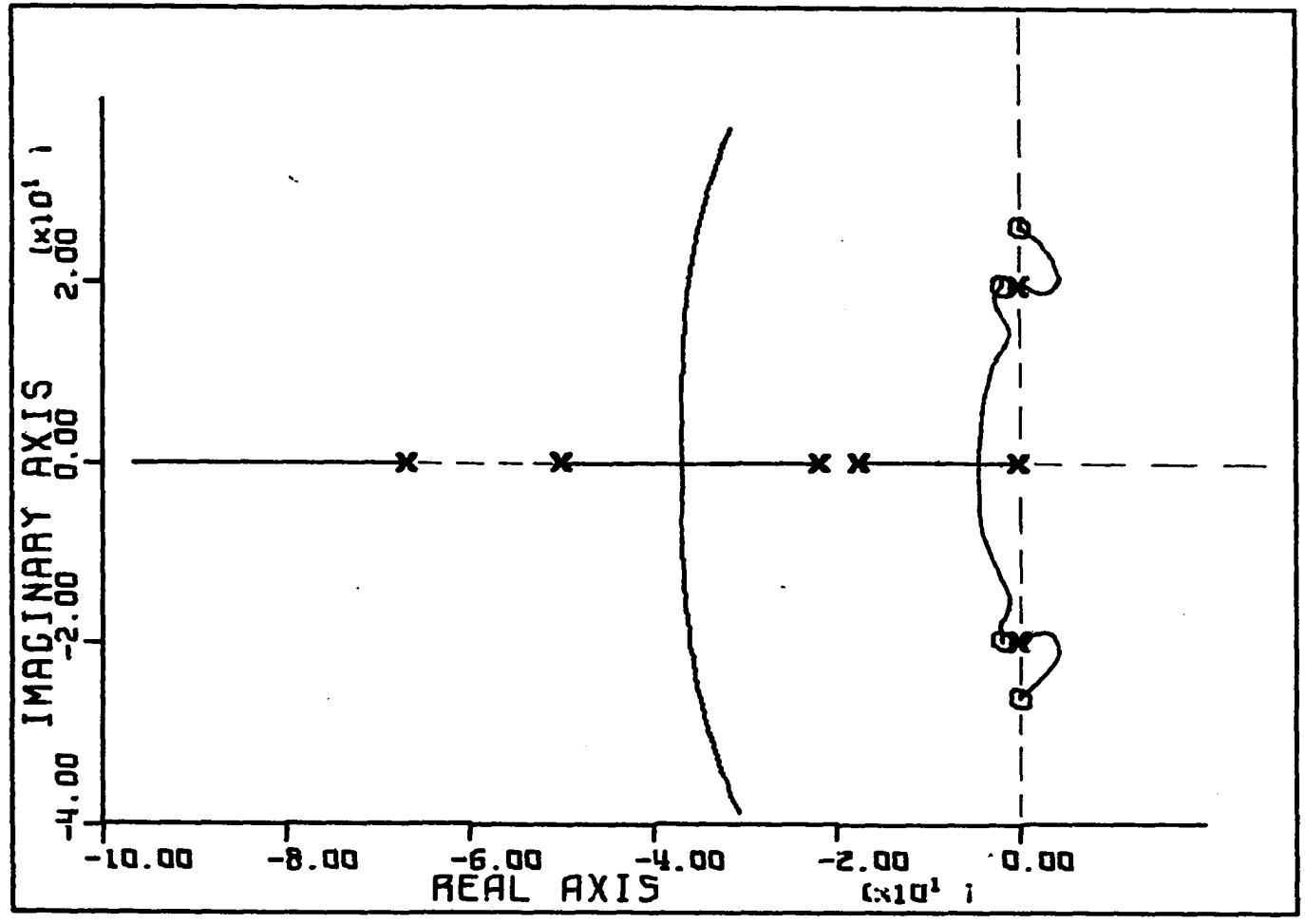

Figure 29. Root-locus diagram of synchronous machine and exciter with bridged-T network placed in exciter forward loop and $K=K_A$, $\omega_o=19.7$ rad/sec, $r=.1$ and $n=2$

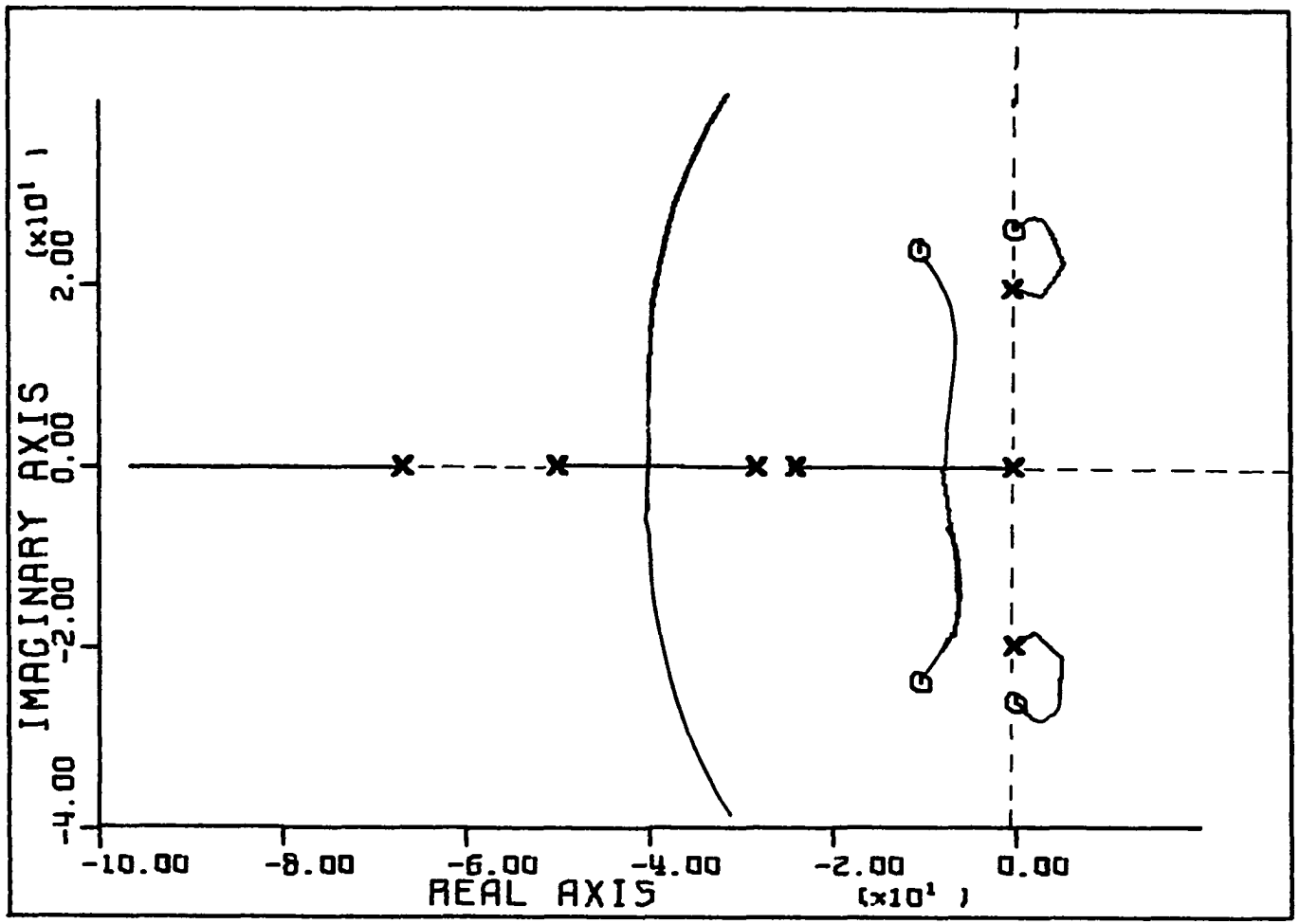

Figure 30. Root-locus diagram of synchronous machine and exciter with bridged-T network placed in exciter forward loop and $K=K_A$, $\omega_o=26$ rad/sec, $r=.4$ and $n=2$

junction having a detrimental effect on system damping. The bridged-T filters out components of this signal near the natural frequency of the machine, and as the root-locus of Figure 28 demonstrated, might be used to improve stability and damping to some extent.

To find a source for additional damping signals we return to the feedback through R_N/R_D, and recognize that signals through this loop will also be filtered by the forward loop bridged-T of the exciter which is an undesirable situation if additional damping near the natural frequency of the machine is desired. A solution is to move the bridged-T to the regulator feedback loop. The root-locus for this condition with no other feedback paths is the same as Figure 28.

F. Bridged-T and Two-stage Lead-lag with Speed Feedback

Additional compensation schemes may be explored after developing an appropriate open-loop transfer function for a bridged-T filter placed in the voltage regulator feedback loop as shown in Figure 31.

The resulting open-loop transfer function is

$$\frac{L_N K_A [K_R R_D F_D K_3 \{2HK_6 s^2+377(K_1K_6-K_2K_5)\}\{s^2+BT1s+BT2\} + sR_N K_2 K_3 F_D(1+T_R s)\{s^2+BT3s+BT2\} + F_N R_D(1+T_R s)\{(1+sK_3T'_{do})(2Hs^2+377K_1)-377K_2K_3K_4\}\{s^2+BT3s+BT2\}]}{\left[L_D(1+T_A s)(K_E+T_E s)\{(1+sK_3T'_{do})(2Hs^2+377K_1)-377K_2K_3K_4\}\right]\left[R_D F_D(1+T_R s)\{s^2+BT3s+BT2\}\right]} \quad [18]$$

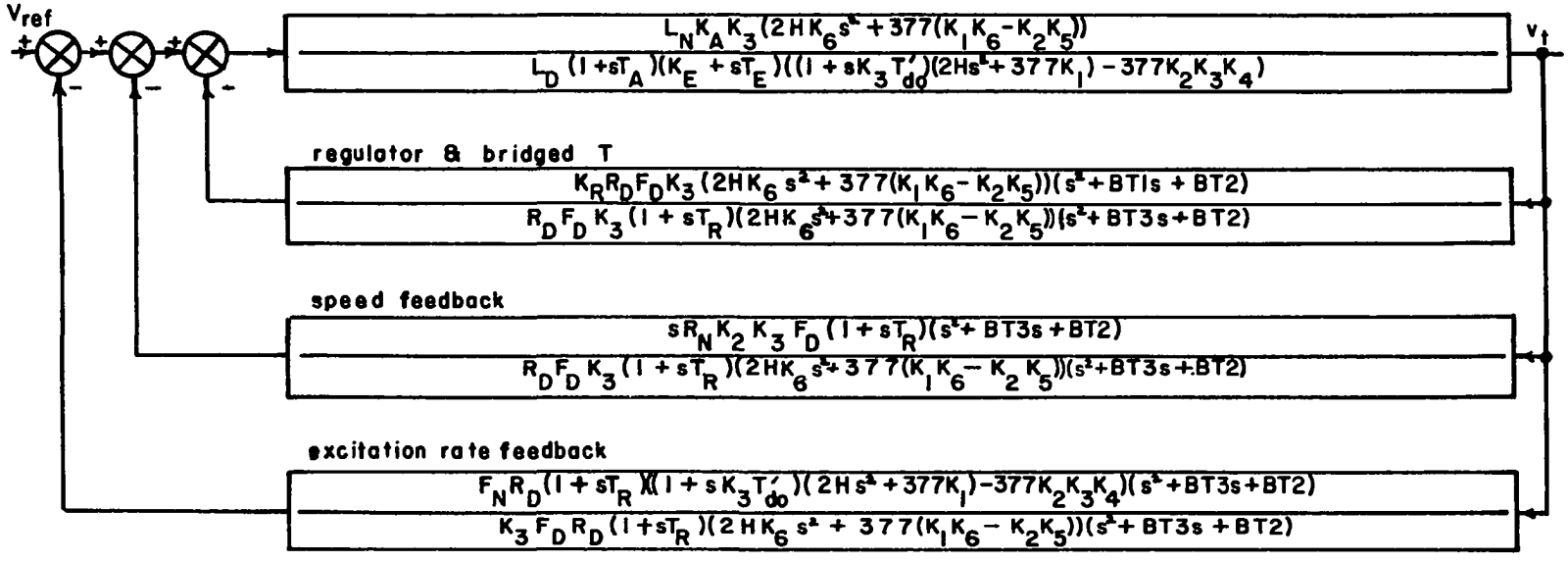

Figure 31. Block diagram showing addition of bridged-T filter to regulator feedback loop

A two-stage lead-lag network is now added to the feedforward loop of the excitation system by setting

$$L_N/L_D = (T_1 s+1)^2/(T_2 s+1)^2 \qquad [19]$$

and speed feedback is added by setting

$$R_N/R_D = GRN \qquad [20]$$

The resulting open-loop transfer function is

$$\frac{(T_1^2 s^2+2T_1 s+1)\,[K_R K_3 K_A\{2HK_6 s^2+377(K_1 K_6-K_2 K_5)\}\{s^2+BT1s+BT2\} + sGRNK_2 K_3 K_A(1+T_R s)\{s^2+BT3s+BT2\}]}{(T_2 s^2+2T_2 s+1)(1+T_A s)(K_E+T_E s)}$$

$$\{(1+sK_3 T'_{do})(2Hs^2+377K_1)-377K_2 K_3 K_4\}(1+T_R s)\{s^2+BT3s+BT2\} \qquad [21]$$

If the following values are chosen for the various parameters, the root-locus shown in Figure 32 results.

$\omega_o = 21$ rad/sec

$r = .1$

$n = 2$

$T_1 = .2$ sec

$T_2 = .05$ sec

$GRN = 3.3$ pu

$K = K_A$ pu

As will be shown later, the idea of Figure 32 results in a stable configuration when it is applied to the nonlinear analog computer model,

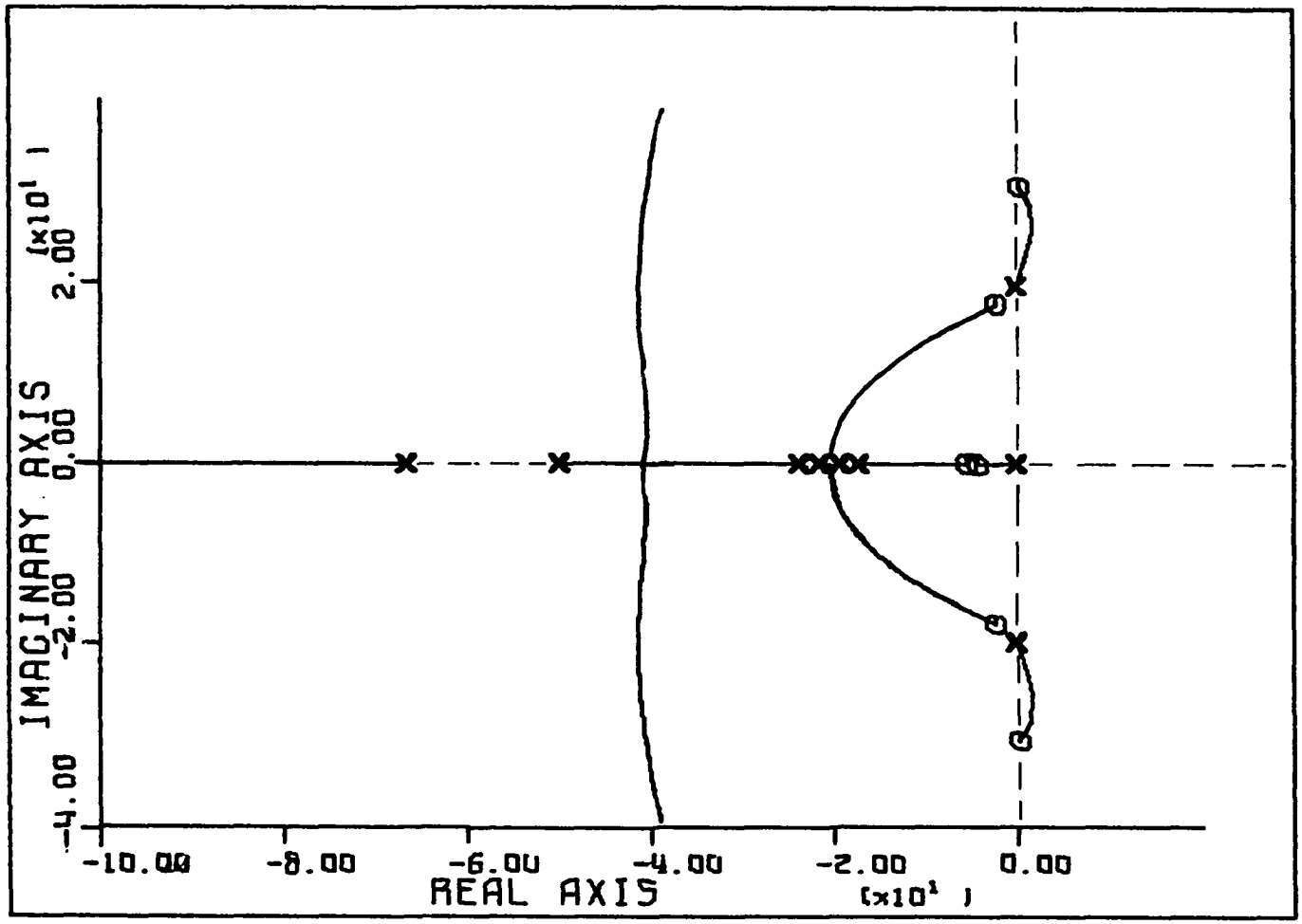

Figure 32. Root-locus of synchronous machine and exciter with bridged-T in regulator loop, 2-stage lead-lag network in exciter feedforward loop and speed feedback through GRN with $K=K_A$, $\omega_o=21$ rad/sec, r=.1, n=2, $T_1=.2$ sec, $T_2=.05$ sec, and GRN=+3.3 pu

so this configuration is superior to that of Figure 28 because much higher values of K_A can be used resulting in a smaller steady-state error.

Also note that this configuration results in the movement of the synchronous machine field pole away from the origin to a location where it does not so completely dominate the system response.

Comparison of Figure 28 and Figure 32 also shows that the complex zeros on the jω-axis have moved upward in the latter. Inspection of Equation 21 shows that these zeros result from the fourth order polynomial in the open-loop transfer function numerator and, further, that the coefficients of the numerator are functions of speed feedback GRN. Also note that GRN does not appear in the denominator of Equation 21 and, therefore, does not change positions of the poles of the open-loop transfer function.

We now explore the effect of GRN on zero locations by manipulating the fourth order polynomial of the numerator into a form appropriate for a root-locus study as shown below.

$$1 + \frac{GRN\ s\{K_AK_3K_2\}\{s^2 + BT3s + BT2\}(1+T_Rs)}{K_EK_3K_A\{2HK_6s^2 + 377(K_1K_6-K_2K_5)\}\{s^2 + BT1s + BT2\}} = 0 \qquad [22]$$

The resulting root-loci for GRN positive and negative are shown in Figures 33 and 34. A feedback path through a positive GRN is preferred as shown in Figure 33 because the locations of all zeros remain in the left half plane. The value of GRN used in the previous example was 3.3 pu. This value was chosen because preliminary analog computer studies indicated it provided a workable solution.

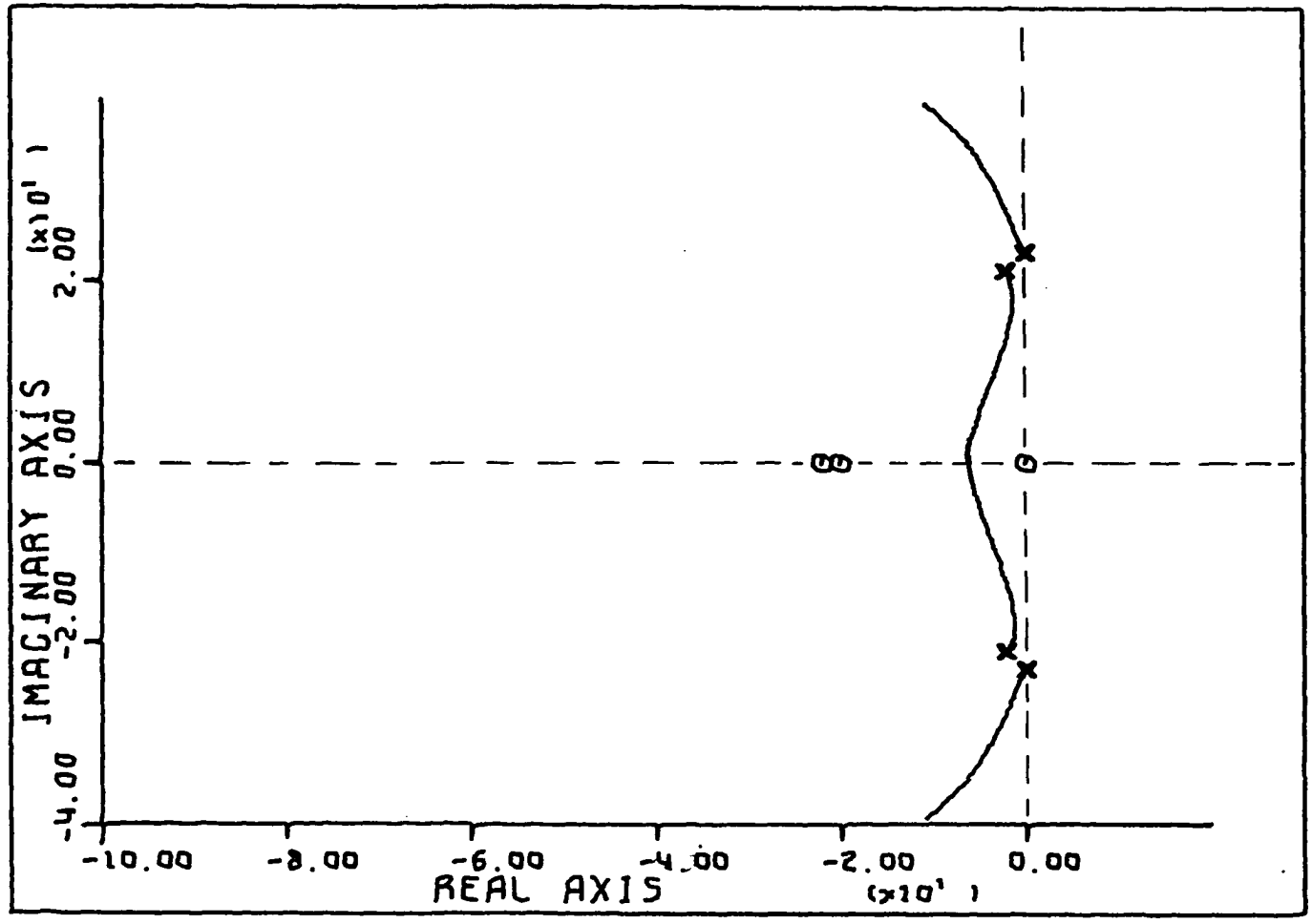

Figure 33. Movement of zeros of Equation 21 with K=+GRN

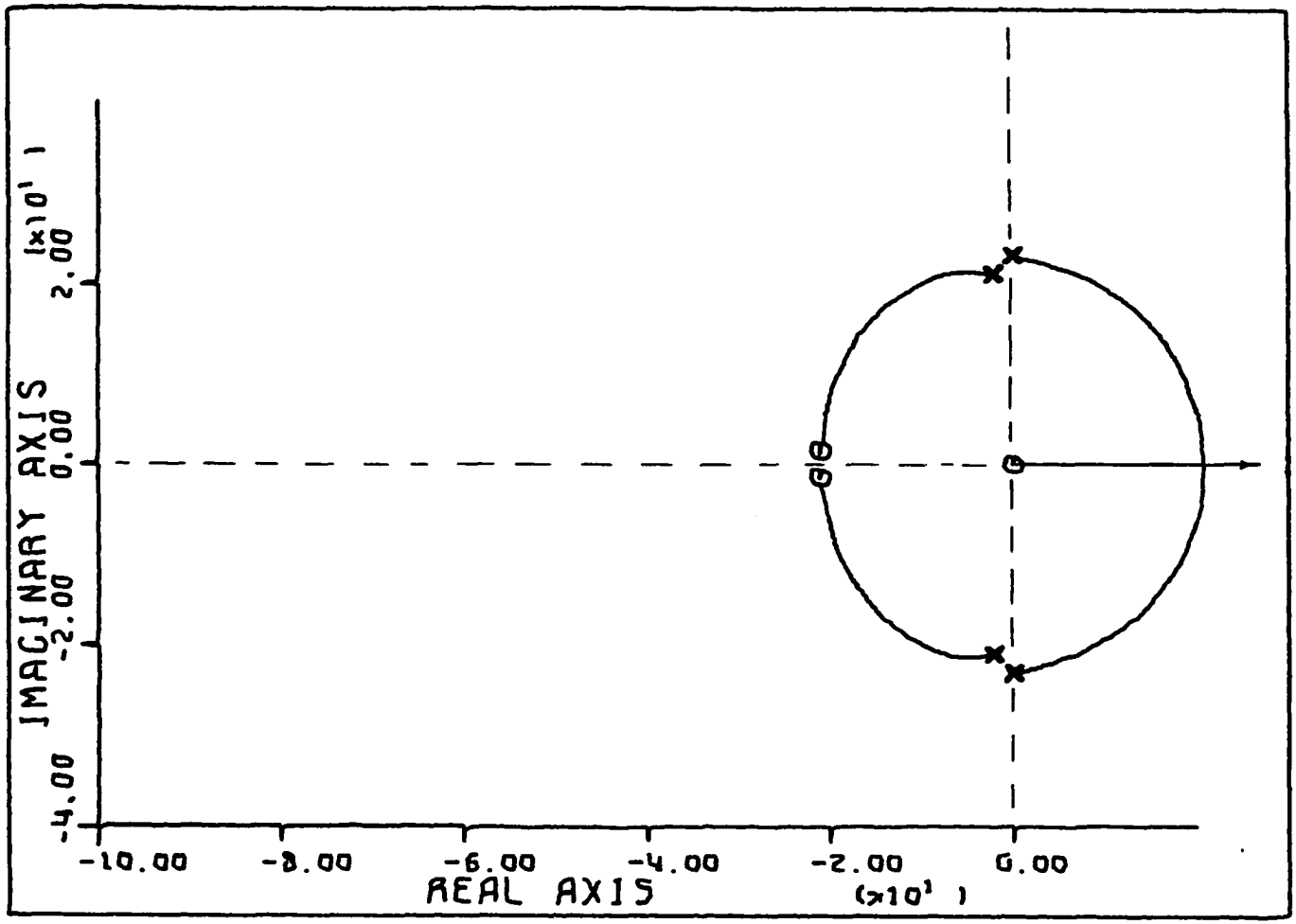

Figure 34. Movement of zeros of Equation 21 with K=-GRN

G. Cancellation of Third Order Polynomial

Another approach to the problem may be explored by considering Equation 14 again. The fundamental problem of compensating this system results from the third order polynomial in the denominator of Equation 14. We note that this same polynomial occurs in one term of the numerator, and it results from excitation system rate feedback. If it were possible to add appropriate compensation networks such that the voltage regulator and speed feedback terms could be combined and the third order polynomial factored from the resulting expression, then this expression could be cancelled from both the numerator and denominator, hopefully giving a more advantageous pole-zero configuration.

An attempt to accomplish the above is made by developing an appropriate speed feedback transfer function noting that a third order polynomial has four coefficients which will result in four equations and thus the maximum number of unknowns is four. A third order expression is needed, so looking at the voltage regulator term which is of order 2 let R_D=As+B where A and B are to be determined. This gives the desired third order expression. Now set R_N=Cs+D to have a physically realizable network, where C and D are also unknowns. The expressions are expanded and coefficients equated as follows.

Numerator of Equation 14:

$$L_N K_A [K_R \{2HK_6 s^2 + 377(K_1 K_6 - K_2 K_5)\} R_D F_D K_3 + s R_N F_D K_3 (1+T_R s) K_2$$

$$+ F_N R_D (1+T_R s)\{(1+sK_3 T'_{do})(2Hs^2 + 377K_1) - 377K_2 K_3 K_4\}] \qquad [23]$$

The common factors from terms 1 and 2 are first factored out as follows.

$$L_N K_A \Big[F_D K_3 [K_R(As+B)\{2HK_6 s^2 + 377(K_1K_6 - K_2K_5)\} + s(Cs+D)(1+T_R s)K_2]$$

$$+ F_N R_D (1+T_R s)\{(1+sK_3 T'_{do})(2Hs^2 + 377K_1) - 377K_2K_3K_4\}\Big] \qquad [24]$$

Expand the above equation.

$$(2HK_6AK_R + T_R CK_2)s^3 + (2HK_6K_R B + (T_R DK_2 + CK_2))s^2$$

$$+ (377(K_1K_6 - K_2K_5)K_R A + DK_2)s + 377(K_1K_6 - K_2K_5)K_R B$$

$$= K_3 T'_{do} 2Hs^3 + 2Hs^2 + 377K_1K_3T'_{do}s + 377(K_1 - K_2K_3K_4) \qquad [25]$$

Equate coefficients.

$$2HK_6K_R A + T_2K_2C = K_3T'_{do}2H \qquad [26a]$$

$$2HK_6K_R B + T_R K_2 D + K_2 C = 2H \qquad [26b]$$

$$377(K_1K_6 - K_2K_5)K_R A + K_2 D = 377K_1K_3T'_{do} \qquad [26c]$$

$$377(K_1K_6 - K_2K_5)K_R B = 377(K_1 - K_2K_3K_4) \qquad [26d]$$

Solve for A, B, C, and D.

From Equation 26d $$B = \frac{(K_1 - K_2K_3K_4)}{K_R(K_1K_6 - K_2K_5)} \qquad [27]$$

Multiply Equation 26b by $-T_R$ and insert Equation 27 for B and add result to Equation 26a. The result is

$$2HK_6K_RA - T_R^2K_2D = K_3T'_{do}2H-2HT_R + \frac{2HK_6T_R(K_1-K_2K_3K_4)}{(K_1K_6-K_2K_5)} \quad [28]$$

Solve Equation 26c for D.

$$D = \frac{(377K_1K_3T'_{do}-377(K_1K_6-K_2K_5)K_RA)}{K_2} \quad [29]$$

Put Equation 29 into Equation 28 and solve for A.

$$A = \frac{377K_1K_3T'_{do}T_R^2+2H(K_3T'_{do}-T_R)(K_1K_6-K_2K_5)+2HK_6T_R(K_1-K_2K_3K_4)}{(2HK_RK_6 + 377(K_1K_6-K_2K_5)K_RT_R^2(K_1K_6-K_2K_5))} \quad [30]$$

From Equation 26a,

$$C = \frac{(K_3T'_{do}2H - 2HK_6K_RA)}{T_RK_2} \quad [31]$$

If the linear constants resulting from Base Case 2 are substituted in the above equations the following values result.

A = 2.57

B = .426

C = 5.15

D = -765.5

So for cancellation under this operating condition the speed feedback transfer function should have the following form.

$$\frac{R_N}{R_D} = \frac{5.15s - 765.5}{2.57s + .462}$$

$$= \frac{2\ (s-149)}{s + .180}$$

If $T_R=0$, corresponding to a fast regulator, then the equations for A, B, and D are simplified as follows. C is indeterminate and may be set equal to zero. Then

$$2HK_6K_RA = K_3T'_{do}2H \qquad [32a]$$

$$2HK_6K_RB + K_2C = 2H \qquad [32b]$$

$$377(K_1K_6-K_2K_5)K_RA + K_2D = 377K_1K_3T'_{do} \qquad [32c]$$

$$377(K_1K_6-K_2K_5)K_RB = 377(K_1-K_2K_3K_4) \qquad [32d]$$

From Equation 32d

$$B = \frac{377(K_1-K_2K_3K_4)}{377(K_1K_6-K_2K_5)K_R} \qquad [27]$$

From Equation 32a

$$A = \frac{K_3T'_{do}2H}{2HK_6K_R} = \frac{K_3T'_{do}}{K_6K_R} \qquad [33]$$

$$D = \frac{377K_1K_3T'_{do}-377(K_1K_6-K_2K_5)K_RA}{K_2} \qquad [34]$$

$$= \frac{377K_1K_3T'_{do}-377(K_1K_6-K_2K_5)K_R\left[\frac{K_3T'_{do}}{K_6K_R}\right]}{K_2}$$

$$= \frac{377K_1K_3T'_{do}K_6-377(K_1K_6-K_2K_5)}{K_2K_6}$$

Set $C = 0$. [35]

The values shown in Table 3 result from the above equations for various transmission line impedances and synchronous machine loadings.

Table 3. Third order polynomial cancellation

	P .333 Q .0	P .666 Q .0	P 1.0 Q .0	P .333 Q .206	P .666 Q .419	P 1.0 Q .62	P .333 Q-.206	P .666 Q-.419
R_E=.02 X_E=.4								
A	2.430	3.270	4.690	2.270	2.440	2.590	3.250	-11.30
B	0.408	0.210	0.030	0.680	0.501	0.425	0.156	0.54
D	-731	-938	-531	-540	-729	-782	-1050	-3359
R_E=0 X_E=.4								
A	2.400	3.290	4.840	2.260	2.400	2.590	3.260	-9.72
B	0.400	0.213	-0.030	0.683	0.501	0.423	0.150	0.61
D	-723	-883	-355	-539	-717	-755	-1012	-3255
R_E=.2 X_E=.4								
A	2.510	3.190	4.070	2.340	2.510	2.650	3.100	-148
B	0.430	0.235	0.161	0.7027	0.522	0.452	0.175	-2.60
D	-762	-1250	-1425	-522.8	-774	-913	-1272	-3342
R_E=1.0 X_E=1.0								
A	3.820	4.500	5.400	3.580	3.740	3.850	5.990	--
B	0.719	0.433	0.249	1.020	0.870	0.797	0.220	--
D	-583	-1042	-1268	-307	-473	-580	-1584	--

The open-loop transfer function that results after the third order polynomial cancellation is

$$OLTF = \frac{L_N K_A [F_D K_3 + F_N(As+B)(1+T_R s)]}{F_D L_D (1+T_A s)(K_E+T_E s)(As+B)(1+T_R s)} \qquad [36]$$

which may be simplified by setting $F_D=L_N=L_D=1$ and $F_N=T_R=0$. Then the open-loop transfer function becomes

$$\frac{K_A K_3}{T_A T_E A(L/T_A+s)(K_E/T_E+s)(B/A+s)} \qquad [37]$$

A root-locus diagram of this system is shown in Figure 35 where $K=K_A$. The root-locus of Figure 35 provides a workable solution. The poles do not move into the right half plane until K_A is greater than 400, but for high K_A the damping is rather poor. From Equation 36 it is noted that two possibilities remain for adding additional compensation to the system. L_N/L_D and F_N/F_D have not been specified. Ideally the number of poles should exceed the number of zeros by two so that asymptotes lie at 90° and 270°. Because of physical realizability it is not possible to add a zero without also adding a pole, so working with F_N/F_D appears to be a better approach than trying series compensation using L_N/L_D.

If F_N and F_D are made first order then the open-loop transfer function has three zeros and five poles, a desirable configuration.

$$\text{Let } F_N/F_D = K_F s/(s+1/T_F) \qquad [38]$$

Arbitrarily pick $1/T_F = 20$ which adds a pole at (-20, 0) to the open-loop transfer functions.

Insert Equation 38 into Equation 36, setting $L_N = L_D = 1$.

$$\text{OLTF} = \frac{K_A[(s+20)K_3+(K_F s)(As+B)(1+T_R s)]}{(s+20)(1+T_A s)(K_E+T_E s)(As+B)(1+T_R s)} \qquad [39]$$

Since T_R is normally very small, set $T_R=0$, so

$$\text{OLTF} = \frac{K_A[(s+20)K_3+(K_F s)(As+B)]}{(s+20)(1+T_A s)(K_E+T_E s)(As+B)} \qquad [40]$$

The numerator is second order and denominator is fourth order so asymptotes are at 90° and 270°. Poles are at -20, $-1/T_A$, $-K_E/T_E$, $-B/A$.

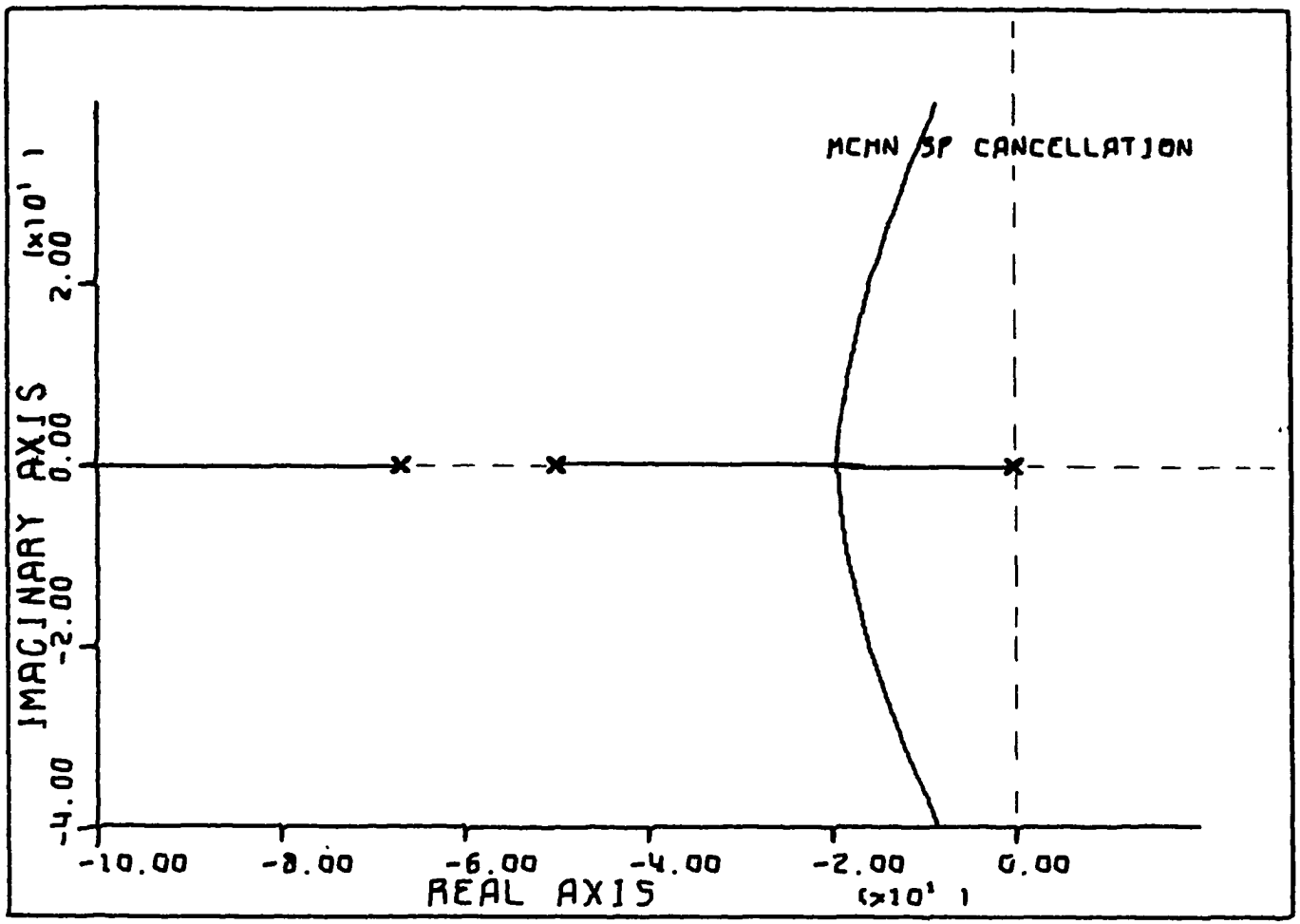

Figure 35. Root-locus resulting from cancellation of torque-angle loop and field poles with $K=K_A$

Explore movement of zeros in numerator as a function of K_F. The numerator is, neglecting K_A,

$$K_F s(As+B) + (s+20)K_3 \qquad [41]$$

which may be put in root-locus form as follows.

$$1 + \frac{K_3(s+20)}{K_F s(As+B)} \qquad [42]$$

$$\text{OLTF} = \frac{K_3(s+20)}{K_F As(s+B/A)} \qquad [43]$$

An arbitrary choice of constants

$$A = 2.6$$

$$B = .426$$

$$K_3 = .262$$

results in the open-loop transfer function

$$\frac{1/K_F\ (.262/2.6)(s+20)}{s(s+.164)} = \frac{1/K_F\ (.164)(s+20)}{s(s+.164)} \qquad [44]$$

The resulting root-locus is shown in Figure 36 for positive K_F and in Figure 37 for negative K_F. From Figure 36 pick $K_F = .00362$ as a suitable value to give appropriate complex zero locations. Putting this value into Equation 34 the root-locus of Figure 38 results where $K=K_A$.

The concept of cancelling the torque-angle loop poles and the field pole with an appropriate speed feedback transfer function produces

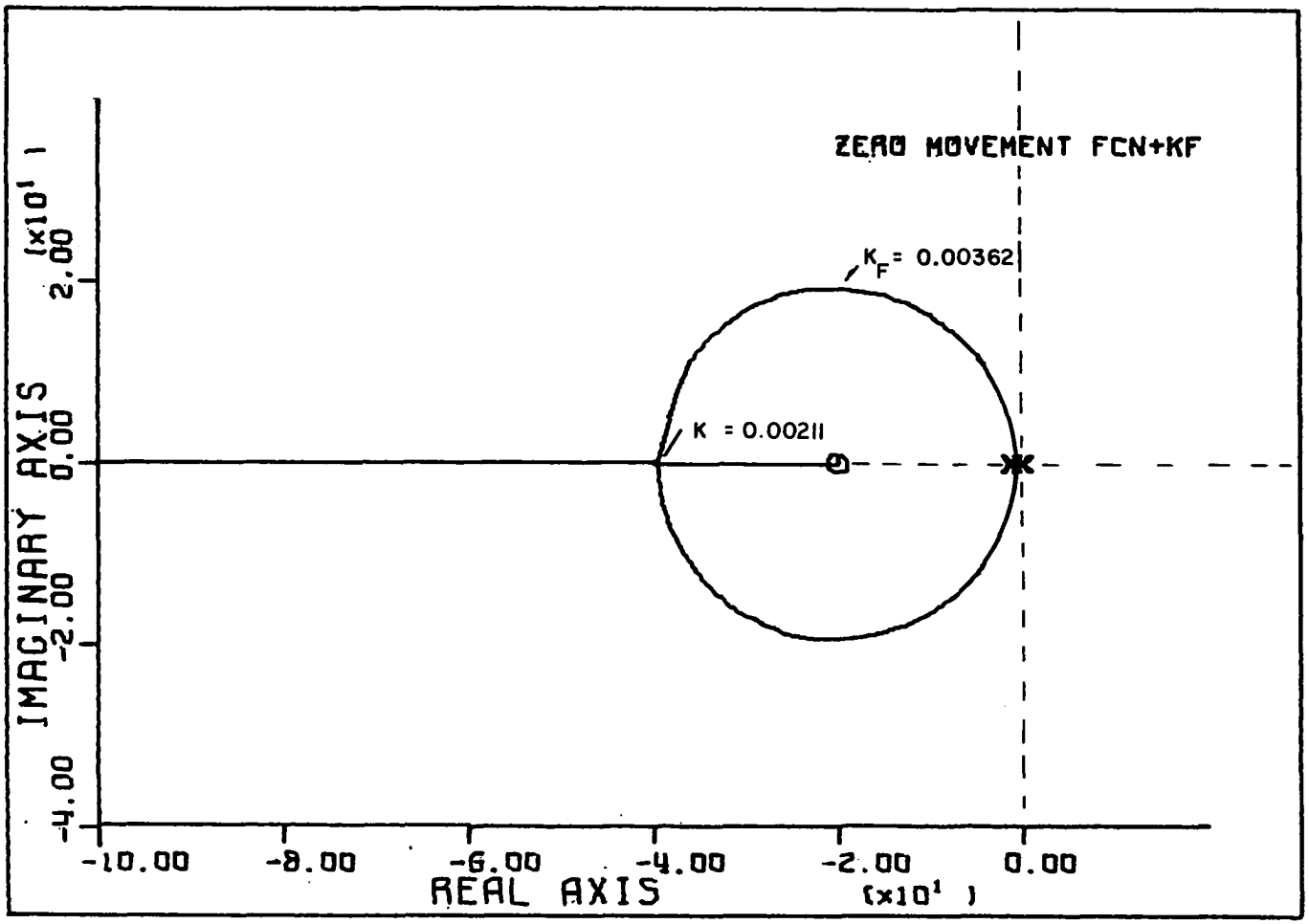

Figure 36. Movement of zeros of Equation 44 with $K=+1/K_F$

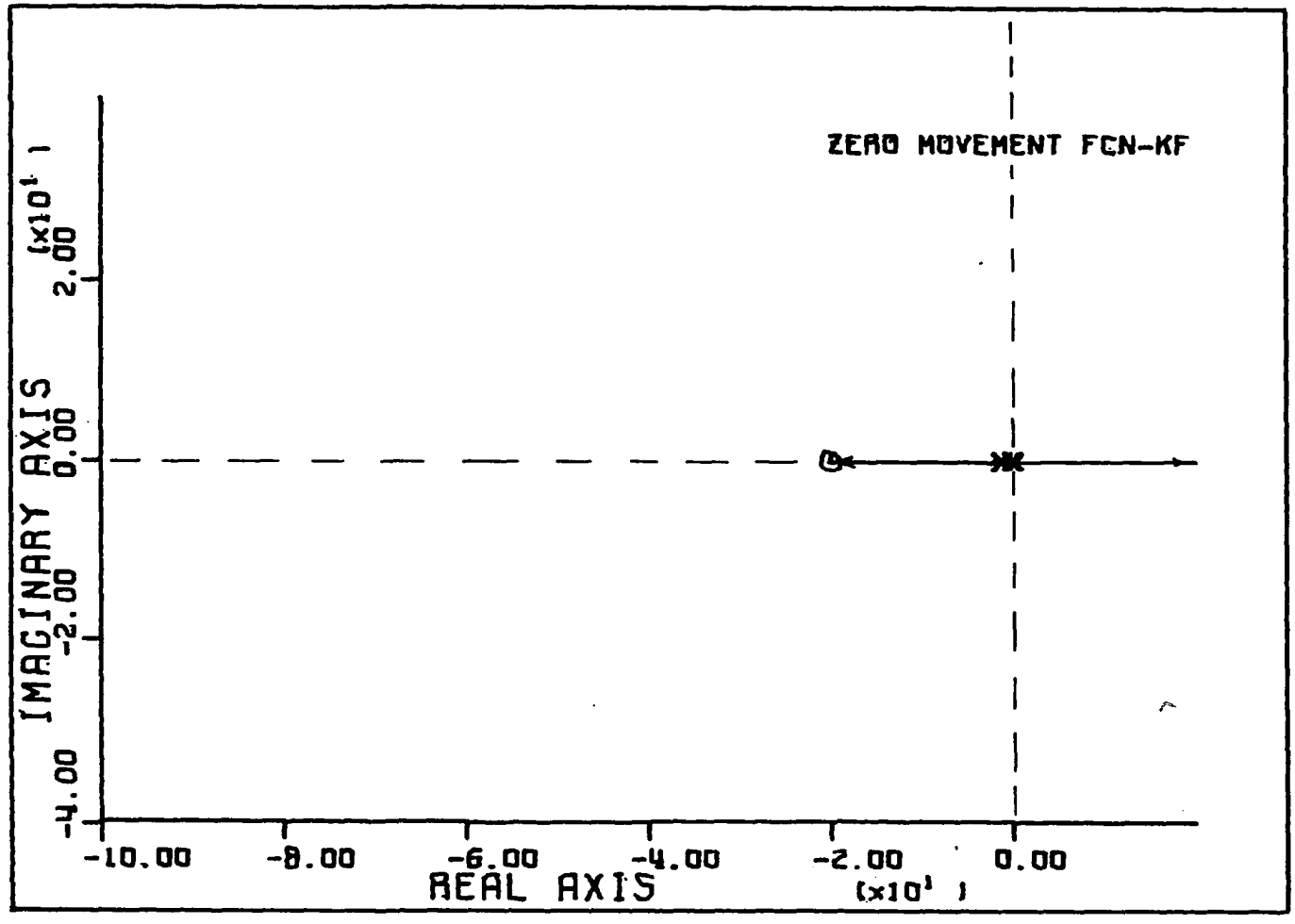

Figure 37. Movement of zeros of Equation 44 with $K=-1/K_F$

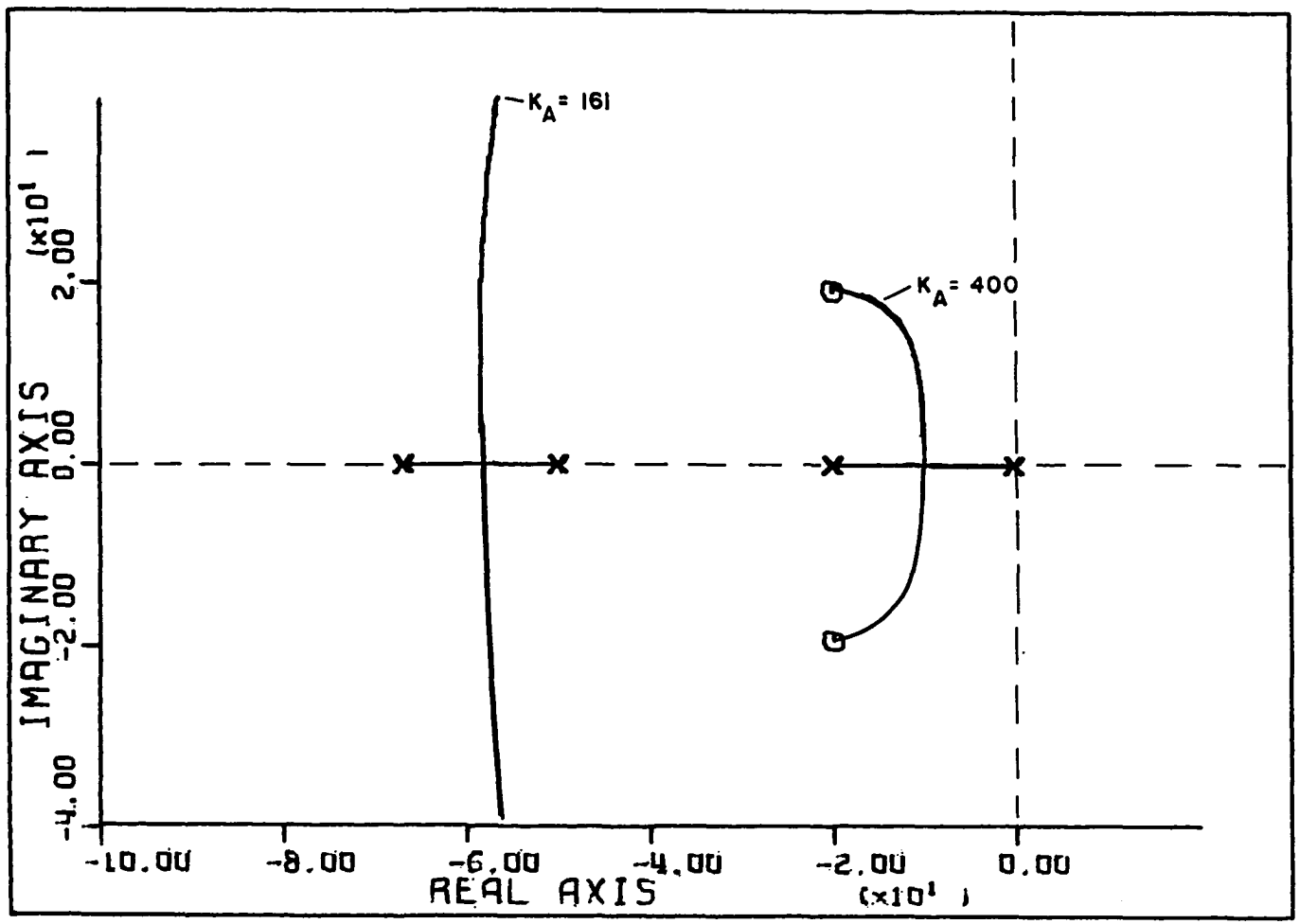

Figure 38. Root-locus after third order pole cancellation and addition of excitation rate feedback

desirable root-locus plots as shown in Figures 35 and 38. Successful implementation of this idea is difficult as will be shown later. Slight inaccuracies in cancellation of the torque-angle loop poles can be tolerated because the poles are fairly far removed from the origin and the resulting residues are small. Extreme accuracy is, however, required to cancel the generator field pole because of its proximity to the origin. If this pole is not cancelled it will dominate the system response, producing an extremely long settling time in the machine terminal voltage.

H. Torque-angle Loop Pole Cancellation by Speed Feedback

It is also possible to develop a transfer function which, when inserted in the speed feedback loop, will cancel the complex pair of torque-angle loop poles. The block diagram of Figure 18 provides an appropriate starting point. The takeoff point for the feedforward loop, K_6, has been moved to δ in Figure 39. Parallel branches K_5 and K_6 are then combined and all feedback paths are moved to v_t as shown in Figure 40. If the excitation system rate feedback loop is neglected, feedback through K_4 is moved to the input summing junction and all feedback paths are arranged so they have a common denominator, the block diagram of Figure 41 results. The open-loop transfer function is

$$\frac{K_3[K_R K_A L_N R_D\{2HK_6 s^2+377(K_1K_6-K_2K_5)\} + sK_AK_2R_NL_N(1+T_Rs)-377K_2K_4L_DR_D(1+T_As)(K_E+T_Es)(1+T_Rs)]}{L_DR_D(1+T_As)(K_E+T_Es)(1+T_Rs)(1+sK_3T'_{do})(2Hs^2+377K_1)} \qquad [45]$$

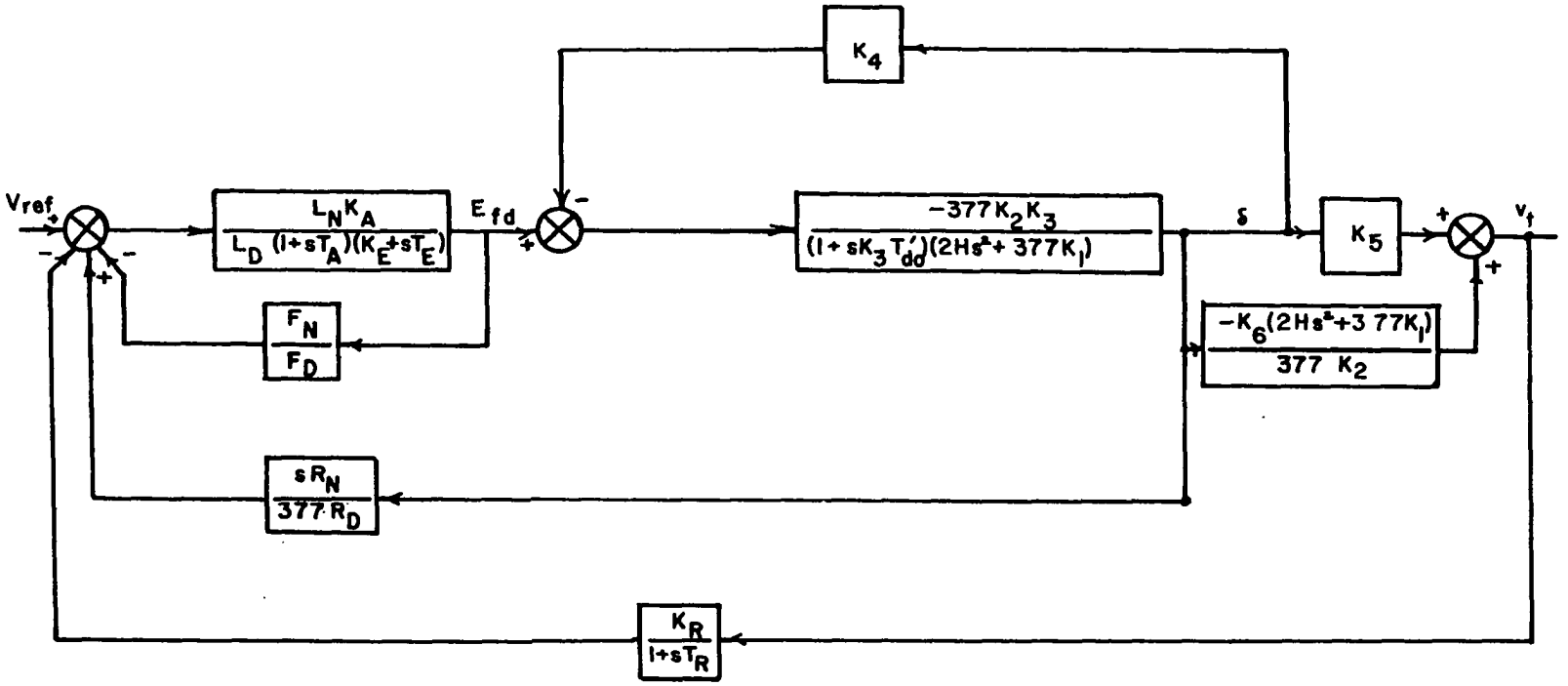

Figure 39. Block diagram of Figure 18 after moving the takeoff point for K_6

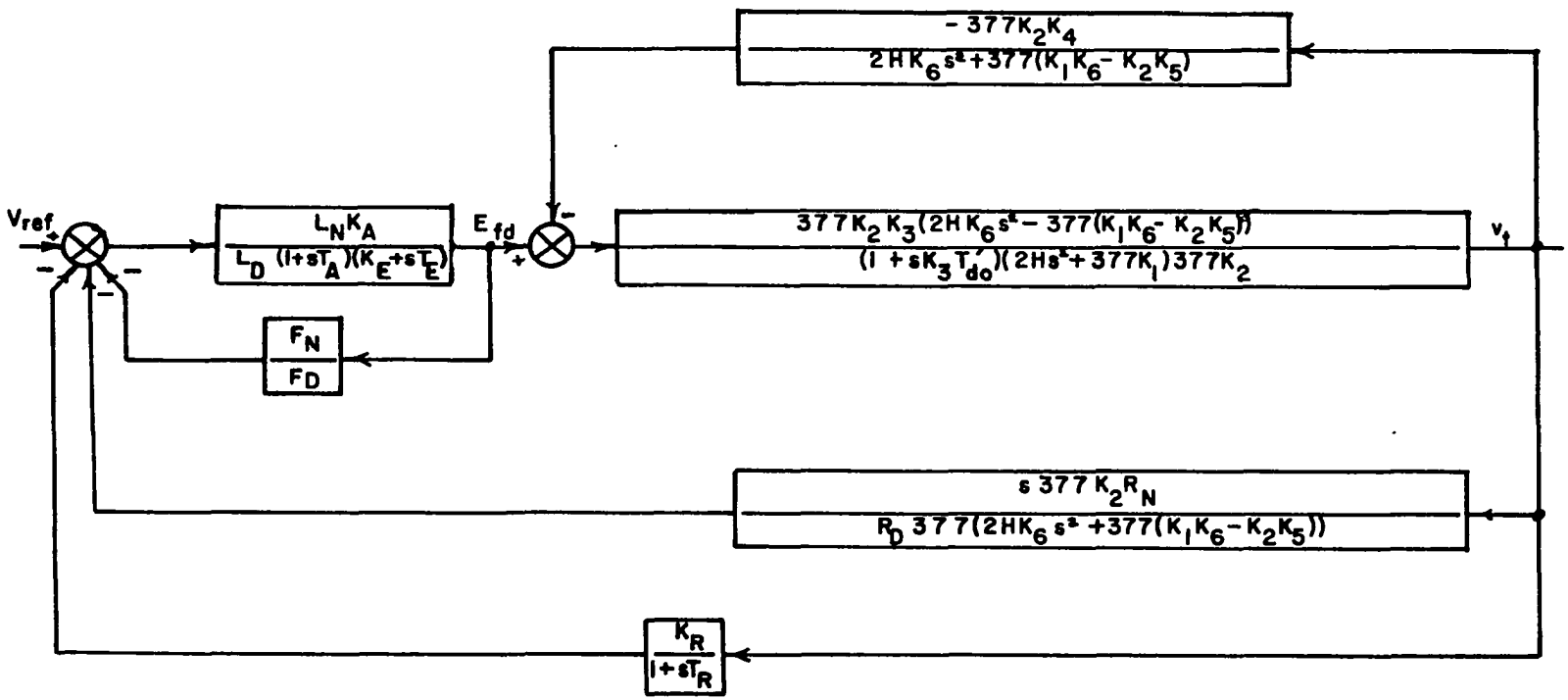

Figure 40. Reduced block diagram of synchronous machine and exciter in which torque-angle loop has not been closed

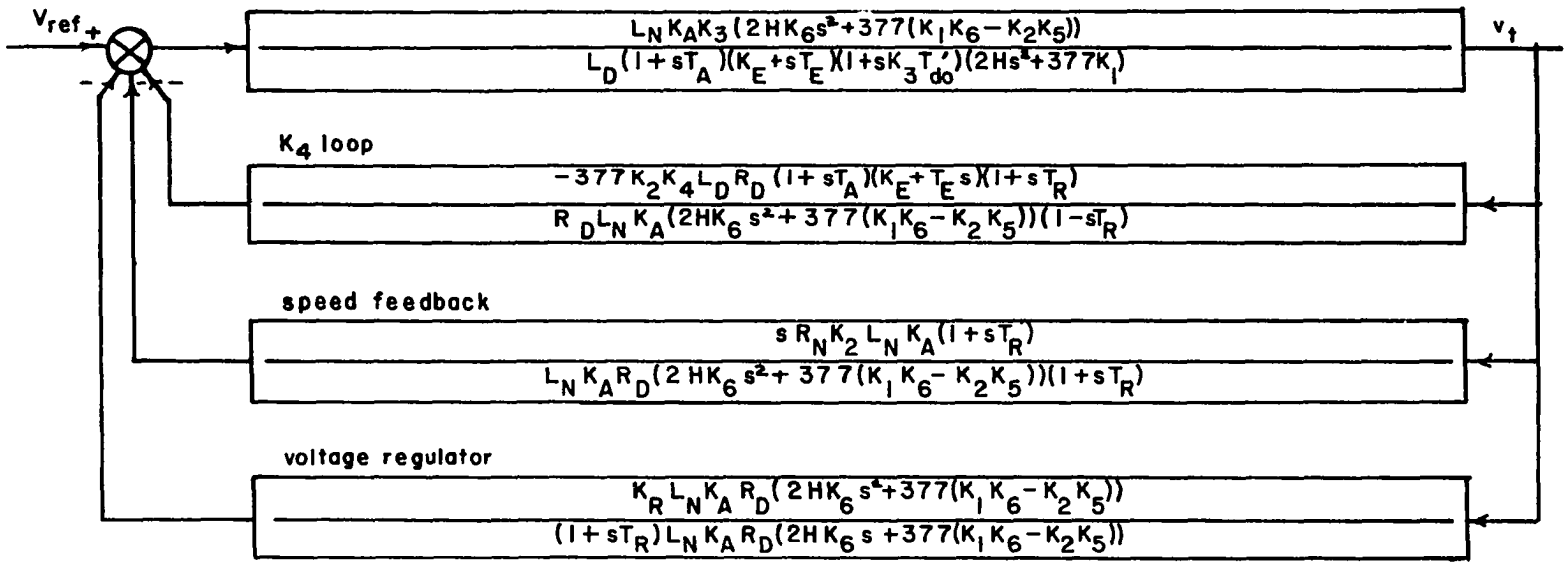

Figure 41. Block diagram after neglecting excitation rate feedback, moving the K_4 loop to the torque summing junction and placing all feedback loops over a common denominator

High-speed exciters make feedback through K_4 negligible and its effect may be neglected (31). T_R is also very small and for this analysis is set equal to zero. The resulting open-loop transfer function is then

$$\frac{K_3K_AL_N[K_RR_D\{2HK_6s^2+377(K_1K_6-K_2K_5)\}+sK_2R_N]}{L_DR_D(1+T_As)(K_E+T_Es)(1+sK_3T'_{do})(2Hs^2+377K_1)} \quad [46]$$

$$\text{Let } R_N/R_D = (Cs+D)/(As+B) \quad [47]$$

This choice of rate feedback transfer function numerator and denominator will result in a third order polynomial while the complex torque-angle loop poles result in a second order polynomial, thus after cancellation a first order zero will remain. Its location is left unspecified by representing it as (Es+F).

The numerator of Equation 46 is now equated to the product of the above zero and the desired complex zeros.

$$K_R(As+B)\{2HK_6s^2+377(K_1K_6-K_2K_5)\}+sK_2(Cs+D) = (Es+F)(2Hs^2+377K_1) \quad [48]$$

If the expressions are expanded and coefficients are equated, the result is

$$2HK_RK_6A = 2HE \quad [49a]$$

$$2HK_6K_RB + K_2C = F2H \quad [49b]$$

$$377(K_1K_6-K_2K_5)K_RA+K_2D = 377K_1E \quad [49c]$$

$$377(K_1K_6-K_2K_5)K_RB = F377K_1 \quad [49d]$$

This system is solved yielding

$$A = \frac{E}{K_R K_6} \qquad [50a]$$

$$B = \frac{K_1 F}{(K_1 K_6 - K_2 K_5) K_R} \qquad [50b]$$

$$C = \frac{-2HFK_5}{(K_1 K_6 - K_2 K_5)} \qquad [50c]$$

$$D = \frac{377EK_5}{K_6} \qquad [50d]$$

If the zero location is fixed at -5 and E = 1, F = 5, the resulting values for these parameters for various tie line impedances and machine loadings are shown in Table 4. The root-locus resulting from this development is shown in Figure 42.

Table 4. Torque-angle loop cancellation using speed feedback

	P .333 Q .0	P .666 Q .0	P 1.0 Q .0	P .333 Q .206	P .666 Q .419	P 1.0 Q .62	P .333 Q-.206	P .666 Q-.419
R_E =.02 X_E=j.4								
A	1.576	2.118	3.04	1.47	1.58	1.68	2.10	-7.38
B	4.225	5.043	8.932	4.91	4.69	4.84	4.41	-3.49
C	5.740	4.240	2.99	5.27	4.35	3.76	5.13	7.82
D	-472.9	-607.1	-344.1	-349.4	-471.8	-506.4	-679.4	-2173.6
R_E=0 X_E=j.4								
A	1.57	2.13	3.13	1.46	1.57	1.68	2.11	-6.29
B	4.26	5.24	10.55	4.94	4.74	4.92	4.54	-2.29
C	5.76	4.19	2.46	5.33	4.39	3.78	5.06	8.66
D	-468.1	-572.0	-230.4	-348.9	-464.2	-488.8	-655.0	-2106.6
R_E=.2 X_E=j.4								
A	1.58	2.01	2.57	1.48	1.59	1.67	2.01	-93.6
B	4.00	4.03	4.80	4.71	4.35	4.31	3.68	116.1
C	5.51	4.36	3.76	4.70	3.99	3.48	5.48	7.96
D	-480.7	-788.8	-898.9	-329.7	-488.4	-575.8	-802.8	-2108.2
R_E=1 X_E=j1								
A	1.31	1.54	1.85	1.22	1.28	1.31	2.04	--
B	4.51	4.28	4.62	4.99	4.76	4.65	4.31	--
C	5.14	4.94	4.47	3.10	3.06	2.84	7.95	--
D	-199.2	-355.9	-433.0	-105.0	-161.7	-198.2	-541.0	--

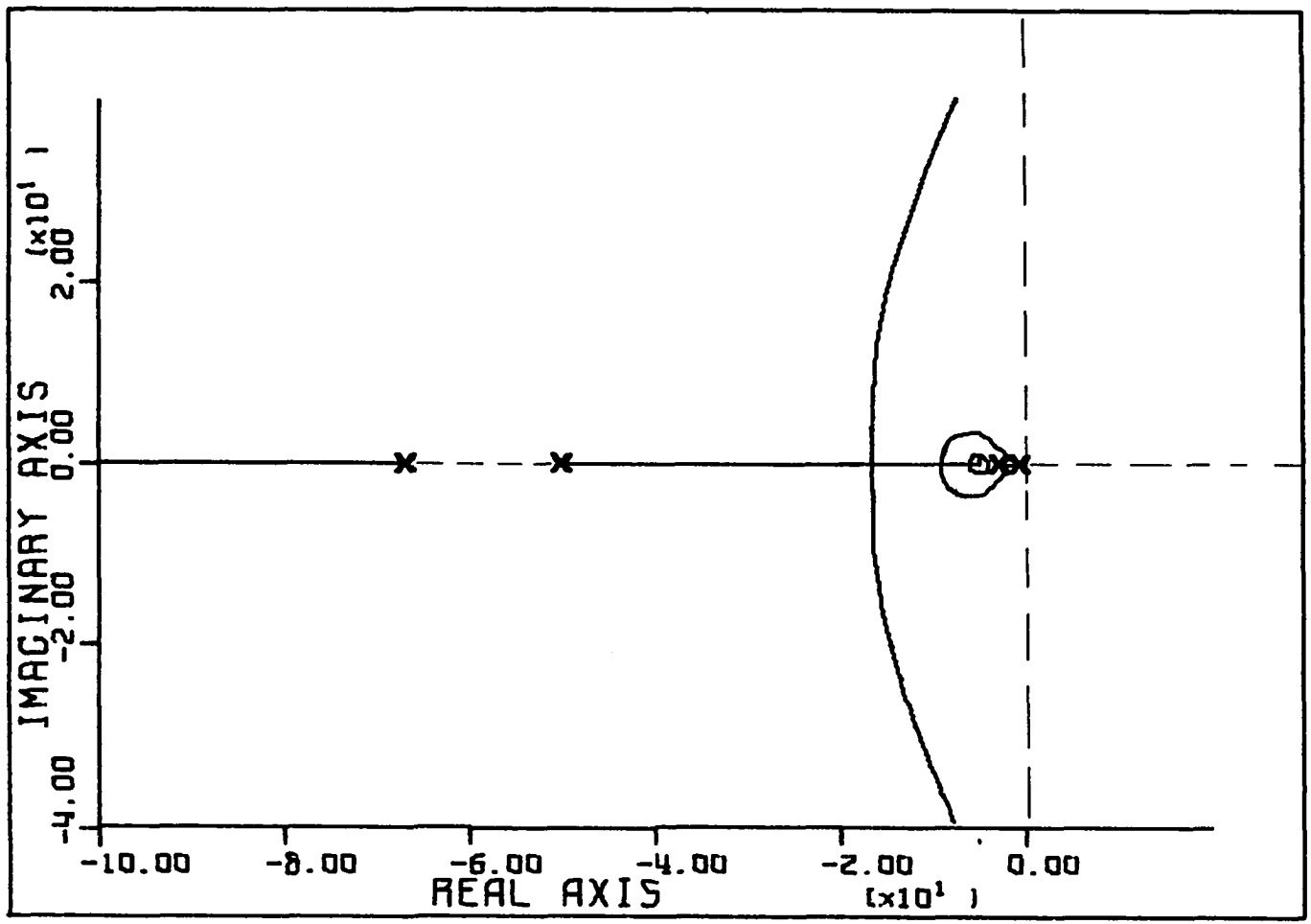

Figure 42. Root-locus showing results of torque-angle loop cancellation

V. ANALOG COMPUTER RESULTS

The ideas developed in the previous section using linear analysis techniques are now studied using a nonlinear analog computer model of a synchronous machine connected to an infinite bus (see Appendix E). The effects of the various compensation schemes are explored by making the following changes in operating conditions of the synchronous machine. Initially the machine is operated with V_{ref} set as in Base Case 2. T_m is increased from zero to full load (0 to 3 pu). Then T_m is increased to 3.3 pu and returned to 3.0 pu. Next V_{ref} is increased and decreased by 5% and finally, T_m is returned to zero.

The strip chart recorder has been operated so that the extreme right and left portions of the graphs indicate zero levels. Variables are given on the left side of the strip charts and recorder gains in volts-per-line are given to the right. The positive direction of all variables is upward. Each tick on the bottom edge of the strip chart pointing upward represents one second of analog computer operation. The auxiliary time markings pointing downward represent one second of operation of the synchronous machine. The analog computer was operated in the fast-second mode, thus one second of synchronous machine operation is simulated by 10 seconds of analog computer operation.

The results shown in the following figures represent a nearly optimum choice of parameter values for each case subject to the constraint that the excitation system amplifier gain remain at 400 pu.

Figure 43 shows the uncompensated system. A 10% increase in mechanical torque results in growing oscillations and an unstable system. Thus

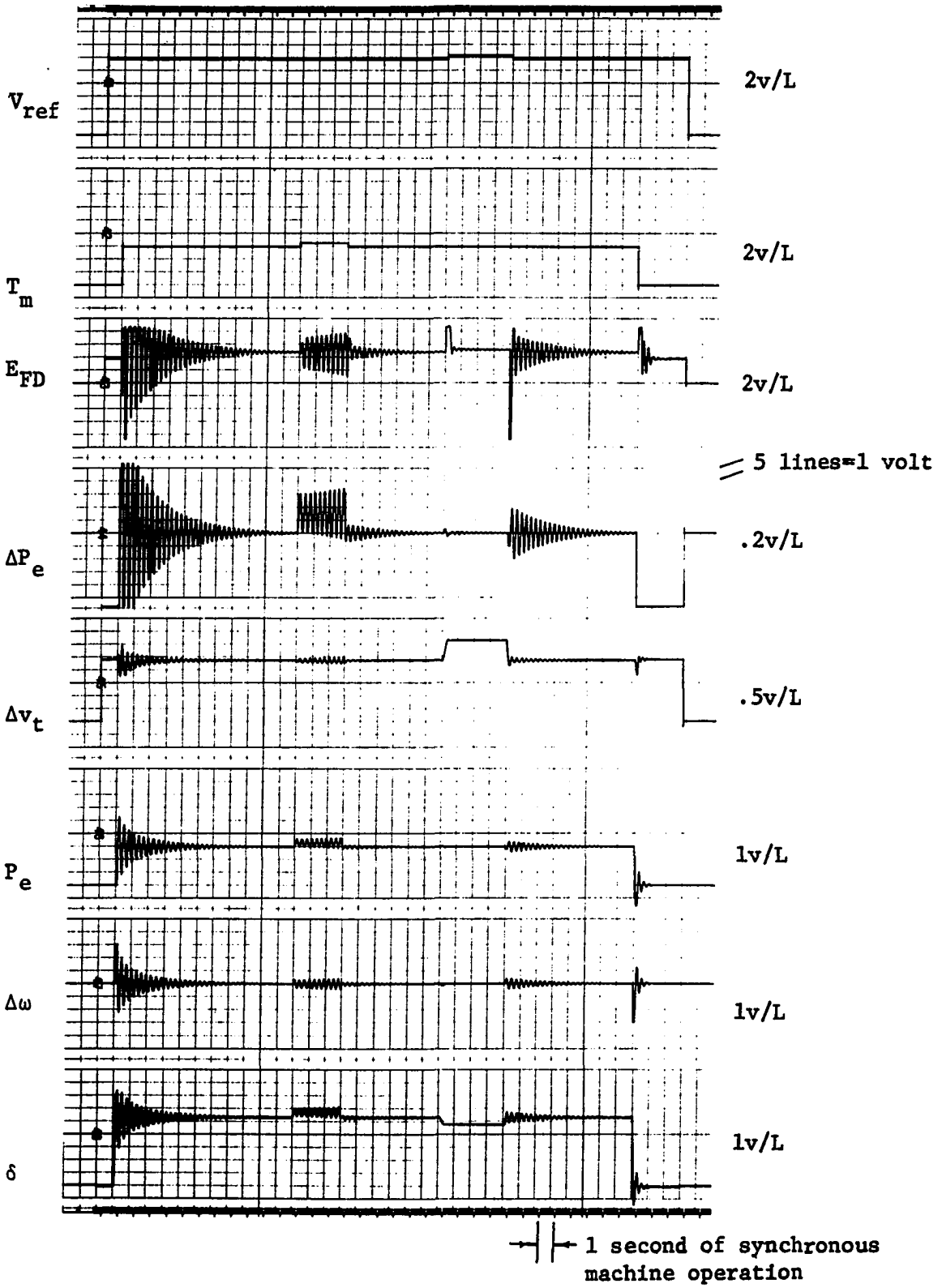

Figure 43. Uncompensated system

the machine is operating near its stability limit under the conditions of Base Case 2. The frequency of oscillation is about 21 radians/sec.

Figure 44 shows the results of adding excitation system rate feed back. This control loop provides a considerable improvement in system performance over the uncompensated system. However, as predicted by the linear model, the response is dominated by a pole near the origin resulting in a long settling time in Δv_t. The field voltage reacts very slowly to changes in both torque and voltage references and this long time constant is reflected in both the terminal voltage Δv_t and machine angle δ.

Figure 45 shows the results of adding a power system stabilizer. The damping of this case is considerably better than that provided by excitation system rate feedback. The initial overshoot in tie line power, ΔP_e, resulting from the 10% increase in the torque reference is almost the same in both cases. The response to a 5% increase in voltage reference results in a much smaller overshoot in the case of the power system stabilizer and the settling time is also greatly improved.

Figures 46a, 46b and 46c show the effects of placing a bridged-T filter in the regulator loop of a synchronous machine tuned to 21, 23 and 19.7 radians per second, respectively.

Linear analysis of the previous section suggested a high degree of sensitivity to the exact frequency to which the bridged-T was tuned. This result is not confirmed here. The three cases, one tuned to the natural frequency of the machine, one above this frequency and one below, are very similar.

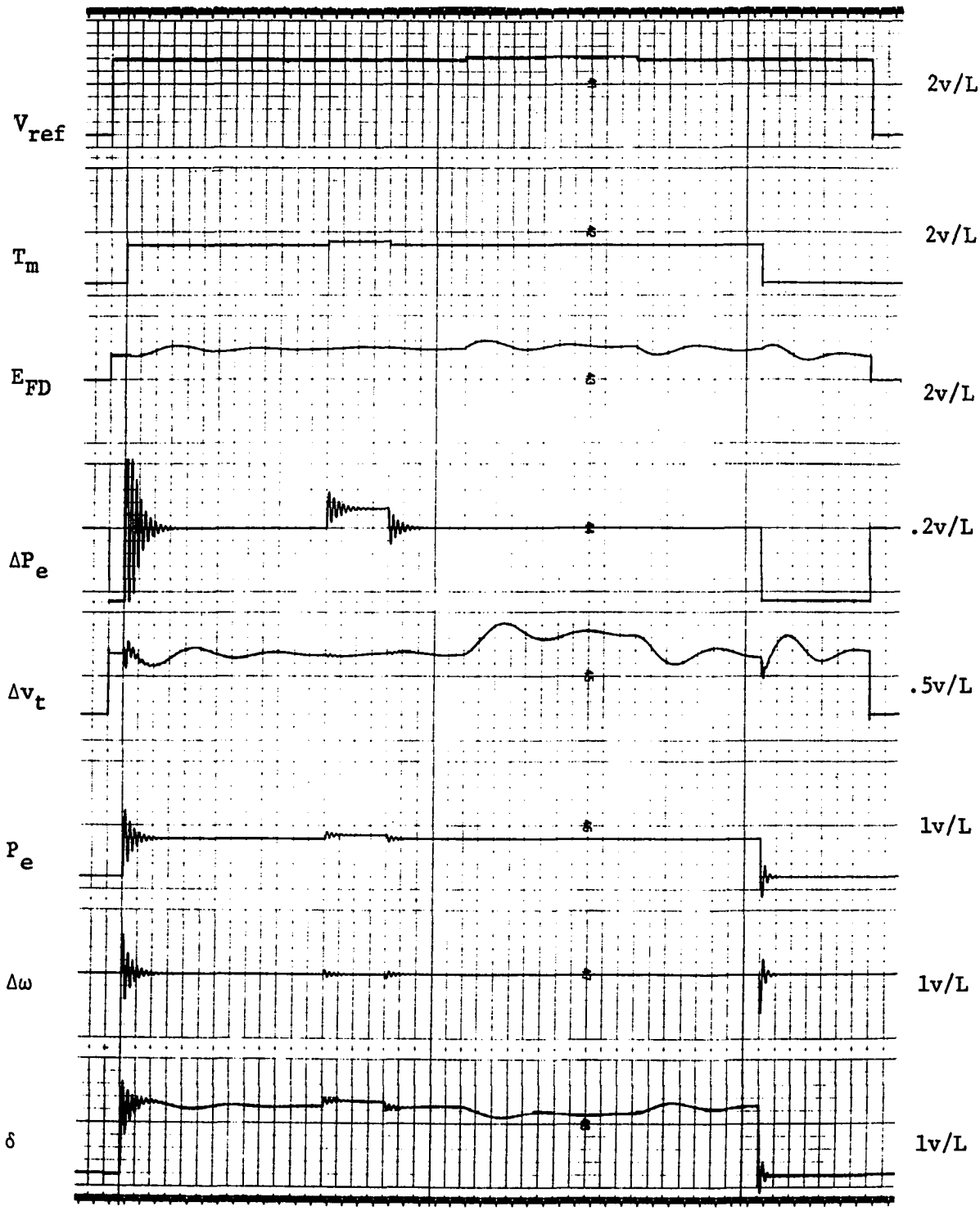

Figure 44. Excitation system rate feedback with K_F=.04 pu and T_F=.05 sec

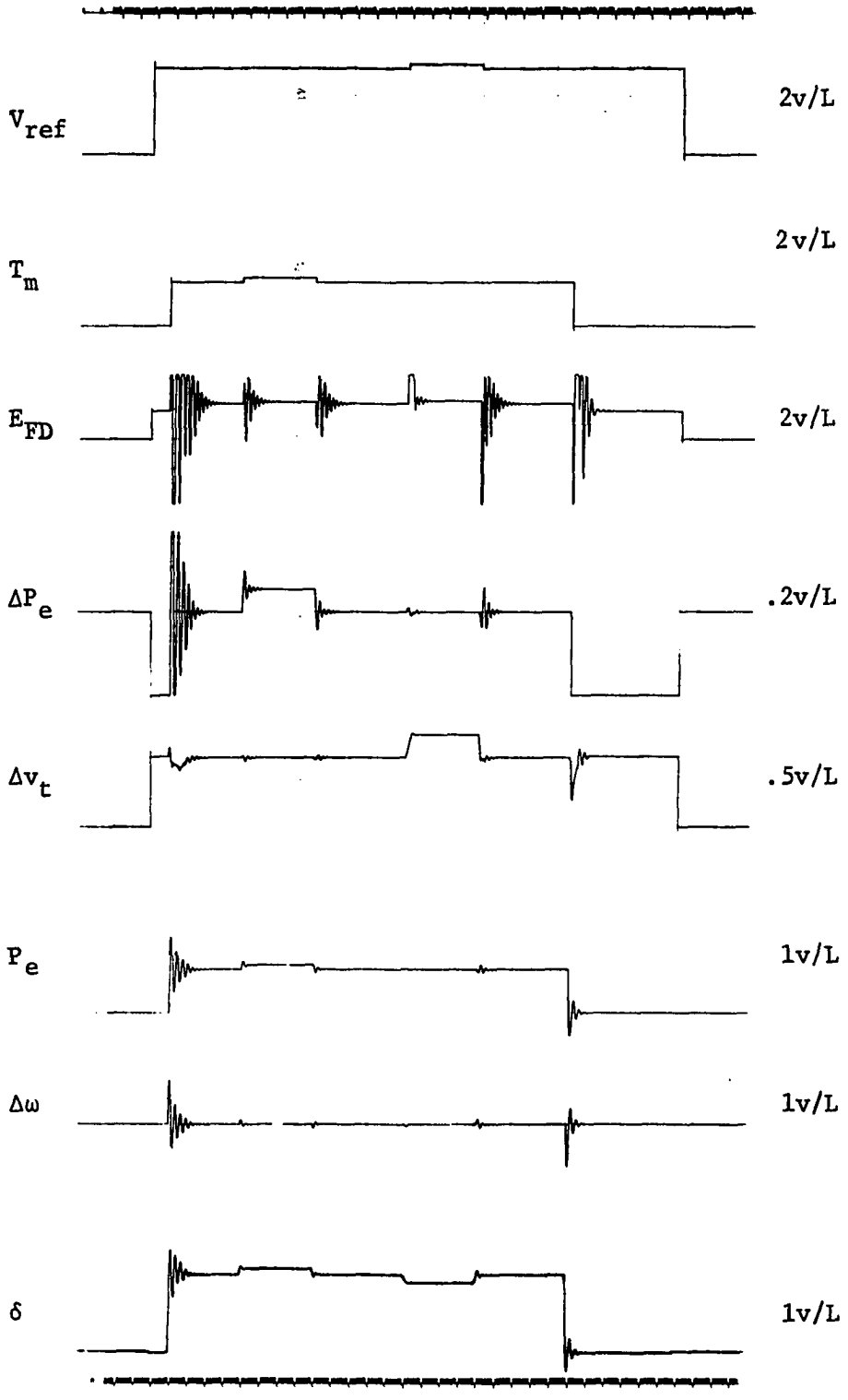

Figure 45. Power system stabilizer with T=3 sec, T_1=.2 sec, T_2=.05 sec and GRN=0.5 pu

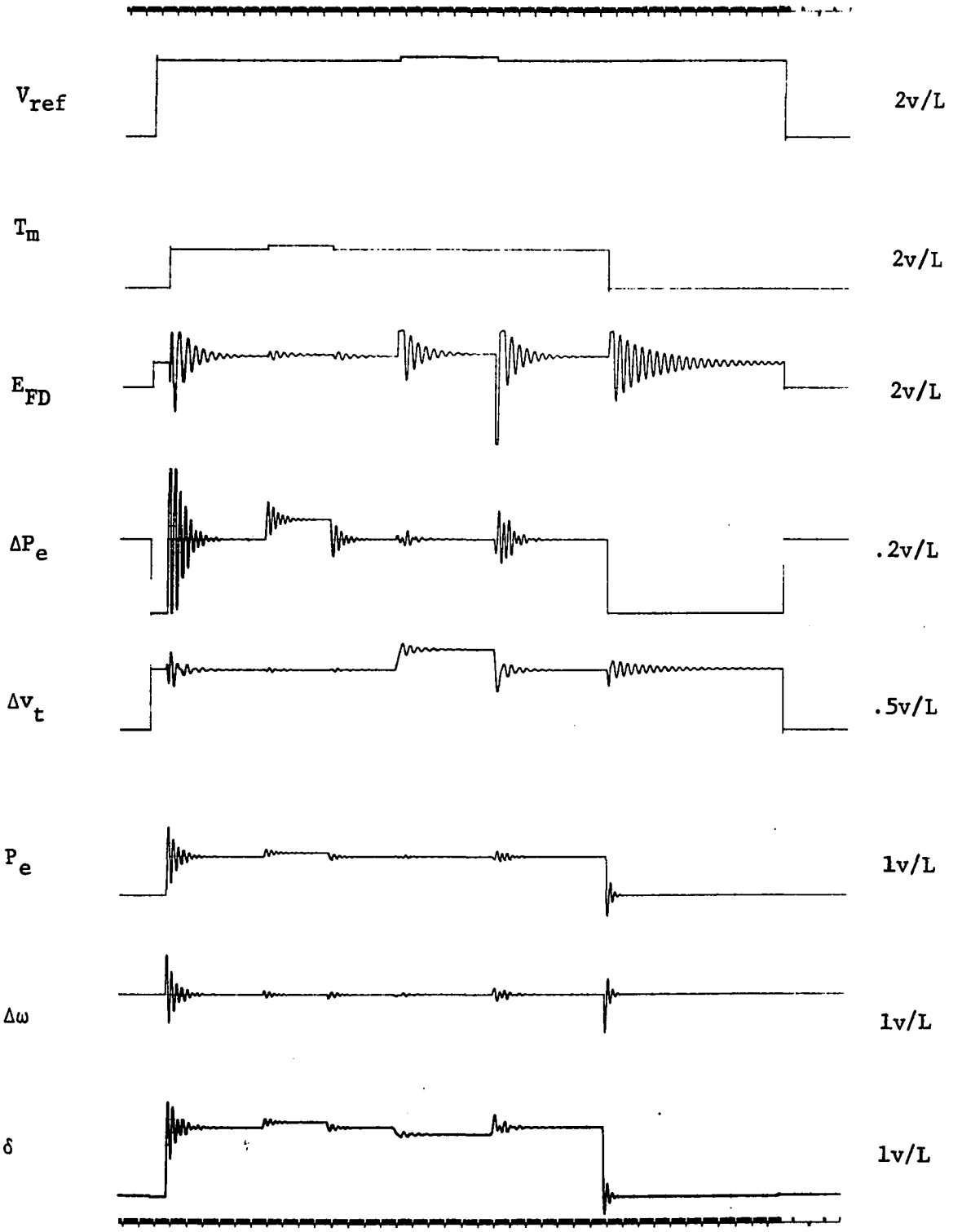

Figure 46a. Bridged-T filter placed in regulator loop with ω_o=21 rad/sec, r=.1 and n=2

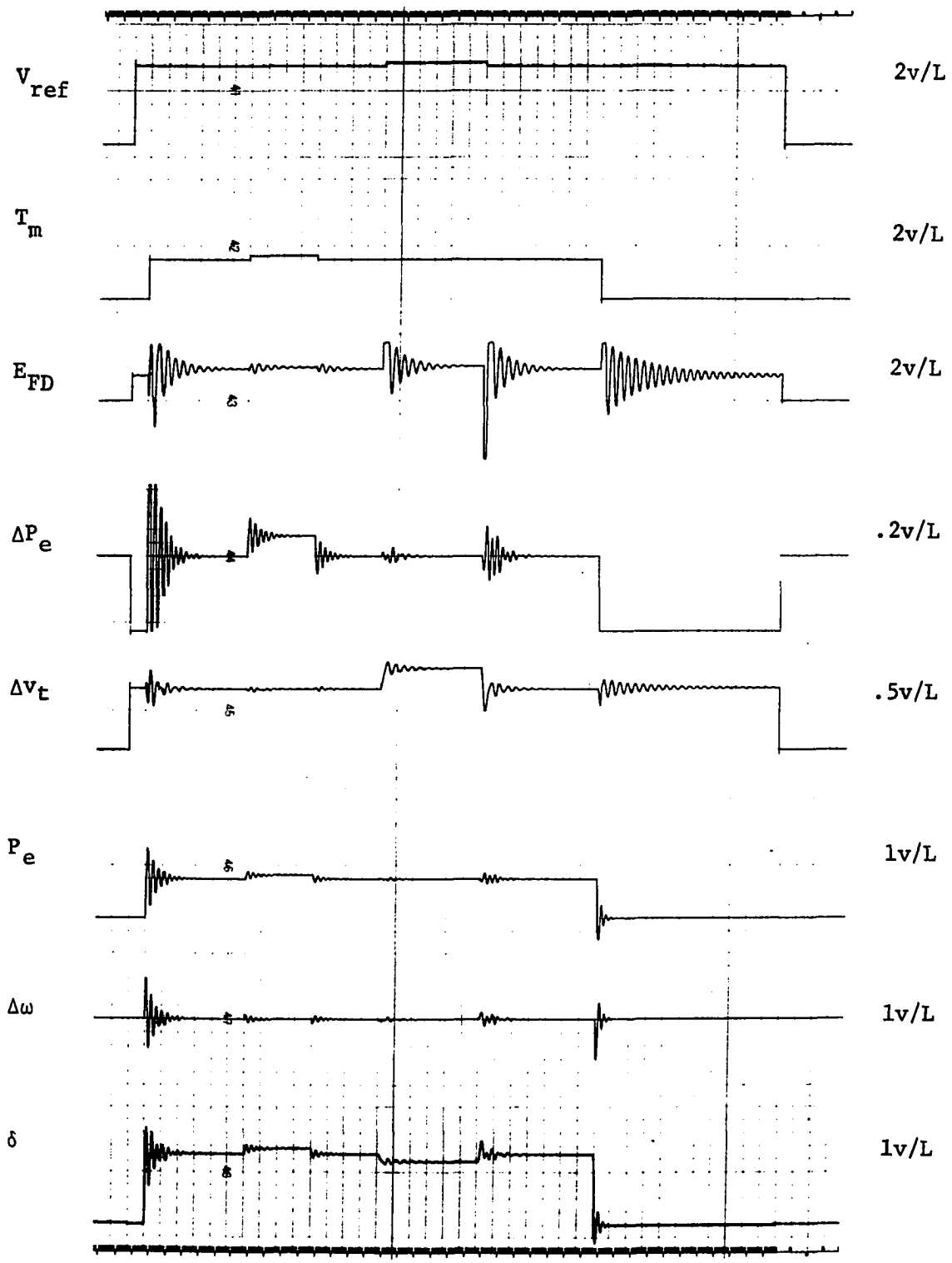

Figure 46b. Bridged-T filter placed in regulator loop with ω_o=23 rad/sec, r=.1 and n=2

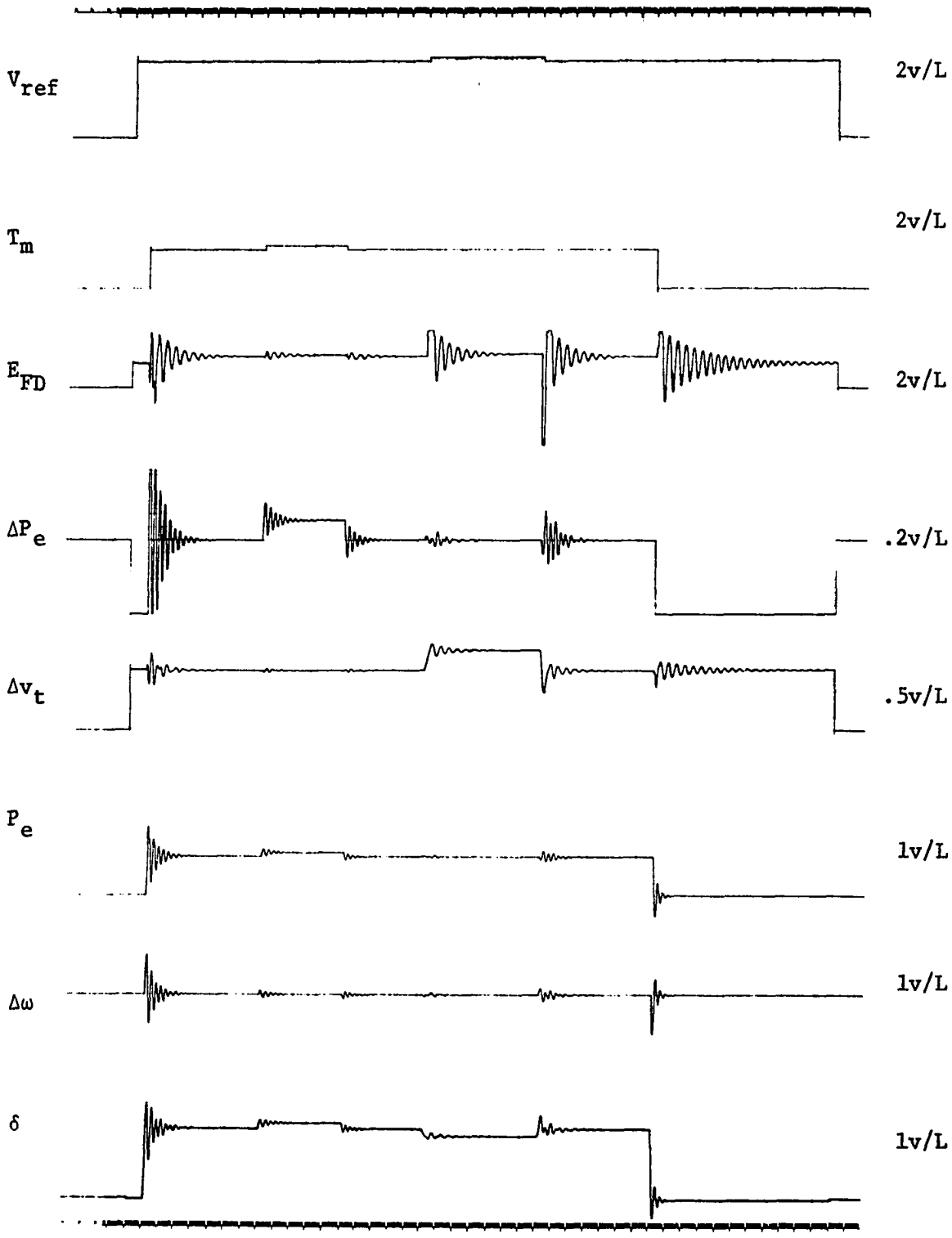

Figure 46c. Bridged-T filter placed in regulator loop with ω_o=19.7 rad/sec, r=.1 and n=2

If the filter is tuned to a higher frequency and if the attenuation at the notch frequency is decreased as shown in Figure 46d, the result is a more oscillatory response to a change in torque and a less oscillatory response to a change in reference voltage.

Figure 47 shows the results of placing a bridged-T filter in the regulator feedback loop, a two-stage lead-lag network in the exciter feedforward loop and feeding an auxiliary signal proportional to rotor speed deviation into the excitation system comparator.

Comparison of Figures 45 and 47 shows that the tie line power resulting from a change in torque reference in the latter has less overshoot and is better damped than in the former. However, the reverse is true for a change in voltage reference. The settling time and damping of the terminal voltage exhibited by both are quite satisfactory.

Figure 48 shows the results of placing a transfer function in the speed deviation feedback path designed to cancel the torque-angle loop poles and the field pole. The initial overshoot is somewhat smaller than the previous cases and the oscillation is quickly damped out. Note that the polarity of the auxiliary signal for this network is opposite to those previously considered. That is, an increase in $\Delta\omega$ results in a decrease in field voltage, thus δ is allowed to make large excursions. (Note the scale change on δ in Figures 48 and 49.) The settling time for this network is very long, indicating that the pole near the origin has not been effectively cancelled.

If excitation rate feedback is added to the above configuration as suggested by the root-locus diagram of Figure 38, Figure 49 results.

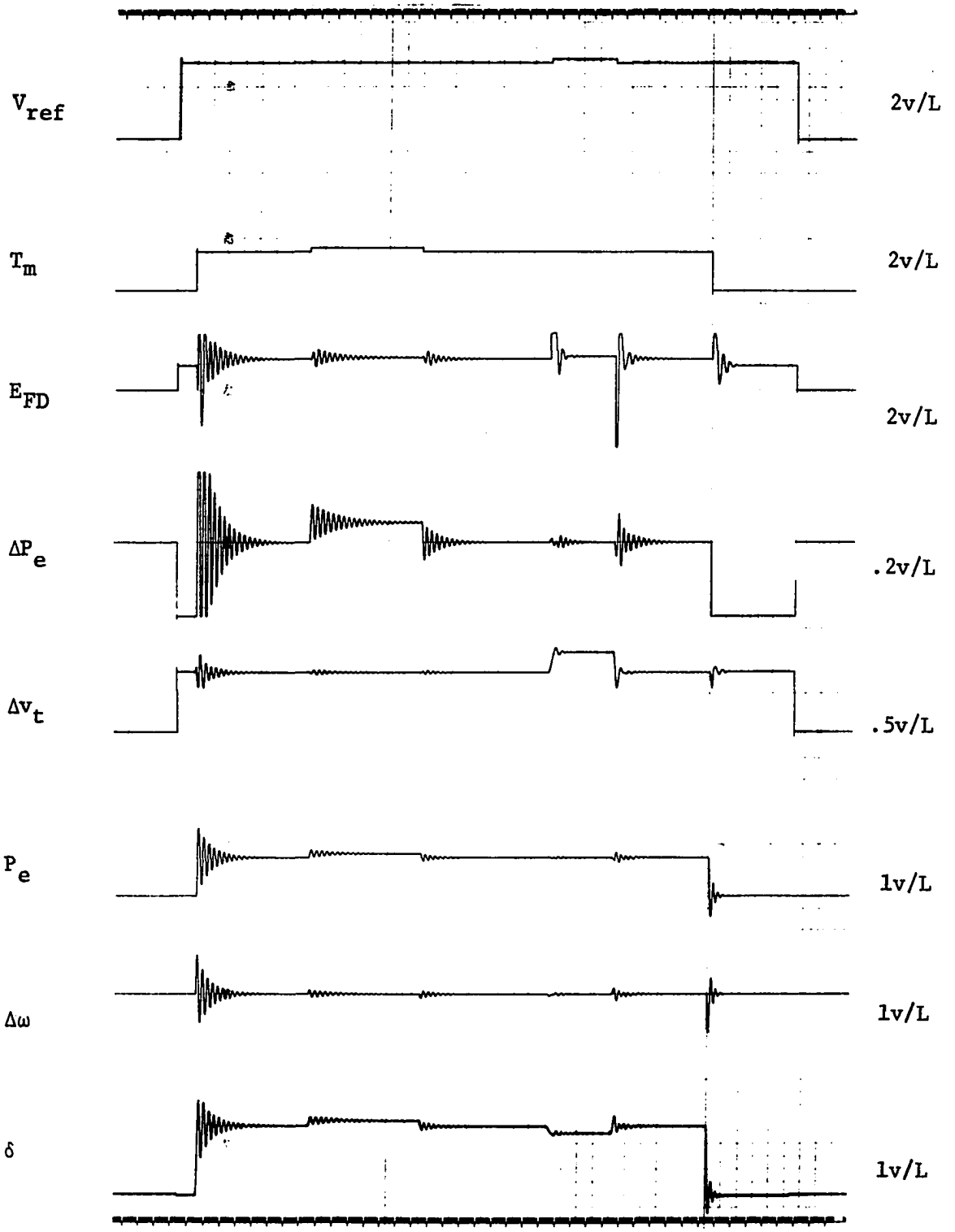

Figure 46d. Bridged-T filter placed in regulator loop with ω_o=26 rad/sec, r=.4 and n=2

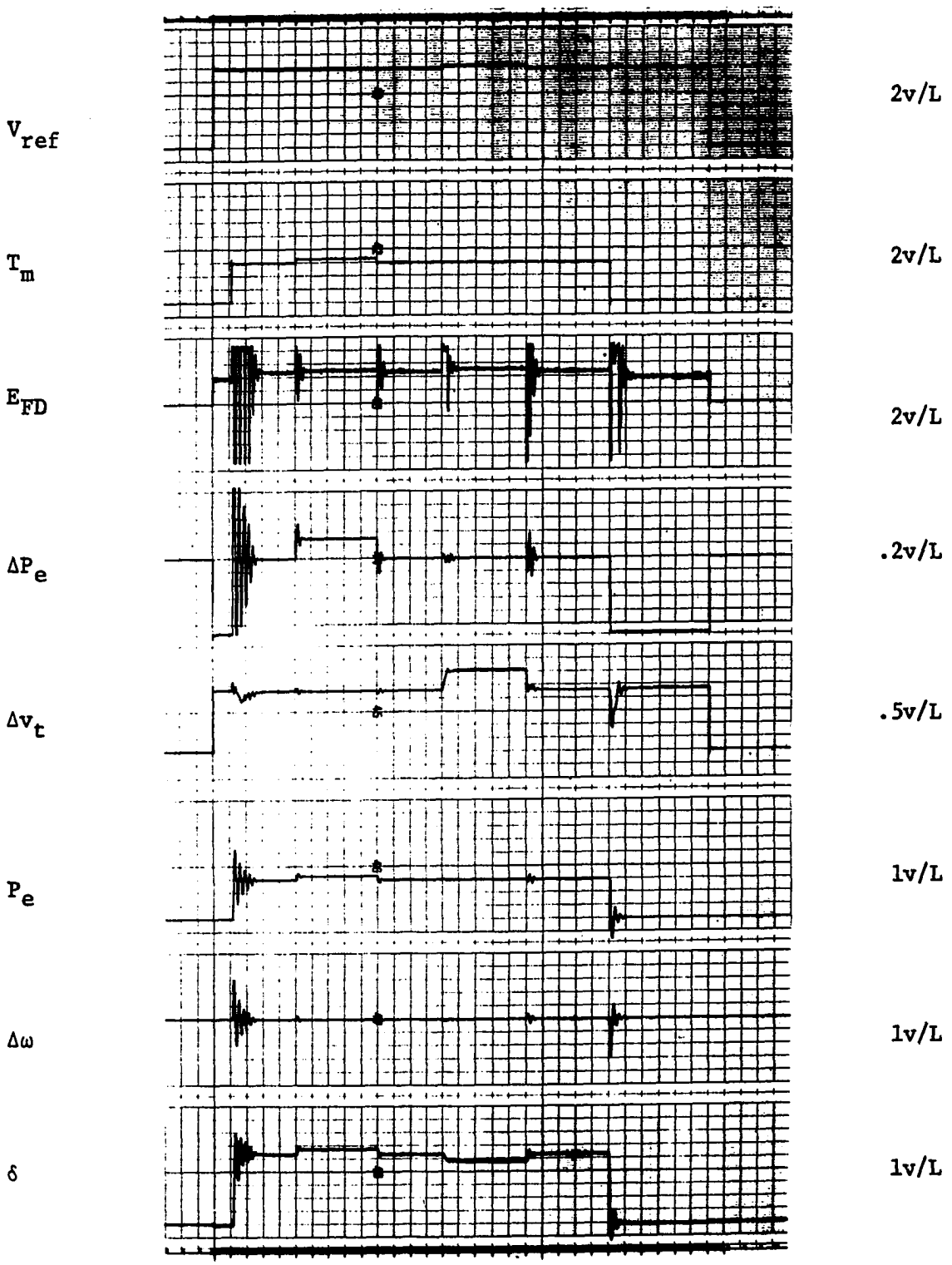

Figure 47. Bridged-T in regulator loop, lead-lag network in exciter forward loop and speed feedback with ω_0=21 rad/sec, r=.1, n=2, T_1=.2 sec, T_2=.05 sec and GRN=0.1571 pu

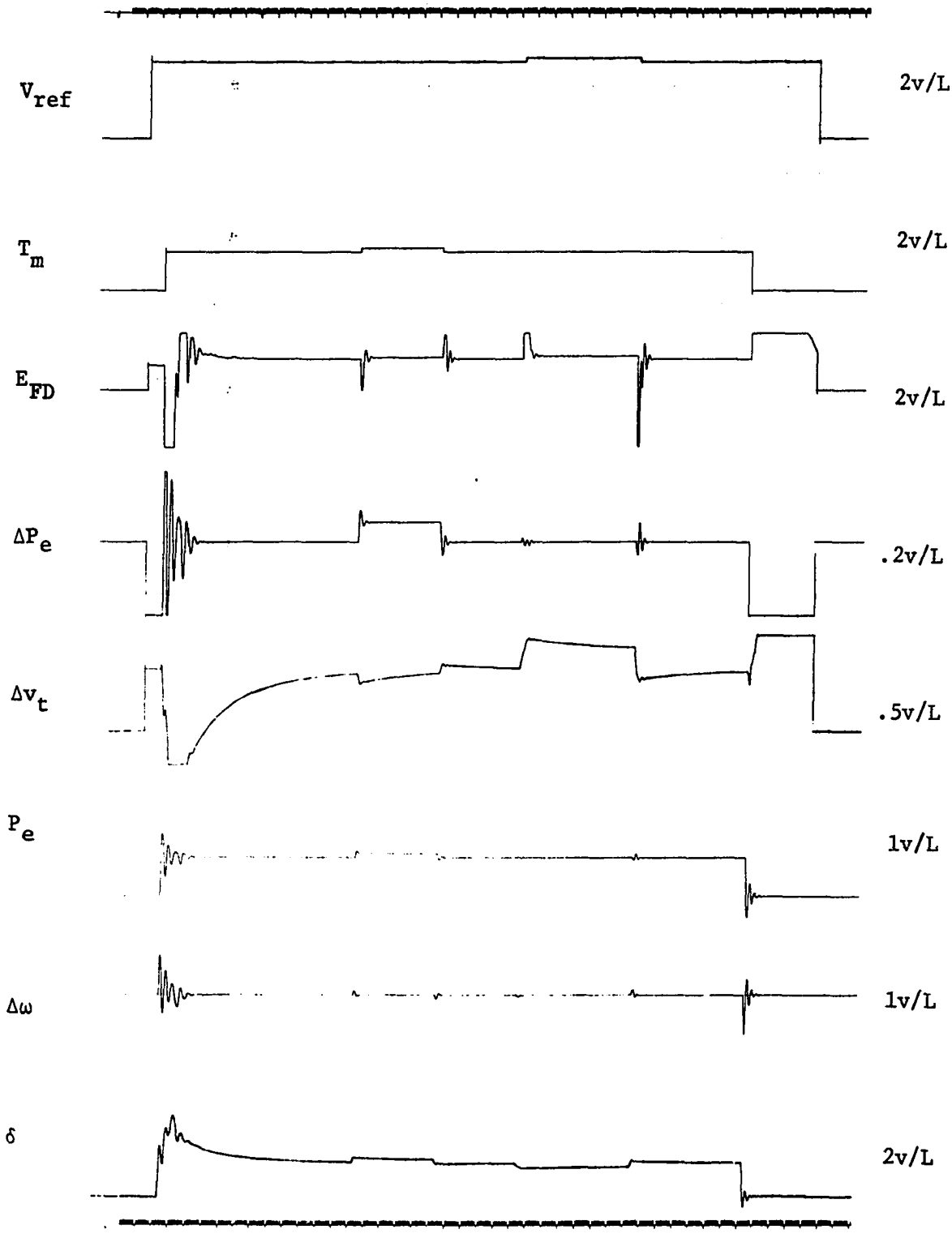

Figure 48. Speed feedback used to cancel torque-angle loop poles and field pole with D/B=80 and B/A=0.164

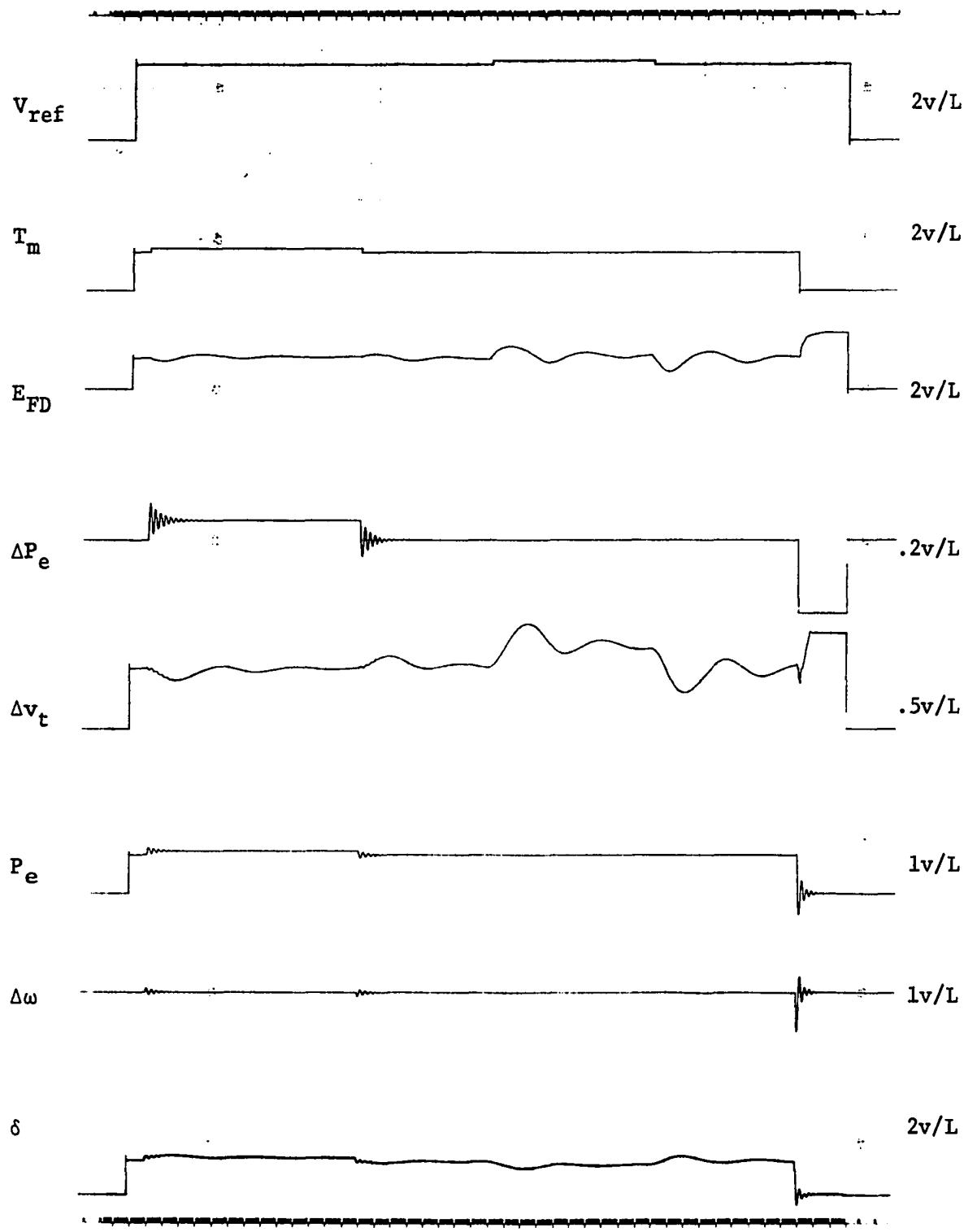

Figure 49. Speed feedback used to cancel torque-angle loop poles and field pole with excitation rate feedback and T_F=0.05 sec, K_F=0.00406 pu, D/B=80 and B/A=0.164 pu

An unstable condition resulted when the T_m was switched from zero to 3 pu with the above compensation network inserted. Therefore, the machine was started and full load placed upon it with the compensation network removed. The network was then switched in and a set of changes in reference levels identical to those described previously was performed, starting with a 10% increase in mechanical torque. The results are comparable to those produced by excitation system rate feedback.

Figure 50 shows the results of placing a transfer function in the speed feedback loop designed to cancel the torque-angle loop poles only. A 10% increase in torque reference results in an overshoot which is less than that observed for either the power system stabilizer or the combination of bridged-T filter, lead-lag network and speed feedback. The overshoot resulting from a 5% increase in V_{ref} is slightly greater than that observed for either of the above systems. As in Figure 48, which shows an attempt to cancel three of the machine poles, the polarity of the speed feedback causes a decrease in E_{FD} for an increase in $\Delta\omega$ leading to excessive excursions in δ.

The following figures show the operation of the synchronous machine against a bus whose voltage is being modulated to produce a sinusoidal variation between 1.02 and 0.98 pu peak value at an adjustable frequency. For the studies involving a modulated bus voltage the generator is operated under conditions of Base Case 1.

Figures 51 and 52 show the performance of the machine with the bridged-T network in the regulator loop, a two-stage lead-lag network in the exciter forward loop and speed feedback through a pure gain. Figures 53 and 54 show the performance of a power system stabilizer.

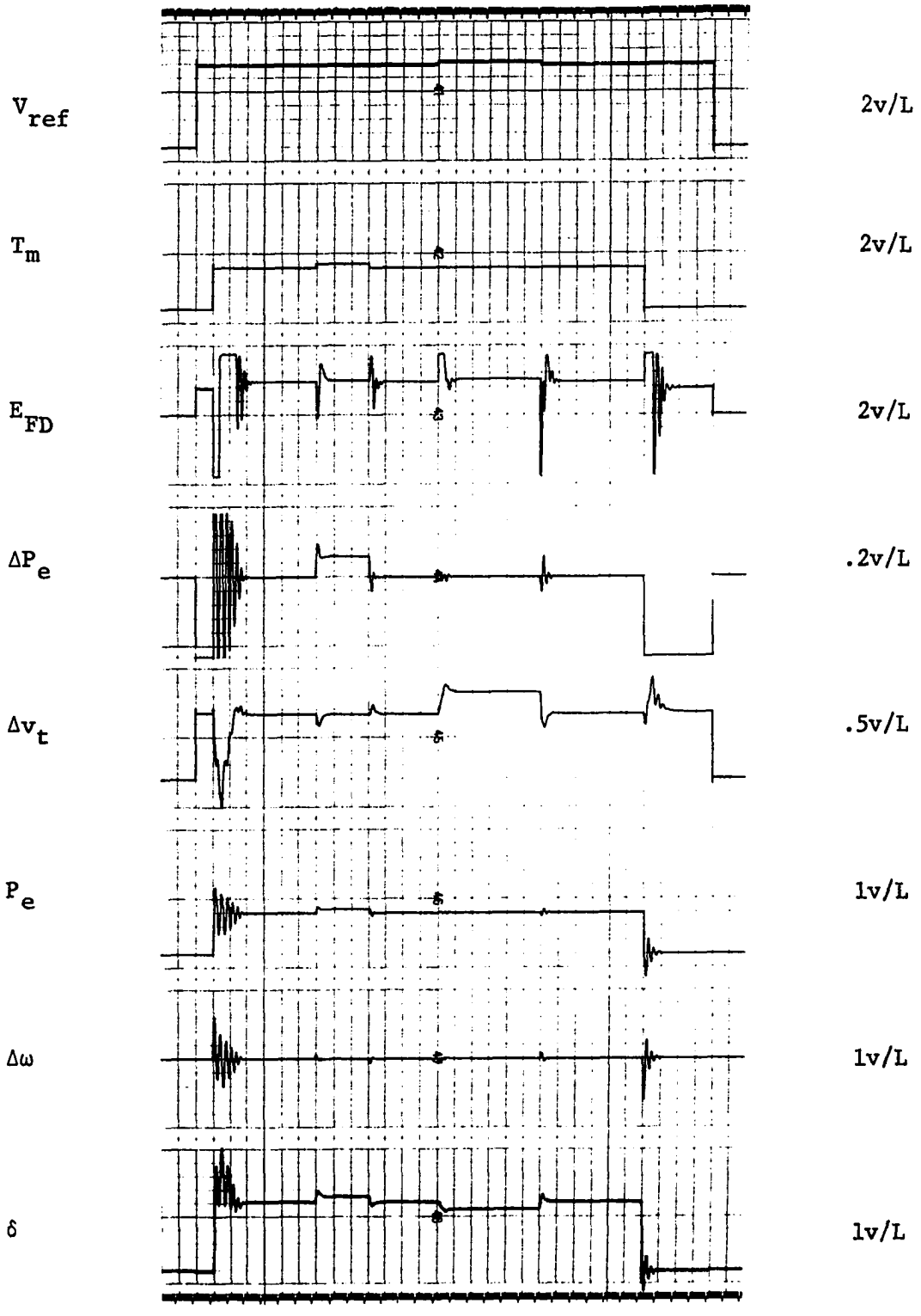

Figure 50. Speed feedback used to cancel torque-angle loop poles with B/A=2.88, C/A=0.845 and B/A+|D|/C=120.0

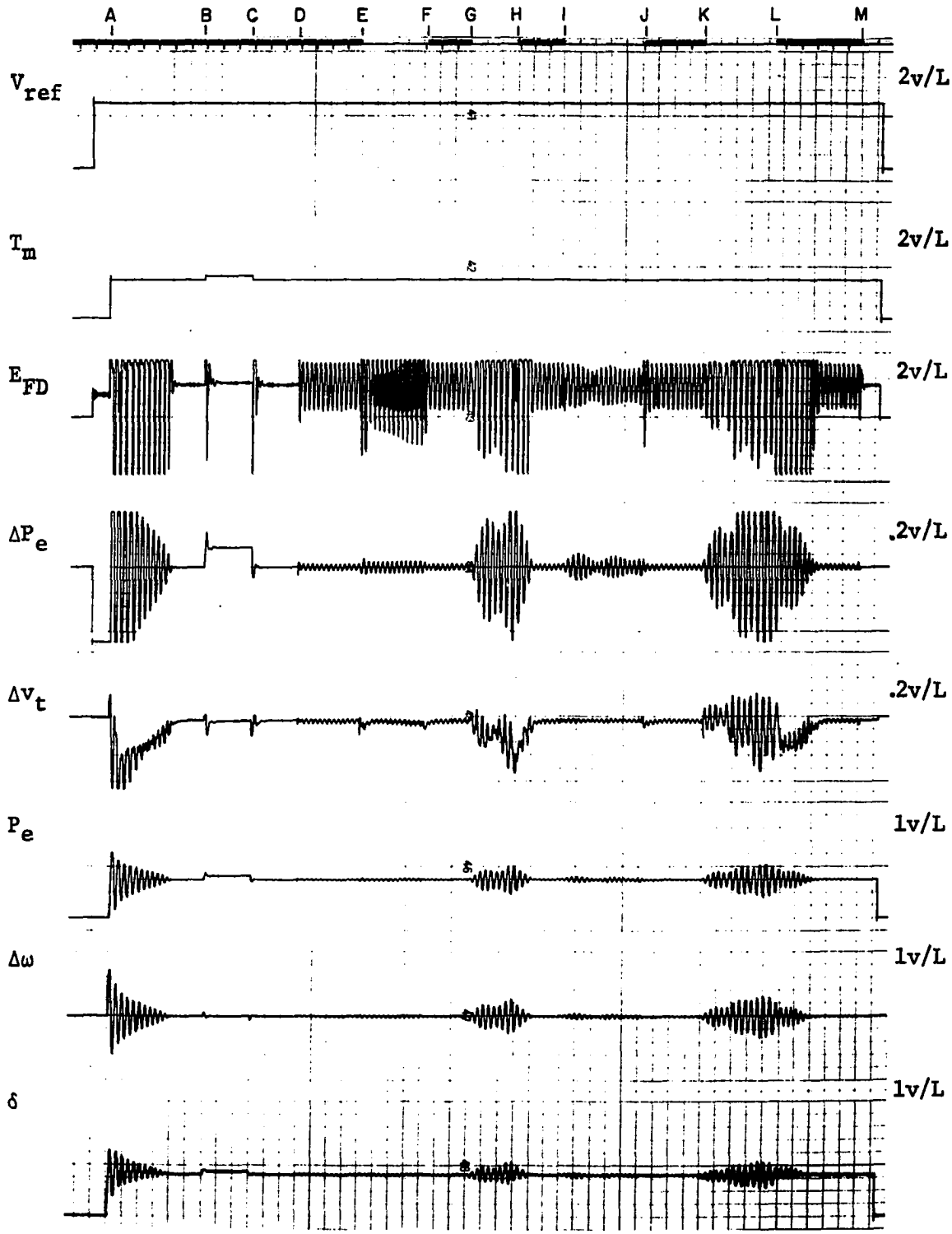

Figure 51. Synchronous machine operating against an infinite bus whose voltage is being modulated at the natural frequency of the machine with bridged-T, lead-lag and speed compensation

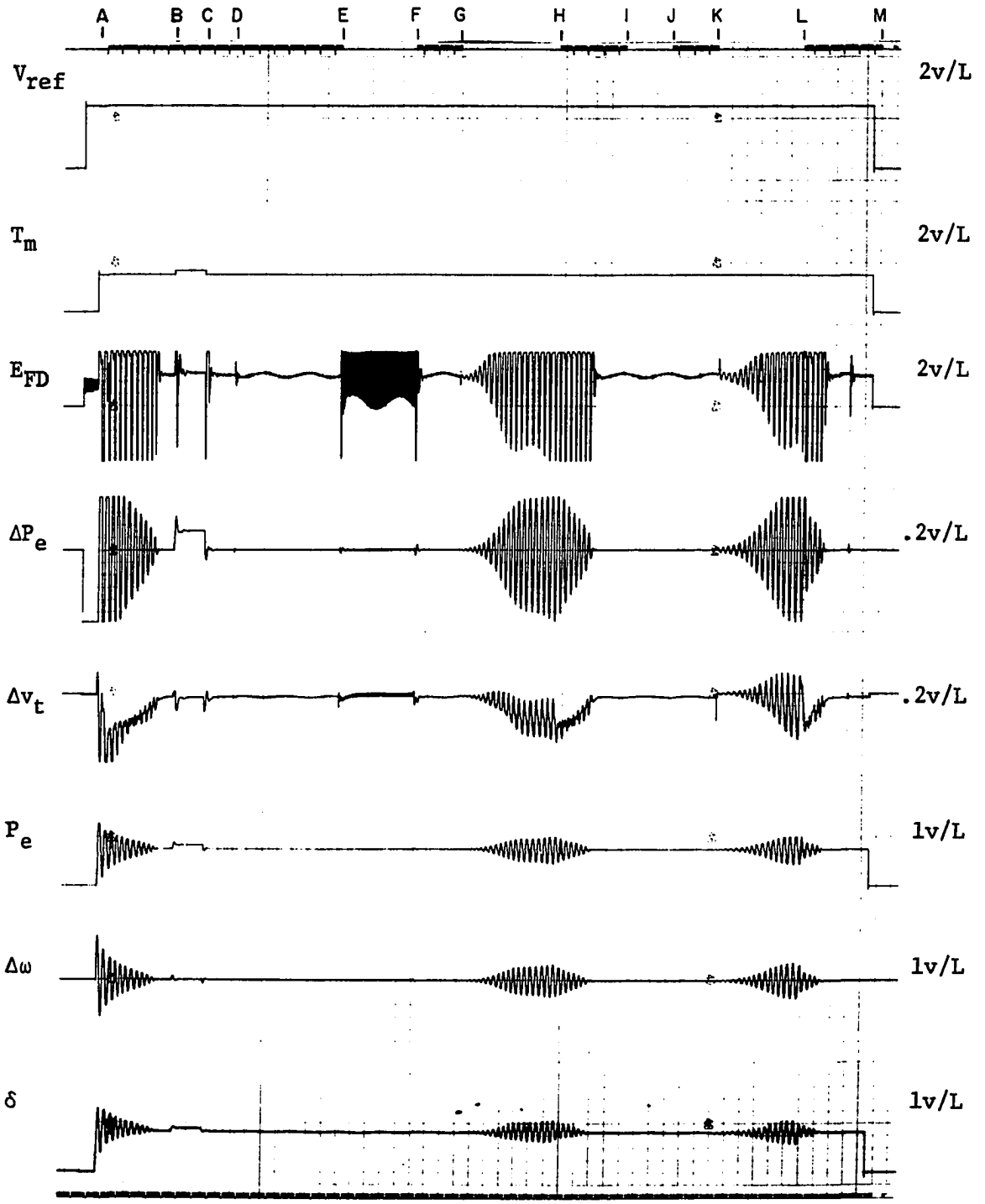

Figure 52. Synchronous machine operating against an infinite bus whose voltage is being modulated at one-tenth the natural frequency of the machine with bridged-T, lead-lag and speed compensation

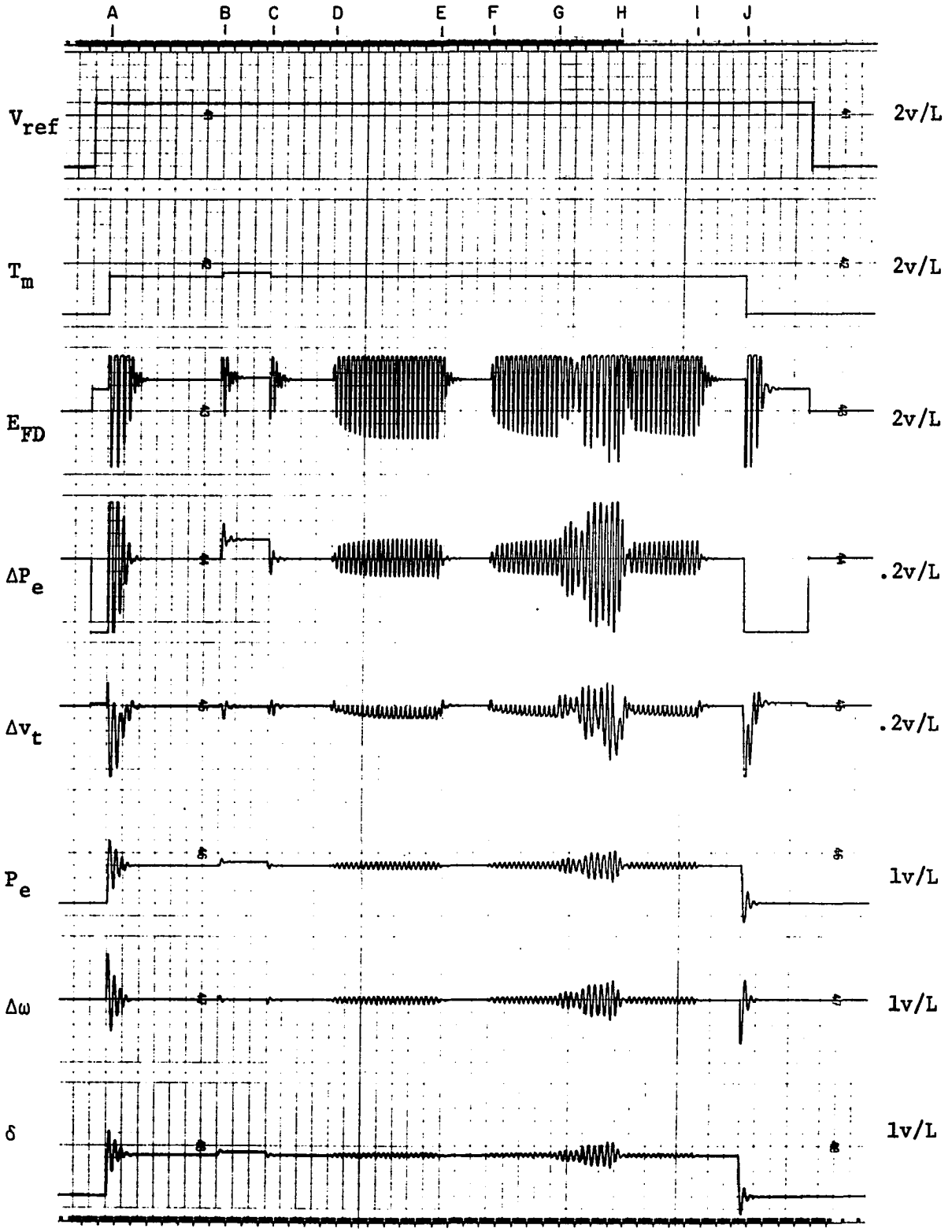

Figure 53. Synchronous machine operating against an infinite bus whose voltage is being modulated at the natural frequency of the machine with power system stabilizer compensation

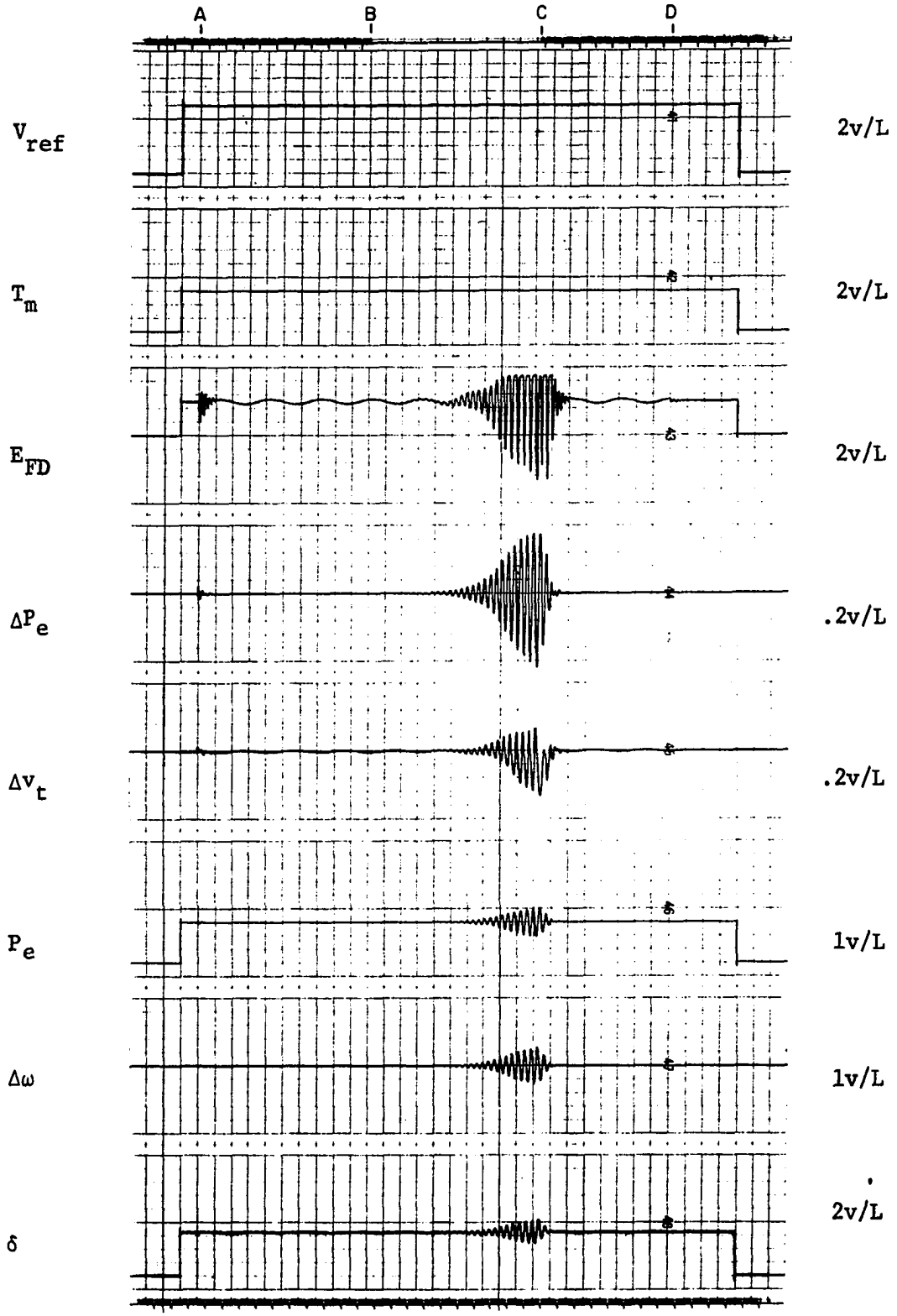

Figure 54. Synchronous machine operating against an infinite bus whose voltage is being modulated at one-tenth the natural frequency of the machine with power system stabilizer compensation

The optimized parameters used for the compensation networks in the first two figures are

T_1 = 0.2 sec r = 0.931

T_2 = 0.05 sec n = 2.49

GRN = 0.3709 pu ω_o = 23.3 rad/sec

and the parameters for the power system stabilizer are

T = 3 sec T_2 = 0.05 sec

T_1 = 0.2 sec GRN = .7714 pu

In Figure 51 the bus voltage was modulated at a frequency equal to the natural frequency of the machine, ω_o = 21 rad/sec. To show how machine performance was affected by a change in operating conditions and the compensation network parameters, the torque reference was changed from zero to 3 pu at point A. The torque reference was then increased and decreased by 10% of full load at points B and C, respectively. This part of Figure 51 is equivalent to the first part of Figure 47, with the exception of the changes in operating conditions and parameters as previously noted. At point D modulation of the bus voltage was begun. The bridged-T network was removed at point E and replaced at F. Similarly the lead-lag network was removed at G and replaced at H and the speed feedback was removed at I and replaced at J. All three compensation networks were removed at K and replaced at L. Finally the modulation of the bus voltage was removed at M.

Removal of the bridged-T network at E increased the excursions of the field voltage and approximately doubled the oscillations of tie line power as shown by ΔP_e. Removal of the lead-lag network at G resulted in large excursions of tie line power and terminal voltage and also allowed

large oscillations to develop in incremental speed $\Delta\omega$ and machine angle δ. Removal of all compensation at K produced an even more severe condition, but when the compensation networks were replaced, the oscillations were damped out.

Figure 52 is similar to Figure 51 except that the bus voltage frequency was reduced to 2.1 rad/sec. Removal of the bridged-T at E resulted in large and high frequency field voltage excursions. Removal of the lead-lag network at G produced results similar to those of the previous figure. Removal of speed feedback when the system was being perturbed at such a low frequency had little effect. Removal of all compensation at K again resulted in large oscillations in the various machine quantities which were damped out after reinsertion of the compensating networks.

Figure 53 is similar to Figure 51 except that a power system stabilizer was used for compensation. The torque reference was changed from zero to 3 pu at A and was increased and decreased by 10% at B and C, respectively. (Compare with Figure 45.) The bus voltage modulation was added at D and removed at E. It was again added at F and the power system stabilizer was removed at G and replaced at H. The bus voltage modulation was removed at I and the torque reference was decreased to zero at J.

Removal of the power system stabilizer allowed the oscillations to grow to comparatively large values, and after it was replaced, the oscillations were again reduced to values comparable to those before the network was removed.

Comparison of Figures 51 and 53 shows that the power system stabilizer was not as effective in controlling either tie line power oscillations or

the terminal voltage fluctuations as the compensation networks of Figure 51.

Figure 54 shows the results of modulating the bus voltage at 2.1 rad/sec. The modulation was added at A. The power system stabilizer was removed at B and replaced at C, and the modulation of the bus voltage was removed at D.

After removal of the power system stabilizer several seconds were required for the oscillations to build up to appreciable levels. After reinsertion of the power system stabilizer the oscillations were quickly damped out.

The performance of five of the compensation networks is summarized in Table 5 for various machine loadings. The compensation network parameters were adjusted to produce the best response to a 10% increase in torque reference with the machine operating under conditions of Base Case 2. The settings used here are the same as those used for Figures 44, 45, 46a and 47, and were not changed as machine loading was varied. The definitions of risetime, settling time and percent overshoot are those given in reference (104). Omissions in the table are the result of an unstable operating condition. The rows labeled ΔP_e give the risetimes, settling time and percent overshoot of the variable ΔP_e resulting from a 10% increase in the torque reference. The rows labeled Δv_t give similar data for the quantity Δv_t resulting from a 5% increase in V_{ref}.

Comparing the bridged-T, lead-lag and speed compensation performance to the power system stabilizer, the following generalizations may be made. There are no significant differences in the risetimes of ΔP_e and Δv_t for the two types of compensation. The settling time for ΔP_e is generally

Table 5. Performance of various compensation networks

	Uncompensated system			Excitation rate feedback		
	rise-time	set-tling time	% over-shoot	rise-time	set-tling time	% over-shoot
T_m = 3.0, pf = .85 lagging						
ΔP_e	0.06	0.22	86.6	0.06	0.22	80.0
Δv_t	0.20	0.60	10.0	0.98	4.20	60.0
T_m = 2.0, pf = .85 lagging						
ΔP_e	0.05	0.26	80.0	0.05	0.25	80.0
Δv_t	0.19	0.35	6.0	1.00	4.10	53.2
T_m = 1.0, pf = .85 lagging						
ΔP_e	0.05	0.25	70.0	0.05	0.23	70.0
Δv_t	0.15	0.325	7.9	1.00	3.60	43.5
T_m = 3.0, pf = 1.0						
ΔP_e				0.09	0.29	87.0
Δv_t				0.90	4.10	69.0
T_m = 2.0, pf = 1.0						
ΔP_e	unstable			0.055	0.27	87.0
Δv_t	0.21	0.34	6.25	1.00	4.20	68.7
T_m = 1.0, pf = 1.0						
ΔP_e	0.06	0.24	67.0	0.055	0.265	73.0
Δv_t	0.155	0.30	6.25	1.00	3.80	57.0
T_m = 1.0, pf = .85 leading						
ΔP_e	0.06	0.27	73.2	0.065	0.28	86.6
Δv_t	0.185	0.45	0.0	1.20	4.40	62.5

Bridged-T only ω_o=21 r=.1 n=2			Bridged-T 2-stage lead-lag and speed			Power system stabilizer		
rise-time	set-tling time	% over-shoot	rise-time	set-tling time	% over-shoot	rise-time	set-tling time	% over-shoot
0.05	0.23	100.0	0.04	0.21	73.4	0.05	0.21	82.6
0.21	0.56	33.0	0.28	0.37	5.0	0.23	0.42	5-10
0.06	0.25	82.0	0.04	0.23	66.0	0.05	0.21	66.0
0.18	0.46	40.0	0.21	0.33	6.0	0.20	0.38	10.0
0.06	0.245	67.0	0.05	0.26	60.0	0.045	0.235	66.0
0.155	0.445	50.0	0.17	0.25	0.0	0.16	0.325	6.0
			0.04	0.22	97.0	0.05	0.255	100.0
			0.21	0.33	3.7	0.20	0.46	20.0
0.05	0.27	87.0	0.04	0.23	67.0	0.045	0.225	76.0
0.20	0.50	38.0	0.23	0.29	0.0	0.20	0.47	10.5
0.06	0.27	67.0	0.05	0.285	53.4	0.05	0.235	60.0
0.145	0.43	57.0	0.135	0.26	14.3	0.15	0.46	2.8
0.06	0.28	80.0	0.05	0.255	53.4	0.045	0.19	63.0
0.18	0.47	35.6	0.225	0.98	0.0	0.25	0.47	7.9

smaller for the power system stabilizer. The settling time for Δv_t is longer for the power system stabilizer and the percent overshoot is also greater.

Comparing the bridged-T to the above two compensation systems, the risetime of Δv_t is generally smaller than the risetimes resulting from either of the above. The settling time and percent overshoot of Δv_t are both generally greater. The risetime of ΔP_e is comparable to the above, but in most cases the settling time is longer and the percent overshoot greater than those above.

Excitation rate feedback produces long risetimes, long settling times, and large overshoots for Δv_t. Considering ΔP_e, however, the risetimes are comparable to those of the power system stabilizer and the settling time and percent overshoot are slightly greater.

It should be noted from Table 5 that the effectiveness of damping through excitation control is related to the power output of the machine. As the load is reduced, the settling time for ΔP_e generally increases.

VI. CONCLUSIONS

The results of this study have shown that for the particular system investigated, that is, a synchronous machine with high-speed excitation connected to an infinite bus through a transmission line, a compensation system consisting of a bridged-T filter in the voltage regulator loop, a lead-lag network in the exciter forward loop and speed feedback without phase compensation, performance is obtained which is superior to that of the power system stabilizer.

For tests in which the infinite bus voltage was modulated at the natural frequency of the synchronous machine, the above compensation system reduced the oscillations of the electrical power output by a factor of four and reduced the oscillations of the field voltage to approximately one-half those resulting from use of the power system stabilizer.

Excitation system rate feedback compensation results in long settling times, especially in Δv_t, and greatly increases the risetime of the field voltage, thus decreasing the ability of the excitation system to produce synchronizing torques.

Attempts to cancel the synchronous generator field pole located near the origin result in extremely long settling times of Δv_t if the cancellation is not exact.

Cancellation of the torque-angle poles using speed feedback is more successful because larger errors can be tolerated in the placement of the bridged-T zeros. The above two compensation techniques result in a decrease in field voltage with an increase in rotor speed allowing the machine rotor angle to make abnormally large excursions due to changes in loading.

VII. BIBLIOGRAPHY

1. Adkins, B. The general theory of electrical machines. John Wiley and Sons, Inc., New York, New York. 1957.

2. Aldred, A. S. Electronic analogue computer simulation of multi-machine power system networks. IEE Proceedings 109A:195-202. 1962.

3. Aldred, A. S. and Doyle, P. A. Electronic-analysis computer study of synchronous machine transient stability. IEE Proceedings 104A:152-160. 1957.

4. Aldred, A. S. and Shackshaft, G. A frequency response method for the predetermination of synchronous-machine stability. IEE Proceedings 107C:2-10. 1960.

5. Aldred, A. S. and Shackshaft, G. The effect of a voltage regulator on the steady-state and transient stability of a synchronous generator. IEE Proceedings 105A:420-427. 1958.

6. Anderson, P. M. Analysis of faulted power systems. Unpublished notes. Electrical Engineering Dept., Iowa State University, Ames, Iowa. 1969.

7. Anderson, P. M. and Fouad, A. A. Power system control and stability. Unpublished notes. Electrical Engineering Dept., Iowa State University, Ames, Iowa. 1968.

8. Boffi, L. V. and Haas, V. B., Jr. Analog computer representation of alternators for parallel operations. AIEE Transactions (C&E) 76:153-158. 1957.

9. Bollinger, K. E. and Fleming, R. G. Design of speed stabilizing transfer functions for a synchronous generator. IEEE Conference paper No. 69 CP 156-PWR. Winter, 1969.

10. Breedon, D. B. and Ferguson, R. W. Fundamental equations for analogue studies of synchronous machines. AIEE Transactions (PAS) 75:297-306. 1956.

11. Brown, R. G. Elements of linear state-space analysis. Unpublished notes. Electrical Engineering Dept., Iowa State University, Ames, Iowa. 1966.

12. Brown, P. G., deMello, F. P., Lenfest, E. H., and Mills, R. J. Effects of excitation, turbine energy control, and transmission on transient stability. IEEE Transactions (PAS) 89:1247-1252. 1970.

13. Brown, R. G. and Nilsson, J. W. Introduction to linear system analysis. John Wiley and Sons, Inc., New York, New York. 1962.

14. Brown, H. E., Shipley, D., Coleman, and Nied, R. E. A study of stability equivalent. IEEE Transactions (PAS) 88:200-207. 1969.

15. Buckley, D. F. Analog computer representation of a synchronous machine. Unpublished M.S. thesis. Library, Iowa State University, Ames, Iowa. 1968.

16. Byerly, R. T., Keay, F. W., and Skooglund, J. W. Damping of power oscillations in salient-pole machines with static exciters. IEEE Transactions (PAS) 89:1009-1021. 1970.

17. Byerly, R. T., Ramey, D. G., and Skooglund, J. W. Power system stability--effect of control system performance. IEEE Conference paper No. 68 EP 706-PWR. ASME/IEEE Joint Power Generation Conference, September, 1968. 1968.

18. Byerly, R. T. and Sherman, D. E. Defining and calculating synchronizing power flows for large transmission networks. IEEE Conference paper No. 71 CP 138-PWR. Winter, 1971.

19. Byerly, R. T., Skooglund, J. W., and Keay, F. W. Control of generator excitation for improved power system stability. American Power Conference Proceedings 1967:1011-1022. 1967.

20. Colombo, A., Redaelli, F., Ruckstuhi, G., and Vian, A. Determination of the dynamic response of electrical system by means of a digital program. IEEE Transactions (PAS) 87:1411-1419. 1968.

21. Concordia, C. Modern concepts of power system stability. Journal of the Institute of Electrical Engineering of Japan 85:4-12. 1965.

22. Concordia, C. Performance of interconnected systems following disturbances. IEEE Spectrum 1965:68-80. 1965.

23. Concordia, C. Steady-state stability of synchronous machines as affected by voltage regulator characteristics. AIEE Transactions 63: 215-220. 1944.

24. Concordia, C. Synchronous machines. John Wiley and Sons, Inc., New York, New York. 1951.

25. Concordia, C. and Kirchmayer, L. K. Tie-line power and frequency control of electric power systems. AIEE Transactions (PAS) 72:562-572. 1953.

26. Concordia, C. and Temoshok, M. Generator excitation system and power system performance. IEEE Conference paper No. 67 CP 536-PWR. Summer, 1967.

27. Crary, S. S. Power system stability. Vols. 1 and 2. John Wiley and Sons, Inc., New York, New York. 1945.

28. Dandeno, P. L., Karas, A. N., McClymont, K. R., and Watson, W. Effect of high speed rectifier excitation systems on generator stability limits. IEEE Transactions (PAS) 87:190-201. 1968.

29. Dave, M. P. and Mukhopadhyay, P. Dynamic stability of a synchronous machine with sampling in the voltage regulator circuits. IEEE Conference paper No. 71 CP 215-PWR. Winter, 1971.

30. Dave, M. P. and Mukhopadhyay, P. Response of single machine connected to bus-bar for variation in power and bus-bar voltage both in magnitude and phase. Part I-cyclic variation. IEEE Conference paper No. 71 CP 213-PWR. Winter, 1971.

31. deMello, F. P. and Concordia, C. Concepts of synchronous machine stability as affected by excitation control. IEEE Transactions (PAS) 88:316-330. 1969.

32. deMello, F. P., Ewart, D. N., and Temoshok, M. Stability of synchronous machines as affected by excitation systems and systems parameters. American Power Conference Proceedings 1965:1150-1159. 1965.

33. DeRusso, P. M., Roy, R. J., and Clase, C. M. State variables for engineers. John Wiley and Sons, Inc., New York, New York. 1967.

34. Dinely, J. L., Morris, A. J., and Preece, C. Optimized transient stability from excitation control of synchronous generators. IEEE Transactions (PAS) 87:1696-1705. 1968.

35. Doherty, R. E. and Nickle, C. A. Synchronous machines. AIEE Transactions 47:912-947. 1926.

36. Dorf, R. C. Modern control systems. Addison-Wesley Publishing Company, Reading, Massachusetts. 1967.

37. Dyrkacz, M. S., Young, C. C., and Maginnis, F. J. A digital transient stability program including the effects of regulator exciter and governor response. AIEE Transactions (PAS) 70:1245-1257. 1960.

38. El-Abiad, A. H. and Nagappan, K. Transient stability region of multimachine power system. IEEE Transactions (PAS) 85:169-179. 1966.

39. Electronic Associates, Inc. Handbook of analog computation. 2nd ed. Publication No. 00800.0001-3. Electronic Associates, Inc., Princeton, New Jersey. 1967.

40. Electronic Associates, Inc. 8800 System reference handbook. Publication No. 00800.1155-2. Electronic Associates, Inc., West Long Branch, New Jersey. 1967.

41. Ellis, H. M., Hardy, J. E., Blythe, A. L., and Skooglund, J. W. Dynamic stability of the Peace River transmission system. IEEE Transactions (PAS) 85:586-601. 1966.

42. El-Sherbiny, M. K. and Fouad, A. A. Digital analysis of excitation control for interconnected power systems. IEEE Transactions (PAS) 90:441-447. 1971.

43. Ewart, D. N. and deMello, F. P. A digital computer program for the automatic determination of dynamic stability limits. IEEE Transactions (PAS) 86:867-875. 1967.

44. Ewart, D. N., Landgren, G. L., Temoshok, M., and Walkey, W. W. Stability studies and tests on a 532 mw cross-compound turbine-generator set. IEEE Transactions (PAS) 84:338-343. 1965.

45. Fitzgerald, A. E., Kingsley, C., Jr., and Kusko, A. Electric machinery. 3rd ed. McGraw-Hill Book Company, Inc., New York, New York. 1971.

46. General Electric Company. Specialty control department. G.E. instructions for supplementary control panel 3S7932LA100, LA101, LA102. General Electric Company, Waynesboro, Virginia. 1969.

47. Gerhart, A. D., Hillesland, T., Jr., Luini, J. F., and Rockfield, M. L., Jr. Power system stabilizer: field testing and digital simulation. IEEE Conference paper No. 71 TP 77-PWR. Winter, 1971.

48. Gless, G. E. Direct method of Liapunov applied to transient power system stability. IEEE Transactions (PAS) 85:159-168. 1966.

49. Grainger, J. J. and Ahmari, R. The effect of non-dynamic parameters of excitation system on stability performance. IEEE Conference paper No. 71 CP 185-PWR. Winter, 1971.

50. Hanson, O. W., Goodwin, C. J., and Dandeno, P. L. Influence of excitation and speed control parameters in stabilizing intersystem oscillations. IEEE Transactions (PAS) 87:1306-1314. 1968.

51. Heffron, W. G. and Phillips, R. A. Effect of a modern amplidyne voltage regulator on underexcited operation of large turbine generators. AIEE Transactions (PAS) 71:692-697. 1952.

52. Hooper, J. S., Adams, G. E., and Conder, J. C. Damping of system oscillations with steam electric generating units. IEEE Conference paper No. 31 CP 66-176. Winter, 1966.

53. Hovey, L. M. Optimum adjustment of hydro governors on Manitoba hydro system. AIEE Transactions (PAS) 81:581-597. 1962.

54. Huelsman, L. P. Circuits, matrices, and linear vector spaces. McGraw-Hill Book Company, Inc., New York, New York. 1963.

55. Humpage, W. D. and Saha, T. N. Digital-computer methods in dynamic response analyses of turbogenerator units. IEE Proceedings 114:1115-1130. 1967.

56. IEEE Committee Report. Bibliography of rotating electric machinery for 1966-1968. IEEE Transactions (PAS) 89:1293-1307. 1970.

57. IEEE Committee Report. Recommended phasor diagram for synchronous machine. IEEE Transactions (PAS) 88:1593-1610. 1969.

58. IEEE Power Generation Committee. Modern concepts of power system dynamics. IEEE Tutorial Course 70M-62-PWR. 1970.

59. IEEE Working Group of the Excitation Systems. Subcommittee of the Power Generating Committee. Computer representation of excitation systems. IEEE Transactions (PAS) 87:1460-1464. 1968.

60. Jacovides, L. J. and Adkins, B. Effect of excitation-regulation on synchronous machine stability. IEE Proceedings 113:1021-1034. 1966.

61. Jones, G. A. Transient stability of a synchronous generator under conditions of bang-bang excitation scheduling. IEEE Transactions (PAS) 84:114-121. 1965.

62. Kashkari, C. N. Effects of feedback signals on transient stability-phase plane approach. IEEE Conference paper No. 71 TP 76-PWR. Winter, 1971.

63. Kasturi, R. and Doraraju, P. Relative dynamic stability regions of power systems. IEEE Transactions (PAS) 89:966-974. 1970.

64. Keay, F. W. and South, W. H. Design of a power system stabilizer sensing frequency deviation. IEEE Transactions (PAS) 90:707-713. 1971.

65. Kimbark, E. W. Power system stability. Vols. 1 and 3. John Wiley and Sons, Inc., New York, New York. 1948.

66. Kirchmayer, L. K. Economic control of interconnected systems. John Wiley and Sons, Inc., New York, New York. 1959.

67. Klopfenstein, A. Experience with system stabilizing excitation controls on the generation of the Southern California Edison Company. IEEE Transactions (PAS) 90:698-706. 1971.

68. Krause, P. C. Simulation of a single machine-infinite bus system. Mimeographed. Electrical Engineering Dept., Purdue University, West Lafayette, Indiana. From report submitted to the Bureau of Reclamation. ca. 1965.

69. Krause, P. C. and Towle, J. N. Synchronous machine damping by excitation control with direct and quadrature axis field windings. IEEE Transactions (PAS) 88:1266-1274. 1969.

70. Kron, G. Regulating system for dynamoelectric machines. U.S. Patent 2,692,967. October 26, 1954.

71. Kron, G. Tensor analysis of networks. John Wiley and Sons, Inc., New York, New York. 1939.

72. Ku, Y. H. Rotating-field theory and general analysis of synchronous and induction machines. IEE Journal 99:410-428. 1952.

73. Ku, Y. H. Transient analysis of rotating machines and stationary networks by means of rotating reference frames. AIEE Transactions (C&E) 70:943-954. 1951.

74. Laughton, M. A. Matrix analysis of dynamic stability in synchronous multimachine systems. IEE Proceedings 113:325-336. 1966.

75. Lewis, W. A. A basic analysis of synchronous machines-Part I. AIEE Transactions (PAS) 77:436-456. 1958.

76. Lewis, W. A. The principles of synchronous machines. Third lithoprinted edition. Illinois Institute of Technology, Chicago Center, Chicago, Illinois. 1959.

77. Lipo, T. A. and Krause, P. C. Stability analysis for variable frequency operation of synchronous machines. IEEE Transactions (PAS) 87: 227-234. 1968.

78. Lokay, H. E. and Bolger, R. L. Effect of turbine-generator representation in system stability studies. IEEE Transactions (PAS) 84:933-942. 1965.

79. Messerle, H. K. Dynamic circuit theory. AIEE Transactions (PAS) 79: 1-12. 1960.

80. Messerle, H. K. Relative dynamic stability of large synchronous generators. IEE Proceedings 103C:234-242. 1956.

81. Miles, J. G. Analysis of overall stability of multi-machine power systems. IEE Proceedings 109A:203-211. 1962.

82. Mittelstadt, W. A. Four methods of power system damping. IEEE Transactions (PAS) 87:1323-1330. 1968.

83. Musil, J. D. Digital stability analysis of power generating units. Unpublished Ph.D. thesis. Library, Iowa State University, Ames, Iowa. 1968.

84. Nagy, I. Analysis of minimum excitation limits of synchronous machines. IEEE Transactions (PAS) 89:1001-1008. 1970.

85. Nanda, J. Some aspects on steady state stability and transient response of a two machine system. IEEE Conference paper No. 71 CP 14-PWR. Winter, 1971.

86. Nandi, Shantanu. Modified simulation of synchronous machine. Unpublished M.S. thesis. Library, Iowa State University, Ames, Iowa. 1971.

87. Neimark, Y. I. On the admissability of linearization in stability investigations (Translated title). Dokl. Akad. Nauk S.S.S.R. 127: 961-964. 1959. Translated by U.S. Department of Commerce, Office of Technical Services, Washington, D.C.

88. Olive, D. W. Digital simulation of synchronous machine transients. IEEE Transactions (PAS) 87:1669-1675. 1968.

89. Olive, D. W. New techniques for the calculation of dynamic stability. IEEE Transactions (PAS) 85:767-782. 1966.

90. Park, R. H. Definition of an ideal synchronous machine and formula for the armature flux linkages. G. E. Review 31:332-334. 1928.

91. Park, R. H. Two reaction theory of synchronous machines-generalized method of analysis, Part 1. AIEE Transactions 48:716-729. 1929.

92. Park, R. H. Two reaction theory of synchronous machines, Part 2. AIEE Transactions 52:352-355. 1933.

93. Passeri, D. P. and Willett, R. M. Variable sampling rate sampled data adaptive control of flexible aerospace vehicles. Unpublished mimeographed paper from Project Themis, a report to the Office of Naval Research, Engineering Research Institute, Iowa State University, Ames, Iowa. 1970.

94. Perry, H. R., Luini, J. F., and Coulter, J. C. Improved stability with low time constant rotating exciter. IEEE Conference paper No. 71 TP 16-PWR. Winter, 1971.

95. Peterson, H. A. and Krause, P. C. Damping of power swings in a parallel AC and DC system. IEEE Transactions (PAS) 85:1231. 1966.

96. Prabhashanker, K. and Janischewsyj, W. Digital simulation of multi-machine power systems for stability studies. IEEE Transactions (PAS) 87:73-80. 1968.

97. Prentice, B. R. Fundamental concepts of synchronous machine reactance. Supplement to 1937 AIEE Transactions 56:1-21. 1937.

98. Ramamoorty, M. and Balgopal. Block diagram approach to power system reliability. IEEE Transactions (PAS) 89:802-811. 1970.

99. Rankin, A. W. Per unit impedances of synchronous machines, Part 1. AIEE Transactions 64:569-575. 1945.

100. Rankin, A. W. Per unit impedances of synchronous machines, Part 2. AIEE Transactions 64:839-841. 1945.

101. Riaz, M. Analogue computer representations of synchronous generators in voltage regulation studies. AIEE Transactions (PAS) 75:1178-1184. 1956.

102. Roemish, W. R., Clemans, C. L., Lloyd, L. W., and Schleif, F. R. An acceleration relay for power systems. IEEE Transactions (PAS) 90: 1150-1154. 1971.

103. Ross, E., Warrent, T., and Thaler, G. Design of servo compensation based on the root locus approach. AIEE Transactions (A&I) 79:272-277. 1960.

104. Savant, C. J., Jr. Control system design. 2nd ed. McGraw-Hill Book Company, Inc., New York, New York. 1964.

105. Schackshaft, G. General-purpose turbo-alternator model. IEE Proceedings 110:703-713. 1963.

106. Schleif, F. R., Hunkins, H. D., Hattan, E. E., and Gish, W. B. Control of rotating exciters for power system damping: pilot applications and experience. IEEE Transactions (PAS) 88:1259-1266. 1969.

107. Schleif, F. R., Hunkins, H. D., Martin, G. E., and Hattan, E. E. Excitation control to improve power line stability. IEEE Transactions (PAS) 87:1426-1434. 1968.

108. Schleif, F. R., Martin, G. E., and Angell, R. R. Damping of system oscillations with a hydrogenerating unit. IEEE Transactions (PAS) 86:438-442. 1967.

109. Schleif, F. R. and White, J. H. Damping for the Northwest-Southwest tieline oscillations--on analog study. IEEE Transactions (PAS) 85: 1239-1247. 1966.

110. Schleif, F. R. and Wilbor, A. B. The coordination of hydraulic turbine governors for power system operation. IEEE Transactions (PAS) 85:750-758. 1966.

111. Schroder, D. C. Generation of supplementary excitation signals by analog computer for increased power system stability. Unpublished mimeographed Annual Report to Affiliate Research Program Sponsors in Power. Engineering Research Institute, Iowa State University, Ames, Iowa. 1971.

112. Schulz, R. R., Temoshok, M., and Farmer, R. G. Dynamic stability tests at four corners. American Power Conference 31st Annual Meeting. April 22-24, 1969.

113. Shier, R. M. and Blythe, A. L. Field tests of dynamic stability using a stabilizing signal and computer program verification. IEEE Transactions (PAS) 87:315-322. 1968.

114. Stagg, G. W. and El-Abiad, A. H. Computer methods in power system analysis. McGraw-Hill Book Company, Inc., New York, New York. 1968.

115. Stapleton, C. A. Root-locus study of synchronous-machine regulation. IEE Proceedings 111:761-768. 1964.

116. Surana, S. L. and Hariharan, M. V. Transient response and transient stability of power systems. IEE Proceedings 115:114-121. 1968.

117. Taylor, D. G. Analysis of synchronous machines connected to power system networks. IEE Proceedings 109:606-611. 1962.

118. Truxal, J. G. Automatic feedback control system synthesis. McGraw-Hill Book Company, Inc., New York, New York. 1955.

119. Truxal, J. G. Control systems--some unusual design problems. In Mishkin, E. and Braun, L., Jr., eds. Adaptive control systems. pp. 91-118. McGraw-Hill Book Company, Inc., New York, New York. 1961.

120. Undrill, J. M. Dynamical stability calculations for an arbitrary number of interconnected synchronous machines. IEEE Transactions (PAS) 87:835-844. 1968.

121. Undrill, J. M. Power system stability studies by the method of Liapunov: Part 1-state space approach to synchronous machine modeling. IEEE Transactions (PAS) 86:791-801. 1967.

122. Undrill, J. M. Power system stability studies by the method of Liapunov: Part 2-the interconnection of hydrogenerating sets. IEEE Transactions (PAS) 86:802-811. 1967.

123. Undrill, J. M. Structure in the computation of power system nonlinear dynamic response. IEEE Transactions (PAS) 88:1-6. 1969.

124. Van Ness, J. E. and Boyle, J. M. Sensitivity of large multiloop control systems. IEEE Transactions on Automatic Control 10:308-315. 1965.

125. Van Ness, J. E. and Goddard, W. F. Formation of the coefficient matrix of a large dynamic system. IEEE Transactions (PAS) 87:80-83. 1968.

126. Warchol, E. J., Schleif, F. R., Gish, W. B., and Church, J. R. Alinement and modeling of Hanford excitation control for system damping. IEEE Transactions (PAS) 90:714-724. 1971.

127. Webster, R. H., Mane, A. P., and Smith, O. J. M. Series capacitor switching to quench electromechanical transients in power systems. IEEE Transactions (PAS) 90:427-433. 1971.

128. Westinghouse Electric Corporation. Electrical transmission and distribution reference book. 4th ed. Westinghouse Electric Corporation, Pittsburgh, Pennsylvania. 1964.

129. Young, C. C. The art and science of dynamic stability analyses. IEEE Conference paper No. 68 CP 702-PWR. ASME/IEEE Joint Power Conference, September, 1968.

130. Young, C. C. and Wever, R. M. A new stability program for predicting dynamic performance of electrical systems. American Power Conference Proceedings 1967:1126-1138. 1967.

131. Yu, Y. N. and Vongsuriya, K. Nonlinear power system stability study by Liapunov function and Zubov's method. IEEE Transactions (PAS) 86:1480-1484. 1967.

132. Yu, Y. N. and Vongsuriya, K. Steady-state stability limits of a regulated synchronous machine connected to an infinite system. IEEE Transactions (PAS) 85:759-767. 1966.

VIII. ACKNOWLEDGMENTS

The author wishes to express his appreciation to his major professor, Dr. P. M. Anderson, for his suggestions and encouragement throughout the investigation. The author also wishes to thank Dr. D. D. Robb for a comprehensive set of notes concerning synchronous machine modeling and choice of base quantities, and Dr. R. M. Willett for his help with the analog computer simulations. The author is also deeply grateful to his wife, Angela, for the many hours she spent in typing the first draft and for her patience and understanding through the years of study leading to this dissertation.

IX. APPENDIX A. DEVELOPMENT OF ANALOG COMPUTER REPRESENTATION OF A SYNCHRONOUS MACHINE

For the purposes of this study it is assumed that a synchronous machine may be adequately represented by six magnetically coupled windings: three stator windings, one field winding, and two amortisseur or damper windings. Magnetic coupling between these windings, and thus the flux linking each winding, is a function of rotor position. The instantaneous terminal voltage of any winding is of the form

$$v = \pm\Sigma ri \pm \Sigma\dot{\lambda} \qquad [A-1]$$

where λ is the flux linkage, r is the winding resistance, and i is the current, with positive current flowing out of the generator terminals.

Figure 55 is a pictorial representation of a synchronous machine. Two sets of reference axes are shown on the figure. Park (91, 92) and others (7, 76) have shown that transformation of quantities from the abc reference frame to the odq reference frame considerably simplifies the matrix equations by eliminating time varying quantities from them. As a result of this simplification, however, two quantities called the speed voltage terms are added to the resistance matrix of the machine.

As shown in Figure 55, the d-axis lies along the centerline of the rotor North pole and leads the axis of phase a by θ degrees. The q-axis lags the d-axis by 90 electrical degrees. Also note that for the current directions shown, $+i_F$ and $+i_D$ magnetize the +d-axis and $+i_Q$ magnetizes the +q-axis.

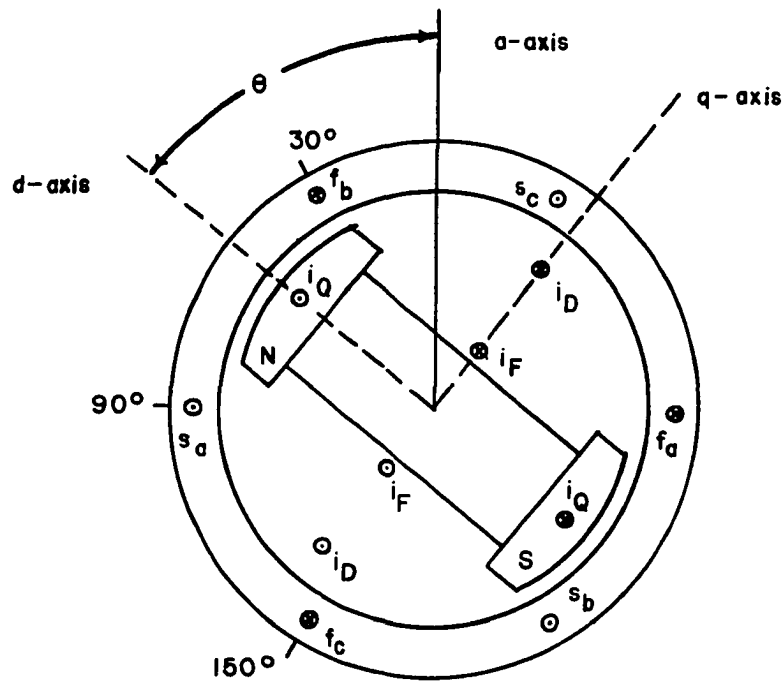

Figure 55. Pictorial representation of a synchronous machine

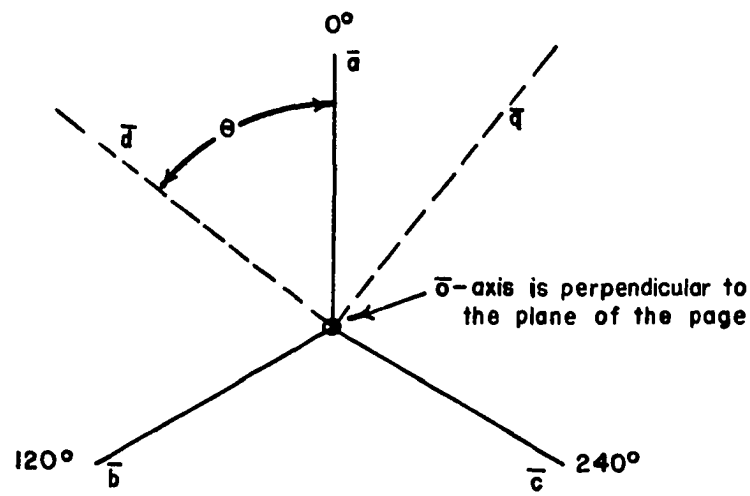

Figure 56. Unit vectors $\bar{a}$, $\bar{b}$, $\bar{c}$ and $\bar{o}$, $\bar{d}$, $\bar{q}$ which form reference frames for synchronous machine

An appropriate Park-type transformation, which conforms with proposed IEEE standards (57), for the reference system shown in Figure 56 is

$$\underline{P} = \sqrt{2/3}\begin{bmatrix} \sqrt{1/2} & \sqrt{1/2} & \sqrt{1/2} \\ \cos\theta & \cos(\theta-120) & \cos(\theta+120) \\ \sin\theta & \sin(\theta-120) & \sin(\theta+120) \end{bmatrix} \qquad [A-2]$$

where $\underline{F}_{odq} = \underline{P}\underline{F}_{abc}$. $\underline{P}^{-1}$ exists and

$$\underline{P}^{-1} = \sqrt{2/3}\begin{bmatrix} \sqrt{1/2} & \cos\theta & \sin\theta \\ \sqrt{1/2} & \cos(\theta-120) & \sin(\theta-120) \\ \sqrt{1/2} & \cos(\theta+120) & \sin(\theta+120) \end{bmatrix} \qquad [A-3]$$

Thus $\underline{F}_{abc} = \underline{P}^{-1}\underline{F}_{odq}$.

Note that $\underline{P}^{-1} = \underline{P}^{t}$ so that the transformation is orthogonal.

Consider transforming the unit vectors $\bar{a}$, $\bar{b}$, $\bar{c}$ in the abc coordinate system of Figure 56 into the odq reference system.

$$\begin{bmatrix} o \\ d \\ q \end{bmatrix} = \sqrt{2/3}\begin{bmatrix} \sqrt{1/2} & \sqrt{1/2} & \sqrt{1/2} \\ \cos\theta & \cos(\theta-120) & \cos(\theta+120) \\ \sin\theta & \sin(\theta-120) & \sin(\theta+120) \end{bmatrix}\begin{bmatrix} \bar{a} \\ \bar{b} \\ \bar{c} \end{bmatrix}$$

The zero vector expressed in terms of $\bar{a}$, $\bar{b}$ and $\bar{c}$ is

$$o = \sqrt{2/3}[\sqrt{1/2}\,\bar{a} + \sqrt{1/2}\,\bar{b} + \sqrt{1/2}\,\bar{c}]$$

and its magnitude is computed as follows,

$$|o| = \sqrt{2/3}\ \sqrt{1/2 + 1/2 + 1/2}$$

$$= 1$$

So $o = \bar{o}$, a unit vector.

Similarly

$$d = \sqrt{2/3}[\bar{a}\cos\theta + \bar{b}\cos(\theta-120) + \bar{c}\cos(\theta+120)]$$

$$|d| = \sqrt{2/3}\ \sqrt{\cos^2 + \cos^2(\theta-120) + \cos^2(\theta+120)}$$

$$= \sqrt{2/3}\sqrt{3/2} = 1$$

So $d = \bar{d}$

and a similar procedure yields

$$q = \bar{q}.$$

Thus the transformation of Equation A-2 defines the relationship between two sets of orthonormal basis vectors.

In Figure 56 unit vectors $\bar{d}$ and $\bar{q}$ lie in the plane of the page, and $\bar{o}$ forms right angles with both $\bar{d}$ and $\bar{q}$ and points out from the page. Unit vectors $\bar{a}$, $\bar{b}$ and $\bar{c}$ are all inclined to the plane formed by the d and q axes by an angle whose cosine equals $\sqrt{2/3}$. The projections of vectors $\bar{a}$, $\bar{b}$ and $\bar{c}$ onto the dq-plane lie at 120° with respect to each other. The fixed reference is a stationary line located in the dq-plane, and $\omega_B t$ is the angle measured from this fixed reference axis to the projection of $\bar{a}$ in the dq-plane. Thus the projections of $\bar{a}$, $\bar{b}$ and $\bar{c}$ in the dq-plane rotate at synchronous speed in a clockwise direction. As the rotor angle,

δ, changes, the d- and q-axes pivot about the $\overline{o}$-axis so that the angle between the fixed reference axis and the q-axis is also equal to δ.

A quantity lying along the a-axis having a magnitude equal to 1 has its length reduced to $\sqrt{2}/\sqrt{3}$ when it is projected into the dq-plane.

Define $$\theta = \omega_B t + \delta + 90^\circ \text{ electrical radians} \qquad [A-4]$$

Figure 57 shows the d- and q-axes after some time interval, t, assuming that the d- and a-axes were coincident at time t = 0. If the rotor had rotated at synchronous speed throughout the interval, the d-axis would lie at the angle labeled $\omega_B t$ in Figure 57. However, since a generator is being considered, assume that the rotor has traveled at some speed greater than ω_B for part of the interval and thus the d-axis is in the position shown. Solving Equation A-4 for δ,

$$\delta = \theta - \omega_B t - 90^\circ \text{ electrical radians} \qquad [A-5]$$

For the case of a generator operating against an infinite bus, the fixed reference axis becomes the angle of the infinite bus voltage. Thus δ is the angle between the infinite bus voltage and the q-axis of the machine. The generator field current produces flux in the +d-axis direction and, since the generated voltage lags the flux by 90 electrical degrees, the generator terminal voltage lies primarily along the q-axis. δ is the angle between the infinite bus voltage and the induced voltage of the machine and for normal generator operation δ is positive.

In order to draw a circuit diagram for the synchronous machine it

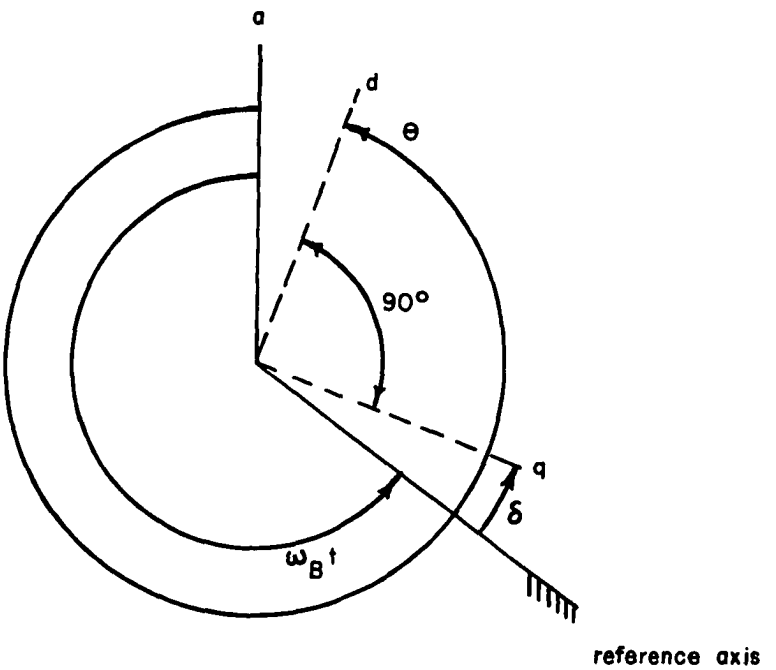

Figure 57. Reference axis

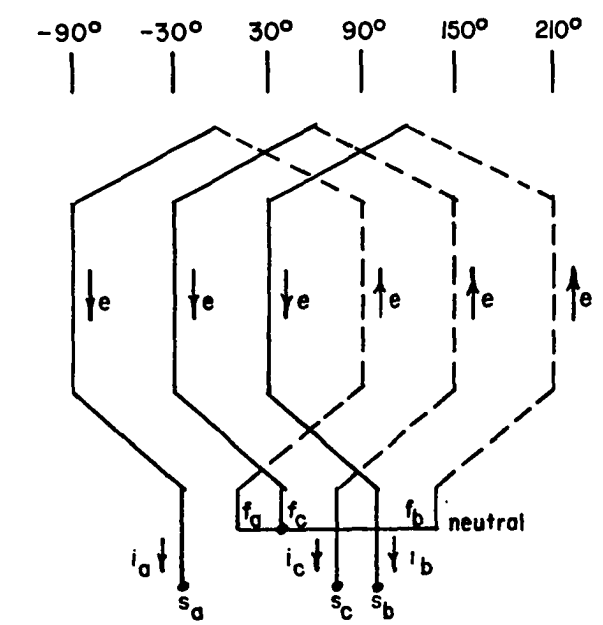

Figure 58. Connection of stator coils to neutral and generator output terminals

is necessary to know how the windings of Figure 55 are connected to the generator neutral and terminals. This information is given in Figure 58.

A. Development of Synchronous Machine Equations

The flux linkage equation for the six circuits of the synchronous machine is

$$\begin{bmatrix} \lambda_a \\ \lambda_b \\ \lambda_c \\ \lambda_F \\ \lambda_D \\ \lambda_Q \end{bmatrix} = \begin{bmatrix} L_{aa} & L_{ab} & L_{ac} & L_{aF} & L_{aD} & L_{aQ} \\ L_{ba} & L_{bb} & L_{bc} & L_{bF} & L_{bD} & L_{bQ} \\ L_{ca} & L_{cb} & L_{cc} & L_{cF} & L_{cD} & L_{cQ} \\ L_{Fa} & L_{Fb} & L_{Fc} & L_{FF} & L_{FD} & L_{FQ} \\ L_{Da} & L_{Db} & L_{Dc} & L_{DF} & L_{DD} & L_{DQ} \\ L_{Qa} & L_{Qb} & L_{Qc} & L_{QF} & L_{QD} & L_{QQ} \end{bmatrix} \begin{bmatrix} i_a \\ i_b \\ i_c \\ i_F \\ i_D \\ i_Q \end{bmatrix} \text{ weber-turns} \qquad [A-6]$$

where

$$L_{jk} = \begin{cases} \text{self-inductance when } j = k \\ \text{mutual inductance when } j \neq k \end{cases}$$

All the inductances in Equation A-6 are functions of rotor position angle, θ, with the exception of L_{FF}, L_{DD} and L_{QQ}; therefore, in a voltage equation $\dot{\lambda} = L\dot{i} + i\dot{L}$ must be used. The inductances in Equation A-6 may be written as follows.

1. Stator self-inductances

$$\begin{aligned} L_{aa} &= L_s + L_m \cos 2\theta \\ L_{bb} &= L_s + L_m \cos 2(\theta-120) \qquad \text{henrys} \qquad L_s > L_m \\ L_{cc} &= L_s + L_m \cos 2(\theta+120) \end{aligned} \qquad [A-7]$$

2. Rotor self-inductances

All rotor self-inductances are constants since slot effects and saturation are being neglected. Let

$$L_{FF} = L_F$$
$$L_{DD} = L_D \quad \text{henrys} \qquad [A-8]$$
$$L_{QQ} = L_Q$$

3. Stator mutual inductances

The phase-to-phase mutual inductances of the stator are negative functions of θ and are written as follows.

$$L_{ab} = L_{ba} = -[M_s + L_m \cos 2(\theta+30)]$$
$$L_{bc} = L_{cb} = -[M_s + L_m \cos 2(\theta-90)] \quad \text{henrys} \quad M_s > L_m \qquad [A-9]$$
$$L_{ca} = L_{ac} = -[M_s + L_m \cos 2(\theta+150)]$$

4. Rotor mutual inductances

The coupling between the d and q axes is zero since there is a 90° displacement between the two, and the mutual inductance between the field and direct axis damper winding is a constant, thus

$$L_{FD} = L_{DF} = M_R$$
$$L_{FQ} = L_{QF} = 0 \quad \text{henrys} \qquad [A-10]$$
$$L_{DQ} = L_{QD} = 0$$

5. Stator-to-field mutual inductances

The mutual inductances from stator windings to field windings are

$$L_{aF} = L_{Fa} = + M_F \cos \theta$$
$$L_{bF} = L_{Fb} = + M_F \cos(\theta-120) \quad \text{henrys} \qquad [A-11]$$
$$L_{cF} = L_{Fc} = + M_F \cos(\theta+120)$$

6. Stator-to-d-axis damper winding mutual inductances

The mutual inductances from stator windings to the direct axis damper winding D are

$$L_{aD} = L_{Da} = + M_D \cos\theta$$
$$L_{bD} = L_{Db} = + M_D \cos(\theta-120) \quad \text{henrys} \qquad [A-12]$$
$$L_{cD} = L_{Dc} = + M_D \cos(\theta+120)$$

7. Stator-to-q-axis damper winding mutual inductances

The mutual inductances from stator windings to the quadrature axis damper winding Q are

$$L_{aQ} = L_{Qa} = + M_Q \sin\theta$$
$$L_{bQ} = L_{Qb} = + M_Q \sin(\theta-120) \quad \text{henrys} \qquad [A-13]$$
$$L_{cQ} = L_{Qc} = + M_Q \sin(\theta+120)$$

The flux linkage equation is now transformed from the abc reference frame to the odq reference frame by premultiplying Equation A-6 by

$$\begin{bmatrix} \underline{P} & \underline{0} \\ \underline{0} & \underline{U_3} \end{bmatrix}$$

where $\underline{P}$ is the Park-type transformation defined in Equation A-2 and $\underline{U_3}$ is the 3x3 unit matrix.

$$\begin{bmatrix} \underline{P} & \underline{0} \\ \underline{0} & \underline{U_3} \end{bmatrix} \underline{\lambda} = \begin{bmatrix} \underline{P} & \underline{0} \\ \underline{0} & \underline{U_3} \end{bmatrix} \underline{L} \begin{bmatrix} \underline{P}^{-1} & \underline{0} \\ \underline{0} & \underline{U_3} \end{bmatrix} \begin{bmatrix} \underline{P} & \underline{0} \\ \underline{0} & \underline{U_3} \end{bmatrix} \underline{i} \qquad [A-14]$$

The result is

$$\begin{bmatrix} \lambda_o \\ \lambda_d \\ \lambda_q \\ \hline \lambda_F \\ \lambda_D \\ \lambda_Q \end{bmatrix} = \left[\begin{array}{ccc|ccc} L_o & 0 & 0 & 0 & 0 & 0 \\ 0 & L_d & 0 & +\sqrt{3/2}M_F & +\sqrt{3/2}M_D & 0 \\ 0 & 0 & L_q & 0 & 0 & +\sqrt{3/2}M_Q \\ \hline 0 & +\sqrt{3/2}M_F & 0 & L_F & M_R & 0 \\ 0 & +\sqrt{3/2}M_D & 0 & M_R & L_D & 0 \\ 0 & 0 & +\sqrt{3/2}M_Q & 0 & 0 & L_Q \end{array}\right] \begin{bmatrix} i_o \\ i_d \\ i_q \\ \hline i_F \\ i_D \\ i_Q \end{bmatrix} \quad \text{weber-turns} \qquad [A\text{-}15]$$

where

$$\begin{aligned} L_d &= L_s + M_s + 3/2\ L_m \\ L_q &= L_s + M_s - 3/2\ L_m \qquad \text{henrys} \\ L_o &= L_s - 2M_s \end{aligned} \qquad [A\text{-}16]$$

Inspection of Equation A-15 shows that the inductances are no longer time varying. The flux linkage equation, Equation A-15, may be partitioned as follows

$$\begin{bmatrix} \underline{\lambda}_{odq} \\ \underline{\lambda}_R \end{bmatrix} = \begin{bmatrix} \underline{L}_{odq} & \underline{L}_m \\ \underline{L}_m^t & \underline{L}_R \end{bmatrix} \begin{bmatrix} \underline{i}_{odq} \\ \underline{i}_R \end{bmatrix} \quad \text{weber-turns} \qquad [A\text{-}17]$$

where

$$\underline{L}_{odq} = \begin{bmatrix} L_o & 0 & 0 \\ 0 & L_d & 0 \\ 0 & 0 & L_q \end{bmatrix} \quad \text{henrys}$$

$$\underline{L}_R = \begin{bmatrix} L_F & M_R & 0 \\ M_R & L_D & 0 \\ 0 & 0 & L_Q \end{bmatrix} \quad \text{henrys}$$

$$\underline{L}_m = \begin{bmatrix} 0 & 0 & 0 \\ +\sqrt{3/2}M_F & +\sqrt{3/2}M_D & 0 \\ 0 & 0 & +\sqrt{3/2}M_Q \end{bmatrix} \quad \text{henrys}$$

The self-inductances of Equation A-15 may be split into mutual and leakage inductance terms where ℓ is a leakage inductance.

$$\begin{bmatrix} \lambda_o \\ \lambda_d \\ \lambda_q \\ \lambda_F \\ \lambda_D \\ \lambda_Q \end{bmatrix} = \begin{bmatrix} (L_o-\ell_o)+\ell_o & 0 & 0 & 0 & 0 & 0 \\ 0 & (L_d-\ell_d)+\ell_d & 0 & +\sqrt{3/2}M_F & +\sqrt{3/2}M_D & 0 \\ 0 & 0 & (L_q-\ell_q)+\ell_q & 0 & 0 & +\sqrt{3/2}M_Q \\ 0 & +\sqrt{3/2}M_F & 0 & (L_F-\ell_F)+\ell_F & M_R & 0 \\ 0 & +\sqrt{3/2}M_D & 0 & M_R & (L_D-\ell_D)+\ell_D & 0 \\ 0 & 0 & +\sqrt{3/2}M_Q & 0 & 0 & (L_Q-\ell_Q)+\ell_Q \end{bmatrix} \begin{bmatrix} i_o \\ i_d \\ i_q \\ i_F \\ i_D \\ i_Q \end{bmatrix} \quad \text{weber-turns} \qquad [A-18]$$

The circuit diagram of the machine is shown in Figure 59, and from it the following voltage equation for the machine may be written.

$$\begin{bmatrix} v_a \\ v_b \\ v_c \\ -v_F \\ 0 \\ 0 \end{bmatrix} = -\begin{bmatrix} r_a & 0 & 0 & 0 & 0 & 0 \\ 0 & r_b & 0 & 0 & 0 & 0 \\ 0 & 0 & r_c & 0 & 0 & 0 \\ 0 & 0 & 0 & r_F & 0 & 0 \\ 0 & 0 & 0 & 0 & r_D & 0 \\ 0 & 0 & 0 & 0 & 0 & r_Q \end{bmatrix} \begin{bmatrix} i_a \\ i_b \\ i_c \\ i_F \\ i_D \\ i_Q \end{bmatrix} - \begin{bmatrix} \dot{\lambda}_a \\ \dot{\lambda}_b \\ \dot{\lambda}_c \\ \dot{\lambda}_F \\ \dot{\lambda}_D \\ \dot{\lambda}_Q \end{bmatrix} + \begin{bmatrix} \underline{v}_n \\ \underline{0} \end{bmatrix} \text{ volts} \qquad [A-19]$$

where

$$\underline{v}_n = -r_n \begin{bmatrix} 1 & 1 & 1 \\ 1 & 1 & 1 \\ 1 & 1 & 1 \end{bmatrix} \begin{bmatrix} i_a \\ i_b \\ i_c \end{bmatrix} - L_n \begin{bmatrix} 1 & 1 & 1 \\ 1 & 1 & 1 \\ 1 & 1 & 1 \end{bmatrix} \begin{bmatrix} \dot{i}_a \\ \dot{i}_b \\ \dot{i}_c \end{bmatrix} \text{ volts} \qquad [A-20]$$

$$= -\underline{R}_n \, \underline{i}_{abc} - \underline{L}_n \, \underline{\dot{i}}_{abc} \text{ volts}$$

If $r_a = r_b = r_c = r$ then

$$\underline{R}_{abc} = r\underline{U}_3 \qquad \text{ohms} \qquad [A-21]$$

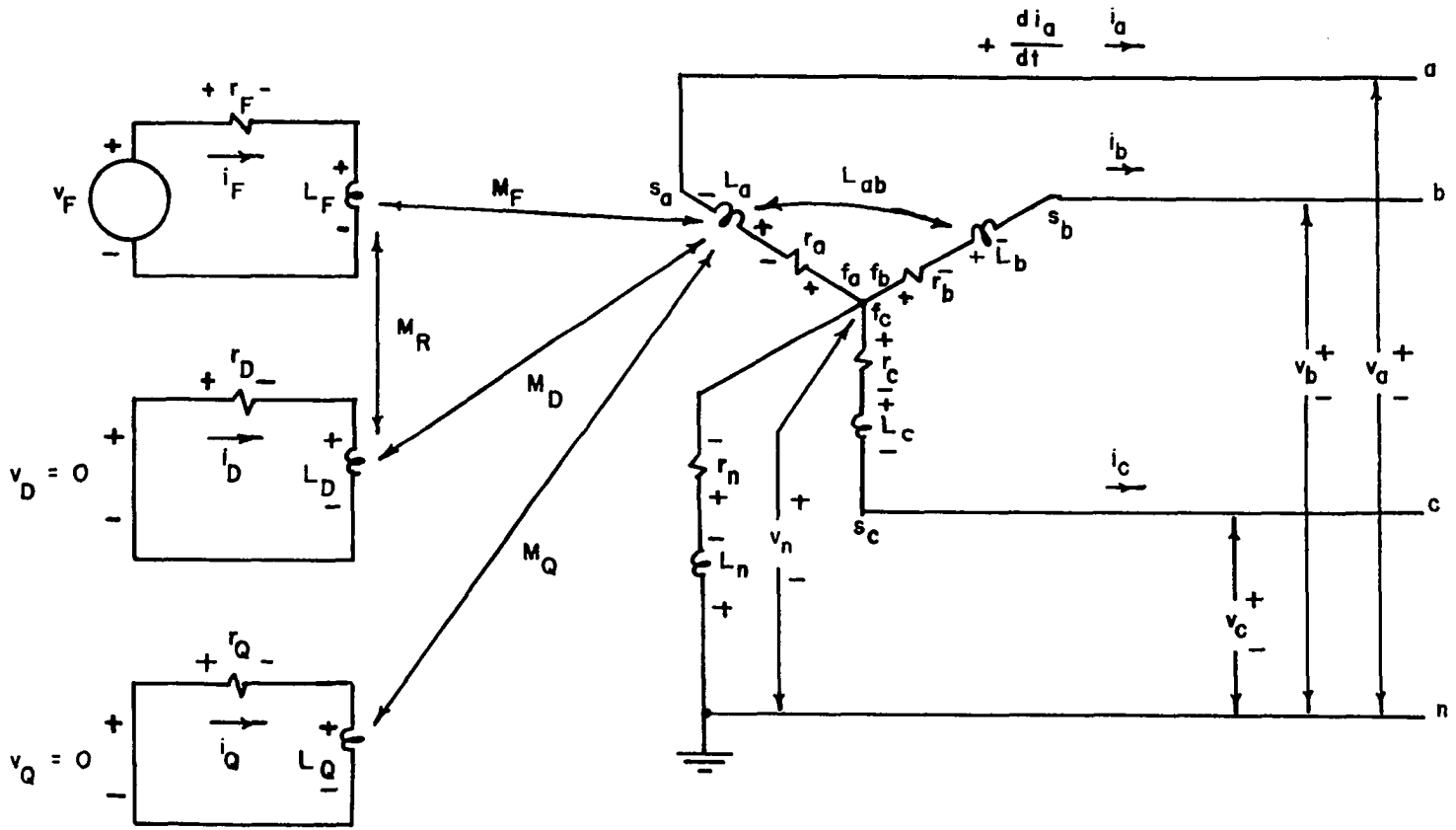

Figure 59. Circuit diagram of synchronous machine

Equation A-19 is now written in partitioned form as follows

$$\begin{bmatrix} \underline{v}_{abc} \\ \underline{v}_R \end{bmatrix} = - \begin{bmatrix} \underline{R}_{abc} & \underline{0} \\ \underline{0} & \underline{R}_R \end{bmatrix} \begin{bmatrix} \underline{i}_{abc} \\ \underline{i}_R \end{bmatrix} - \begin{bmatrix} \dot{\underline{\lambda}}_{abc} \\ \dot{\underline{\lambda}}_R \end{bmatrix} + \begin{bmatrix} \underline{v}_n \\ \underline{0} \end{bmatrix} \text{ volts} \qquad [A-22]$$

Equation A-22 is transformed by premultiplying by $\begin{bmatrix} \underline{P} & \underline{0} \\ \underline{0} & \underline{U}_3 \end{bmatrix}$.

$$\begin{bmatrix} \underline{P} & \underline{0} \\ \underline{0} & \underline{U}_3 \end{bmatrix} \begin{bmatrix} \underline{v}_{abc} \\ \underline{v}_R \end{bmatrix} = - \begin{bmatrix} \underline{P} & \underline{0} \\ \underline{0} & \underline{U}_3 \end{bmatrix} \begin{bmatrix} \underline{R}_{abc} & \underline{0} \\ \underline{0} & \underline{R}_R \end{bmatrix} \begin{bmatrix} \underline{P}^{-1} & \underline{0} \\ \underline{0} & \underline{U}_3 \end{bmatrix} \begin{bmatrix} \underline{P} & \underline{0} \\ \underline{0} & \underline{U}_3 \end{bmatrix} \begin{bmatrix} \underline{i}_{abc} \\ \underline{i}_R \end{bmatrix}$$

$$- \begin{bmatrix} \underline{P} & \underline{0} \\ \underline{0} & \underline{U}_3 \end{bmatrix} \begin{bmatrix} \dot{\underline{\lambda}}_{abc} \\ \dot{\underline{\lambda}}_R \end{bmatrix} + \begin{bmatrix} \underline{P} & \underline{0} \\ \underline{0} & \underline{U}_3 \end{bmatrix} \begin{bmatrix} \underline{v}_n \\ \underline{0} \end{bmatrix} \text{ volts} \qquad [A-23]$$

Each term of Equation A-23 is now evaluated separately.

Voltage term:

$$\begin{bmatrix} \underline{P} & \underline{0} \\ \underline{0} & \underline{U}_3 \end{bmatrix} \begin{bmatrix} \underline{v}_{abc} \\ \underline{v}_R \end{bmatrix} = \begin{bmatrix} v_o \\ v_d \\ v_q \\ -v_F \\ 0 \\ 0 \end{bmatrix} \text{ volts} \qquad [A-24]$$

Resistance term:

$$\begin{bmatrix} \underline{P} & \underline{0} \\ \underline{0} & \underline{U}_3 \end{bmatrix} \begin{bmatrix} \underline{R}_{abc} & \underline{0} \\ \underline{0} & \underline{R}_R \end{bmatrix} \begin{bmatrix} \underline{P}^{-1} & \underline{0} \\ \underline{0} & \underline{U}_3 \end{bmatrix} = \begin{bmatrix} \underline{P}\underline{R}_{abc}\underline{P}^{-1} & \underline{0} \\ \underline{0} & \underline{R}_R \end{bmatrix} = \begin{bmatrix} \underline{R}_{abc} & \underline{0} \\ \underline{0} & \underline{R}_R \end{bmatrix} \text{ohms} \qquad [A-25]$$

Current term:

$$\begin{bmatrix} \underline{P} & \underline{0} \\ \underline{0} & \underline{U}_3 \end{bmatrix} \begin{bmatrix} \underline{i}_{abc} \\ \underline{i}_R \end{bmatrix} = \begin{bmatrix} i_o \\ i_d \\ i_q \\ i_F \\ i_D \\ i_Q \end{bmatrix} \text{ amps} \qquad [A-26]$$

Flux linkage terms:

$$\begin{bmatrix} \underline{P} & \underline{0} \\ \underline{0} & \underline{U}_3 \end{bmatrix} \begin{bmatrix} \dot{\underline{\lambda}}_{abc} \\ \dot{\underline{\lambda}}_R \end{bmatrix} = \begin{bmatrix} P\dot{\underline{\lambda}}_{abc} \\ \dot{\underline{\lambda}}_R \end{bmatrix} \quad \text{volts} \qquad [A\text{-}27]$$

$\underline{P\dot{\lambda}}_{abc}$ is computed as follows. By definition,

$$\underline{\lambda}_{odq} = \underline{P\lambda}_{abc}$$

Differentiating,

$$\dot{\underline{\lambda}}_{odq} = \underline{P\dot{\lambda}}_{abc} + \dot{\underline{P\lambda}}_{abc} \qquad [A\text{-}28]$$

So

$$\underline{P\dot{\lambda}}_{abc} = \dot{\underline{\lambda}}_{odq} - \dot{\underline{P\lambda}}_{abc} = \dot{\underline{\lambda}}_{odq} - \underline{\dot{P}P^{-1}\lambda}_{odq} \qquad [A\text{-}29]$$

Differentiating the top partition of Equation A-15, the following matrix equation results where the right side is a 3x1 vector.

$$\begin{bmatrix} \dot{\lambda}_o \\ \dot{\lambda}_d \\ \dot{\lambda}_q \end{bmatrix} = \begin{bmatrix} L_o\dot{i}_o & & \\ L_d\dot{i}_d & +\sqrt{3/2}M_F\dot{i}_F & +\sqrt{3/2}M_D\dot{i}_D \\ L_q\dot{i}_q & +\sqrt{3/2}M_Q\dot{i}_Q & \end{bmatrix} \quad \text{volts} \qquad [A\text{-}30]$$

Also using Equation A-2 and Equation A-3

$$\underline{\dot{P}P^{-1}} = \omega \begin{bmatrix} 0 & 0 & 0 \\ 0 & 0 & -1 \\ 0 & 1 & 0 \end{bmatrix} \qquad [A\text{-}31]$$

and finally from Equation A-15 and Equation A-31

$$\underline{\dot{P}P^{-1}\lambda}_{odq} = \begin{bmatrix} 0 & & \\ -\omega L_q i_q & -\omega\sqrt{3/2}M_Q i_Q & \\ +\omega L_d i_d & +\omega\sqrt{3/2}M_F i_F & +\omega\sqrt{3/2}M_D i_D \end{bmatrix} \quad \text{volts} \qquad [A\text{-}32]$$

Differentiating the bottom partition of Equation A-15 yields

$$\dot{\underline{\lambda}}_R = \begin{bmatrix} +\sqrt{3/2}M_F\dot{i}_d & +L_F\dot{i}_F & +M_R\dot{i}_D \\ +\sqrt{3/2}M_D\dot{i}_d & +M_R\dot{i}_F & +L_D\dot{i}_D \\ +\sqrt{3/2}M_Q\dot{i}_q & +L_Q\dot{i}_Q & \end{bmatrix} \quad \text{volts} \qquad [A-33]$$

Neutral voltage term:

$$\begin{bmatrix} \underline{P} & \underline{0} \\ \underline{0} & \underline{U}_3 \end{bmatrix} \begin{bmatrix} \underline{v}_n \\ \underline{0} \end{bmatrix} \triangleq \begin{bmatrix} \underline{v}^n_{odq} \\ \underline{0} \end{bmatrix} \quad \text{volts} \qquad [A-34]$$

$$\underline{v}^n_{odq} = \underline{P}\underline{v}_n = -\underline{P}\underline{R}_n\underline{P}^{-1}\underline{P}\underline{i}_{abc} - \underline{P}\underline{L}_n\underline{P}^{-1}\underline{P}\dot{\underline{i}}_{abc}$$

$$= -\underline{P}\underline{R}_n\underline{P}^{-1}\underline{i}_{odq} - \underline{P}\underline{L}_n\underline{P}^{-1}\dot{\underline{i}}_{odq} \qquad [A-35]$$

$$-\underline{P}\underline{R}_n\underline{P}^{-1} = -3r_n \begin{bmatrix} 1 & 0 & 0 \\ 0 & 0 & 0 \\ 0 & 0 & 0 \end{bmatrix} \quad \text{ohms} \qquad [A-36]$$

So

$$-\underline{P}\underline{R}_n\underline{P}^{-1}\underline{i}_{odq} = -3r_n i_o \qquad [A-37]$$

and similarly

$$-\underline{P}\underline{L}_n\underline{P}^{-1}\dot{\underline{i}}_{odq} = -3L_n\dot{i}_o$$

Finally,

$$\begin{bmatrix} \underline{v}^n_{odq} \\ \underline{0} \end{bmatrix} = - \begin{bmatrix} 3r_n i_o \\ 0 \\ 0 \\ 0 \\ 0 \end{bmatrix} - \begin{bmatrix} 3L_n\dot{i}_o \\ 0 \\ 0 \\ 0 \\ 0 \end{bmatrix} \qquad [A-38]$$

Inserting the above results into Equation A-23 and expanding to 6x6 notation the following machine voltage equation results.

$$\begin{bmatrix} v_o \\ v_d \\ v_q \\ -v_F \\ 0 \\ 0 \end{bmatrix} = - \begin{bmatrix} r+3r_n & 0 & 0 & 0 & 0 & 0 \\ 0 & r & +\omega L_q & 0 & 0 & +\omega\sqrt{3/2}M_Q \\ 0 & -\omega L_d & r & -\omega\sqrt{3/2}M_F & -\omega\sqrt{3/2}M_D & 0 \\ 0 & 0 & 0 & r_F & 0 & 0 \\ 0 & 0 & 0 & 0 & r_D & 0 \\ 0 & 0 & 0 & 0 & 0 & r_Q \end{bmatrix} \begin{bmatrix} i_o \\ i_d \\ i_q \\ i_F \\ i_D \\ i_Q \end{bmatrix}$$

$$- \begin{bmatrix} L_o+3L_n & 0 & 0 & 0 & 0 & 0 \\ 0 & L_d & 0 & +\sqrt{3/2}M_F & +\sqrt{3/2}M_D & 0 \\ 0 & 0 & L_q & 0 & 0 & +\sqrt{3/2}M_Q \\ 0 & +\sqrt{3/2}M_F & 0 & L_F & M_R & 0 \\ 0 & +\sqrt{3/2}M_D & 0 & M_R & L_D & 0 \\ 0 & 0 & +\sqrt{3/2}M_Q & 0 & 0 & L_Q \end{bmatrix} \begin{bmatrix} \dot{i}_o \\ \dot{i}_d \\ \dot{i}_q \\ \dot{i}_F \\ \dot{i}_D \\ \dot{i}_Q \end{bmatrix} \text{ volts} \qquad [A-39]$$

Using Equation A-15 and Equation A-39 the machine voltage equations may also be written as follows where $p = d/dt$ and $p_u = d/dt_u$.

$$\begin{bmatrix} v_o \\ v_d \\ v_q \\ -v_F \\ 0 \\ 0 \end{bmatrix} = - \begin{bmatrix} r+3r_n+3L_np & 0 & 0 & 0 & 0 & 0 \\ 0 & r & 0 & 0 & 0 & 0 \\ 0 & 0 & r & 0 & 0 & 0 \\ 0 & 0 & 0 & r_F & 0 & 0 \\ 0 & 0 & 0 & 0 & r_D & 0 \\ 0 & 0 & 0 & 0 & 0 & r_Q \end{bmatrix} \begin{bmatrix} i_o \\ i_d \\ i_q \\ i_F \\ i_D \\ i_Q \end{bmatrix}$$

$$- \begin{bmatrix} p & 0 & 0 & 0 & 0 & 0 \\ 0 & p & \omega & 0 & 0 & 0 \\ 0 & -\omega & p & 0 & 0 & 0 \\ 0 & 0 & 0 & p & 0 & 0 \\ 0 & 0 & 0 & 0 & p & 0 \\ 0 & 0 & 0 & 0 & 0 & p \end{bmatrix} \begin{bmatrix} \lambda_o \\ \lambda_d \\ \lambda_q \\ \lambda_F \\ \lambda_D \\ \lambda_Q \end{bmatrix} \text{ volts} \qquad [A-40]$$

B. Interpretations of Voltage Equations

1. The zero-sequence equation is uncoupled from the other equations and thus it may be solved separately once the initial conditions are known.
2. The voltage equations are like those of a passive network except for speed voltage terms in the resistance matrix which result from the elimination of time-varying inductance coefficients. The resistance matrix is nonlinear as a result of the presence of products involving ω.
3. All of the mutuals are reciprocal, as in a passive network. This results from the particular Park-type transformation used here and is not true in general.

C. Per-unit Conversion

The large numerical difference between the stator voltages in the kilovolt range and the much lower field voltage makes it desirable to normalize all equations to a convenient base value and express all variables in per unit or percent of base value. In order that the same equations are valid both in dimensional form and in per unit, Lewis (76) makes the following suggestions concerning the choice of base quantities.

1. If the circuits are coupled, the same volt-amp base and same time base should be chosen for each circuit.
2. Base mutual stator-to-rotor inductance should be the geometric mean of the base self-inductances of stator and rotor.

3. For coupled windings having no relative motion the base mutual inductance should also be chosen as the geometric mean of the base self-impedances.

The stator base quantities are defined as follows where subscript "B" denotes a base quantity and "u" denotes a per-unit quantity.

1. Stator bases (valid for all odq-axis quantities)

S_B = stator rated volt-amps per phase

V_B = stator rated line-to-neutral voltage, rms

ω_B = rated synchronous speed of machine

$I_B = S_B/V_B$ = stator rated line current, rms amps

$t_B = 1/\omega_B$ seconds

$\lambda_B = V_B t_B = V_B/\omega_B = L_B I_B$ weber-turns

$R_B = V_B/I_B$ ohms

$L_B = V_B t_B/I_B = V_B/\omega_B I_B = R_B/\omega_B$ henrys

2. Normalized time

$\omega_u t_u = \omega t$

$(\omega/\omega_B)(t/t_B) = \omega t$

Choose $t_B = 1/\omega_B$ sec

Then $\omega t = \omega t$

When differentiating, $t_u = t/t_B = \omega_B t$

So $\dfrac{d(\ )}{dt_u} = \dfrac{d(\ )}{d(t/t_B)} = t_B \dfrac{d(\ )}{dt} = 1/\omega_B \dfrac{d(\ )}{dt}$

3. Rotor bases

Let I_{FB} be that field current (all other i=0) which generates V_B rms or $\dfrac{V_{Bmax}}{\sqrt{2}}$ on the air gap line when $\omega = \omega_B$. Define I_{DB} and I_{QB} similarly.

Find v_q when stator-generated voltage equals V_B.

$$\begin{bmatrix} v_a \\ v_b \\ v_c \end{bmatrix} = \begin{bmatrix} \sqrt{2}V_B \sin\theta \\ \sqrt{2}V_B \sin(\theta-120) \\ \sqrt{2}V_B \sin(\theta+120) \end{bmatrix}$$

Using Equation A-2,

$$v_q = \sqrt{2/3}\sqrt{2}\, V_B \left[\sin^2\theta + \sin^2(\theta-120) + \sin^2(\theta+120)\right]$$

$$= \sqrt{3}\, V_B$$

From Equation A-39,

$$v_q = \omega L_d i_d - r i_q + \omega\sqrt{3/2}M_F i_F + \omega\sqrt{3/2}M_D i_D - L_q \dot{i}_q - \sqrt{3/2}M_Q \dot{i}_Q$$

Setting

$$i_d = i_D = i_q = i_Q = 0,$$

$$v_q = \omega_B\sqrt{3/2}M_F i_F = \sqrt{3}\, V_B$$

Thus the rms equivalent of i_f reflected in the stator is (using capital I for rms)

$$I_{FB} = \sqrt{2}V_B/(\omega_B M_F) = \sqrt{2}S_B/(\omega_B M_F I_B)$$

A similar procedure yields the following

$$I_{DB} = \sqrt{2}V_B/(\omega_B M_D) = \sqrt{2}S_B/(\omega_B M_D I_B)$$

$$I_{QB} = \sqrt{2}V_B/(\omega_B M_Q) = \sqrt{2}S_B/(\omega_B M_Q I_B)$$

4. <u>Field bases</u>

$$I_{FB} = \sqrt{2}V_B/(\omega_B M_F)$$

$$V_{FB} = S_B/I_{FB} = \omega_B M_F I_B/\sqrt{2}$$

$$R_{FB} = V_{FB}/I_{FB} = (\omega_B M_F)^2/2R_B$$

$$L_{FB} = V_{FB}/\omega_B I_{FB} = \omega_B M_F^2/2R_B$$

$$\lambda_{FB} = V_{FB}/\omega_B = M_F I_B/\sqrt{2}$$

5. D bases

(For Q bases replace D by Q in following equations.)

$$I_{DB} = \sqrt{2}V_B/\omega_B M_D$$

$$V_{DB} = \omega_B M_D I_B/\sqrt{2}$$

$$R_{DB} = (\omega_B M_D)^2/2R_B$$

$$L_{DB} = V_{DB}/\omega_B I_{DB} = \omega_B M_D^2/2R_B$$

$$\lambda_{DB} = V_{DB}/\omega_B = M_D I_B/\sqrt{2}$$

6. Base mutuals: stator-to-rotor

$$M_{FB} = \sqrt{L_B L_{FB}} = \sqrt{\frac{V_B}{\omega_B I_B} \cdot \frac{\omega_B M_F I_B}{\sqrt{2}} \cdot \frac{\omega_B M_F}{\sqrt{2}\ V_B} \cdot \frac{1}{\omega_B}}$$

$$= M_F/\sqrt{2}$$

Similarly,

$$M_{DB} = M_D/\sqrt{2}$$

$$M_{QB} = M_Q/\sqrt{2}$$

7. Base mutuals: rotor-to-rotor

$$M_{RB} = \sqrt{L_{FB} L_{DB}} = \sqrt{\frac{\omega_B M_F^2}{2\ V_B/I_B} \cdot \frac{\omega_B M_D^2}{2\ V_B/I_B}}$$

$$= \frac{I_B M_F M_D \omega_B}{2\ V_B} = \frac{M_F M_D}{2\ L_B} = \frac{M_{FB} M_{DB}}{L_B}$$

So

$$M_F/M_{FB} = \sqrt{2} = M_{Fu}$$

$$M_D/M_{DB} = \sqrt{2} = M_{Du}$$

$$M_Q/M_{QB} = \sqrt{2} = M_{Qu}$$

and $M_{Fu} = M_{Du} = M_{Qu}$

8. Normalize the flux linkage Equation A-15

For the zero sequence equation we write

$$\lambda_{ou}\lambda_B = L_o i_{ou} I_B$$

$$\lambda_{ou} = L_o i_{ou} \frac{I_B}{\lambda_B}$$

$$= L_o i_{ou} \frac{I_B \omega_B}{V_B}$$

$$\lambda_{ou} = L_{ou} i_{ou}.$$

The d-axis equation may be written as

$$\lambda_{du}\lambda_B = L_d i_{du} I_B + \sqrt{3/2} M_F i_{Fu} I_{FB} + \sqrt{3/2} M_D i_{Du} I_{DB}$$

$$\lambda_{du} = L_d i_{du} \frac{I_B \omega_B}{V_B} + \sqrt{3/2} M_F i_{Fu} \frac{I_{FB} \omega_B}{V_B} + \sqrt{3/2} M_D i_{Du} \frac{I_{DB} \omega_B}{V_B}$$

$$\lambda_{du} = L_{du} i_{du} + \sqrt{3/2} M_F i_{Fu} \frac{\sqrt{2}\, V_B}{\omega_B M_F} \frac{\omega_B}{V_B} + \sqrt{3/2} M_D i_{Du} \frac{\sqrt{2}\, V_B}{\omega_B M_D} \frac{\omega_B}{V_B}$$

$$\lambda_{du} = L_{du} i_{du} + \sqrt{3/2} M_{Fu} i_{Fu} + \sqrt{3/2} M_{Du} I_{Du}.$$

Similarly the q-axis equation becomes

$$\lambda_{qu}\lambda_B = L_q i_{qu} I_B + \sqrt{3/2} M_Q i_{Qu} I_{QB}$$

or

$$\lambda_{qu} = L_{qu} i_{qu} + \sqrt{3/2} M_{Qu} i_{Qu}.$$

The field equation is similarly computed to be

$$\lambda_{Fu}\lambda_{FB} = +\sqrt{3/2} M_F i_{du} I_B + L_F i_{Fu} I_{FB} + M_R i_{Du} I_{DB}$$

or

$$\lambda_{Fu} = \sqrt{3/2}\, M_{Fu} i_{du} + L_{Fu} i_{Fu} + M_{Ru} i_{Du}.$$

In a similar fashion we compute

$$\lambda_{Du} = \sqrt{3/2}\, M_{Du} i_{du} + M_{Ru} i_{Fu} + L_{Du} i_{Du}$$

$$\lambda_{Qu} = +\sqrt{3/2}\, M_{Qu} i_{qu} + L_{Qu} i_{Qu}.$$

From the above equations the following normalized flux linkage equation results which has the same form as the dimensional equation, A-15.

$$\begin{bmatrix} \lambda_o \\ \lambda_d \\ \lambda_q \\ \lambda_F \\ \lambda_D \\ \lambda_Q \end{bmatrix} = \begin{bmatrix} L_o & 0 & 0 & 0 & 0 & 0 \\ 0 & L_d & 0 & +\sqrt{3/2}M_F & +\sqrt{3/2}M_D & 0 \\ 0 & 0 & L_q & 0 & 0 & +\sqrt{3/2}M_Q \\ 0 & +\sqrt{3/2}M_F & 0 & L_F & +M_R & 0 \\ 0 & +\sqrt{3/2}M_D & 0 & +M_R & L_D & 0 \\ 0 & 0 & +\sqrt{3/2}M_Q & 0 & 0 & L_Q \end{bmatrix} \begin{bmatrix} i_o \\ i_d \\ i_q \\ i_F \\ i_D \\ i_Q \end{bmatrix} \quad \text{per unit} \qquad [A\text{-}41]$$

9. Normalize voltage Equation A-39

The zero sequence equation may be written as

$$v_{ou} V_B = -(r+3r_n)\, i_{ou} I_B - (L_o+3L_n)\omega_B \frac{d}{dt_u} i_{ou} I_B$$

$$v_{ou} = -(r_u+3r_{nu}) i_{ou} - (L_{ou}+3L_{nu}) \frac{d}{dt_u} i_{ou}$$

The d-axis voltage is similarly computed as follows.

$$v_{du} V_B = -r i_{du} I_B - \omega L_q i_{qu} I_B - \omega\sqrt{3/2}\, M_Q i_{Qu} I_{QB}$$

$$-L_d \omega_B \frac{d}{dt_u} i_{du} I_B - \sqrt{3/2}\, M_F \omega_B \frac{d}{dt_u} i_{Fu} I_{FB} - \sqrt{3/2}\, M_D \omega_B \frac{d}{dt_u} i_{Du} I_{DB}$$

$$v_{du} = -r_u i_{du} - \omega_u L_q i_{qu} \frac{\omega_B I_B}{V_B} - \omega_u \sqrt{3/2}\, M_Q i_{Qu} \frac{\omega_B I_{QB}}{V_B}$$

$$-L_d \frac{\omega_B I_B}{V_B} \frac{d}{dt_u} i_{du} - \sqrt{3/2}\, M_F \frac{\omega_B I_{FB}}{V_B} \frac{d}{dt_u} i_{Fu} - \sqrt{3/2}\, M_D \frac{\omega_B I_{DB}}{V_B} \frac{d}{dt_u} i_{Du}$$

$$= -r_u i_{du} - \omega_u L_{qu} i_{qu} - \omega_u \sqrt{3/2}\, M_Q i_{Qu} \frac{\omega_B}{V_B} \frac{\sqrt{2} V_B}{\omega_B M_Q}$$

$$-L_{du} \frac{d}{dt_u} i_{du} - \sqrt{3/2}\, M_F \frac{\omega_B}{V_B} \frac{\sqrt{2} V_B}{\omega_B M_F} \frac{d}{dt_u} i_{Fu} - \sqrt{3/2}\, M_D \frac{\omega_B}{V_B} \frac{\sqrt{2} V_B}{\omega_B M_D} \frac{d}{dt_u} i_{Du}$$

$$v_{du} = -r_u i_{du} - \omega_u L_{qu} i_{qu} - \omega_u \sqrt{3/2}\, M_{Qu} i_{Qu}$$

$$-L_{du} \frac{d}{dt_u} i_{du} - \sqrt{3/2}\, M_{Fu} \frac{d}{dt_u} i_{Du}$$

The q-axis voltage is computed as follows.

$$v_{qu} V_B = \omega_u \omega_B L_d i_{du} I_B - r i_{qu} I_B + \omega_u \omega_B \sqrt{3/2}\, M_F i_{Fu} I_{FB}$$

$$+\omega_u \omega_B \sqrt{3/2}\, M_D i_{Du} I_{DB} - L_q \omega_B \frac{d}{dt_u} i_{qu} I_B - \sqrt{3/2}\, M_Q \omega_B \frac{d}{dt_u} i_{Qu} I_{QB}$$

or

$$v_{qu} = \omega_u i_{du} L_{du} - i_{qu} r_u + \omega_u i_{Fu} \sqrt{3/2}\, M_{Fu}$$

$$+\omega_u i_{Du} \sqrt{3/2}\, M_{Du} - L_{qu} \frac{d}{dt_u} i_{qu} - \sqrt{3/2}\, M_{Qu} \frac{d}{dt_u} i_{Qu}$$

The field voltage equation becomes

$$-v_{Fu} V_{FB} = -r_F i_{Fu} I_{FB} - \sqrt{3/2}\, M_F \omega_B \frac{d}{dt_u} i_{du} I_B$$

$$-L_F \omega_B \frac{d}{dt_u} i_{Fu} I_{FB} - M_R \omega_B \frac{d}{dt_u} i_{Du} I_{DB}$$

or

$$-v_{Fu} = -r_{Fu}i_{Fu} - \sqrt{3/2}\, M_{Fu} \frac{d}{dt_u} i_{du} - L_{Fu} \frac{d}{dt_u} i_{Fu} - M_{Ru} \frac{d}{dt_u} i_{Du}.$$

Similarly the damper winding voltages are

$$0 = v_{Du}V_{DB} = -r_D i_{Du} I_{DB} - \sqrt{3/2}\, M_D \omega_B \frac{d}{dt_u} i_{du} I_B$$

$$-M_R \omega_B \frac{d}{dt_u} i_{Fu} I_{FB} - L_D \omega_B \frac{d}{dt_u} i_{Du} I_{DB}$$

$$= -r_{Du}i_{Du} - \sqrt{3/2}\, M_{Du} \frac{d}{dt_u} i_{du} - \omega_B M_{Ru} \frac{d}{dt_u} i_{Fu} - L_{Du} \frac{d}{dt_u} i_{Du}$$

and

$$0 = v_{Qu}V_{QB} = -r_Q i_{Qu} I_{QB} - \sqrt{3/2}\, M_Q \omega_B \frac{d}{dt_u} i_{qu} I_B - L_Q \omega_B \frac{d}{dt_u} i_{Qu} I_{QB}$$

$$0 = -r_{Qu}i_{Qu} - \sqrt{3/2}\, M_{Qu} \frac{d}{dt_u} i_{qu} - L_{Qu} \frac{d}{dt_u} i_{Qu}.$$

The resulting machine equation in per unit is

$$\begin{bmatrix} v_o \\ v_d \\ v_q \\ -v_F \\ 0 \\ 0 \end{bmatrix} = -\begin{bmatrix} r_u+3r_n & 0 & 0 & 0 & 0 & 0 \\ 0 & r & +\omega L_q & 0 & 0 & +\omega\sqrt{3/2}M_Q \\ 0 & -\omega L_d & r & -\omega\sqrt{3/2}M_F & -\omega\sqrt{3/2}M_D & 0 \\ 0 & 0 & 0 & r_F & 0 & 0 \\ 0 & 0 & 0 & 0 & r_D & 0 \\ 0 & 0 & 0 & 0 & 0 & r_Q \end{bmatrix} \begin{bmatrix} i_o \\ i_d \\ i_q \\ i_F \\ i_D \\ i_Q \end{bmatrix}$$

(continued on next page)

$$-\begin{bmatrix} L_o+3L_n & 0 & 0 & 0 & 0 & 0 \\ 0 & L_d & 0 & +\sqrt{3/2}M_F & +\sqrt{3/2}M_D & 0 \\ 0 & 0 & L_q & 0 & 0 & +\sqrt{3/2}M_Q \\ 0 & +\sqrt{3/2}M_F & 0 & L_F & M_F & 0 \\ 0 & +\sqrt{3/2}M_D & 0 & M_R & L_D & 0 \\ 0 & 0 & +\sqrt{3/2}M_Q & 0 & 0 & L_Q \end{bmatrix} \begin{bmatrix} \dot{i}_o \\ \dot{i}_d \\ \dot{i}_q \\ \dot{i}_F \\ \dot{i}_D \\ \dot{i}_Q \end{bmatrix} \quad \text{per unit} \qquad [A\text{-}42]$$

Comparison with Equation A-39 shows that the above per-unit equation has the same form as the dimensional one.

10. Normalized voltage equations using flux linkage as a variable

Normalizing Equation A-40 we compute the following.

$$v_{ou}V_B/V_B = -(r+3r_n)\, i_{ou}\frac{I_B}{V_B} - 3L_n\omega_B \frac{d}{dt_u} i_{ou}\frac{I_B}{V_B} - \frac{\omega_B}{V_B}\frac{d}{dt_u}\lambda_o$$

$$v_{ou} = -(r_u+3r_{nu})\, i_{ou} - 3L_{nu}\frac{d}{dt_u} i_{ou} - \frac{d}{dt_u}\lambda_{ou}$$

$$v_{du}\frac{V_B}{V_B} = -\, ri_{du}\frac{I_B}{V_B} - \frac{\omega_B}{V_B}\frac{d}{dt_u}\lambda_d - \frac{\omega_u}{V_B}\omega_B\lambda_q$$

$$v_{du} = -\, r_u i_{du} - \frac{d}{dt_u}\lambda_{du} - \omega_u\lambda_{qu}$$

$$v_{qu}\frac{V_B}{V_B} = -\, ri_{qu}I_B + \omega_u\frac{\omega_B}{V_B}\lambda_d - \frac{\omega_B}{V_B}\frac{d}{dt_u}\lambda_q$$

$$v_{qu} = -\, r_u i_{qu} + \omega_u\lambda_{du} - \frac{d}{dt_u}\lambda_{qu}$$

$$-v_{Fu}\frac{V_{FB}}{V_{FB}} = -\, r_F\, i_{Fu}\frac{I_{FB}}{V_{FB}} - \frac{\omega_B}{V_{FB}}\frac{d}{dt_u}\lambda_F$$

$$-v_{Fu} = -r_{Fu}\, i_{Fu} - \frac{d}{dt_u}\lambda_{Fu}$$

$$0 = v_{Du}\frac{V_{DB}}{V_{DB}} = -r_D\, i_{Du}\frac{I_{DB}}{V_{DB}} - \frac{\omega_B}{V_{DB}}\frac{d}{dt_u}\lambda_D$$

$$0 = -r_{Du}\, i_{Du} - \frac{d}{dt_u}\lambda_{Du}$$

$$0 = v_{qu}\frac{V_{QB}}{V_{QB}} = -r_q\, i_{qu}\frac{I_{QB}}{V_{QB}} - \frac{\omega_B}{V_{QB}}\frac{d}{dt_u}\lambda_Q$$

$$0 = -r_{Qu}\, i_{Qu} - \frac{d}{dt_u}\lambda_{Qu}$$

Writing the above equations in matrix form the following expression results.

$$\begin{bmatrix} v_o \\ v_d \\ v_q \\ -v_F \\ 0 \\ 0 \end{bmatrix} = -\begin{bmatrix} r+3r_n+3L_n p_u & 0 & 0 & 0 & 0 & 0 \\ 0 & r & 0 & 0 & 0 & 0 \\ 0 & 0 & r & 0 & 0 & 0 \\ 0 & 0 & 0 & r_F & 0 & 0 \\ 0 & 0 & 0 & 0 & r_D & 0 \\ 0 & 0 & 0 & 0 & 0 & r_Q \end{bmatrix}\begin{bmatrix} i_o \\ i_d \\ i_q \\ i_F \\ i_D \\ i_Q \end{bmatrix}$$

$$-\begin{bmatrix} p_u & 0 & 0 & 0 & 0 & 0 \\ 0 & p_u & +\omega & 0 & 0 & 0 \\ 0 & -\omega & p_u & 0 & 0 & 0 \\ 0 & 0 & 0 & p_u & 0 & 0 \\ 0 & 0 & 0 & 0 & p_u & 0 \\ 0 & 0 & 0 & 0 & 0 & p_u \end{bmatrix}\begin{bmatrix} \lambda_o \\ \lambda_d \\ \lambda_q \\ \lambda_F \\ \lambda_D \\ \lambda_Q \end{bmatrix} \quad \text{per unit} \qquad [A\text{-}43]$$

D. Equivalent Circuit Using Mutual and Leakage Inductances

From the preceding discussion it is apparent that with the machine base quantities chosen in this development the dimensional and per unit equations are the same. Consider the flux linkage Equation A-18 written in per-unit form with λ_o now referred to as λ_o^*.

$$\begin{bmatrix} \lambda_o^* \\ \lambda_d \\ \lambda_q \\ \lambda_F \\ \lambda_D \\ \lambda_Q \end{bmatrix} = \begin{bmatrix} (L_o-\ell_o)+\ell_o & 0 & 0 & 0 & 0 & 0 \\ 0 & (L_d-\ell_d)+\ell_d & 0 & +\sqrt{3/2}M_F & +\sqrt{3/2}M_D & 0 \\ 0 & 0 & (L_q-\ell_q)+\ell_q & 0 & 0 & +\sqrt{3/2}M_Q \\ 0 & +\sqrt{3/2}M_F & 0 & (L_F-\ell_F)+\ell_F & M_R & 0 \\ 0 & +\sqrt{3/2}M_D & 0 & M_R & (L_D-\ell_D)+\ell_D & 0 \\ 0 & 0 & +\sqrt{3/2}M_Q & 0 & 0 & (L_Q-\ell_Q)+\ell_Q \end{bmatrix} \begin{bmatrix} i_o \\ i_d \\ i_q \\ i_F \\ i_D \\ i_Q \end{bmatrix} \text{ per unit} \quad [A-44]$$

Set i_d = 1.0 pu and all other currents equal to 0. The d-axis mutual λ's are

$$(L_d-\ell_d) = \sqrt{3/2}M_F = \sqrt{3/2}M_D \quad [A-45]$$

If i_F = 1.0 pu and all other currents are zero then the d-axis mutuals are

$$\sqrt{3/2}M_F = (L_F-\ell_F) = M_R \quad [A-46]$$

and similarly when i_D = 1.0 pu

$$\sqrt{3/2}M_D = M_R = (L_D-\ell_D) \quad [A-47]$$

Similar evaluations of the q-axis mutual λ's yield the following results.

$$(L_q-\ell_q) = \sqrt{3/2}M_Q \quad [A-48]$$

$$\sqrt{3/2}M_Q = (L_Q-\ell_Q) \quad [A-49]$$

The per-unit mutual inductances in the d-axis are all observed to be equal so define the magnetizing inductance in the d-axis as follows.

$$L_{AD} = (L_d - \ell_a) = \sqrt{3/2}M_F = \sqrt{3/2}M_D = (L_F - \ell_F) = M_R = (L_D - \ell_D) \qquad [A\text{-}50]$$

The per-unit mutual inductances in the q-axis are also the same and the magnetizing inductance in the q-axis may be defined as follows.

$$L_{AQ} = (L_q - \ell_a) = \sqrt{3/2}M_Q = (L_Q - \ell_Q) \qquad [A\text{-}51]$$

where

$$\ell_a = \ell_d = \ell_q$$

is the armature leakage inductance in per unit and is the same in both axes.

Define

$$\lambda_{AD} = L_{AD}(i_d + i_F + i_D) \qquad \text{per unit} \qquad [A\text{-}52]$$

$$\lambda_{AQ} = L_{AQ}(i_q + i_Q) \qquad [A\text{-}53]$$

The flux linkage Equation A-44 may now be rewritten in terms of mutual and leakage flux linkages.

$$\begin{aligned} \lambda_o^* &= L_o i_o \\ \lambda_d &= \lambda_{AD} + \ell_a i_d \\ \lambda_q &= \lambda_{AQ} + \ell_a i_q \\ \lambda_F &= \lambda_{AD} + \ell_F i_F \\ \lambda_D &= \lambda_{AD} + \ell_D i_D \\ \lambda_Q &= \lambda_{AQ} + \ell_Q i_Q \end{aligned} \qquad \text{per unit} \qquad [A\text{-}54]$$

The machine voltage Equation A-42 may also be rewritten in terms of mutual and leakage flux linkages.

$$
\begin{aligned}
v_o &= -(r+3r_n)i_o - p\lambda_o \qquad \text{where } \lambda_o = i_o(L_o+3L_n) \\
v_d &= -ri_d - \omega\lambda_q - p\lambda_{AD} - \ell_a p i_d \\
v_q &= -ri_q + \omega\lambda_d - p\lambda_{AQ} - \ell_a p i_q \\
-v_F &= -r_F i_F - p\lambda_F = -r_F i_F - p\lambda_{AD} - \ell_F p i_F \\
0 &= -r_D i_D - p\lambda_{AD} - \ell_D p i_D \\
0 &= -r_Q i_Q - p\lambda_{AQ} - \ell_Q p i_Q
\end{aligned}
\qquad \text{per unit} \qquad [A\text{-}55]
$$

The equivalent circuits for voltage Equation A-55 are shown in Figure 60.

E. Development of Analog Computer Equations for a Synchronous Generator

Eliminate currents between flux linkage equation, Equation A-54, and the voltage equation, Equation A-55.

$$
\begin{aligned}
i_o &= \frac{\lambda_o}{L_o + 3L_n} \\
i_d &= \frac{\lambda_d - \lambda_{AD}}{\ell_a} \\
i_q &= \frac{\lambda_q - \lambda_{AQ}}{\ell_a} \\
i_F &= \frac{\lambda_F - \lambda_{AD}}{\ell_F} \\
i_D &= \frac{\lambda_D - \lambda_{AD}}{\ell_D} \\
i_Q &= \frac{\lambda_Q - \lambda_{AQ}}{\ell_Q}
\end{aligned}
\qquad \text{per unit} \qquad [A\text{-}56]
$$

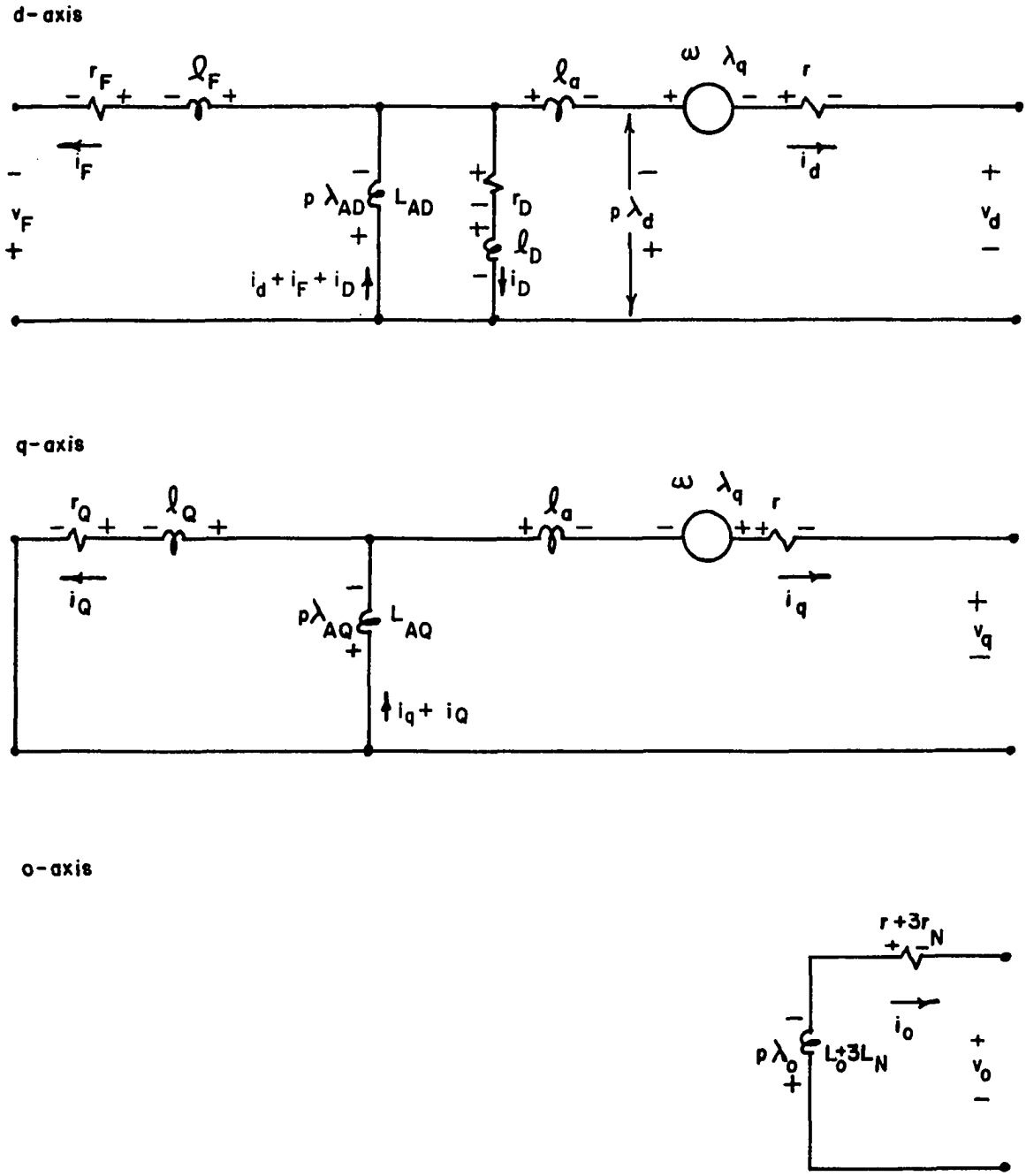

Figure 60. Equivalent circuits for synchronous machine

From Equation A-52,

$$\lambda_{AD} = L_{AD}\left[\frac{\lambda_d - \lambda_{AD}}{\ell_a} + \frac{\lambda_F - \lambda_{AD}}{\ell_F} + \frac{\lambda_D - \lambda_{AD}}{\ell_D}\right] \qquad [A-52]$$

$$\lambda_{AD} = L_{AD}\left[\frac{\lambda_d}{\ell_a} + \frac{\lambda_F}{\ell_F} + \frac{\lambda_D}{\ell_D} - \lambda_{AD}\left[\frac{1}{\ell_a} + \frac{1}{\ell_F} + \frac{1}{\ell_D}\right]\right]$$

$$\lambda_{AD}\left[\frac{1}{L_{AD}} + \frac{1}{\ell_a} + \frac{1}{\ell_F} + \frac{1}{\ell_D}\right]L_{AD} = \left[\frac{\lambda_d}{\ell_a} + \frac{\lambda_F}{\ell_F} + \frac{\lambda_D}{\ell_D}\right]L_{AD}$$

Define

$$L_{MD} = \frac{1}{\frac{1}{L_{AD}} + \frac{1}{\ell_a} + \frac{1}{\ell_F} + \frac{1}{\ell_D}} \qquad [A-57]$$

So

$$\lambda_{AD} = L_{MD}\left[\frac{\lambda_d}{\ell_a} + \frac{\lambda_F}{\ell_F} + \frac{\lambda_D}{\ell_D}\right] \qquad [A-58]$$

Similarly from Equation A-53,

$$\lambda_{AQ} = L_{AQ}\,[i_q + i_Q] \qquad [A-53]$$

$$\lambda_{AQ} = L_{AQ}\left[\frac{\lambda_q - \lambda_{AQ}}{\ell_a} + \frac{\lambda_Q - \lambda_{AQ}}{\ell_Q}\right]$$

$$= L_{AQ}\left[\frac{\lambda_q}{\ell_a} + \frac{\lambda_Q}{\ell_Q} - \lambda_{AQ}\left[\frac{1}{\ell_a} + \frac{1}{\ell_Q}\right]\right]$$

$$\lambda_{AQ}\left[\frac{1}{L_{AQ}} + \frac{1}{\ell_a} + \frac{1}{\ell_a}\right]L_{AQ} = L_{AQ}\left[\frac{\lambda_q}{\ell_a} + \frac{\lambda_Q}{\ell_a}\right]$$

Define

$$L_{MQ} = \frac{1}{\frac{1}{L_{AQ}} + \frac{1}{\ell_a} + \frac{1}{\ell_Q}} \qquad [A-59]$$

So

$$\lambda_{AQ} = L_{MQ}\left[\frac{\lambda_q}{\ell_a} + \frac{\lambda_Q}{\ell_Q}\right] \qquad [A-60]$$

Eliminate currents from Equation A-55 using Equation A-56.

$$v_{ou} = -(r_u+3r_{nu})\frac{\lambda_o}{L_{ou}+3L_{nu}} - \frac{d}{dt_u}\lambda_{ou}$$

$$\frac{d}{dt_u}\lambda_{ou} = -v_{ou} - \frac{(r_u+3r_{nu})}{(L_{ou}+3L_{nu})}\lambda_{ou}$$

But

$$\frac{d}{dt_u} = \frac{1}{\omega_B}\frac{d}{dt}$$

so

$$\lambda_{ou} = -\omega_B\int v_{ou} + \frac{r_u+3r_{nu}}{L_{ou}+3L_{nu}}\lambda_{ou}\ dt. \qquad [A-61]$$

To compute λ_{du}, write

$$v_{du} = -r_u\left[\frac{\lambda_{du}-\lambda_{ADu}}{\ell_{au}}\right] - \omega_u\lambda_{qu} - \frac{d}{dt_u}\lambda_{ADu} - \ell_{au}\frac{d}{dt_u}\frac{\lambda_{du}-\lambda_{ADu}}{\ell_{au}}$$

$$v_{du} = \frac{-r_u}{\ell_{au}}(\lambda_{du}-\lambda_{ADu}) - \omega_u\lambda_{qu} - \frac{d}{dt_u}\lambda_{du}$$

and

$$\lambda_{du} = \omega_B \int -v_{du} + \frac{r_u}{\ell_{au}} (\lambda_{ADu} - \lambda_{du}) - \frac{\omega}{\omega_B} \lambda_{qu} \quad dt. \qquad [A-62]$$

Similarly for λ_{qu}, compute

$$v_{qu} = -r_u \frac{\lambda_{qu}-\lambda_{AQu}}{\ell_{au}} + \omega_u \lambda_{du} - \frac{d}{dt_u} \lambda_{AQu} - \ell_{au} \frac{d}{dt_u} \frac{\lambda_{qu}-\lambda_{AQu}}{\ell_{au}}$$

$$v_{qu} = -r_u \frac{\lambda_{qu}-\lambda_{AQu}}{\ell_{au}} + \omega_u \lambda_{du} - \frac{d}{dt_u} \lambda_{qu}$$

$$\lambda_{qu} = \omega_B \int -v_{qu} - \frac{r_u(\lambda_{qu}-\lambda_{AQu})}{\ell_{au}} + \frac{\omega}{\omega_B} \lambda_{du} \quad dt. \qquad [A-63]$$

λ_{Fu} is computed from

$$-v_{Fu} = -r_{Fu} \frac{(\lambda_{Fu}-\lambda_{ADu})}{\ell_{Fu}} - \frac{d}{dt_u} \lambda_{Fu}$$

or

$$\lambda_{Fu} = \omega_B \int v_{Fu} + \frac{r_{Fu}}{\ell_{Fu}} (\lambda_{ADu}-\lambda_{Fu}) \quad dt. \qquad [A-64]$$

Finally λ_{Du} and λ_{Qu} are computed as follows.

$$0 = \frac{-r_{Du}}{\ell_{Du}} (\lambda_{Du}-\lambda_{ADu}) - \frac{d}{dt_u} \lambda_{ADu} - \ell_{Du} \frac{d}{dt_u} \frac{(\lambda_{Du}-\lambda_{ADu})}{\ell_{Du}}$$

$$\lambda_{Du} = \omega_B \int + \frac{r_{Du} (\lambda_{ADu}-\lambda_{Du})}{\ell_{Du}} dt. \qquad [A-65]$$

and

$$0 = -r_{Qu} \frac{(\lambda_{Qu}-\lambda_{AQu})}{\ell_{Qu}} - \frac{d}{dt_u} \lambda_{AQu} - \ell_{Qu} \frac{d}{dt_u} \frac{(\lambda_{Qu}-\lambda_{AQu})}{\ell_{Qu}}$$

$$\lambda_{Qu} = \omega_B \int \frac{r_{Qu}}{\ell_{Qu}} (\lambda_{AQu} - \lambda_{Qu})\, dt. \qquad [A-66]$$

1. Torque equations

The equation of motion of the machine rotor may be expressed as

$$J \frac{2}{p} \frac{d\omega}{dt} = T_m - T_e \quad \text{newton-meters} \qquad [A-67]$$

where

ω = speed of rotor in radians/sec

p = the number of poles of the machine

T_m, T_e = mechanical and electrical torque, respectively newton-meters

J = rotor inertia kilogram-meter^2

This equation may be converted to per unit as follows. From fundamental concepts

$$P = \omega T \quad \text{where P is power in watts} \qquad [A-68]$$

Since base speed and base power (base volt-amps) have already been defined, base torque is defined as follows.

$$\omega_B T_B = S_B = V_B I_B$$

$$T_B = S_B/\omega_B \qquad [A-69]$$

Base moment of inertia may also be defined as follows.

$$T = J \frac{d\omega}{dt} \qquad [A-70]$$

so $T_B = J_B\, \omega_B / t_B$

$$\text{or} \quad J_B = T_B/\omega_B^2 \quad \text{since} \quad t_B = 1/\omega_B \qquad [A\text{-}71]$$

Equation A-67 is now normalized.

$$\frac{2}{p} J_u J_B \frac{d\omega_u \omega_B}{dt_u t_B} = T_{mu} T_B - T_{eu} T_B$$

and

$$\frac{2}{p} J_u \frac{d\omega_u}{dt_u} = T_{mu} - T_{eu} \qquad [A\text{-}72]$$

Rather than specify the moment of inertia of a machine rotor, manufacturers generally supply the inertia constant H where

$$H = \frac{\text{internally stored energy at synchronous speed}}{\text{rated KVA of machine}} \quad \text{sec} \qquad [A\text{-}73]$$

and $J = 2\,\omega_B H$. Again base H is defined in terms of previously defined base quantities.

$$J_B = \omega_B H_B$$

$$H_B = \frac{J_B}{\omega_B} = \frac{T_B}{\omega_B^3} \qquad [A\text{-}74]$$

$$\text{Then} \quad J_u J_B = 2\omega_B H_u H_B$$

$$J_u = 2\,H_u \qquad [A\text{-}75]$$

As noted previously all base quantities are defined in terms of the rated values of the machine. S_B is the rated single-phase output of the machine and the rated KVA of the machine is then $3S_B$. From Equations A-69 and A-71,

$$J_B = \frac{S_B}{\omega_B{}^3}$$

so the moment of inertia of a machine operating at rated conditions is

$$J_{rated} = \frac{S_{rated}}{(\omega_{rated})^3}$$

expressed in terms of single-phase quantities, or

$$J = 3J_{rated} = \frac{3S_{rated}}{(\omega_{rated})^3} = 3J_B$$

expressed in terms of 3-phase quantities.

From Equation A-73

$$H = \frac{1/2\ J\omega^2}{3S} \quad \text{at rated conditions}$$

$$= \frac{1/2\ J_B\omega_B{}^2}{S_B}$$

$$= \frac{1}{2\omega_B}$$

But $H = H_u H_B = 1/2\ \omega_B$

so $H_u = 1/2$

and $H_B = 1/\omega_B$

Equation A-72 is now expressed in terms of H_u.

$$\frac{d\omega_u}{dt_u} = \frac{p}{2}\left[\frac{1}{2\ H_u}\right]\left[T_{mu} - T_{eu}\right] \qquad [A-76]$$

Define

$$T_{au} = T_{mu} - T_{eu} \qquad [A-77]$$

Equation A-76 is now integrated to find ω_u.

$$\omega_u = \frac{p}{2}\left[\frac{1}{2H_u}\right]\int T_{au}\, dt_u + \omega_{ou} \qquad [A-78]$$

where ω_{ou} is the initial value and equals 1. For purposes of analog computer simulation, integration should be with respect to time rather than normalized time so Equation A-78 is modified as follows.

$$\omega_u = \frac{p}{2}\frac{1}{2H_u\left[\frac{1}{\omega_B}\right]}\int T_{au}\,\frac{dt_u}{\omega_B} + 1.$$

so

$$\omega_u = \frac{p}{2}\left[\frac{1}{2H}\right]\int T_{au}\, dt + 1. \qquad [A-79]$$

where H and t have dimensions of seconds but ω and T are in per unit.

Define

$$\Delta\omega_u \triangleq \frac{p}{2}\left[\frac{1}{2H}\right]\int T_{au}\, dt \qquad [A-80]$$

Then

$$\omega_u = \Delta\omega_u + 1 \qquad [A-81]$$

From Equation A-4

$$\theta = \omega_B t + \delta + 90° \text{ electrical radians} \qquad [A-4]$$

Define

$$\omega \triangleq \dot{\theta} = \omega_B + \dot{\delta} \qquad [A-82]$$

and converting Equation A-81 to dimensional quantities by multiplying by ω_B

$$\omega = \Delta\omega + \omega_B \qquad \text{[A-83]}$$

Compare this with Equation A-82.

$$\Delta\omega = \dot{\delta} \quad \text{radians/sec} \qquad \text{[A-84]}$$

Integrating Equation A-84

$$\delta = \int \Delta\omega \, dt + \delta_o \quad \text{radians} \qquad \text{[A-85]}$$

So

$$\delta = \left(57.3 \frac{\text{degrees}}{\text{radian}}\right)\left[\omega_B \int \Delta\omega_u \, dt + \delta_o\right] \text{ mechanical degrees} \qquad \text{[A-86]}$$

2. Electrical torque equation

The following dimensional equation for electrical torque is given by Lewis (75).

$$T_e = \frac{p}{2}[\lambda_d i_q - \lambda_q i_d] \quad \text{newton-meters} \qquad \text{[A-87]}$$

Normalizing

$$T_{eu}T_B = \frac{p}{2}[\lambda_d i_{qu} I_B - \lambda_q i_{du} I_B]$$

$$T_{eu} = \frac{p}{2}[\lambda_{du} i_{qu} - \lambda_{qu} i_{du}] \qquad \text{[A-88]}$$

The above choices of base quantities cause the dimensional equations and normalized equations to have the same form. Note, howver, that S_B which serves as a base for power is defined in terms of rated line-to-neutral machine terminal voltage and rated line current. A machine delivering 1 pu terminal voltage and 1 pu terminal current has a 3 Ø power output of 3 pu. With the above choices of bases, a two-pole machine

operating as above has mechanical and electrical torques of approximately 3 pu also.

If the generator were unloaded, differentiation would need to be performed on the analog computer to develop the terminal voltages. Placing a large resistance on the machine terminals allows the terminal voltage quantities to be measured without actually performing the differentiation (68). The following equations relate generator currents i_q and i_d, transmission line currents i_{qt} and i_{dt}, and terminal voltages v_q and v_d.

$$v_q = R(i_q - i_{qt}) \qquad [A-89]$$

$$v_d = R(i_d - i_{dt}) \qquad [A-90]$$

where R is the resistance placed at the machine terminals.

The rms equivalent magnitude of the machine terminal voltage is found from v_d and v_q as follows.

$$v_{todq} = \sqrt{3}V_{tabc} = \sqrt{v_d^2 + v_q^2} \qquad [A-91]$$

3. Infinite bus equations

Assume the synchronous machine is connected to an infinite bus through a transmission line having impedance $R_E + jX_E$ ohms.

V_B = stator base line-to-neutral voltage rms

= infinite bus voltage line-to-neutral rms

Define the abc infinite bus voltages as follows.

$$\begin{aligned} V_{a\infty} &= \sqrt{2}V_B \cos \omega_B t \\ V_{b\infty} &= \sqrt{2}V_B \cos(\omega_B t - 120) \quad \text{volts} \\ V_{c\infty} &= \sqrt{2}V_B \cos(\omega_B t + 120) \end{aligned} \qquad [A-92]$$

A circuit diagram showing phase a of a synchronous machine connected to an infinite bus through a transmission line is shown in Figure 61. From this figure the following matrix equation is written since phases b and c are similar.

$$\underline{v}_{abc} = \underline{V}_{abc\infty} + R_E\underline{i}_{abc} + L_E\dot{\underline{i}}_{abc} \quad \text{volts} \qquad [A\text{-}93]$$

The above equation is transformed to the odq reference system using the Park-type transformation as follows.

$$\underline{Pv}_{abc} = \underline{PV}_{abc\infty} + R_E\underline{Pi}_{abc} + L_E\dot{\underline{Pi}}_{abc} \quad \text{volts} \qquad [A\text{-}94]$$

where

$$\underline{V}_{abc\infty} = \sqrt{2}V_B \begin{bmatrix} \cos\ \omega_B t \\ \cos(\omega_B t - 120) \\ \cos(\omega_B t + 120) \end{bmatrix} \quad \text{volts} \qquad [A\text{-}95]$$

Transforming the above equation and using the fact that $\theta = \omega_B t + \delta + 90$,

$$\underline{V}_{odq\infty} = \sqrt{3}V_B \begin{bmatrix} 0 \\ -\sin\ \delta \\ \cos\ \delta \end{bmatrix} \quad \text{volts} \qquad [A\text{-}96]$$

$\dot{\underline{Pi}}_{abc}$ is computed as follows. By definition

$$\underline{i}_{odq} = \underline{Pi}_{abc}$$

Differentiating

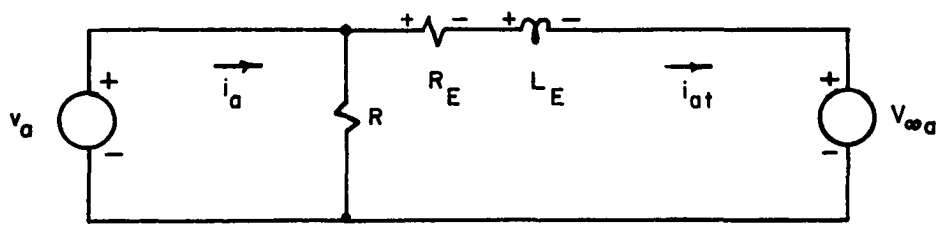

Figure 61. Synchronous machine connected to an infinite bus through a transmission line

$$\dot{\underline{i}}_{odq} = \dot{\underline{Pi}}_{abc} + \underline{P\dot{i}}_{abc}$$

So

$$\dot{\underline{Pi}}_{abc} = \dot{\underline{i}}_{odq} - \underline{P\dot{i}}_{abc} = \dot{\underline{i}}_{odq} - \underline{\dot{P}P^{-1}i}_{odq} \qquad [A\text{-}97]$$

where

$$\underline{\dot{P}P^{-1}} = \omega \begin{bmatrix} 0 & 0 & 0 \\ 0 & 0 & -1 \\ 0 & 1 & 0 \end{bmatrix} \qquad [A\text{-}31]$$

Equation A-94 is now rewritten as follows using Equation A-97.

$$\underline{v}_{odq} = \underline{V}_{odq\infty} + R_E\underline{i}_{odq} + L_E\dot{\underline{i}}_{odq} - L_E\underline{\dot{P}P^{-1}i}_{odq} \qquad [A\text{-}98]$$

If the above quantities are substituted into Equation A-98 the following matrix equation results.

$$\begin{bmatrix} v_o \\ v_d \\ v_q \end{bmatrix} \underline{=} \sqrt{3}V_B \begin{bmatrix} 0 \\ -\sin\delta \\ +\cos\delta \end{bmatrix} + R_E \begin{bmatrix} i_o \\ i_d \\ i_q \end{bmatrix} + L_E \begin{bmatrix} \dot{i}_o \\ \dot{i}_d \\ \dot{i}_q \end{bmatrix} - \omega L_E \begin{bmatrix} 0 & 0 & 0 \\ 0 & 0 & -1 \\ 0 & 1 & 0 \end{bmatrix} \begin{bmatrix} i_o \\ i_d \\ i_q \end{bmatrix} \qquad [A\text{-}99]$$

Currents are subscripted with "t" to indicate currents flowing from the generator terminals to the infinite bus, and the d- and q-axes voltage equations are solved for $\dot{i}_{dt}$ and $\dot{i}_{qt}$, respectively, yielding

$$i_{dt} = \frac{1}{L_E P}\left[v_d + \sqrt{3}V_B \sin\delta - R_E i_{dt} - \omega L_E i_{qt}\right] \qquad [A\text{-}100]$$

$$i_{qt} = \frac{1}{L_E P}\left[v_q - \sqrt{3}V_B \cos\delta - R_E i_{qt} + \omega L_E i_{dt}\right] \qquad [A\text{-}101]$$

The equations are normalized as follows.

$$i_{dtu}I_B = \frac{\omega_B}{L_{Eu}p}\left[v_{du}\frac{V_B}{L_B\omega_B} + \sqrt{3}\sin\delta\frac{V_B}{L_B\omega_B} - R_{Eu}i_{du}\frac{R_BI_B}{L_B\omega_B} - \omega_uL_{Eu}i_{qu}\frac{\omega_BL_BI_B}{\omega_BL_B}\right] \quad [A\text{-}102]$$

Dividing through by I_B

$$i_{dtu} = \frac{\omega_B}{L_{Eu}}\int\left[v_{du} + \sqrt{3}\sin\delta - R_{Eu}i_{dtu} - \omega_uL_{Eu}i_{qtu}\right]dt \quad [A\text{-}103]$$

Similarly,

$$i_{qtu}I_B = \frac{\omega_B}{L_{Eu}p}\left[v_{qu}\frac{V_B}{\omega_BL_B} - \sqrt{3}\cos\delta\frac{V_B}{\omega_BL_B} - R_{Eu}i_{qtu}\frac{R_BI_B}{\omega_BL_B} + \omega_uL_{Eu}i_{qtu}\frac{\omega_BL_BI_B}{\omega_BL_B}\right] \quad [A\text{-}104]$$

Dividing through by I_B

$$i_{qtu} = \frac{\omega_B}{L_{Eu}}\int\left[v_{qu} - \sqrt{3}\cos\delta - R_{Eu}i_{qtu} + \omega_uL_{Eu}i_{dtu}\right]dt \quad [A\text{-}105]$$

The equations necessary to represent a synchronous machine on an analog computer are implemented as shown in Figures 62-66. In these figures "a" denotes the time scaling factor and LC denotes a level change in voltages.

F. Governor Representation

A simplified representation of the governor system of a synchronous machine is shown in block diagram form in Figure 67 (7). Typical constants are as follows (19).

$$\lambda_{ADu} = L_{MDu}\left[\frac{\lambda_{du}}{\ell_{au}} + \frac{\lambda_{Fu}}{\ell_{Fu}} + \frac{\lambda_{Du}}{\ell_{Du}}\right] \qquad [A-58]$$

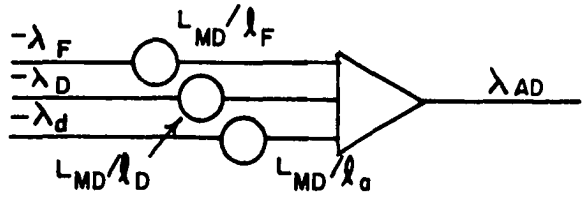

$$\lambda_{du} = \omega_B \int \left[-v_{du} + \frac{r_u}{\ell_{au}}(\lambda_{ADu}-\lambda_{du}) - \frac{\omega}{\omega_B}\lambda_{qu}\right] dt \qquad [A-62]$$

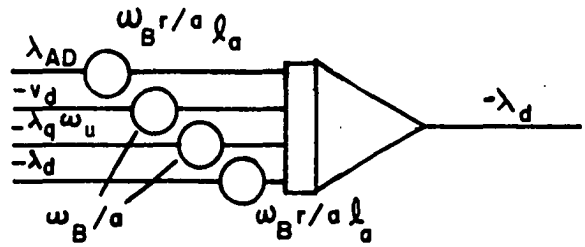

$$\lambda_{Fu} = \omega_B \int \left[v_{Fu} + \frac{r_{Fu}}{\ell_{Fu}}(\lambda_{ADu}-\lambda_{Fu})\right] dt \qquad [A-64]$$

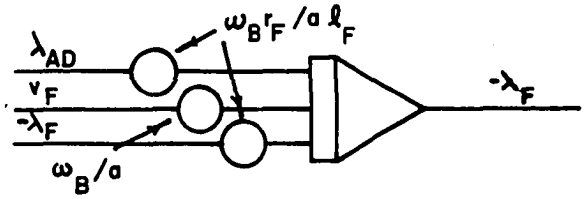

$$\lambda_{Du} = \omega_B \int \frac{r_{Du}(\lambda_{ADu}-\lambda_{Du})}{\ell_{Du}} dt \qquad [A-65]$$

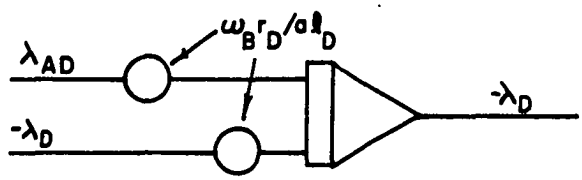

Figure 62. Analog computer implementation of direct axis equations

$$\lambda_{AQu} = L_{MQu}\left[\frac{\lambda_{qu}}{\ell_{au}} + \frac{\lambda_{Qu}}{\ell_{Qu}}\right] \qquad \text{[A-60]}$$

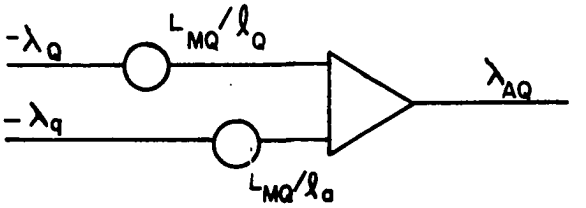

$$\lambda_{qu} = \omega_B \int \left[-v_{qu} - \frac{r_u(\lambda_{qu}-\lambda_{AQu})}{\ell_{au}} + \frac{\omega}{\omega_B}\lambda_{du}\right] dt \qquad \text{[A-63]}$$

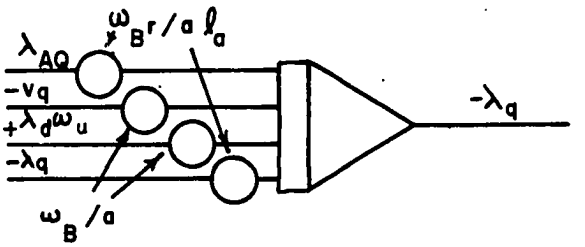

$$\lambda_{Qu} = \omega_B \int \frac{r_{Qu}(\lambda_{AQu}-\lambda_{Qu})}{\ell_{Qu}} dt \qquad \text{[A-66]}$$

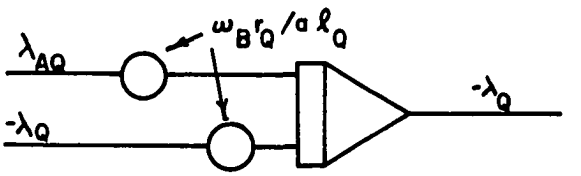

Figure 63. Analog computer implementation of quadrature axis equations

$$T_{eu} = \frac{p}{2}\left[\lambda_{du} i_{qu} - \lambda_{qu} i_{du}\right] \qquad \text{[A-88]}$$

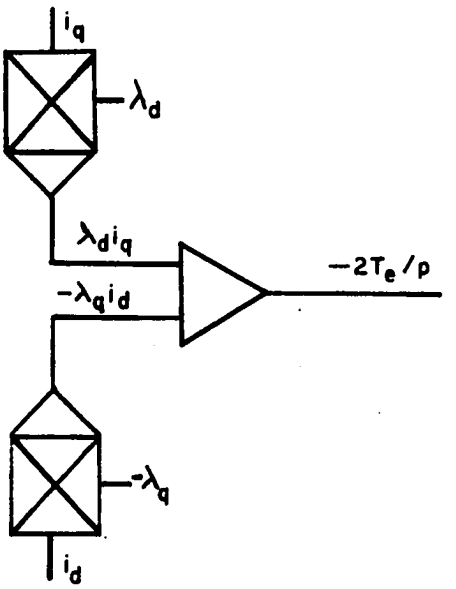

$$T_{au} = T_{mu} - T_{eu} \qquad \text{[A-77]}$$

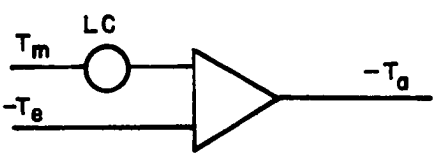

Figure 64. Analog computer implementation of torque equations

$$\Delta\omega_u = \frac{p}{2}\frac{1}{2H}\int T_{au}\,dt \qquad \text{[A-80]}$$

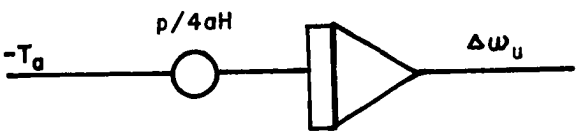

$$\omega_u = \Delta\omega_u + 1 \qquad \text{[A-81]}$$

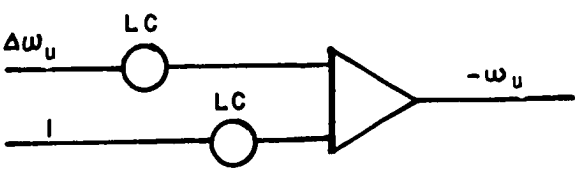

$$\delta = 57.3\left[\omega_B \int \Delta\omega_u\,dt + \delta_o\right] \qquad \text{[A-86]}$$

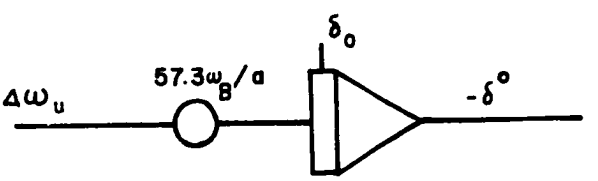

Figure 65. Analog computer implementation of mechanical equations

$$i_{dtu} = \frac{\omega_B}{L_{Eu}} \int \left[v_{du} + \sqrt{3} \sin\delta - R_{Eu} i_{dtu} - \omega_u L_{Eu} i_{qtu} \right] dt \qquad [A\text{-}103]$$

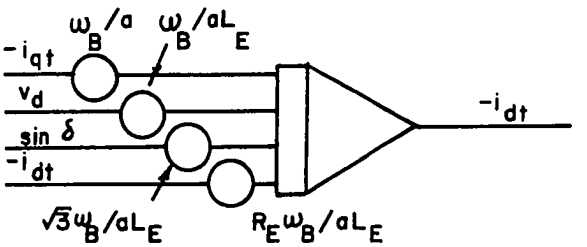

$$i_{qtu} = \frac{\omega_B}{L_{Eu}} \int \left[v_{qu} - \sqrt{3} \cos\delta - R_{Eu} i_{qtu} + \omega_u L_{Eu} i_{dtu} \right] dt \qquad [A\text{-}105]$$

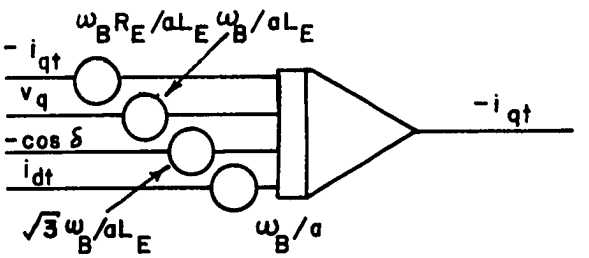

$$v_{du} = R_u(i_{du} - i_{dtu}) \qquad [A\text{-}90]$$

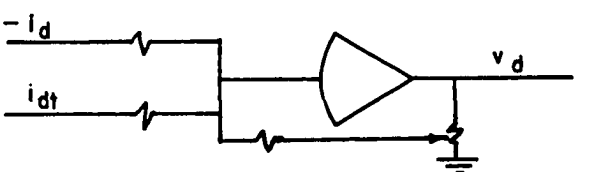

$$v_{qu} = R_u(i_{qu} - i_{qtu}) \qquad [A\text{-}89]$$

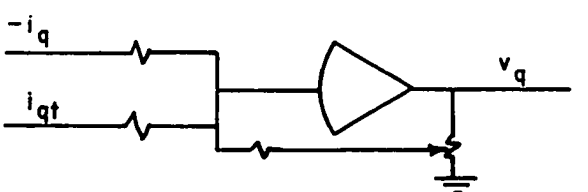

Figure 66. Analog computer implementation of load equations

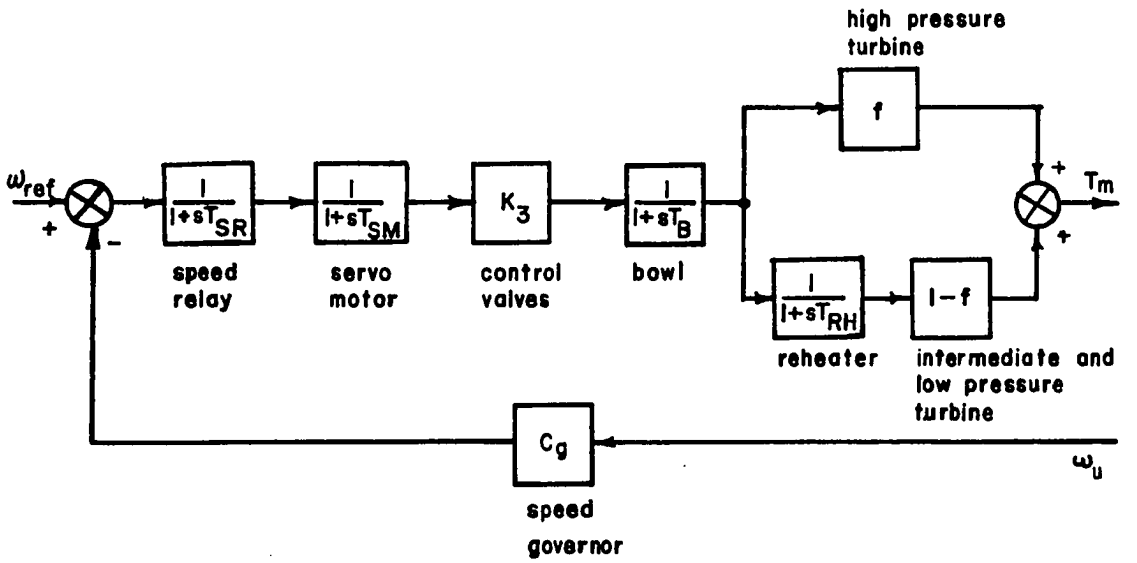

Figure 67. Block diagram of the governing system of a synchronous machine

T_{SR}	=	.05	sec	f	=	.23	
T_{SM}	=	.15	sec	K_3	=	.70	pu
T_B	=	.10	sec	C_g	=	20.	pu
T_{RH}	=	10.0	sec				

The analog computer diagram is developed using Appendix B of (40) and is shown in Figure 68.

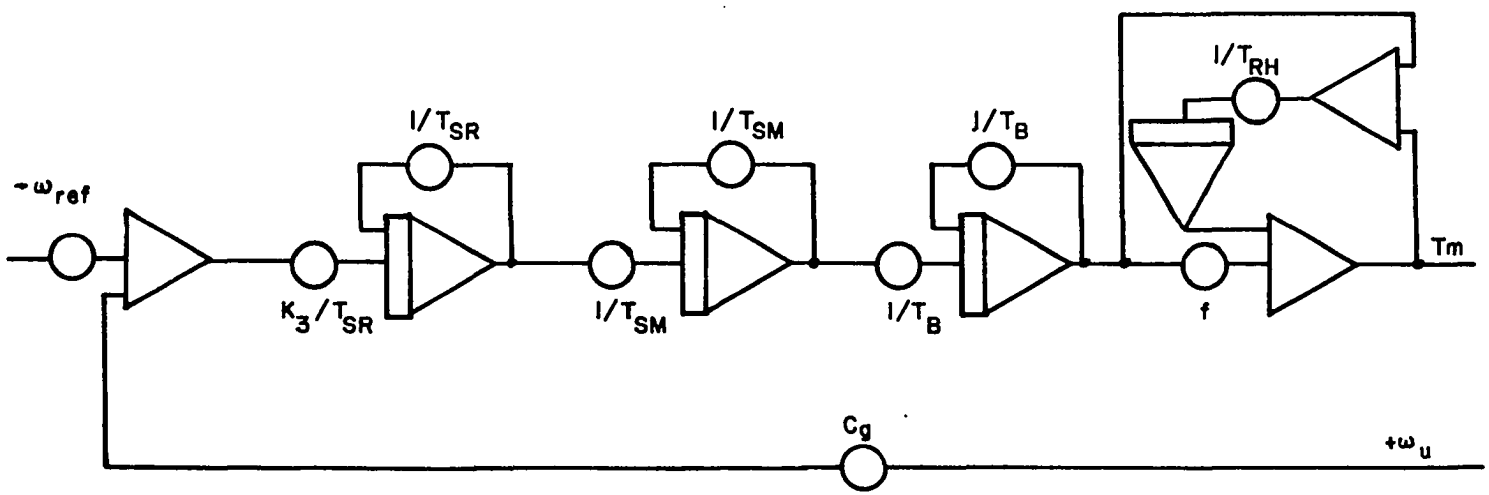

Figure 68. Analog computer diagram of the governing system of a synchronous machine

X. APPENDIX B. DEVELOPMENT OF A LINEAR MODEL OF A SYNCHRONOUS MACHINE

The following nonlinear equation was developed in Appendix A and is repeated here for convenience.

$$\begin{bmatrix} v_o \\ v_d \\ v_q \\ -v_F \\ 0 \\ 0 \end{bmatrix} = -\begin{bmatrix} r+3r_n & 0 & 0 & 0 & 0 & 0 \\ 0 & r & +\omega L_q & 0 & 0 & +\omega\sqrt{3/2}M_Q \\ 0 & -\omega L_d & r & -\omega\sqrt{3/2}M_F & -\omega\sqrt{3/2}M_D & 0 \\ 0 & 0 & 0 & r_F & 0 & 0 \\ 0 & 0 & 0 & 0 & r_D & 0 \\ 0 & 0 & 0 & 0 & 0 & r_Q \end{bmatrix}\begin{bmatrix} i_o \\ i_d \\ i_q \\ i_F \\ i_D \\ i_Q \end{bmatrix}$$

$$-\begin{bmatrix} L_o+3L_n & 0 & 0 & 0 & 0 & 0 \\ 0 & L_d & 0 & +\sqrt{3/2}M_F & +\sqrt{3/2}M_D & 0 \\ 0 & 0 & L_q & 0 & 0 & +\sqrt{3/2}M_Q \\ 0 & +\sqrt{3/2}M_F & 0 & L_F & M_R & 0 \\ 0 & +\sqrt{3/2}M_D & 0 & M_R & L_D & 0 \\ 0 & 0 & +\sqrt{3/2}M_Q & 0 & 0 & L_Q \end{bmatrix}\begin{bmatrix} \dot{i}_o \\ \dot{i}_d \\ \dot{i}_q \\ \dot{i}_F \\ \dot{i}_D \\ \dot{i}_Q \end{bmatrix} \quad \text{per unit} \qquad [A\text{-}42]$$

The above equations are now linearized as follows where all initial conditions are assumed to be steady state, i.e., $\dot{i}(0)=0$ and initial values are constants.

$$\begin{aligned}(v_{do}+v_{d\Delta}) = \; & -r(i_{do}+i_{d\Delta}) - (\omega_o+\omega_\Delta)L_q(i_{qo}+i_{q\Delta}) \\ & - (\omega_o+\omega_\Delta)\sqrt{3/2}M_Q(i_{Qo}+i_{Q\Delta}) - L_d(\dot{i}_{do}+\dot{i}_{d\Delta}) \\ & - \sqrt{3/2}M_F(\dot{i}_{Fo}+\dot{i}_{F\Delta}) - \sqrt{3/2}M_D(\dot{i}_{Do}+\dot{i}_{D\Delta})\end{aligned}$$

$$v_{do} = -ri_{do} - \omega_o L_q i_{qo} - \omega_o \sqrt{3/2} M_Q i_{Qo} \qquad [B\text{-}1]$$

$$v_{d\Delta} = -ri_{d\Delta} - \omega_o L_q i_{q\Delta} - L_q i_{qo} \omega_\Delta - \omega_o \sqrt{3/2} M_Q i_{Q\Delta}$$

$$- \sqrt{3/2} M_Q i_{Qo} \omega_\Delta - L_d \dot{i}_{d\Delta} - \sqrt{3/2} M_F \dot{i}_{F\Delta} - \sqrt{3/2} M_D \dot{i}_{D\Delta} \qquad [B\text{-}2]$$

$$(v_{qo}+v_{q\Delta}) = +(\omega_o+\omega_\Delta) L_d (i_{do}+i_{d\Delta}) - r(i_{qo}+i_{q\Delta})$$

$$+(\omega_o+\omega_\Delta) \sqrt{3/2} M_F (i_{Fo}+i_{F\Delta}) + (\omega_o+\omega_\Delta) \sqrt{3/2} M_D (i_{Do}+i_{D\Delta})$$

$$-L_q (\dot{i}_{qo}+\dot{i}_{q\Delta}) - \sqrt{3/2} M_q (\dot{i}_{Qo}+\dot{i}_{Q\Delta})$$

$$v_{qo} = +\omega_o L_d i_{do} - ri_{qo} + \omega_o \sqrt{3/2} M_F i_{Fo} + \omega_o \sqrt{3/2} M_D i_{Do} \qquad [B\text{-}3]$$

$$v_{q\Delta} = +L_d i_{do} \omega_\Delta + \omega_o L_d i_{d\Delta} - ri_{q\Delta} + \omega_o \sqrt{3/2} M_F i_{F\Delta}$$

$$+\sqrt{3/2} M_F i_{Fo} \omega_\Delta + \omega_o \sqrt{3/2} M_D i_{D\Delta} + \sqrt{3/2} M_D i_{Do} \omega_\Delta$$

$$-L_q \dot{i}_{q\Delta} - \sqrt{3/2} M_Q \dot{i}_{Q\Delta} \qquad [B\text{-}4]$$

$$-(v_{Fo}+v_{F\Delta}) = -r_F (i_{Fo}+i_{F\Delta}) - \sqrt{3/2} M_F (\dot{i}_{do}+\dot{i}_{d\Delta})$$

$$-L_F (\dot{i}_{Fo}+\dot{i}_{F\Delta}) - M_R (\dot{i}_{Do}+\dot{i}_{D\Delta})$$

$$-v_{Fo} = -r_F i_{Fo} \qquad [B\text{-}5]$$

$$-v_{F\Delta} = -r_F i_{F\Delta} - \sqrt{3/2} M_F \dot{i}_{d\Delta} - L_F \dot{i}_{F\Delta} - M_R \dot{i}_{D\Delta} \qquad [B\text{-}6]$$

$$(v_{Do}+v_{D\Delta})=0 = -r_D (i_{Do}+i_{D\Delta}) - \sqrt{3/2} M_D (\dot{i}_{do}+\dot{i}_{d\Delta})$$

$$-M_R (\dot{i}_{Fo}+\dot{i}_{F\Delta}) - L_D (\dot{i}_{Do}+\dot{i}_{D\Delta})$$

$$0 = -r_D i_{Do} \qquad [B\text{-}7]$$

$$0 = -r_D i_{D\Delta} - \sqrt{3/2}M_D \dot{i}_{d\Delta} - M_R \dot{i}_{F\Delta} - L_D \dot{i}_{D\Delta} \quad [B\text{-}8]$$

$$(v_{Qo}+v_{Q\Delta})=0 = -r_Q(i_{Qo}+i_{Q\Delta}) - \sqrt{3/2}M_Q(\dot{i}_{qo}+\dot{i}_{q\Delta}) - L_Q(\dot{i}_{Qo}+\dot{i}_{Q\Delta})$$

$$0 = -r_Q i_{Qo} \quad [B\text{-}9]$$

$$0 = -r_Q i_{Q\Delta} - \sqrt{3/2}M_Q \dot{i}_{q\Delta} - L_Q \dot{i}_{Q\Delta} \quad [B\text{-}10]$$

The above equations are rewritten in matrix form as follows.

$$\begin{bmatrix} v_{d\Delta} \\ v_{q\Delta} \\ -v_{F\Delta} \\ 0 \\ 0 \end{bmatrix} = -\begin{bmatrix} r & \omega_o L_q & 0 & 0 & +\omega_o\sqrt{3/2}M_Q \\ -\omega_o L_d & r & -\omega_o\sqrt{3/2}M_F & -\omega_o\sqrt{3/2}M_D & 0 \\ 0 & 0 & r_F & 0 & 0 \\ 0 & 0 & 0 & r_D & 0 \\ 0 & 0 & 0 & 0 & r_Q \end{bmatrix} \begin{bmatrix} i_{d\Delta} \\ i_{q\Delta} \\ i_{F\Delta} \\ i_{D\Delta} \\ i_{Q\Delta} \end{bmatrix}$$

$$-\begin{bmatrix} L_d & 0 & \sqrt{3/2}M_F & \sqrt{3/2}M_D & 0 \\ 0 & L_q & 0 & 0 & \sqrt{3/2}M_Q \\ \sqrt{3/2}M_F & 0 & L_F & M_R & 0 \\ \sqrt{3/2}M_D & 0 & M_R & L_D & 0 \\ 0 & \sqrt{3/2}M_Q & 0 & 0 & L_Q \end{bmatrix} \begin{bmatrix} \dot{i}_{d\Delta} \\ \dot{i}_{q\Delta} \\ \dot{i}_{F\Delta} \\ \dot{i}_{D\Delta} \\ \dot{i}_{Q\Delta} \end{bmatrix} - \omega_\Delta \begin{bmatrix} +L_q i_{qo} + \sqrt{3/2}M_Q i_{Qo} \\ -L_d i_{do} - \sqrt{3/2}M_F i_{Fo} - \sqrt{3/2}M_D i_{Do} \\ 0 \\ 0 \\ 0 \end{bmatrix}$$

[B-11]

Since at steady state $i_D = i_Q = 0$, the following equations represent the steady-state conditions.

$$\begin{bmatrix} v_{do} \\ v_{qo} \\ -v_{Fo} \end{bmatrix} = -\begin{bmatrix} r & \omega_o L_q & 0 \\ -\omega_o L_d & r & -\omega_o\sqrt{3/2}M_F \\ 0 & 0 & -r_F \end{bmatrix} \begin{bmatrix} i_{do} \\ i_{qo} \\ i_{Fo} \end{bmatrix} \quad [B\text{-}12]$$

The torque equation may be written in terms of currents and inductances using Equations A-49 through A-53.

$$T_e = \frac{p}{2}[\lambda_d i_q - \lambda_q i_d] \quad [A\text{-}87]$$

$$= \frac{p}{2}[\{L_{AD}(i_d+i_F+i_D)+\ell_a i_d\}i_q - \{L_{AQ}(i_q+i_Q) + \ell_a i_q\}i_d] \quad [B\text{-}13]$$

Neglecting amortisseur effects

$$T_e = \frac{p}{2}[\{(L_d-\ell_a)i_d + \ell_a i_d + L_{AD}i_F\}\, i_q - \{(L_q-\ell_a)i_q + \ell_a i_q\}i_d]$$

$$= \frac{p}{2}[L_d i_d i_q + L_{AD}i_F i_q - L_q i_q i_d]$$

$$= \frac{p}{2}[L_{AD}i_F i_q + (L_d-L_q)i_d i_q] \quad [B\text{-}14]$$

Linearize Equation B-14

$$(T_{eo}+T_{e\Delta}) = \frac{p}{2}[L_{AD}(i_{Fo}+i_{F\Delta})(i_{qo}+i_{q\Delta}) + (L_d-L_q)(i_{do}+i_{d\Delta})(i_{qo}+i_{q\Delta})]$$

$$T_{eo} = \frac{p}{2}[L_{AD}i_{Fo} + (L_d-L_q)i_{do}]\, i_{qo} \quad [B\text{-}15]$$

$$T_{e\Delta} = \frac{p}{2}[L_{AD}(i_{Fo}i_{q\Delta} + i_{qo}i_{F\Delta}) + (L_d-L_q)(i_{do}i_{q\Delta} + i_{qo}i_{d\Delta})]$$

$$= \frac{p}{2}[\{L_{AD}i_{Fo} + (L_d-L_q)i_{do}\}\, i_{q\Delta} + i_{qo}\{L_{AD}i_{F\Delta} + (L_d-L_q)i_{d\Delta}\}] \quad [B\text{-}16]$$

Define

$$E_{qo} = \omega_o L_{AD}i_{Fo} + \omega_o(L_d-L_q)i_{do} \quad [B\text{-}17]$$

$$E_{q\Delta} = \omega_o L_{AD}i_{F\Delta} + \omega_o(L_d-L_q)i_{d\Delta} \quad [B\text{-}18]$$

Then since $\omega_o = 1.0$ pu

$$T_{eo} = \frac{p}{2} E_{qo} i_{qo} \quad [B-19]$$

$$T_{e\Delta} = \frac{p}{2}[E_{qo} i_{q\Delta} + i_{qo} E_{q\Delta}] \quad [B-20]$$

Define $E'_{q\Delta}$ such that

$$E_{q\Delta} = E'_{q\Delta} - \omega_o(L_q - \ell_a) i_{d\Delta} \quad [B-21]$$

$$E'_{q\Delta} = E_{q\Delta} + \omega_o(L_q - \ell_a) i_{d\Delta}$$

$$= \omega_o L_{AD} i_{F\Delta} + \omega_o(L_d - L_q) i_{d\Delta} + \omega_o L_q i_{d\Delta} - \omega_o \ell_a i_{d\Delta}$$

$$= \omega_o L_{AD} i_{F\Delta} + \omega_o(L_d - \ell_a) i_{d\Delta} = \omega_o L_{AD} i_{F\Delta} + \omega_o L_{AD} i_{d\Delta} \quad [B-22]$$

$$E'_{qo} = \omega_o L_{AD} i_{Fo} + \omega_o(L_d - \ell_a) i_{do} \quad [B-23]$$

The linearized machine terminal voltage may be found as follows for the balanced case.

$$|v_t| = |v_{todq}| = \sqrt{v_d^2 + v_q^2}$$

$$(v_{to} + v_{t\Delta})^2 = (v_{do} + v_{d\Delta})^2 + (v_{qo} + v_{q\Delta})^2$$

So

$$v_{to}^2 = v_{do}^2 + v_{qo}^2 \quad [B-24]$$

$$v_{t\Delta} = \frac{-v_{do}}{v_{to}} v_{d\Delta} + \frac{v_{qo}}{v_{to}} v_{q\Delta} \quad [B-25]$$

where the minus sign is added to the first term since v_{do} is negative.

Transmission line equations given in Equation A-98 are linearized as follows.

$$\sin(\delta_o+\delta_\Delta) = \sin\delta_o \cos\delta_\Delta + \cos\delta_o \sin\delta_\Delta$$

$$\cos(\delta_o+\delta_\Delta) = \cos\delta_o \cos\delta_\Delta - \sin\delta_o \sin\delta_\Delta$$

which for small δ become

$$\sin(\delta_o+\delta_\Delta) = \sin\delta_o + \delta_\Delta \cos\delta_o \qquad [B-26]$$

$$\cos(\delta_o+\delta_\Delta) = \cos\delta_o - \delta_\Delta \sin\delta_o \qquad [B-27]$$

$$v_d = -\sqrt{3}\, V_B \sin\delta + R_E i_d + L_E \dot{i}_d + \omega L_E i_q$$

$$(v_{do}+v_{d\Delta}) = -\sqrt{3}\, V_B (\sin\delta_o + \delta_\Delta \cos\delta_o) + R_E(i_{do}+i_{d\Delta})$$

$$+ L_E(\dot{i}_{do}+\dot{i}_{d\Delta}) + (\omega_o+\omega_\Delta)L_E(i_{qo}+i_{q\Delta})$$

$$v_{do} = -\sqrt{3}\, V_B \sin\delta_o + R_E i_{do} + \omega_o L_E i_{qo} \qquad [B-28]$$

$$v_{d\Delta} = -\sqrt{3}\, V_B \cos\delta_o\delta_\Delta + R_E i_{d\Delta} + L_E \dot{i}_{d\Delta}$$

$$+ \omega_o L_E i_{q\Delta} + L_E i_{qo}\omega_\Delta \qquad [B-29]$$

$$v_q = \sqrt{3}\, V_B \cos\delta + R_E i_q + L_E \dot{i}_q - \omega L_E i_d$$

$$(v_{qo}+v_{q\Delta}) = \sqrt{3}\, V_B (\cos\delta_o - \delta_\Delta \sin\delta_o) + R_E(i_{qo}+i_{q\Delta})$$

$$+ L_E(\dot{i}_{qo}+\dot{i}_{q\Delta}) - (\omega_o+\omega_\Delta)L_E(i_{do}+i_{d\Delta})$$

$$v_{qo} = \sqrt{3}\, V_B \cos\delta_o + R_E i_{qo} - \omega_o L_E i_{do} \qquad [B-30]$$

$$v_{q\Delta} = -\sqrt{3}\, V_B \sin\delta_o\, \delta_\Delta + R_E i_{q\Delta} + L_E \dot{i}_{q\Delta}$$

$$- \omega_o L_E i_{d\Delta} - L_E i_{do}\omega_\Delta \qquad [B-31]$$

A. Synchronous Machine Phasor Diagrams

In this section the mathematical relationships necessary to solve for the synchronous machine initial conditions are developed. If balanced operation is assumed, these relationships may be represented in a two dimensional vector space, and following reference (31) these diagrams will be called synchronous machine phasor diagrams.

Using Equation A-3

$$\underline{v}_{abc} = \underline{P}^{-1} \underline{v}_{odq} \qquad [B-32]$$

so

$$v_a = \sqrt{2/3}[v_d \cos\theta + v_q \sin\theta] \qquad [B-33]$$

where $\theta = (\omega_B t + \delta + 90°)$ [A-4]

and where it is implied that $\delta = \delta_o$ throughout this development.

Substituting from Equation B-12 for v_d and v_q

$$v_a = \sqrt{2/3}[(-ri_{do}-\omega_o L_q i_{qo}) \cos(\omega_B t+\delta+90°)$$

$$+ (+\omega_o L_d i_{do}-ri_{qo}+\omega_o\sqrt{3/2}M_F i_{Fo})\cos(\omega_B t+\delta)]$$

since $\sin(\omega_B t+\delta+90°) = \cos(\omega_B t+\delta)$.

This equation may be written in phasor form as follows.

$$\bar{V}_a = -r\left[\frac{i_{do}}{\sqrt{3}} \angle\delta+90° + \frac{i_{qo}}{\sqrt{3}} \angle\delta\right] - X_q \frac{i_{qo}}{\sqrt{3}} \angle\delta+90°$$

$$+ X_d \frac{i_{do}}{\sqrt{3}} \angle\delta + E_F \angle\delta \qquad [B-34]$$

where $E_F = \frac{\omega_o M_F i_{Fo}}{\sqrt{2}}$ [B-35]

Also $\underline{i}_{abc} = \underline{P}^{-1} \underline{i}_{odq}$ and using Equation A-3 [B-36]

$$i_a = \sqrt{2/3}[i_d \cos \theta + i_q \sin \theta]$$

which may also be written in phasor form as follows.

$$\bar{I}_a = \frac{i_d}{\sqrt{3}} \angle \delta + 90° + \frac{i_q}{\sqrt{3}} \angle \delta \quad [B-37]$$

Define

$$\bar{I}_a \triangleq +\bar{I}_d + \bar{I}_q \quad [B-38]$$

Then

$$\bar{I}_d = \frac{+i_d}{\sqrt{3}} \angle \delta+90° \quad [B-39]$$

$$\bar{I}_q = \frac{i_q}{\sqrt{3}} \angle \delta \quad [B-40]$$

where $\bar{I}_d$ and $\bar{I}_q$ are rms "stator equivalent" quantities (6).

Solving Equation B-34 for $\bar{E}_F$ and using Equations B-38, B-39 and B-40

$$E_F \angle \delta = \bar{V}_a + r\bar{I}_a + X_q I_q \angle \delta+90° - X_d I_d \angle \delta \quad [B-41]$$

which may be written as

$$\bar{E}_F = \bar{V}_a + r\bar{I}_a + jX_q \bar{I}_q + jX_d \bar{I}_d \quad [B-42]$$

The resulting phasor diagram is shown in Figure 69.

Define

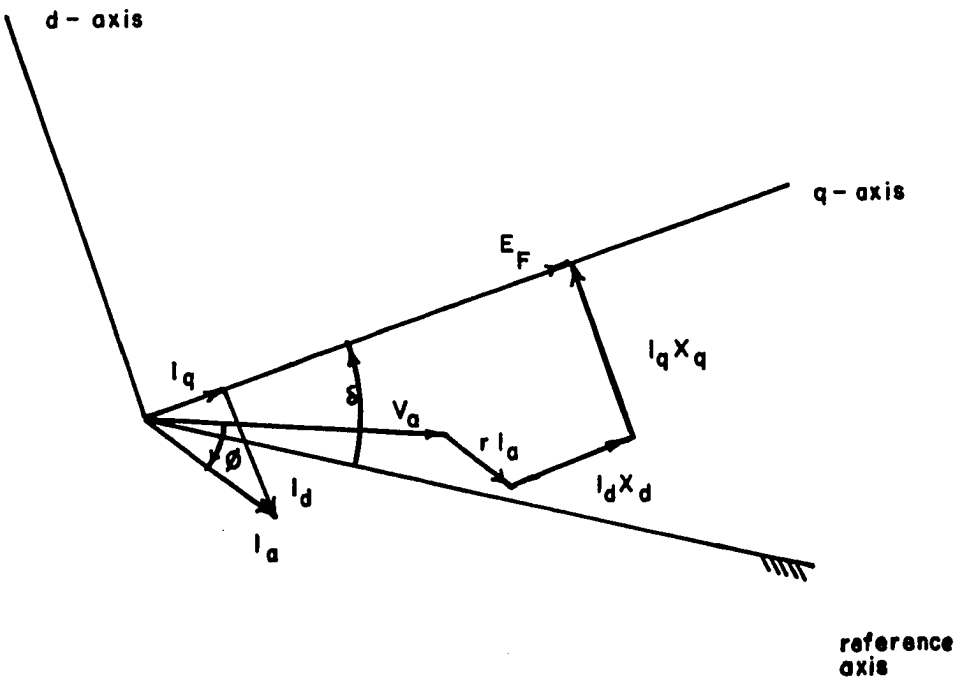

Figure 69. Phasor diagram of a synchronous machine

$$v_{tabc} = v_a \qquad [B-43]$$

So from Equation B-33

$$v_{tabc} \triangleq v_a = \sqrt{2/3}[v_d \cos\theta + v_q \sin\theta]$$

$$= \sqrt{2/3}[v_d \cos(\omega_B t+\delta+90°) + v_q \cos(\omega_B t+\delta)] \qquad [B-44]$$

Rewriting the above equation in phasor form

$$\bar{V}_{tabc} = \bar{V}_a = \frac{v_d}{\sqrt{3}} \angle \delta+90° + \frac{v_q}{\sqrt{3}} \angle \delta \qquad [B-45]$$

Define

$$\bar{V}_a = +\bar{V}_d + \bar{V}_q \qquad [B-46]$$

Then

$$\bar{V}_d = \frac{+v_d}{\sqrt{3}} \angle \delta+90° \qquad [B-47]$$

$$\bar{V}_q = \frac{v_q}{\sqrt{3}} \angle \delta \qquad [B-48]$$

where $\bar{V}_d$ and $\bar{V}_q$ are rms "stator equivalent" quantities.

Let α be the angle from the q-axis to the terminal voltage and ϕ be the angle between terminal voltage and current.

Then

$$v_t \angle \delta-\alpha = \sqrt{3}\,\bar{V}_a = +v_d \angle \delta+90° + v_q \angle \delta \qquad [B-49]$$

and

$$i_t \angle \delta-\alpha-\phi = \sqrt{3}\,\bar{I}_a = +i_d \angle \delta+90° + i_q \angle \delta \qquad [B-50]$$

From Equation B-34 neglecting armature resistance r

$$v_t \angle\underline{\delta-\alpha} = -X_q i_q \angle\underline{\delta+90°} + X_d i_d \angle\underline{\delta} + \omega_o L_{AD} i_{Fo} \angle\underline{\delta}$$

Add and subtract $X_q i_{do} \angle\underline{\delta}$

$$v_t \angle\underline{\delta-\alpha} = -X_q i_q \angle\underline{\delta+90°} + X_{AD} i_{Fo} \angle\underline{\delta} + (X_d - X_q) i_d \angle\underline{\delta} + X_q i_d \angle\underline{\delta}$$

Using Equation B-17

$$v_t \angle\underline{\delta-\alpha} = -X_q i_q \angle\underline{\delta+90°} + E_{qo} \angle\underline{\delta} + X_q i_d \angle\underline{\delta} \qquad [B-51]$$

$$E_{qo} \angle\underline{\delta} = v_t \angle\underline{\delta-\alpha} + X_q i_q \angle\underline{\delta+90°} - X_q i_d \angle\underline{\delta}$$

$$= v_t \angle\underline{\delta-\alpha} + jX_q i_q \angle\underline{\delta} + jX_q i_d \angle\underline{\delta+90°}$$

$$= v_t \angle\underline{\delta-\alpha} + \sqrt{3} jX_q \frac{i_d}{\sqrt{3}} \angle\underline{\delta+90°} + \frac{i_q}{\sqrt{3}} \angle\underline{\delta}$$

$$= v_t \angle\underline{\delta-\alpha} + j\sqrt{3}\, X_q \, (+\bar{I}_d + \bar{I}_q)$$

$$= v_t \angle\underline{\delta-\alpha} + j\sqrt{3}\, X_q \, (\bar{I}_a) \qquad [B-52]$$

$\bar{I}_a$ may be decomposed into currents in phase with and lagging v_t by 90°. Define

$$i_r \angle\underline{\delta-\alpha} = \sqrt{3}\, I_a \cos\phi \angle\underline{\delta-\alpha} \qquad [B-53]$$

$$i_x \angle\underline{\delta-\alpha-90°} = \sqrt{3}\, I_a \sin\phi \angle\underline{\delta-\alpha-90°} \qquad [B-54]$$

Inserting the above equations into Equation B-52

$$E_{qo} \angle\underline{\delta} = v_t \angle\underline{\delta-\alpha} + jX_q (i_r \angle\underline{\delta-\alpha} + i_x \angle\underline{\delta-\alpha-90°})$$

$$= v_t \angle\underline{\delta-\alpha} + X_q i_r \angle\underline{\delta-\alpha+90°} + X_q i_x \angle\underline{\delta-\alpha}$$

Thus

$$|E_{qo}| = \sqrt{(v_t + X_q i_x)^2 + (X_q i_r)^2} \qquad [B-55]$$

If the variables in Figure 61 are transformed to the odq coordinate system and if R is assumed to be large, thus its effect negligible, the following equation results.

$$\begin{aligned} v_B \angle 0° &= v_t \angle \delta-\alpha - (R_E+jX_E) i_t \angle \delta-\alpha-\phi \\ &= v_t \angle \delta-\alpha - (R_E+jX_E)(i_r \angle \delta-\alpha + i_x \angle \delta-\alpha-90°) \\ &= v_t \angle \delta-\alpha - (R_E+jX_E)(i_r \angle \delta-\alpha - j i_x \angle \delta-\alpha-90°) \\ &= v_t \angle \delta-\alpha - R_E i_r \angle \delta-\alpha + jR_E i_x \angle \delta-\alpha - jX_E i_r \angle \delta-\alpha - X_E i_x \angle \delta-\alpha \\ &= (v_t - R_E i_r - X_E i_x) \angle \delta-\alpha + j(-X_E i_r + R_E i_x) \angle \delta-\alpha \end{aligned} \qquad [B-56]$$

The resulting phasor diagram is shown in Figure 70 where all subscript "o" have been deleted. α may be found from Figure 70 as follows.

$$\sin \alpha = i_r X_q / E_{qo} \qquad [B-57]$$

$$\cos \alpha = (v_t + i_x X_q)/E_{qo} \qquad [B-58]$$

$$\begin{aligned} i_{qo} &= i_r \cos \alpha - i_x \sin \alpha \\ &= i_r (v_t + i_x X_q)/E_{qo} - (i_x i_r X_q)/E_{qo} \end{aligned} \qquad [B-59]$$

$$\begin{aligned} i_{do} &= -i_r \sin \alpha - i_x \cos \alpha \\ &= -i_r X_q/E_{qo} - (i_x v_t + i_x X_q)/E_{qo} \end{aligned} \qquad [B-60]$$

Find δ from Figure 70.

$$v_B \cos \delta = v_t \cos \alpha - (i_x X_E + i_r R_E) \cos \alpha + (R_E i_x - X_E i_r) \sin \alpha$$

$$v_B \cos \delta = (v_t - i_x X_E - i_r R_E)(v_t + i_x X_q)/E_{qo} + (R_E i_x - X_E i_r)(i_r X_q)/E_{qo}$$

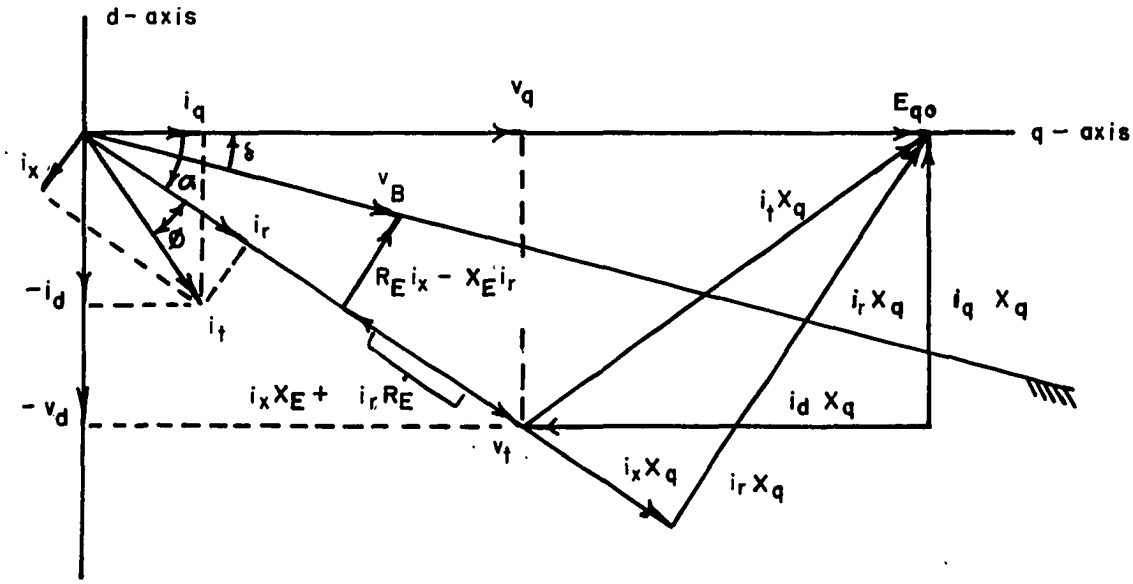

Figure 70. Phasor diagram of a synchronous machine connected to an infinite bus through a transmission line

$$\cos\delta = v_t[v_t + i_x (X_q - X_E) - i_r R_E]/E_{qo} v_B - [X_q X_E (i_r^2 + i_x^2)]/E_{qo} v_B \quad [B-61]$$

The q-axis component of terminal voltage is

$$v_q = v_t \cos\alpha = v_t (v_t + i_x X_q)/E_{qo} \quad [B-62]$$

The d-axis component of terminal voltage is

$$v_d = -i_{qo} X_q \quad [B-63]$$

B. Synchronous Machine Terminal Voltage

The loading of a synchronous machine is normally given in terms of the power output and the power factor. If the infinite bus voltage and tie line impedance are also given, the terminal voltage may be found as follows.

Let

$$\bar{I}_a = I_a \angle -\phi^\circ$$
$$\bar{V}_a = V_a \angle 0^\circ$$
$$\bar{V}_B = V_B \angle \gamma^\circ$$

Then from Figure 61 neglecting R

$$\bar{V}_B = \bar{V}_a - (R_E + jX_E)\bar{I}_a \quad [B-64]$$

The single-phase power output of the machine is

$$P = V_a I_a \cos\phi \quad [B-65]$$

where $$\phi = \tan^{-1} Q/P = \cos^{-1} P/S \quad [B-66]$$

$$I_a = P/(V_a \cos \phi)$$

$$\bar{I}_a = P/(V_a \cos \phi) \angle -\phi \qquad [B-67]$$

So

$$\bar{V}_B = \bar{V}_a - (R_E + jX_E) \frac{P}{V_a \cos \phi} (\cos \phi - j \sin \phi) \qquad [B-68]$$

$$= \bar{V}_a - \frac{R_E P}{V_a} - \frac{X_E P}{V_a} \tan \phi - j \left[\frac{X_E P}{V_a} - \frac{R_E P}{V_a} \tan \phi \right] \qquad [B-69]$$

$$|\bar{V}_B|^2 = \bar{V}_B \bar{V}_B^* \qquad [B-70]$$

$$= -2P(R_E + X_E \tan \phi) + V_a^2 + \frac{P^2(R_E^2 + X_E^2)}{V_a^2 \cos^2 \phi} \qquad [B-71]$$

Define

$$C = V_B^2 + 2P(R_E + X_E \tan \phi) \qquad [B-72]$$

Then

$$C = V_a^2 + \frac{P^2(R_E^2 + X_E^2)}{V_a^2 \cos^2 \phi} \qquad [B-73]$$

and

$$V_a^4 - C V_a^2 + P^2(R_E^2 + X_E^2)/\cos^2 \phi = 0 \qquad [B-74]$$

$$V_a = \sqrt{\frac{C \pm \sqrt{C^2 - 4 P^2(R_E^2 + X_E^2)/\cos^2\phi}}{2}} \qquad [B-75]$$

To transform from the phasor domain to the corresponding instantaneous rotor quantities, the phasor quantities (rms magnitudes) are multiplied by $\sqrt{3}$. Thus

$$v_B = \sqrt{3}\, V_B \qquad [B-76]$$

$$v_t = \sqrt{3}\, V_a \qquad [B-77]$$

$$i_t = \sqrt{3}\, I_a \qquad [B-78]$$

C. Development of a Linear Model of a Synchronous Machine Connected to an Infinite Bus

Assumptions: Terms resulting from the following effects are neglected.

1) Amortisseur effects
2) Armature resistance
3) Armature $\dot{\lambda}$ terms
4) Saturation
5) Load $\dot{\lambda}$ terms
6) Load ω_Δ terms

The required linearized equations are repeated for convenience neglecting above effects.

1. Machine equations

$$v_{d\Delta} = -\omega_o L_q i_{q\Delta} \qquad [B-79]$$

$$v_{q\Delta} = \omega_o L_d i_{d\Delta} + \omega_o L_{AD} i_{F\Delta} \qquad [B-80]$$

$$-v_{F\Delta} = -r_F i_F - L_{AD}\, i_{d\Delta} - L_F\, \dot{i}_{F\Delta} \qquad [B-81]$$

$$v_{t\Delta} = -v_{do}/v_{to}\, v_{d\Delta} + v_{qo}/v_{to}\, v_{q\Delta} \qquad [B-25]$$

$$E_{q\Delta} = \omega_o L_{AD} i_{F\Delta} + \omega_o (L_d - L_q)\, i_{d\Delta} \qquad [B-18]$$

$$E'_{q\Delta} = \omega_o L_{AD} i_{F\Delta} + \omega_o L_{AD} i_{d\Delta} \qquad [B-22]$$

$$T_{e\Delta} = p/2[E_{qo} i_{q\Delta} + i_{qo} E_{q\Delta}] \qquad [B-20]$$

2. Machine load equations

$$v_{q\Delta} = -\sqrt{3}\, V_B \sin \delta_o\, \delta_\Delta + R_E i_{q\Delta} - \omega_o L_E i_{d\Delta} \qquad [B-82]$$

$$v_{d\Delta} = -\sqrt{3}\, V_B \cos \delta_o\, \delta_\Delta + R_E i_{d\Delta} + \omega_o L_E i_{q\Delta} \qquad [B-83]$$

Replace $v_{q\Delta}$ in Equation B-73 by Equation B-71.

$$\omega_o L_{AD} i_{F\Delta} + \omega_o L_d i_{d\Delta} = -\sqrt{3}\, V_B \sin \delta_o\, \delta_\Delta + R_E i_{q\Delta} - \omega_o L_E i_{d\Delta}$$

Use Equation B-18, adding and subtracting $\omega_o L_q i_{d\Delta}$

$$\omega_o L_{AD} i_{F\Delta} + \omega_o L_d i_{d\Delta} - \omega_o L_q i_{d\Delta} + \sqrt{3}\, V_B \sin \delta_o\, \delta_\Delta = R_E i_{q\Delta} - \omega_o L_E i_{d\Delta} - \omega_o L_q i_{d\Delta}$$

So

$$E_{q\Delta} + \sqrt{3}\, V_B \sin \delta_o\, \delta_\Delta = R_E i_{q\Delta} - (\omega_o L_E + \omega_o L_q)\, i_{d\Delta} \qquad [B\text{-}84]$$

Combine Equation B-79 and Equation B-83.

$$-\omega_o L_q i_{q\Delta} = -\sqrt{3}\, V_B \cos \delta_o\, \delta_\Delta + R_E i_{d\Delta} + \omega_o L_E i_{q\Delta}$$

Rearranging.

$$\sqrt{3}\, V_B \cos \delta_o\, \delta_\Delta = R_E i_{d\Delta} + (\omega_o L_E + \omega_o L_q)\, i_{q\Delta} \qquad [B\text{-}85]$$

Equations B-84 and B-85 are solved for $i_{d\Delta}$ and $i_{q\Delta}$ as follows.

$$\begin{bmatrix} \sqrt{3}\, V_B \cos \delta_o\, \delta_\Delta \\ E_{q\Delta} + \sqrt{3}\, V_B \sin \delta_o\, \delta_\Delta \end{bmatrix} = \begin{bmatrix} R_E & (\omega_o L_E + \omega_o L_q) \\ -(\omega_o L_E + \omega_o L_q) & R_E \end{bmatrix} \begin{bmatrix} i_{d\Delta} \\ i_{q\Delta} \end{bmatrix}$$

$$i_{d\Delta} = \frac{(\sqrt{3}\, V_B \cos \delta_o\, \delta_\Delta) R_E - (E_{q\Delta} + \sqrt{3}\, V_B \sin \delta_o\, \delta_\Delta)(\omega_o L_E + \omega_o L_q)}{D} \qquad [B\text{-}86]$$

$$i_{q\Delta} = \frac{(E_{q\Delta} + \sqrt{3}\, V_B \sin \delta_o\, \delta_\Delta) R_E + (\sqrt{3}\, V_B \cos \delta_o\, \delta_\Delta)(\omega_o L_E + \omega_o L_q)}{D} \qquad [B\text{-}87]$$

where $D = R_E^2 + (\omega_o L_E + \omega_o L_q)^2$ [B-88]

Replace $E_{q\Delta}$ with E'_q as follows.

$$E_{q\Delta} = E'_{q\Delta} - \omega_o(L_q - \ell_d)\, i_{d\Delta} \qquad [B\text{-}21]$$

$$i_{d\Delta} = \frac{(\sqrt{3}\, V_B \cos\delta_o\, \delta_\Delta)R_E - (E'_{q\Delta} + \sqrt{3}\, V_B \sin\delta_o\, \delta_\Delta)(\omega_o L_E + \omega_o L_q)}{D}$$

$$+ \frac{\omega_o(L_q - \ell_d)\, i_{d\Delta}\, (\omega_o L_E + \omega_o L_q)}{D}$$

$$i_{d\Delta}\left[1 - \frac{\omega_o^2(L_q - \ell_d)(L_E + L_q)}{R_E^2 + (\omega_o L_E + \omega_o L_q)^2}\right]$$

$$= \frac{(\sqrt{3}\, V_B \cos\delta_o\, \delta_\Delta)R_E - (E'_{q\Delta} + \sqrt{3}\, V_B \sin\delta_o\, \delta_\Delta)(\omega_o L_E + \omega_o L_q)}{D}$$

$$i_{d\Delta}\, \frac{R_E^2 + (\omega_o L_E + \omega_o L_q)^2 - \omega_o^2(L_q - \ell_d)(L_q + L_E)}{D}$$

$$= \frac{(\sqrt{3}\, V_B \cos\delta_o\, \delta_\Delta)R_E - (E'_{q\Delta} + \sqrt{3}\, V_B \sin\delta_o\, \delta_\Delta)(\omega_o L_E + \omega_o L_q)}{D}$$

$$i_{d\Delta}\, \frac{R_E^2 + \omega_o^2 L_E + 2\omega_o^2 L_E L_q + \omega_o^2 L_q^2 - \omega_o^2 L_q^2 + \omega_o^2 \ell_d L_q - \omega_o^2 L_q L_E + \omega_o^2 \ell_d L_E}{D}$$

$$= \frac{(\sqrt{3}\, V_B \cos\delta_o\, \delta_\Delta)R_E - (E'_{q\Delta} + \sqrt{3}\, V_B \sin\delta_o\, \delta_\Delta)(\omega_o L_E + \omega_o L_q)}{D}$$

$$i_{d\Delta}\, \frac{R_E^2 + (\omega_o L_E + \omega_o \ell_d)(\omega_o L_E + \omega_o L_q)}{D}$$

$$= \frac{(\sqrt{3}\, V_B \cos\delta_o\, \delta_\Delta)R_E - (E'_{q\Delta} + \sqrt{3}\, V_B \sin\delta_o\, \delta_\Delta)(\omega_o L_E + \omega_o L_q)}{D}$$

Define

$$A = R_E^2 + (\omega_o L_E + \omega_o \ell_d)(\omega_o L_E + \omega_o L_q)$$

So

$$i_{d\Delta} = \frac{(\sqrt{3}\, V_B \cos \delta_o\, \delta_\Delta) R_E - (E'_{q\Delta} + \sqrt{3}\, V_B \sin \delta_o\, \delta_\Delta)(\omega_o L_E + \omega_o L_q)}{A} \qquad [B\text{-}89]$$

Similarly from Equations B-87 and B-21

$$i_{q\Delta} = \frac{(E'_{q\Delta} + \sqrt{3}\, V_B \sin \delta_o\, \delta_\Delta) R_E}{D}$$

$$+ \frac{(\sqrt{3}\, V_B \cos \delta_o\, \delta_\Delta)(\omega_o L_E + \omega_o L_q) - R_E \omega_o (L_q - \ell_d) i_{d\Delta}}{D}$$

$$i_{q\Delta} = \frac{(E'_{q\Delta} + \sqrt{3}\, V_B \sin \delta_o\, \delta_\Delta) R_E}{D}$$

$$+ \frac{(\sqrt{3}\, V_B \cos \delta_o\, \delta_\Delta)(\omega_o L_E + \omega_o L_q)}{D} - \left[\left[\frac{R_E \omega_o (L_q - \ell_d)}{D} \right] \right.$$

$$\left. \left[\frac{\sqrt{3}\, V_B \cos \delta_o\, \delta_\Delta) R_E - (E'_{q\Delta} + \sqrt{3}\, V_B \sin \delta_o\, \delta_\Delta)(\omega_o L_E + \omega_o L_q)}{A} \right] \right]$$

$$= E'_{q\Delta} \left[\frac{R_E}{D} + \frac{R_E \omega_o (L_q - \ell_d)(\omega_o L_E + \omega_o L_q)}{DA} \right]$$

$$+ \sqrt{3}\, V_B \sin \delta_o\, \delta_\Delta \left[\frac{R_E}{D} + \frac{R_E \omega_o (L_q - \ell_d)(\omega_o L_E + \omega_o L_q)}{DA} \right]$$

$$+ \sqrt{3}\, V_B \cos \delta_o\, \delta_\Delta \left[\frac{(\omega_o L_E + \omega_o L_q)}{D} - \frac{R_E \omega_o (L_q - \ell_d) R_E}{DA} \right]$$

$$= E'_{q\Delta} \frac{\left[R_E R_E^2 + (\omega_o L_E + \omega_o \ell_d)(\omega_o L_E + \omega_o L_q) + R_E \omega_o (L_q - \ell_d)(\omega_o L_E + \omega_o L_q)\right]}{AD}$$

$$+ \sqrt{3}\, V_B \sin \delta_o\, \delta_\Delta \left[\frac{R_E}{D} + \frac{R_E \omega_o (L_q - \ell_d)(\omega_o L_E + \omega_o L_q)}{DA}\right]$$

$$+ \sqrt{3}\, V_B \cos \delta_o\, \delta_\Delta \left[\frac{(\omega_o L_E + \omega_o L_q)[R_E^2 + (\omega_o L_E + \omega_o \ell_d)(\omega_o L_E + \omega_o L_q)] - R_E^2 \omega_o (L_q - \ell_d)}{AD}\right]$$

$$i_{q\Delta} = E'_{q\Delta} \left[R_E [R_E^2 + \omega_o^2 L_E^2 + \omega_o^2 \ell_d L_E + \omega_o^2 L_E L_q \right.$$

$$\left. \frac{+\omega_o^2 L_q \ell_d + \omega_o^2 L_q L_E + \omega_o^2 L_q^2 - \omega_o^2 L_E \ell_d - \omega_o^2 \ell_d L_q]}{AD}\right]$$

$$+ \sqrt{3}\, V_B \sin \delta_o\, \delta_\Delta \left[\frac{R_E}{D} + \frac{R_E \omega_o (L_q - \ell_d)(\omega_o L_E + \omega_o L_q)}{AD}\right]$$

$$+ \sqrt{3}\, V_B \cos \delta_o\, \delta_\Delta \left[R_E^2 \omega_o L_E + R_E^2 \omega_o L_q - R_E^2 \omega_o L_q + \omega_o^2 R_E^2 \ell_d \right.$$

$$\left. \frac{+(\omega_o L_E + \omega_o L_q)(\omega_o L_E + \omega_o \ell_d)(\omega_o L_E + \omega_o L_q)}{AD}\right]$$

$$= E'_{q\Delta} \left[R_E [R_E^2 + (\omega_o L_E + \omega_o L_q)^2]\right] + \sqrt{3}\, V_B \sin \delta_o\, \delta_\Delta \left[\frac{R_E D}{AD}\right]$$

$$+ \sqrt{3}\, V_B \cos \delta_o\, \delta_\Delta \left[\frac{(\omega_o L_E + \omega_o \ell_d)[R_E^2 + (\omega_o L_E + \omega_o L_q)^2]}{AD}\right]$$

$$= \frac{(E'_{q\Delta} + \sqrt{3}\, V_B \sin \delta_o\, \delta_\Delta) R_E + \sqrt{3}\, V_B \cos \delta_o\, \delta_\Delta\, (\omega_o L_E + \omega_o \ell_d)}{A} \qquad \text{[B-90]}$$

From Equation B-81

$$-v_{F\Delta} = -r_F i_{F\Delta} - \sqrt{3/2}\, M_F\, \dot{i}_{d\Delta} - L_F \dot{i}_{F\Delta} \qquad \text{[B-91]}$$

$$= -r_F i_{F\Delta} - d/dt[L_{AD} i_{d\Delta} + L_F i_{F\Delta}]$$

But $L_F - \ell_F = L_{AD}$, so

$$-v_{F\Delta} = -r_F i_{F\Delta} - d/dt[L_{AD} i_{d\Delta} + L_F i_{F\Delta} - \ell_F i_{F\Delta} + \ell_F i_{F\Delta}]$$

$$= -r_F i_{F\Delta} - d/dt[L_{AD} i_{d\Delta} + L_{AD} i_{F\Delta} + \ell_F i_{F\Delta}]$$

$$= -r_F i_{F\Delta} - d/dt[E'_{q\Delta} + \ell_F i_{F\Delta}]$$

$$\text{and } d/dt\, E'_{q\Delta} = v_{F\Delta} - r_F i_{F\Delta} - \ell_F \dot{i}_{F\Delta} \qquad \text{[B-92]}$$

Multiply above by L_F/r_F.

$$T'_{do}\, d/dt\, E'_{q\Delta} = (L_F/r_F)v_{F\Delta} - (L_F/r_F) r_F i_F - (L_F/r_F)\ell_F \dot{i}_F$$

where $T'_{do} = L_F/r_F$ = open circuit time constant of field.

Assuming a solution of the form

$$i_F = K\, e^{-t/(L_F/r_F)}$$

then

$$\dot{i}_F = (-r_F/L_F) K\, e^{-t/(L_F/r_F)} = (-r_F/L_F) i_F$$

so

$$\frac{T'_{do}\, dE'_{q\Delta}}{dt} = E_{fd\Delta} - (L_F - \ell_F) i_F$$

and since $\omega_o = 1.0$ pu

$$T'_{do}\, \frac{dE'_{q\Delta}}{dt} = E_{fd\Delta} - \omega_o L_{AD} i_{F\Delta} \qquad \text{[B-93]}$$

$$\text{where } E_{fd\Delta} = (L_F/r_F) v_{F\Delta} \qquad \text{[B-94]}$$

Using Equation B-71 with Equation B-22

$$E'_{q\Delta} = v_{q\Delta} - \omega_o \ell_d i_{d\Delta}$$

$$v_{q\Delta} = E'_{q\Delta} + \omega_o \ell_d i_{d\Delta} \qquad [B-95]$$

If Equations B-95 and B-79 are inserted in Equation B-25, the following expression for terminal voltage results.

$$v_{t\Delta} = \frac{v_{do}}{v_{to}} \omega_o L_q i_{q\Delta} + \frac{v_{qo}}{v_{to}} \left[E'_{q\Delta} + \omega_o \ell_d i_d \right] \qquad [B-96]$$

Eliminate $i_{d\Delta}$ and $i_{q\Delta}$ using Equations B-89 and B-90.

$$v_{t\Delta} = \frac{v_{do}}{v_{to}} \omega_o L_q \left[\frac{(E'_{q\Delta} + \sqrt{3}\, V_B \sin \delta_o\, \delta_\Delta) R_E + (\sqrt{3}\, V_B \cos \delta_o\, \delta_\Delta)(\omega_o L_E + \omega_o \ell_d)}{A} \right]$$

$$+ \frac{v_{qo}}{v_{to}} \left[E'_{q\Delta} + \omega_o \ell_d \left[\frac{(\sqrt{3}\, V_B \cos \delta_o \delta_\Delta) R_E - (E'_{q\Delta} + \sqrt{3}\, V_B \sin \delta_o \delta_\Delta)(\omega_o L_E + \omega_o L_q)}{A} \right] \right]$$

$$v_{t\Delta} = K_5\, \delta_\Delta + K_6\, E'_{q\Delta} \qquad [B-97]$$

where

$$K_5 = \frac{v_{do}\ \omega_o L_q}{v_{to}} \left[\frac{\sqrt{3}\, V_B \sin \delta_o R_E + \sqrt{3}\, V_B \cos \delta_o (\omega_o L_E + \omega_o \ell_d)}{A} \right]$$

$$+ \frac{v_{qo}}{v_{to}} \omega_o \ell_d \left[\frac{\sqrt{3}\, V_B \cos \delta_o R_E - \sqrt{3}\, V_B \sin \delta_o (\omega_o L_E + \omega_o L_q)}{A} \right] \qquad [B-98]$$

$$K_6 = \frac{v_{do}\ \omega_o L_q R_E}{v_{to}\ A} + \frac{v_{qo}}{v_{to}} \left[1 - \frac{\omega_o \ell_d (\omega_o L_E + \omega_o L_q)}{A} \right] \qquad [B-99]$$

From Equation B-93

$$T'_{do}\frac{dE'_{q\Delta}}{dt} = E_{fd\Delta} - \omega_o L_{AD} i_{F\Delta} \qquad [B\text{-}100]$$

By definition,

$$E'_{q\Delta} = \omega_o L_{AD} i_{F\Delta} + \omega_o (L_d - \ell_d) i_{d\Delta} \qquad [B\text{-}22]$$

so

$$i_{F\Delta} = \frac{E'_{q\Delta} - \omega_o (L_d - \ell_d) i_{d\Delta}}{\omega_o L_{AD}}$$

Take LaPlace transform of Equation B-100 using above.

$$sT'_{do}E'_{q\Delta} = E_{fd\Delta} - E'_{q\Delta} + \omega_o (L_d - \ell_d) i_{d\Delta}$$

$$(1+sT'_{do})E'_{q\Delta} = E_{fd\Delta} + \omega_o (L_d - \ell_d)\left[\frac{\sqrt{3}V_B \cos \delta_o \delta_\Delta) R_E - (E'_{q\Delta} + 3V_B \sin \delta_o \delta_\Delta)(\omega_o L_E + \omega_o L_q)}{A}\right]$$

$$\left[1+sT'_{do} + \frac{\omega_o (L_d - \ell_d)(\omega_o L_E + \omega_o L_q)}{A}\right] E'_{q\Delta} =$$

$$E_{fd} + \omega_o (L_d - \ell_d)\left[\frac{\sqrt{3}\, V_B \cos \delta_o R_E - (\omega_o L_E + \omega_o L_q)\sqrt{3}\, V_B \sin \delta_o}{A}\right] \delta_\Delta$$

Multiply by $\left[1 + \frac{\omega_o (L_d - \ell_d)(\omega_o L_E + \omega_o L_q)}{A}\right]^{-1}$

Changing L's to X's since $\omega_o = 1.0$ pu

$$1 + sT'_{do}\left[1 + \frac{(X_d - X'_d)(X_q + X_E)}{A}\right]^{-1} E'_{q\Delta} = \left[1 + \frac{(X_d - X'_d)(X_q + X_E)}{A}\right]^{-1} E_{fd\Delta}$$

$$+\left[1+\frac{(X_d-X_d')(X_q+X_E)}{A}\right]^{-1}\frac{X_d-X_d'}{A}\sqrt{3}\,V_B[R_E\cos\delta_o-(X_q+X_E)\sin\delta_o]\,\delta_\Delta$$

Define

$$K_3 \triangleq \left[1+\frac{(X_d-X_d')(X_q+X_E)}{A}\right]^{-1} \qquad \text{[B-101]}$$

So

$$1+sT_{do}'K_3E_{q\Delta}' = K_3E_{fd\Delta}+K_3\sqrt{3}\,V_B\frac{(X_d-X_d')}{A}[R_E\cos\delta_o-(X_q+X_E)\sin\delta_o]\,\delta_\Delta$$

Define

$$K_4 = \sqrt{3}\,V_B\frac{(X_d-X_d')}{A}[-R_E\cos\delta_o+(X_q+X_E)\sin\delta_o] \qquad \text{[B-102]}$$

So

$$E_{q\Delta}' = \frac{K_3E_{fd\Delta}}{1+sT_{do}'K_3}-\frac{K_3K_4}{1+sT_{do}'K_3}\delta_\Delta \qquad \text{[B-103]}$$

Substituting Equation B-90 and Equation B-21, with Equation B-81 substituted into it, into Equation B-20, and setting p = 2

$$T_{e\Delta} = E_{qo}\left[\frac{(E_{q\Delta}'+\sqrt{3}\,V_B\sin\delta_o\delta_\Delta)R_E+(\sqrt{3}\,V_B\cos\delta_o\delta_\Delta)(\omega_oL_E+\omega_o\ell_d)}{A}\right]$$

$$+i_{qo}\left[E_{q\Delta}'-\omega_o(L_q-\ell_d)\left[\frac{(\sqrt{3}V_B\cos\delta_o\delta_\Delta)R_E-(E_{q\Delta}'+\sqrt{3}V_B\sin\delta_o\delta_\Delta)(\omega_oL_E+\omega_oL_q)}{A}\right]\right]$$

$$=\left[\frac{E_{qo}\sqrt{3}\,V_B\,R_E\sin\delta_o+E_{qo}\sqrt{3}\,V_B\cos\delta_o\,(\omega_oL_E+\omega_o\ell_d)}{A}\right.$$

$$- \frac{i_{qo}\omega_o(L_q-\ell_d)\sqrt{3}\ V_B \cos\delta_o R_E + i_{qo}\omega_o(L_q-\ell_d)\sqrt{3}\ V_B \sin\delta_o(\omega_o L_E+\omega_o L_q)}{A} \Bigg] \delta$$

$$+ \frac{E_{qo}E'_{q\Delta}R_E}{A} + i_{qo}E'_{q\Delta} + \frac{i_{qo}\omega_o(L_q-\ell_d)(\omega_o L_E+\omega_o L_q)\ E'_{q\Delta}}{A}$$

$$T_{e\Delta} = K_1\delta_\Delta + K_2E'_{q\Delta} \qquad \text{[B-104]}$$

where

$$K_1 = \frac{E_{qo}\sqrt{3}\ V_B}{A}[R_E \sin\delta_o + (\omega_o L_E+\omega_o\ell_d)\cos\delta_o] \qquad \text{[B-105]}$$

$$+ \frac{i_{qo}\sqrt{3}\ V_B}{A}[\omega_o(L_q-\ell_d)(\omega_o L_E+\omega_o L_q)\sin\delta_o - \omega_o(L_q-\ell_d)\cos\delta_o R_E]$$

$$K_2 = \frac{R_E E_{qo}}{A} + i_{qo}\left[1 + \frac{\omega_o(L_q-\ell_d)(\omega_o L_E+\omega_o L_q)}{A}\right] \qquad \text{[B-106]}$$

The following equations describe the linearized system of a generator connected to an infinite bus through impedance $R_E + jX_E$ where the constants have been previously defined.

$$E'_{q\Delta} = \frac{K_3E_{fd\Delta}}{1 + sT'_{do}K_3} - \frac{K_3K_4}{1 + sT'_{do}K_3}\delta_\Delta \quad \text{pu} \qquad \text{[B-103]}$$

$$T_{e\Delta} = K_1\delta_\Delta + K_2E'_{q\Delta} \quad \text{pu} \qquad \text{[B-104]}$$

$$v_{t\Delta} = K_5\delta_\Delta + K_6E'_{q\Delta} \quad \text{pu} \qquad \text{[B-97]}$$

$$\Delta\omega_u = p/2\ 1/2H \int T_{au}\,dt \quad \text{pu} \qquad \text{[A-80]}$$

$$\delta_\Delta = 377 \int \Delta\omega_u\,dt \quad \text{radians} \qquad \text{[A-85]}$$

The block diagram resulting from the above equations is shown in Figure 71 where all subscript "Δ's" have been deleted.

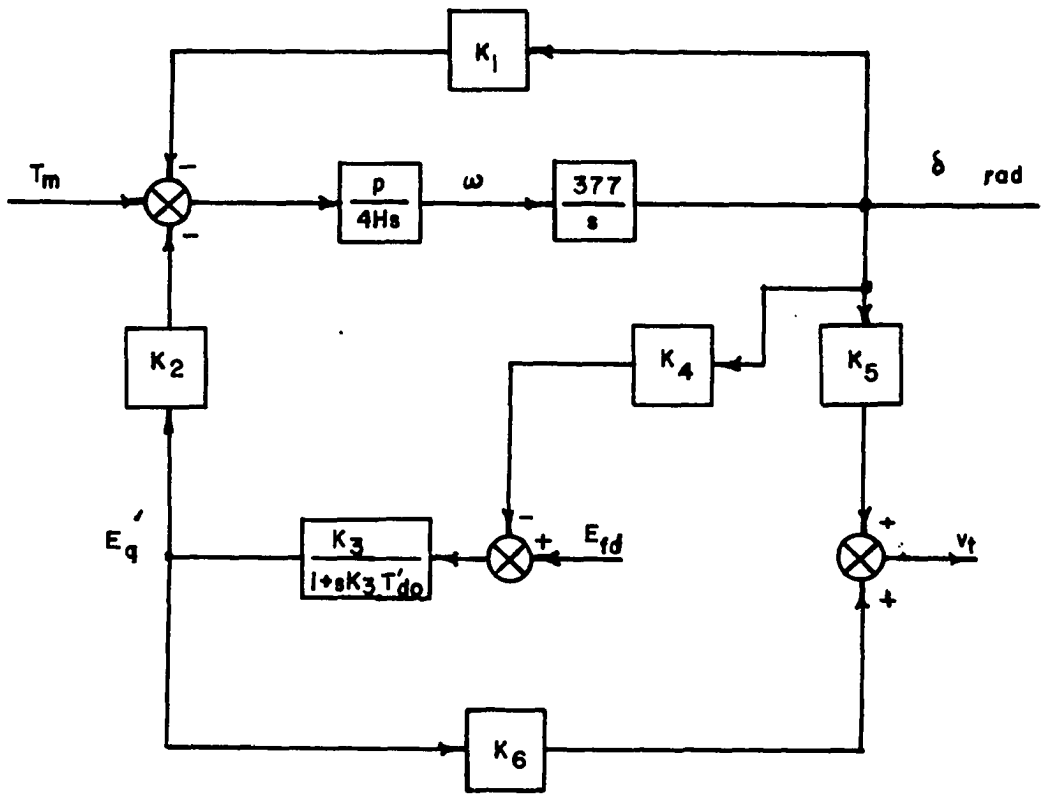

Figure 71. Block diagram of simplified synchronous machine

XI. APPENDIX C. COMPUTER PROGRAM TO CALCULATE INITIAL VALUES AND LINEAR PARAMETERS

```
C  THE FOLLOWING PROGRAM CALCULATES INITIAL CONDITIONS FOR A SYNCHRONOUS
C  MACHINE CONNECTED TO AN INFINITE BUS THROUGH A TRANSMISSION LINE AND
C  PARAMETERS FOR A LINEAR MODEL OF THE ABOVE SYSTEM.
C
C  DATA INPUT IS AS FOLLOWS:
C
C  THE FIRST CARD CONTAINS LINE RESISTANCE, LINE REACTANCE, DIRECT AXIS
C  SYNCHRONOUS REACTANCE, DIRECT AXIS LEAKAGE REACTANCE, AND QUADRATURE
C  AXIS SYNCHRONOUS REACTANCE (5F10.5).
C
C  ONE OR MORE CARDS ARE USED TO SPECIFY THE OPERATING CONDITION.
C  ONE OPERATING CONDITION PER CARD.
C  EACH CARD CONTAINS THE SINGLE PHASE POWER OUTPUT, SINGLE PHASE VAR OUTPUT,
C  AND THE INFINITE BUS VOLTAGE. (3F10.5)
C
C  A 999 CARD (F10.5) TERMINATES ONE CASE,  THAT IS ONE SET OF OPERATING
C  CONDITIONS FOR A GIVEN SYSTEM PARAMETER CARD.  THE ABOVE DATA SET MAY BE
C  REPEATED FOR ANOTHER SET OF SYSTEM PARAMETERS AND OPERATING CONDITIONS.
C
C  A 888 CARD (F10.5) TERMINATES COMPUTATION.
C
C  A SAMPLE DATA SET FOLLOWS.
C
C    .02       .4       1.7       .15      1.64
C   1.0        .62       .828
C   1.0        .62      1.0
C 999.         .0        .0
C 888.
1        REAL VBABC/0.0/, EQO/0.0/, IDOODQ/0.0/, IQOODQ/0.0/,
        1VTOODQ/0.0/, VDOODQ/0.0/, VQOODQ/0.0/, DELTA/0.0/, VBODQ/0.0/
2        REAL  X(5)
3      201 READ(5,1)   (X(I), I = 1,5)
4        1 FORMAT(5F10.5)
5         FLAG = X(1)
6         IF(FLAG.EQ.888.) GO TO 200
7      100 CONTINUE
```

```
      READ(5,2) P, Q, VBABC
    2 FORMAT(3F10.5)
      IF(P.EQ.999.)  GO TO 201
      WRITE(6,3)
    3 FORMAT('1', 'THE MACHINE AND LINE PARAMETERS ARE')
      WRITE(6,4)  (X(I), I=1,5)
    4 FORMAT ('0', 14X, 'RE  =', F8.3/15X,'XE  =', F8.3/
     115X, 'XD  =', F8.3/ 15X,'XD'' =',F8.3/ 15X,'XQ  =',F8.3)
      CALL CINVAL(X, P, Q, VBABC, VBODQ, EQO, IDOODQ, IQOODQ, VTOODQ,
     1VDOODQ, VQOODQ, DELTA)
      CALL CONST( X,DELTA, EQO, VBODQ, IQOODQ, IDOODQ, VDOODQ, VQOODQ,
     1 VTOODQ)
      GO TO 100
  200 CONTINUE
      STOP
      END


      SUBROUTINE CONST (XX, DELTA, EQO, VBODQ, IQOODQ, IDOODQ, VDOODQ,
     1VQOODQ, VTOODQ)
      REAL  XX(5), C(6), EQO, VBODQ,  IQOODQ, IDOODQ, SINDEL, COSDEL
      REAL VDOODQ, VQOODQ, VTOODQ, DELTA
      SINDEL = SIN(DELTA)
      COSDEL = COS(DELTA)
      A = XX(1)*XX(1) + (XX(2) +XX(4))*(XX(5)+XX(2))
      C(1) = (EQO*VBODQ/A)*(XX(1)*SINDEL + (XX(4)+XX(2))*COSDEL)
     1 +(IQOODQ*VBODQ/A)*((XX(5)-XX(4))*(XX(5)+XX(2))*SINDEL
     1 -(XX(5)-XX(4))*COSDEL*XX(1))
      C(2) = XX(1)*EQO/A +IQOODQ*(1.+(XX(5)-XX(4))*(XX(5)+XX(2))/A)
      C(3) = 1./(1.+(XX(3)-XX(4))*(XX(5)+XX(2))/A)
      C(4) =-(VBODQ*(XX(3)-XX(4))/A)*(XX(1)*COSDEL-(XX(5)+XX(2))*SINDEL)
      C(5)=(VDOODQ*XX(5)/(VTOODQ*A))*(XX(1)*VBODQ*SINDEL+VBODQ*COSDEL
     1*(XX(2)+XX(4)))
     1 +(VQOODQ*XX(4)/(VTOODQ*A))*(XX(1)*VBODQ*COSDEL-VBODQ*SINDEL
     1*(XX(2)+XX(5)))
      C(6) = (VQOODQ/VTOODQ)*(1.-XX(4)*(XX(5)+XX(2))/A)
```

```
     1 +VDOODQ*XX(2)*XX(1)/(VTOODQ*A)
      WRITE(6,1)
    1 FORMAT('0', 'THE LINEARIZED MACHINE CONSTANTS ARE')
      DO 10 I = 1,6
      WRITE(6,2)  I, C(I)
    2 FORMAT('0', 5X, 'C',  I1, 2X, '=', F8.4)
   10 CONTINUE
      RETURN
      END


      SUBROUTINE CINVAL (XX,P,Q,VBABC,VBODQ,EQO,IDOODQ,IQOODQ,VTOODQ,
     1VDOODQ,VQOODQ,DELTA)
      REAL XX(5), P, Q, VBABC, VBODQ, EQO, IDOODQ, IQOODQ, VTOODQ,
     1VDOODQ, VQOODQ, DELTA, TTHETA, IIPODQ, IIQODQ, RT3
      RT3 = SQRT(3.)
      VBODQ = RT3*VBABC
      TTHETA = Q/P
      THETA = ATAN(TTHETA)
      CTHETA = COS(THETA)
      CONS = VBABC*VBABC + 2.*P*(XX(1)+XX(2)*TTHETA)
      B24AC = CONS*CONS -4.*P*P*(XX(1)*XX(1)+XX(2)*XX(2))/(CTHETA*
     1CTHETA)
      IF(B24AC) 10,20,20
   10 WRITE(6,11)
   11 FORMAT('0', 'B**2-4AC IS LESS THAN ZERO')
      GO TO 100
   20 VTABC =SQRT((CONS+SQRT(B24AC))/2.)
      VTOODQ = RT3*VTABC
      IIPODQ = RT3*P/VTABC
      IIQODQ = RT3*Q/VTABC
      EQO = SQRT((VTOODQ+XX(5)*IIQODQ)**2+(XX(5)*IIPODQ)**2)
      COSDEL = (VTOODQ*(VTOODQ+IIQODQ*(XX(5)-XX(2))-IIPODQ*XX(1))
     1-XX(5)*XX(2)*(IIPODQ*IIPODQ+IIQODQ*IIQODQ))/(RT3*VBABC*EQO)
      DELTA =  ARCOS(COSDEL)
      DELDEG = DELTA*180./3.1416
      SINDEL = SIN(DELTA)
```

```
      IQOODQ = (IIPODQ*(VTOODQ+IIQODQ*XX(5))-IIQODQ*IIPODQ*XX(5))/EQO
      IDOODQ =-(IIPODQ*IIPODQ*XX(5)+IIQODQ*(VTOODQ+IIQODQ*XX(5)))/EQO
      VDOODQ = -IQOODQ*XX(5)
      VQOODQ = (VTOODQ*(VTOODQ+IIQODQ*XX(5)))/EQO
      TEO = EQO*IQOODQ
      WRITE(6,12)
   12 FORMAT('0', 'THE INITIAL CONDITIONS FOR THE MACHINE ARE')
      WRITE(6,14)  P, Q, VBABC, VTOODQ, VTABC,  IDOODQ, IQOODQ, VDOODQ,
     1 VQOODQ, DELDEG, TEO
   14 FORMAT('0',     'SINGLE PHASE POWER OUTPUT', 26X, '=', F8.3/
     11X, 'SINGLE PHASE VAR OUTPUT', 28X, '=',  F8.3/
     11X, 'INFINITE BUS VOLTAGE (ABC)', 25X, '=', F8.3/
     11X, 'TERMINAL VOLTAGE (ODQ)', 29X, '=', F8.3/
     11X, 'TERMINAL VOLTAGE (ABC)', 29X,'=', F8.3/
     11X, 'DIRECT AXIS CURRENT', 32X, '=', F8.3/
     11X, 'QUADRATURE AXIS CURRENT', 28X, '=', F8.3/
     11X, 'DIRECT AXIS TERMINAL VOLTAGE', 23X, '=', F8.3/
     11X, 'QUADRATURE AXIS TERMINAL VOLTAGE', 19X, '=', F8.3/
     1 1X, 'DELTA=ANGLE FROM INFINITE BUS TO Q-AXIS IN DEGREES =', F8.3/
     11X, 'MECHANICAL TORQUE', 34X,'=', F8.3)
  100 CONTINUE
      RETURN
      END
```

THE MACHINE AND LINE PARAMETERS ARE

RE = 0.020
XE = 0.400
XD = 1.700
XD' = 0.150
XQ = 1.640

THE INITIAL CONDITIONS FOR THE MACHINE ARE

SINGLE PHASE POWER OUTPUT	=	1.000
SINGLE PHASE VAR OUTPUT	=	0.620
INFINITE BUS VOLTAGE (ABC)	=	0.828
TERMINAL VOLTAGE (ODQ)	=	1.732
TERMINAL VOLTAGE (ABC)	=	1.000
DIRECT AXIS CURRENT	=	-1.927
QUADRATURE AXIS CURRENT	=	0.666
DIRECT AXIS TERMINAL VOLTAGE	=	-1.093
QUADRATURE AXIS TERMINAL VOLTAGE	=	1.343
DELTA=ANGLE FROM INFINITE BUS TO Q-AXIS IN DEGREES	=	67.047
MECHANICAL TORQUE	=	3.000

THE LINEARIZED MACHINE CONSTANTS ARE

C1 = 3.7128

C2 = 2.5507

C3 = 0.2620

C4 = 3.7049

C5 = -0.5861

C6 = 0.5598

THE MACHINE AND LINE PARAMETERS ARE

RE = 0.020
XE = 0.400
XD = 1.700
XD' = 0.150
XQ = 1.640

THE INITIAL CONDITIONS FOR THE MACHINE ARE

SINGLE PHASE POWER OUTPUT	=	1.000
SINGLE PHASE VAR OUTPUT	=	0.620
INFINITE BUS VOLTAGE (ABC)	=	1.000
TERMINAL VOLTAGE (ODQ)	=	2.031
TERMINAL VOLTAGE (ABC)	=	1.172
DIRECT AXIS CURRENT	=	-1.591
QUADRATURE AXIS CURRENT	=	0.700
DIRECT AXIS TERMINAL VOLTAGE	=	-1.148
QUADRATURE AXIS TERMINAL VOLTAGE	=	1.675
DELTA=ANGLE FROM INFINITE BUS TO Q-AXIS IN DEGREES	=	53.750
MECHANICAL TORQUE	=	3.000

THE LINEARIZED MACHINE CONSTANTS ARE

C1 = 4.8866

C2 = 2.6731

C3 = 0.2620

C4 = 3.9067

C5 = -0.8004

C6 = 0.5958

XII. APPENDIX D. EXCITATION SYSTEM AND COMPENSATION NETWORKS

The generator used in this study is equipped with an amplidyne voltage regulator having a response ratio of 0.5. Because high response ratio exciters tend to decrease system damping, thus contributing to the dynamic stability problem, the above exciter-regulator was replaced in these studies with one having a higher response ratio (58). A rotating-rectifier exciter with static voltage regulator having parameters given by Perry et al. (94) was used. This particular exciter had a response ratio of 2.23.

The excitation system was modeled by using the Type 2 excitation system representation suggested in an IEEE Committee Report (59). A block diagram representation is shown in Figure 72 and appropriate constants are given in Table 6. In order to conserve analog computer components, the takeoff point for the rate compensation network was moved as shown in Figure 73.

Table 6. Exciter parameters

K_A = 400		$v_{R\ max}$ = 8.26 pu	
T_A = 0.02		$v_{R\ min}$ = -8.26 pu	
T_E = 0.015		$S_{E\ max}$ = 0.86	
K_E = 1.0		$S_{E\ 0.75\ max}$ = 0.50	
K_F = 0.04		T_R = 0	
T_F = 0.05		K_R = 1.0	
		$E_{FD\ max}$ = 4.45 pu	

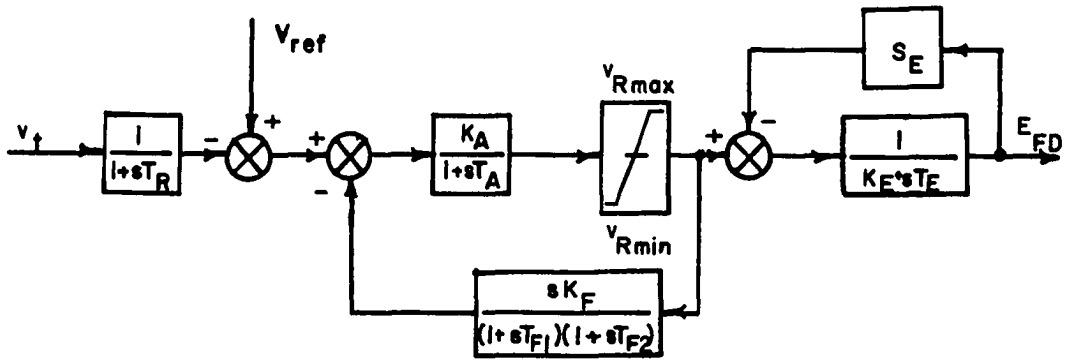

Figure 72. Type 2 excitation system representation, rotating-rectifier system

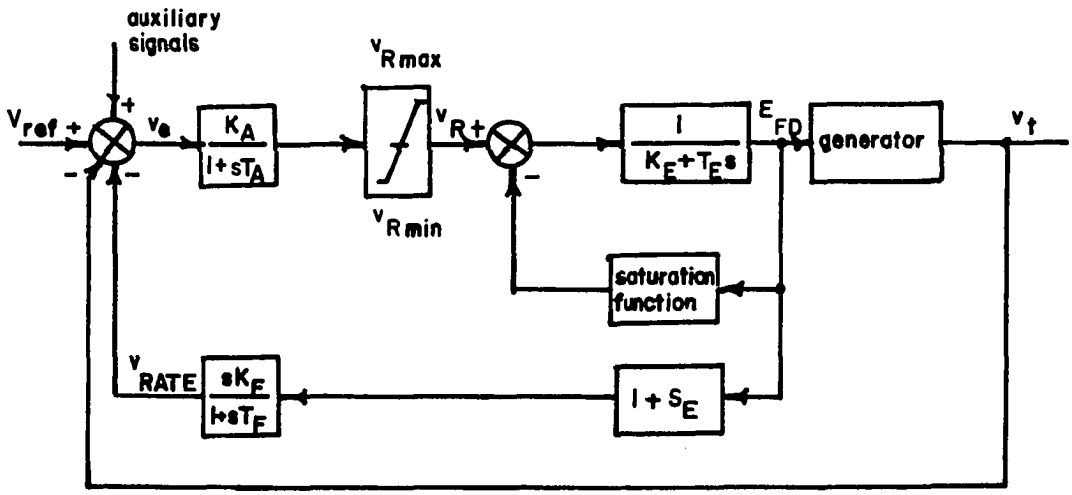

Figure 73. Type 2 excitation system as modified for analog computer representation

Perry et al. (94) did not give parameters for saturation or for voltage regulator limiting so typical values of S_E for this type of excitation system were taken from the IEEE Committee Report (59).

$$S_{E\ max} = 0.86 \qquad [D\text{-}1]$$

$$S_{E\ 0.75\ max} = 0.50 \qquad [D\text{-}2]$$

From these two values, an exciter saturation curve was constructed as shown in Figure 74. Values read from this curve are tabulated in Table 7. S_E is then computed and S_E vs E_{FD} is shown in Figure 75. Table 7 also contains the product $E_{FD}S_E$ as a function of E_{FD}. The linear approximation of this curve is shown in Figure 76. This function was simulated on the analog computer using a manual diode function generator to represent exciter saturation effects as shown in Figure 77.

Table 7. Saturation function

E_{FD}	A	B	$S_E = \frac{A}{B} - 1$	$E_{FD} \times S_E$
0			0.366	0
0.5	0.688	0.5	0.366	1.83
1.0	1.366	1.0	0.366	3.66
1.5	2.050	1.5	0.366	5.50
2.0	2.750	2.0	0.373	7.45
2.5	3.500	2.5	0.400	10.00
3.0	4.350	3.0	0.450	13.50
3.5	5.330	3.5	0.522	18.30
4.0	6.500	4.0	0.625	25.00
4.5	8.600	4.5	0.910	40.80

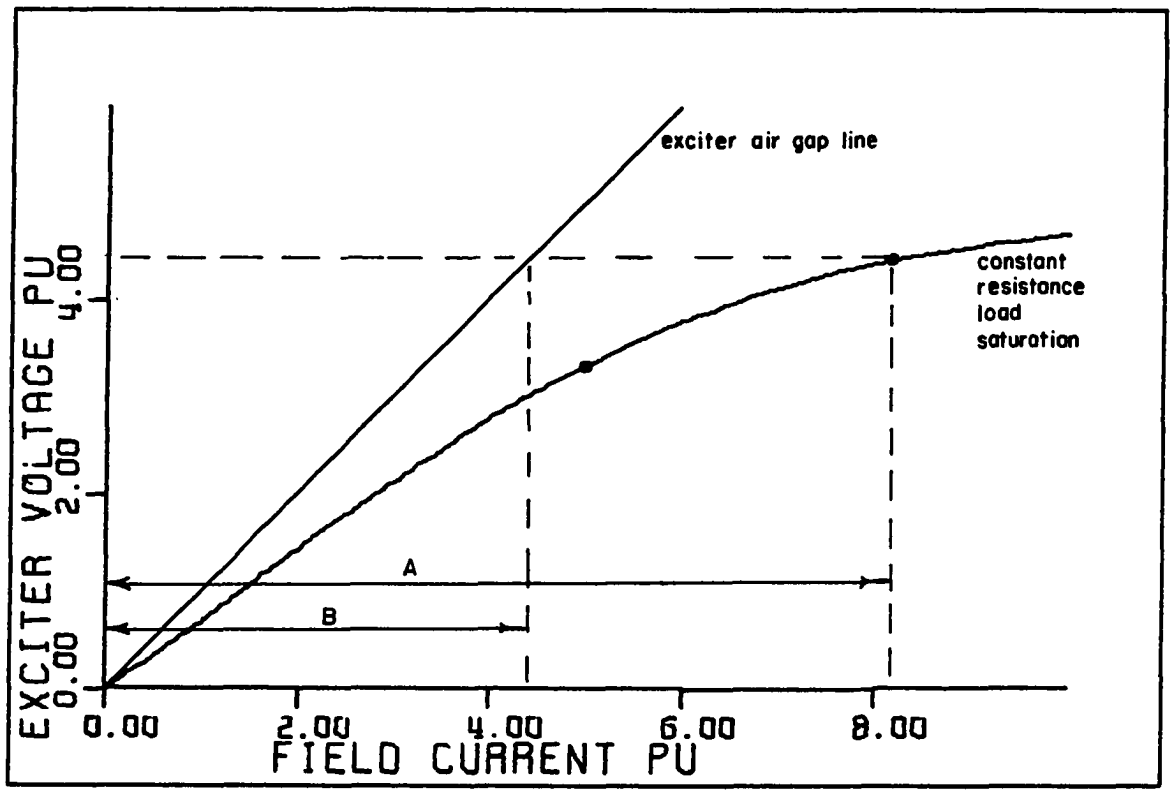

Figure 74. Exciter saturation curve

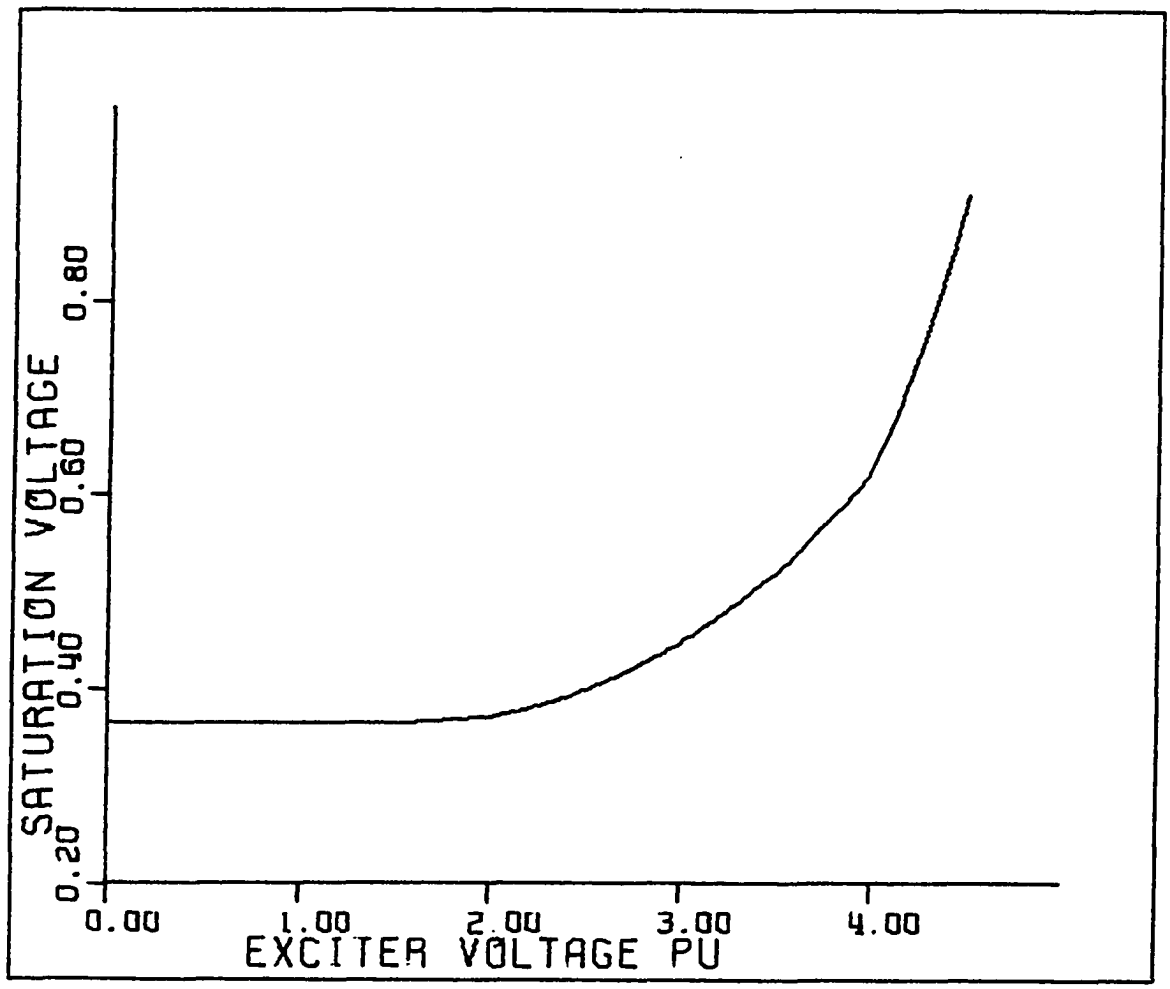

Figure 75. Saturation function

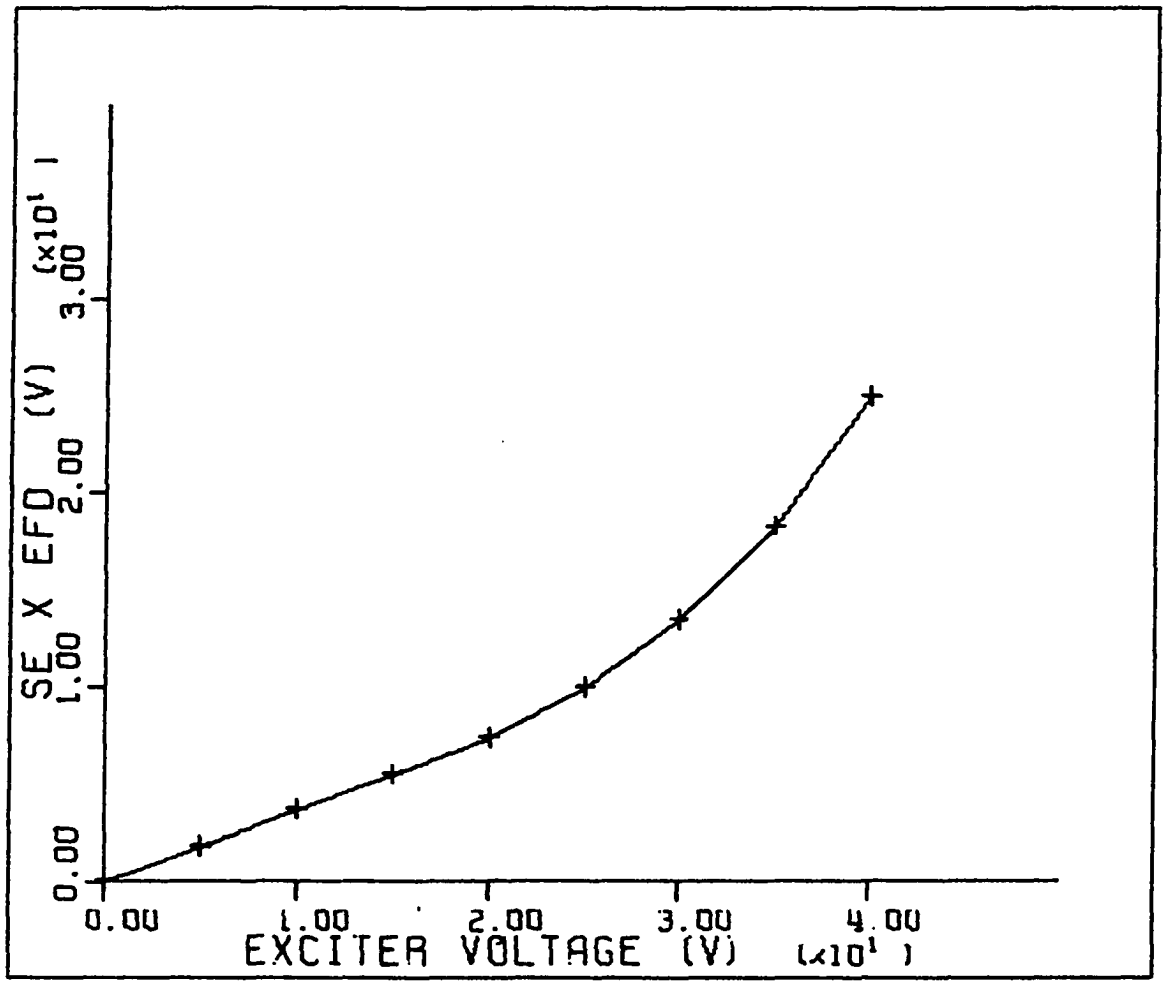

Figure 76. Curve used to set DFG on analog computer

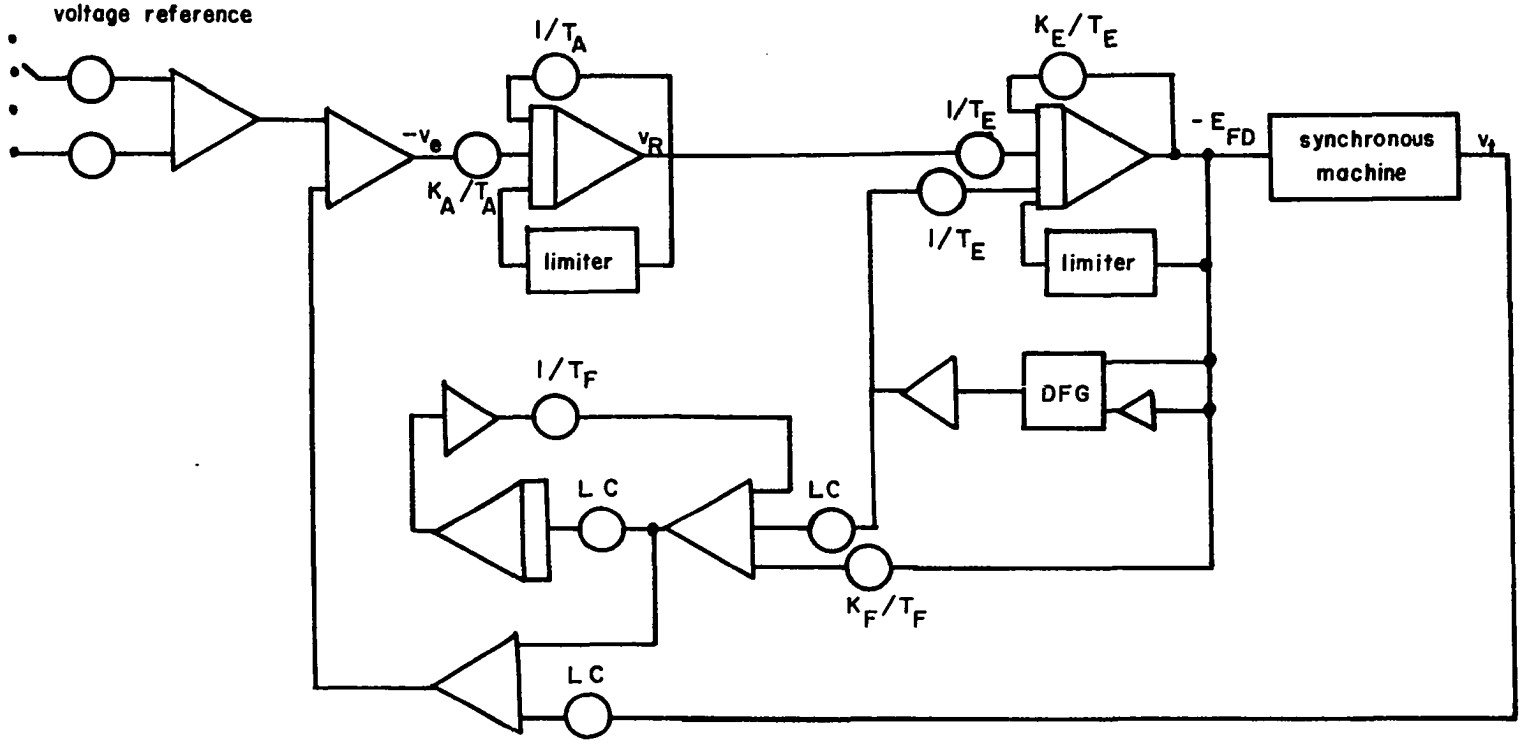

Figure 77. Analog computer diagram of the excitation system

Limiting values for $v_{R\ max}$ were not given but may be calculated from

$$v_{R\ max} - (K_E + S_{E\ max})E_{FD\ max} = 0 \qquad [D-3]$$

Using data from Table 7

$$v_{R\ max} = 8.26\ pu \qquad [D-4]$$

The analog computer diagram of the excitation system is shown in Figure 77.

A. Mathematical Development of Excitation System Equations

The equations necessary to describe the dynamic and steady-state performance of the excitation system are developed from Figure 73 as follows (7).

1. Potential transformer and rectifier

A suitable input signal for the excitation system may be generated by connecting the phase voltages of the synchronous machine to potential transformers which have their secondaries connected to bridge rectifiers. Three bridges may be connected in series and produce an output voltage, v_{dc}, which is proportional to synchronous machine terminal voltage. This circuitry may be represented by a first order system having the following transfer function

$$v_{dc} = \frac{K_R\ v_t}{1 + sT_R} \qquad [D-5]$$

where K_R is a proportionality constant and T_R is the time constant due to filtering or smoothing in the transformer-rectifier assembly. Generally T_R is small and in this study it is assumed to be negligible.

2. Reference comparator

This component compares v_{dc} to a fixed reference potential which is proportional to the desired machine terminal voltage. The difference is v_e the error voltage where

$$v_e = V_{ref} - v_{dc} \qquad [D-6]$$

Auxiliary signals from the rate feedback network or other sources are also fed into the comparator and may be considered as changes in the reference voltage V_{ref}.

3. Amplifier

The error voltage, v_e, is amplified by some means, for example, a rotating, magnetic or electronic amplifier, and then used to drive the exciter. Linear voltage amplification K_A is assumed with time constant T_A. The transfer function is

$$v_R = \frac{K_A v_e}{1 + sT_A} \qquad [D-7]$$

Amplifier saturation is represented by limiting, that is

$$v_{R\ min} < v_R < v_{R\ max}$$

4. Exciter

The exciter is represented as shown in Figure 73 where S_E is a function of E_{FD} and represents the effects of saturation. The transfer function for the exciter is

$$E_{FD} = \frac{v_R - S_E E_{FD}}{K_E + T_E s} \qquad [D-8]$$

5. Rate feedback compensator

The performance of the excitation system can be stabilized by using rate feedback compensation to decrease system gain during transients. A transfer function representing this feedback is

$$v_{rate} = \frac{sK_F E_{FD}}{1 + sT_F} \qquad [D-9]$$

6. Bridged-T filter

The transfer function of a bridged-T network may be written as (104)

$$\frac{C}{R} = \frac{s^2 + rn\,\omega_o s + \omega_o^2}{s^2 + n\,\omega_o s + \omega_o^2} \qquad [D-10]$$

where ω_o is the frequency where the notch is to occur, r is the notch ratio, i.e., the ratio of the amplitude at ω_o to the amplitude at zero frequency, and n is the relative width of the notch.

The filter produces two zeros located at

$$\frac{-rn\,\omega_o \pm \omega_o \sqrt{(rn)^2 - 4}}{2} \qquad [D-11]$$

and two poles at

$$\frac{-n\,\omega_o \pm \omega_o \sqrt{n^2 - 4}}{2}$$

An analog computer diagram for implementation of a transfer function having the form of Equation D-10 is given in Appendix B of (39). The resulting analog computer diagram for a bridged-T network is shown in Figure 78.

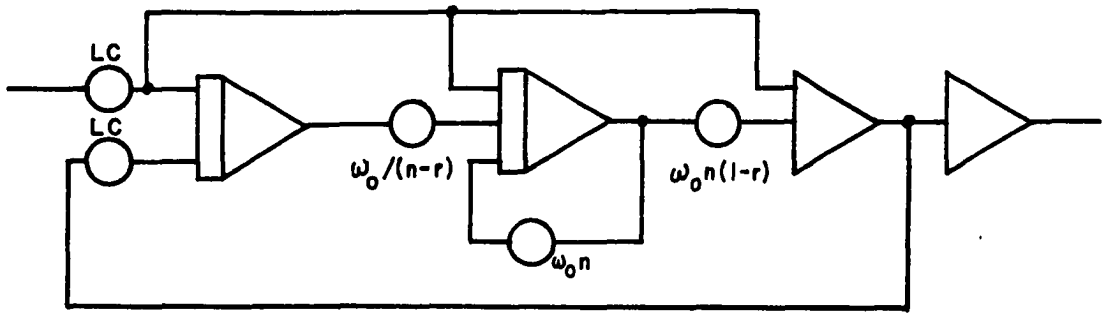

Figure 78. Analog computer diagram for a bridged-T filter

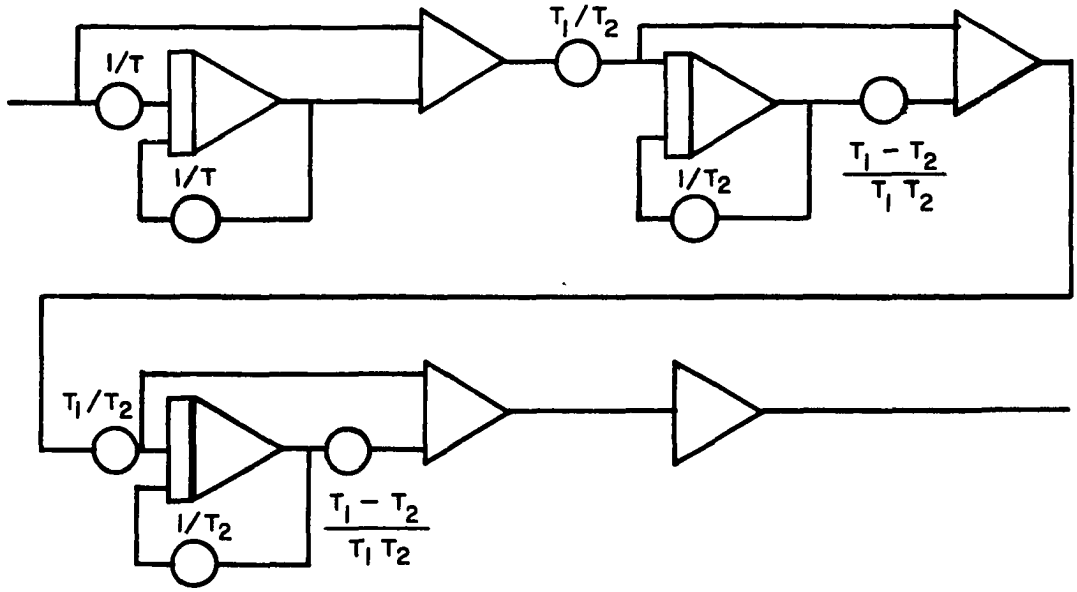

Figure 79. Analog computer diagram for a power system stabilizer

7. Power system stabilizer

The transfer function for a power system stabilizer is

$$\frac{C}{R} = \frac{Ks}{1 + sT} \frac{(1 + sT_1)}{(1 + sT_2)} \frac{(1 + sT_1)}{(1 + sT_2)} \qquad [D-12]$$

The analog computer diagram for this transfer function is again developed using (39) and the result is shown in Figure 79.

8. Two-stage lead-lag network

The power system stabilizer contains a two-stage lead-lag network so a transfer function for the latter can be obtained from Equation D-12 by omitting the first factor. The associated analog computer diagram is shown in Figure 80.

9. Speed feedback compensation networks

The transfer function necessary to cancel the torque-angle loop and field poles using speed feedback was previously shown to be

$$\frac{D}{As + B} \quad \text{if } T_R = 0$$

The analog computer simulation of this transfer function is again developed using Appendix B of (39). The resulting analog computer diagram is shown in Figure 81 part (a). The compensator used to cancel the torque-angle loop poles only has a transfer function of the following form.

$$\frac{Cs - |D|}{As + B}$$

The resulting analog computer diagram is shown in Figure 81 part (b).

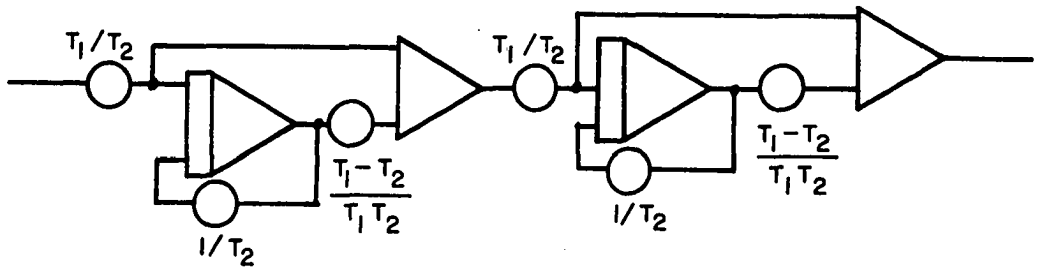

Figure 80. Analog computer diagram for a two-stage lead-lag network

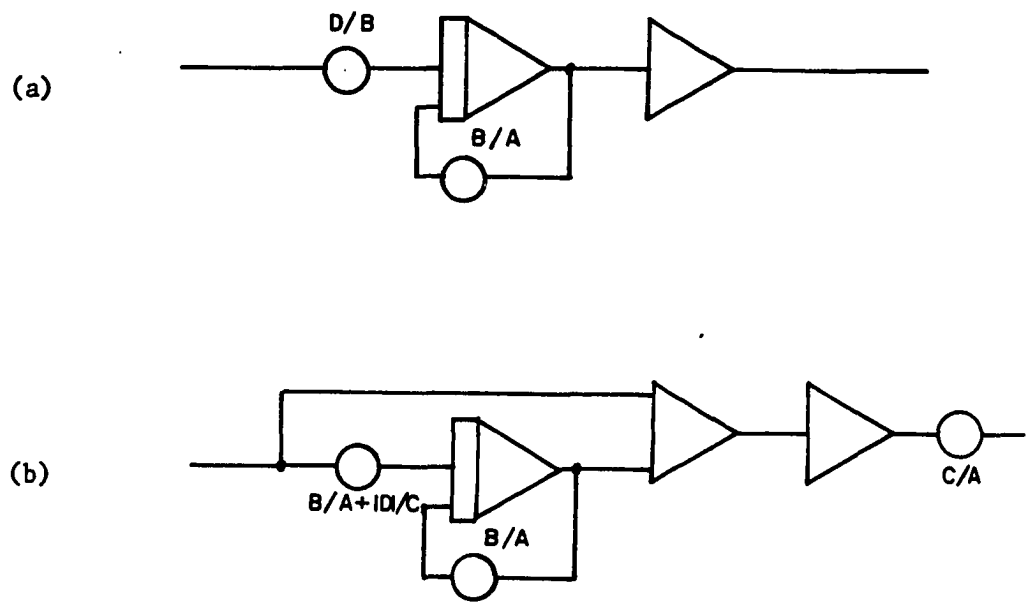

Figure 81. Analog computer diagrams for speed feedback compensators:
(a) used to cancel torque-angle loop poles and field pole,
(b) used to cancel torque-angle loop poles

XIII. APPENDIX E. ANALOG COMPUTER REPRESENTATION

In this appendix the data used for the analog computer studies of Chapter V are presented. Tables of potentiometer settings are given and the final analog computer diagram showing the interconnections of various components is also included. All values are in per unit unless otherwise noted.

A. Data

Generator (7)

$L_d = 1.70$	$\ell_D = 0.055$	$r_Q = 0.0198$
$L_q = 1.64$	$L_D = 1.605$	$R = 100$
$\ell_a = 0.15$	$\ell_Q = 0.036$	$L_{MD} = 0.02818$
$L_{AD} = 1.55$	$L_Q = 1.526$	$L_{MQ} = 0.02846$
$L_{AQ} = 1.49$	$r = 0.001126$	
$\ell_f = 0.101$	$r_F = 0.00805$	
$L_F = 1.65$	$r_D = 0.0132$	

$H = 2.37$ sec
$T'_{do} = 5.90$ sec

Exciter (94)

$K_A = 400$	$S_{E\ max} = 0.86$	
$T_A = 0.02$ sec	$S_{E\ 0.75\ min} = 0.50$	
$T_E = 0.015$ sec	$T_R = 0.0$ sec	
$K_E = 1.0$	$K_R = 1.0$	
$K_F = 0.04$	$E_{FD\ max} = 4.45$	
$T_F = 0.05$ sec		
$v_{R\ max} = 8.26$		
$v_{R\ min} = 8.26$		

Governor (17)

$T_{SR} = 0.05$ sec	$T_{RH} = 10.0$ sec	$C_g = 20$
$T_{SM} = 0.15$ sec	$f = 0.23$	
$T_B = 0.10$ sec	$K_3 = 0.7$	

Power system stabilizer (31)

$T = 3.0$ sec	$T_1 = 0.2$ sec	$T_2 = 0.05$ sec

Two-stage lead-lag network

$T_1 = 0.2$ sec	$T_2 = 0.05$ sec

Bridged-T (104) tuned to natural frequency of machine

$\omega_o = 21$ rad/sec	$n = 2$	$r = 0.1$

Potentiometer settings for the synchronous machine, excitation system, governor, and the compensation networks are given in Tables 8, 9, 10 and 11. The analog computer diagram is shown in Figure 82. Analog switches are provided for changing voltage and torque reference levels and for inserting the various compensation networks. Potentiometers normally used to supply initial conditions to the integrators are omitted to conserve analog computer components. Initial conditions are established as follows.

The speed is held constant when the simulation is started by holding integrator 210 in IC. Flux linkages are allowed to build up, and after steady-state conditions have been established, amplifier 210 is allowed to integrate. Switch 411 is then closed applying load to the machine. Positive or negative increments of machine loading are accomplished by switching 011 to the right or left respectively.

A similar arrangement using switch 021 allows incremental changes in the voltage reference level which is established by potentiometer 613. The squaring and square root circuitry necessary to generate the terminal voltage v_t is somewhat noisy, so amplifier 610 is used as a filter to reduce the noise level. A 0.001 μf feedback capacitor is connected in the feedback path of amplifier 610 by appropriate logic patching.

Components used in the two-stage lead-lag network placed in the forward loop of the exciter are also used in the power system stabilizer. The governor is omitted due to lack of analog computer components.

Although they are not essential to the basic simulation, two additional quantities are computed. The electrical power output of the machine is available at amplifier 213 and the change in terminal voltage

Table 8. Potentiometer settings for synchronous machine

Potentiometer number	Potentiometer settings	Amplifier gain	Constant	Numerical substitutions	Value	Scaling	Value x scaling
000	0.0283	1	$r\omega_B/\ell_a$	.001126(377)/.15	2.8300	50/50x1/100=0.010	0.0283
001	0.9040	1	$r_D\omega_B/\ell_D$	.0132(377)/.055	90.400	50/50x1/100=0.010	0.9040
002	0.6960	1	L_{MD}/ℓ_F	.02818/.101	0.2785	50/20=2.500	0.6960
003	0.2665	10	$1/\ell_a$	1/.15	6.6660	20/50=0.400	2.6650
010	0.0283	1	$r\omega_B/\ell_a$	.001126(377)/.15	2.8300	50/50x1/100=0.010	0.0283
011	0.2070	10	$r_Q\omega_B/\ell_Q$	.0198(377)/.036	207.00	50/50x1/100=1.000	2.0700
012	0.7906	1	L_{MQ}/ℓ_Q	.02846/.036	0.7906	50/50=1.000	0.7906
013	0.2665	10	$1/\ell_a$		6.6660	20/50=0.400	2.6650
100	0.4710	10	ω_B		377.00	50/40x1/100=0.0125	4.7100
101	0.9040	1	$r_D\omega_B/\ell_D$		90.400	50/50x1/100=0.010	0.9040
102	0.5120	1	L_{MD}/ℓ_D	.02818/.055	0.5120	50/50=1.000	0.5120
103	0.2665	10	$1/\ell_a$		6.6660	20/50=0.400	2.6650
110	0.4710	10	ω_B		377.00	50/40x1/100=0.0125	4.7100
111	0.2070	10	$r_Q\omega_B/\ell_Q$		207.00	50/50x1/100=0.010	2.0700
112	0.0050	1	R	100.	100.00	40/20=2.000	200.00
113	0.0050	1	R	100.	100.00	40/20=2.000	200.00

Table 8 (Continued)

Potentiometer number	Potentiometer settings	Amplifier gain	Constant	Numerical substitutions	Value	Scaling	Value x scaling
200	0.7540	10	ω_B		377.00	50/25x1/100=0.020	7.5400
201	0.1212	.1	$r_F\omega_B/\ell_F$	.000805(377)/.101	3.0300	20/50x1/100=0.004	0.01212
202	0.1879	1	L_{MD}/ℓ_a	.02818/.15	0.1879	50/50=1.000	0.1879
210	0.7540	10	ω_B		377.00	50/25x1/100=0.020	7.5400
211	0.0283	1	$r\omega_B/\ell_a$	.001126(377)/.15	2.8300	50/50x1/100=0.010	0.0283
212	0.5000	1	ω_B/ω_B		1.0000	50/100=0.500	0.5000
213	0.1000	1	L.C.	1	1.0000	50/500=0.100	0.1000
300	0.0283	1	$r\omega_B/\ell_a$	.001126(377)/.15	2.8300	50/50x1/100=0.010	0.0283
301	0.3030	.1	$r_F\omega_B/\ell_F$		3.0300	20/20x1/100=0.010	0.0303
302	0.0778	.1	$\omega_B$xbase change	377(162v/157KV)	0.3890	20/10x1/100=0.020	0.00778
303	0.1055	1	p/2 1/2H	1/2 (2.37)	0.2110	500/10x1/100=0.500	0.1055
400	0.0188	10	$R_E\omega_B/L_E$	.02(377)/.4	18.850	20/20x1/100=0.010	0.1885
401	0.4710	10	ω_B/L_E	377/.4	944.00	20/40x1/100=0.005	4.7100
402	0.7540	10	ω_B		377.00	20/10x1/100=0.020	7.5400
403	0.4710	10	ω_B/L_E		944.00	20/40x1/100=0.005	4.7100
410	0.2160	1	$57.3\omega_B$	57.3(377)	21,600	$.5/500x1/100=10^{-5}$	0.2160

Table 8 (Continued)

Potentiometer number	Potentiometer settings	Amplifier gain	Constant	Numerical substitutions	Value	Scaling	Value x scaling
412	0.1897	1	L_{MQ}/ℓ_a	.02846/.15	0.1897	50/50x1=1.000	0.1897
413	0.2665	10	$1/\ell_a$		6.6660	20/50x1=0.400	2.6650
500	0.3264	10	$\sqrt{3}\omega_B/L_E$	3(377)/.4	1632.0	20/100x1/100=0.002	3.2640
501	0.7540	10	ω_B		377.00	20/10x1/100=0.020	7.5400
502	0.3264	10	$\sqrt{3}\omega_B/L_E$		1632.0	20/100x1/100=0.002	3.2640
503	0.0188	10	$R_E\omega_E/L_E$		18.850	20/20x1/100=0.010	0.1885
612	0.0291	1	5% full load				
613	0.5905	1	full load				
610	0.0300	1	10% full load .3 pu		0.3000	10/100=0.100	0.0300
611	0.3000	1	full load T_M 3 pu		3.0000	10/100=0.100	0.3000

Table 9. Potentiometer settings for excitation system

Potentiometer number	Potentiometer settings	Amplifier gain	Constant	Numerical substitutions	Value	Scaling	Value x scaling
600	0.0200	1	L.C.	1.0		100/50x1/100=0.020	0.0200
602	0.9990	10	$1/T_F$	1/.05	20.000	50/100=0.500	10.000
701	0.5000	1	$1/T_A$	1/.02	50.000	1/1x1/100=0.010	0.5000
800	0.4000	10	K_A/T_A	400/.02	20,000	1/50x1/100=0.0002	4.0000
801	0.6667	10	$1/T_E$	1/.015	66.670	10/1x1/100=0.100	6.6670
802	0.6667	1	$1/T_E$	1/.015	66.670	10/10x1/100=0.010	0.6667
803	0.6667	1	K_E/T_E	1.0/.015	66.670	10/10x1/100=0.010	0.6667
810	0.7210	1	L.C.	$1/\sqrt{3}$	0.5770	50/40x1=1.250	0.7210
812	0.4000	10	K_F/T_F	.04/.05	0.8000	50/10=5.000	4.0000
813	0.5000	10	L.C.		1.0000	50/10=5.000	5.0000

Table 10. Potentiometer settings for governor

Potentiometer number	Potentiometer settings	Amplifier gain	Constant	Numerical substitutions	Value	Scaling	Value x scaling
222	0.1400	10	K_3/T_{SR}	20x.7	14.000	10/1x1/100=.100	1.4000
233	0.0667	1	$1/T_{SM}$	6.6667	6.6670	10/10x1/100=.010	0.0667
020	0.1000	1	$1/T_B$	10.000	10.000	10/10x1/100=.010	0.1000
230	0.1000	1	$1/T_B$	10.000	10.000	10/10x1/100=.010	0.1000
220	0.2000	1	$1/T_{SR}$	20.000	20.000	10/10x1/100=.010	0.2000
223	0.2300	1	f	0.23	0.23	10/10=1.00	0.2300
232	0.4000	10	C_g	20	20	1/50=.020	0.4000
221	0.0667	1	$1/T_{SM}$	6.666	6.666	10/10x1/100=.010	0.0667
231	0.0010	1	$1/T_{RH}$	.1	.1	10/10x1/100=.010	0.0010
203	0.2000	1	ω_{ref} corresponding to $T_m = 0$				
610	0.0045	1	ω_{ref} corresponding to $T_m = 0.3$				
611	0.0452	1	ω_{ref} corresponding to $T_m = 3.0$				

Table 11. Miscellaneous potentiometer settings

Potentiometer number	Potentiometer settings	Amplifier gain	Constant	Numerical substitutions	Value	Scaling	Value x scaling
Power system stabilizer							
021	0.0333	.1	1/T	1/3	0.3330	500/500x1/100=.010	.00333
220	0.0333	.1	1/T	1/3	0.3330	500/500x1/100=.010	.00333
221	0.2000	1	$1/T_2$	1/.05	20.000	500/500x1/100=.010	0.2000
222	0.0400	1	T_1/T_2	.2/.05	4.000	50/50x1/100=.010	0.0400
223	0.0400	1	T_1/T_2	.2/.05	4.000	500/500x1/100=.010	0.0400
230	0.1500	10	T_1-T_2/T_1T_2	(.2-.05)/.2(.05)	15.000	5/50=.100	1.5000
231	0.2000	1	$1/T_2$	1/.05	20.000	50/50x1/100=.010	0.2000
232	0.1500	10	T_1-T_2/T_1T_2	(.2-.05)/.2(.05)	15.000	50/500x1=.100	1.5000
601	0.5000						
Two-stage lead-lag network							
221	0.2000	1	$1/T_2$	1/.05	20.000	10/10x1/100=.010	0.2000
222	0.4000	1	T_1/T_2	.2/.05	4.0000	10/1x1/100=.100	0.4000
223	0.4000	1	T_1/T_2	.2/.05	4.0000	10/1x1/100=.100	0.4000
230	0.1500						

Table 11 (Continued)

Potentiometer number	Potentiometer settings	Amplifier gain	Constant	Numerical substitutions	Value	Scaling	Value x scaling
Two-stage lead-lag network							
231	0.2000	1	$1/T_2$	1/.05	20.000	10/10x1/100=.010	0.2000
232	0.1500	10	T_1-T_2/T_1T_2	(.2-.05)/.2(.05)	15.000	1/10=.100	1.5000
Bridged-T network							
022	0.1000	1	L.C.	1	1.0000	40/4x1/100=.100	0.1000
023	0.0100	1	L.C.	1	1.0000	40/40x1/100=.010	0.0100
030	0.1167	1	$\omega_o/n-r$	21/(2-.2)	11.670	40/40x1/100=.010	0.1167
031	0.4200	1	$\omega_o n$	21(2)	42.000	40/40x1/100=.010	0.4200
032	0.3780	10	$\omega_o(n-r_n)$	21(2)(1-.1)	37.800	4/40x1=.100	3.7800
Infinite bus modulator							
020	0.0441	1	ω_o^2	21^2	441.00	$50/50x1/100^2=.0001$	0.0441
203	0.5000	IC	L.C.	1	1.0	50/100=.500	0.5000
033	0.8280	1	1	1	1.0	82.8/100=.828	0.8280
233	0.0332	1	.02	.02	0.02	82.8/50=1.65	0.0332

Table 11 (Continued)

Potentiometer number	Potentiometer settings	Amplifier gain	Constant	Numerical substitutions	Value	Scaling	Value x scaling
Speed compensation used to cancel torque-angle loop and field poles							
020	0.0164	0.1	B/A	.425/2.59	0.164	1/100=0.010	0.00164
233	0.1840	10	D/B	-782/.425	-1840	50/500x1/100=0.001	1.8400
Speed compensation used to cancel torque-angle loop poles							
020	0.0288	1	B/A	4.84/1.68	2.88	50/50x1/100=0.010	0.0288
021	0.1000	1	L.C.	1.00	1.00	50/500=0.100	0.1000
233	0.1370	1	B/A+|D|/C	4.84/1.68+506.4/3.76	137.38	50/500x1/100=0.001	0.1370
601	0.2240	10	C/A	3.76/1.68	2.24	50/50=1.000	2.2400

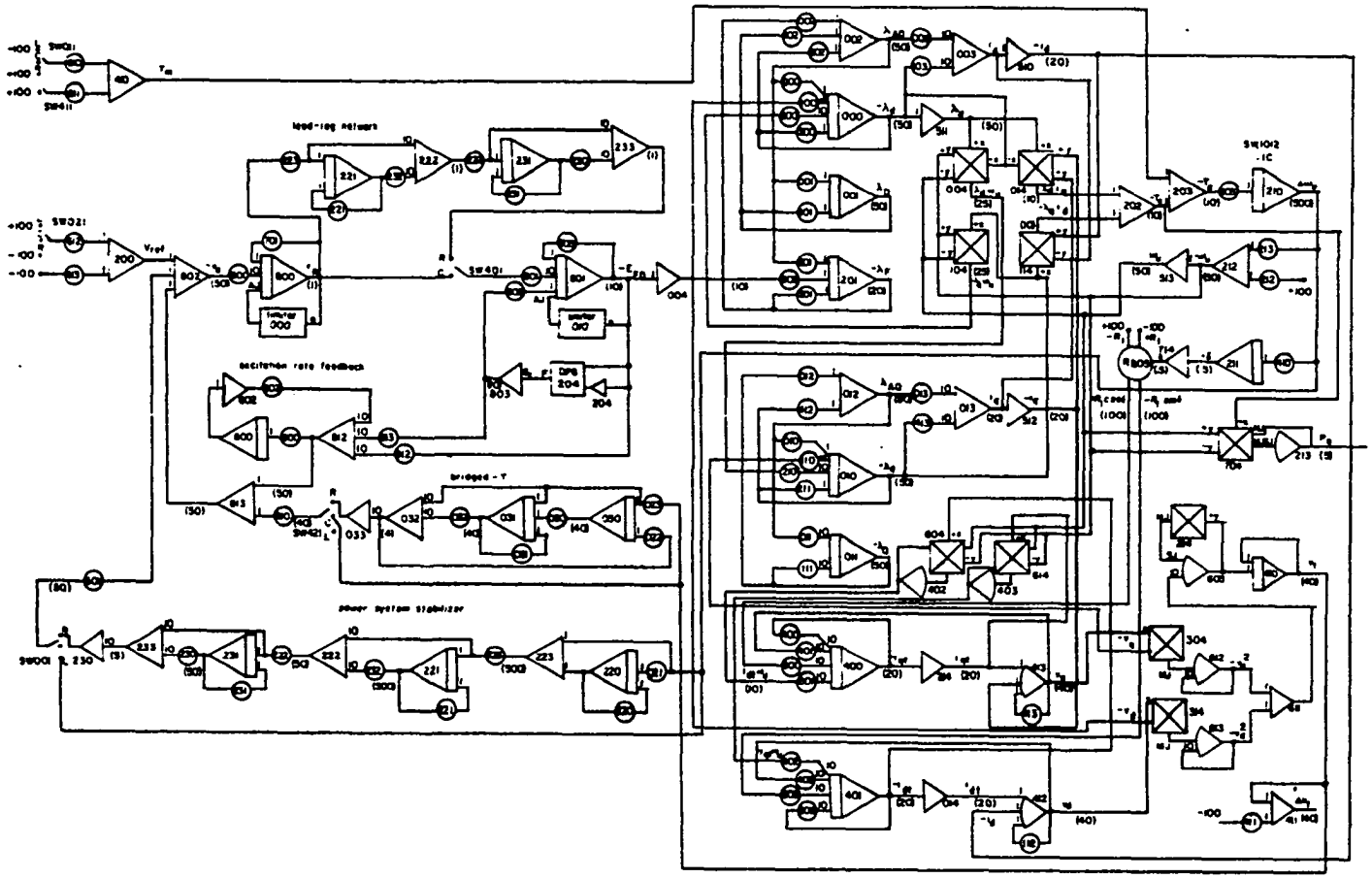

Figure 82. Composite analog computer diagram

is produced at amplifier 411. Excitation system rate feedback is removed by setting potentiometers 812 and 813 to zero or by removing the connection from the output of amplifier 812 to the input of amplifier 813.

The time scaling factor, a, for the simulation was 100. Thus, one second of synchronous machine operation is represented by 100 seconds of analog computer time if the simulation is operated at the medium-second speed. Normally it was found desirable to speed up the analog computer simulation by a factor of ten so the computer was operated in the fast-second mode. Thus, one second of synchronous machine operation is equivalent to 10 seconds of operation on the analog computer.

While establishing the initial conditions of the simulation the analog computer was operated at milliseconds slow speed to minimize the time necessary to establish a steady-state condition. The time mode was then switched to fast or medium seconds and the particular test was then conducted. The simulation would not operate at millisecond medium or fast speeds, thus oscilloscope displays and the repetitive operation mode could not be used to optimize parameters. All variables were observed and recorded using the digital voltmeter and a strip chart recorder.

Figure 83 shows the analog computer simulation of the governor control system. Potentiometer settings are given in Table 10.

The analog computer circuitry necessary to modulate the infinite bus voltage is shown in Figure 84 and potentiometer settings are given in Table 11. These values result in the infinite bus voltage being set at a value corresponding to Base Case 1. The modulation increases and decreases the infinite bus voltage by 2% peak at a frequency

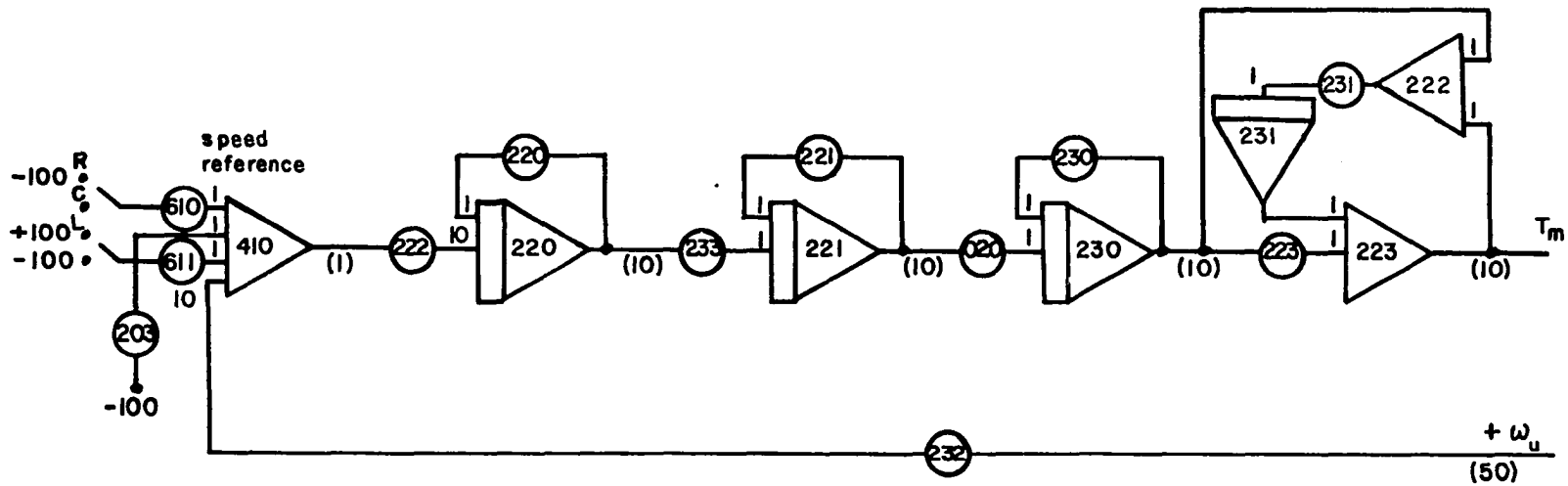

Figure 83. Analog computer diagram of governor control system

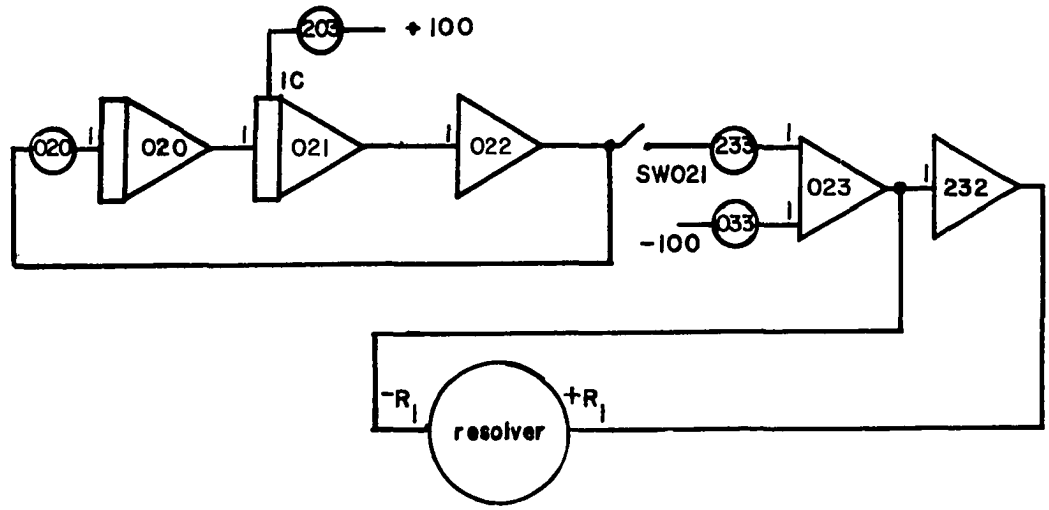

Figure 84. Analog computer diagram of circuit used to modulate infinite bus voltage

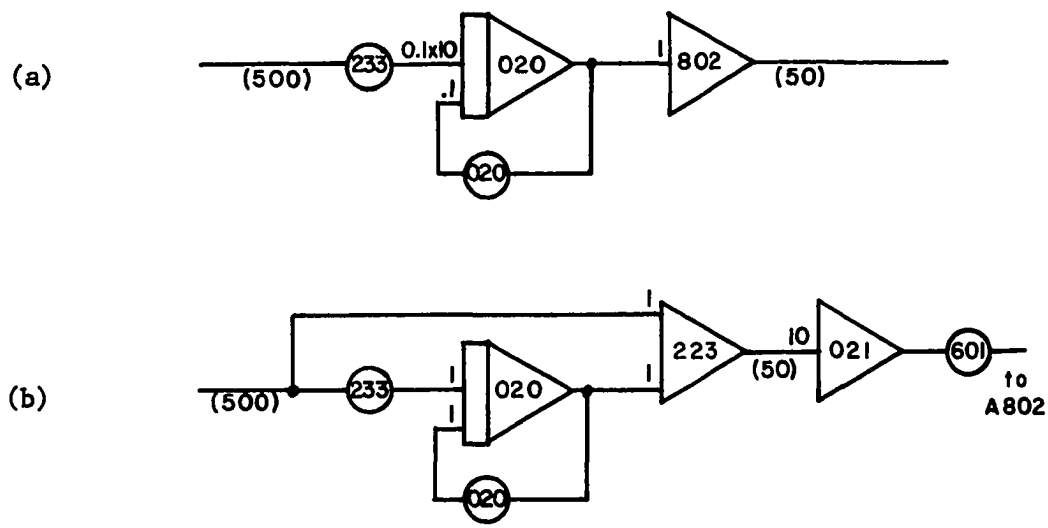

Figure 85. Analog computer diagrams of speed feedback compensation networks: (a) cancellation of torque-angle loop poles and field pole, (b) cancellation of torque-angle loop pole

approximately equal to that of the uncompensated machine for the given potentiometer values.

Potentiometer settings for the speed feedback network used to cancel the torque-angle loop plus the field pole and the torque-angle loop poles alone are also given in Table 11. The analog computer diagrams for these compensators are shown in Figure 85.

B. Base Case Calculations

Two test cases have been calculated for the synchronous machine. In the first, the machine was assumed to be operating at rated conditions, that is, full load, 0.85 power factor lagging, and terminal voltage equal to 1.0 pu. This case provided a means of checking nameplate quantities against model performance under steady-state conditions and also provided a check on the excitation system since full load field current is given in the machine specifications. The machine was connected through a transmission line having $Z = 0.02 + j.4$ pu impedance to an infinite bus with its voltage adjusted so that the machine delivered rated power at rated power factor and rated terminal voltage.

The second test case was intended to represent the operating conditions of a fully loaded machine supplying power over a long transmission line. The loading was the same as in Base Case 1, that is, rated power output at 0.85 pf lagging, and the same tie line impedance was used. The infinite bus voltage was set at 1.0 pu and the terminal voltage was then adjusted to obtain the desired var loading.

Hand calculations for these two cases were made and the results,

along with digital and analog computer outputs, are summarized in Table 12 for Case 1 and in Table 13 for Case 2.

Figure 86 is similar to Figure 82 except the voltages (in volts) at the outputs of various analog computer components have been added. These voltages result from establishing conditions of Base Case 1 and allowing the simulation to come to a steady-state condition. Figure 87 shows the voltages resulting from the establishment of Base Case 2 conditions on the machine.

The dynamic performance of the synchronous machine without excitation and governing systems is shown in Figures 88, 89 and 90. Excitation was adjusted to produce machine loading as in Base Case 1. After establishing steady-state conditions the mechanical torque was increased from zero to 3.0 pu (full load). T_m was then increased and decreased by ten percent of full load. Next the voltage reference was increased and decreased by five percent and finally T_m was reduced to zero.

The variable is shown on the left and the scale factor is shown on the right. The width of one strip chart recording is 50 lines. Extreme left and right portions of the graphs indicate zero voltage levels. The positive direction is upward, and the distance between downward timing marks corresponds to one second of synchronous machine operation. The various references were switched at the same relative times in each of the figures. Thus the three figures are in effect a strip chart recording 24 channels wide.

Figures 91 and 92 show the dynamic performance of the synchronous machine with both exciter and governor control systems included. Excitation system rate feedback was included because the uncompensated system

Table 12. Base Case 1

Variable	Hand computation pu	Digital computer pu	Analog computer		
			Analog computer component	Voltage volts	Per unit
$P_{1\phi}$	1.0	1.0			
$Q_{1\phi}$	0.62	0.62			
V_{ref}	1.00805		A200	50.48	1.008
V_{Babc}	0.828	0.828	A023	82.80	0.828
			A232	82.80	0.828
v_{todq}	1.732	1.732	A610	69.40	1.732
V_{tabc}	1.0	1.0			
v_d	-1.09	-1.093	A412	-43.60	-1.090
v_q	1.342	1.343	A413	53.95	1.346
v_F	0.00239				
E_{FD}	2.31		A004	25.12	2.512
i_d	-1.921	-1.927	A003	-38.35	1.918
i_q	0.664	0.666	A013	13.39	0.668
i_F	2.975				
i_D	0.0				
i_Q	0.0				
i_{dt}			A014	-38.14	-1.908
i_{qt}			A214	13.12	0.656
I_{tabc}	1.176				
λ_{AD}	1.630		A002	81.90	1.636
λ_{AQ}	0.989		A012	49.56	0.992
λ_d	1.342		A511	67.45	1.348

Table 12 (Continued)

Variable	Hand computation pu	Digital computer pu	Analog computer		
			Analog computer component	Voltage volts	Per unit
λ_q	1.089		A010	54.58	1.092
λ_F	1.930		A201	39.19	1.956
λ_D	1.630		A001	81.90	1.638
λ_Q	0.989		A011	49.59	
T_m	3.0	3.0	A410	30.00	3.000
P_e	2.981		A213	14.97	2.995
ω	1.0	1.0	A513	50.00	1.000
$\Delta\omega$	0.0		A210	0.00	0.000
δ	67.1°	67.047°	A714	33.25	66.5°
v_R	3.66		A800	3.53	3.530
v_e	0.00805		A802	0.45	0.009
v_{rate}	0.0		A812	0.00	0.000

Table 13. Base Case 2

Variable	Hand computation pu	Digital computer pu	Analog computer		
			Analog computer component	Voltage volts	Per unit
$P_{1\phi}$	1.0	1.0			
$Q_{1\phi}$	0.62	0.62			
V_{ref}	1.1808		A200	59.04	1.182
V_{Babc}	1.0	1.0	A023	100.00	1.000
			A232	100.00	1.000
v_{todq}	2.030	2.031	A610	81.20	2.030
V_{tabc}	1.172	1.172			
v_d	-1.145	-1.148	A412	-49.05	-1.226
v_q	1.672	1.675	A413	64.65	1.610
v_F	0.00227				
E_{FD}	2.195		A004	27.27	2.727
i_d	-1.589	-1.591	A003	-33.76	1.688
i_q	0.698	0.700	A013	13.70	0.685
i_F	2.820				
i_D	0.0				
i_Q	0.0				
i_{dt}			A014	-33.52	-1.678
i_{qt}			A214	13.38	0.668
I_{tabc}	1.002				
λ_{AD}	1.914		A002	93.38	1.866
λ_{AQ}	1.042		A012	50.77	1.030
λ_d	1.675		A511	80.76	1.613

Table 13 (Continued)

Variable	Hand computation pu	Digital computer pu	Analog computer		
			Analog computer component	Voltage volts	Per unit
λ_q	1.147		A010	55.92	1.118
λ_F	2.200		A201	44.35	2.218
λ_D	1.914		A001	93.37	1.868
λ_Q	1.042		A011	50.81	1.016
T_m	3.0		A410	29.99	2.999
P_e	2.995		A213	14.96	2.990
ω	1.0		A513	50.00	1.000
$\Delta\omega$	0.0		A210	0.00	0.000
δ	53.8°		A714	28.78	57.5°
v_R	3.045		A800	3.84	3.840
v_e	0.0076		A802	0.50	0.010
v_{rate}	0.0		A812	0.00	0.000

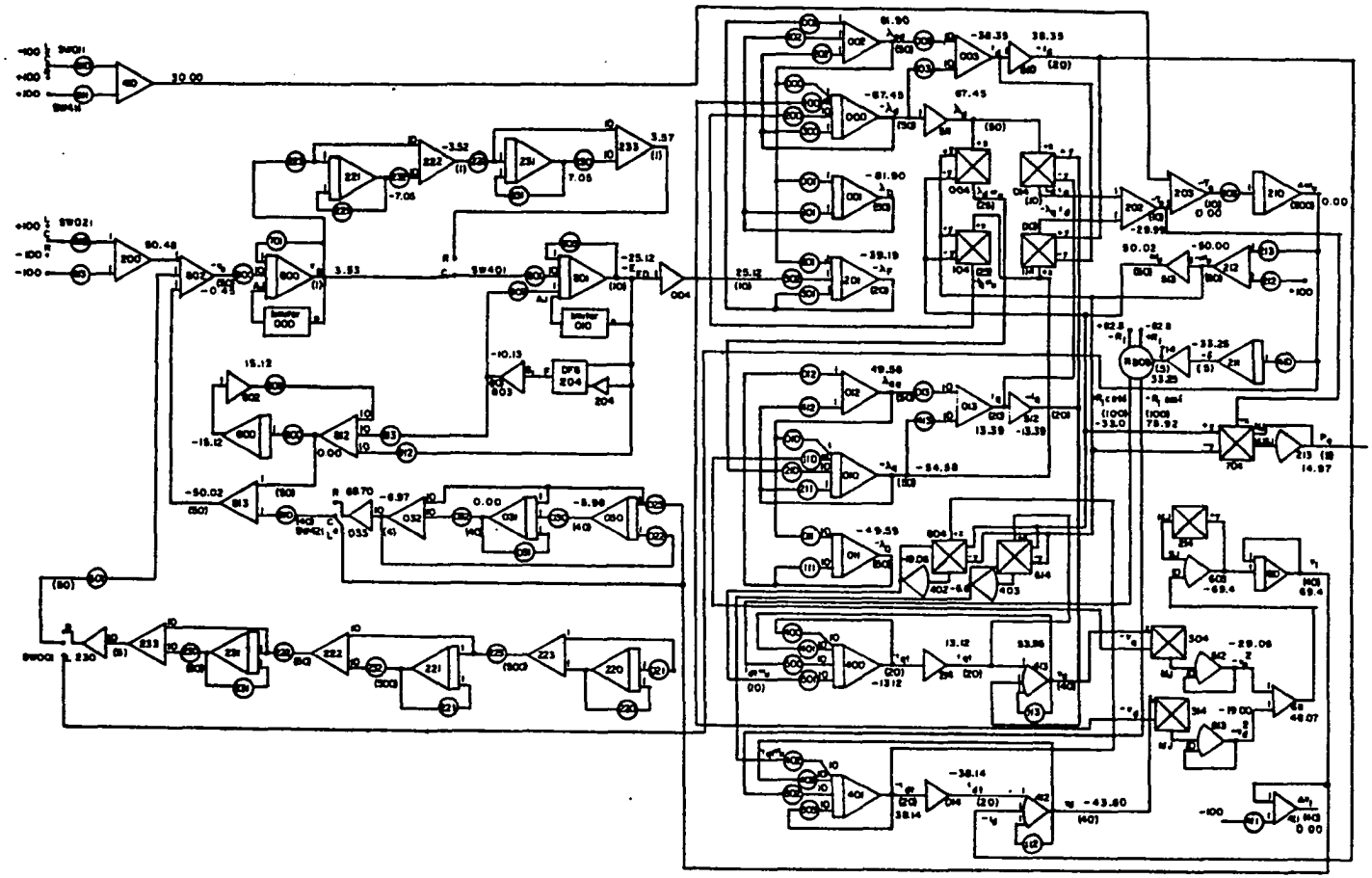

Figure 86. Steady-state voltages under conditions of Base Case 1

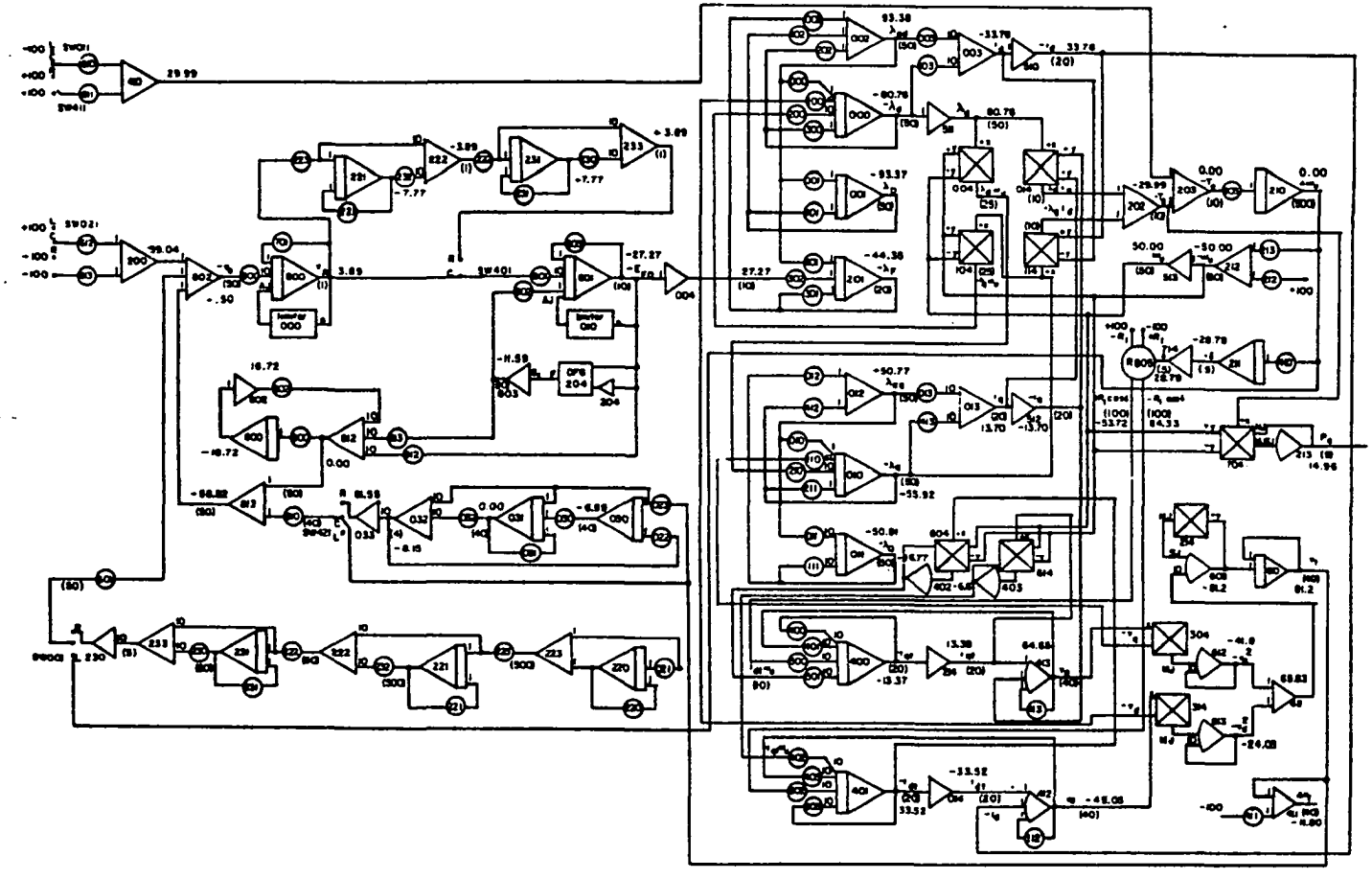

Figure 87. Steady-state voltages under conditions of Base Case 2

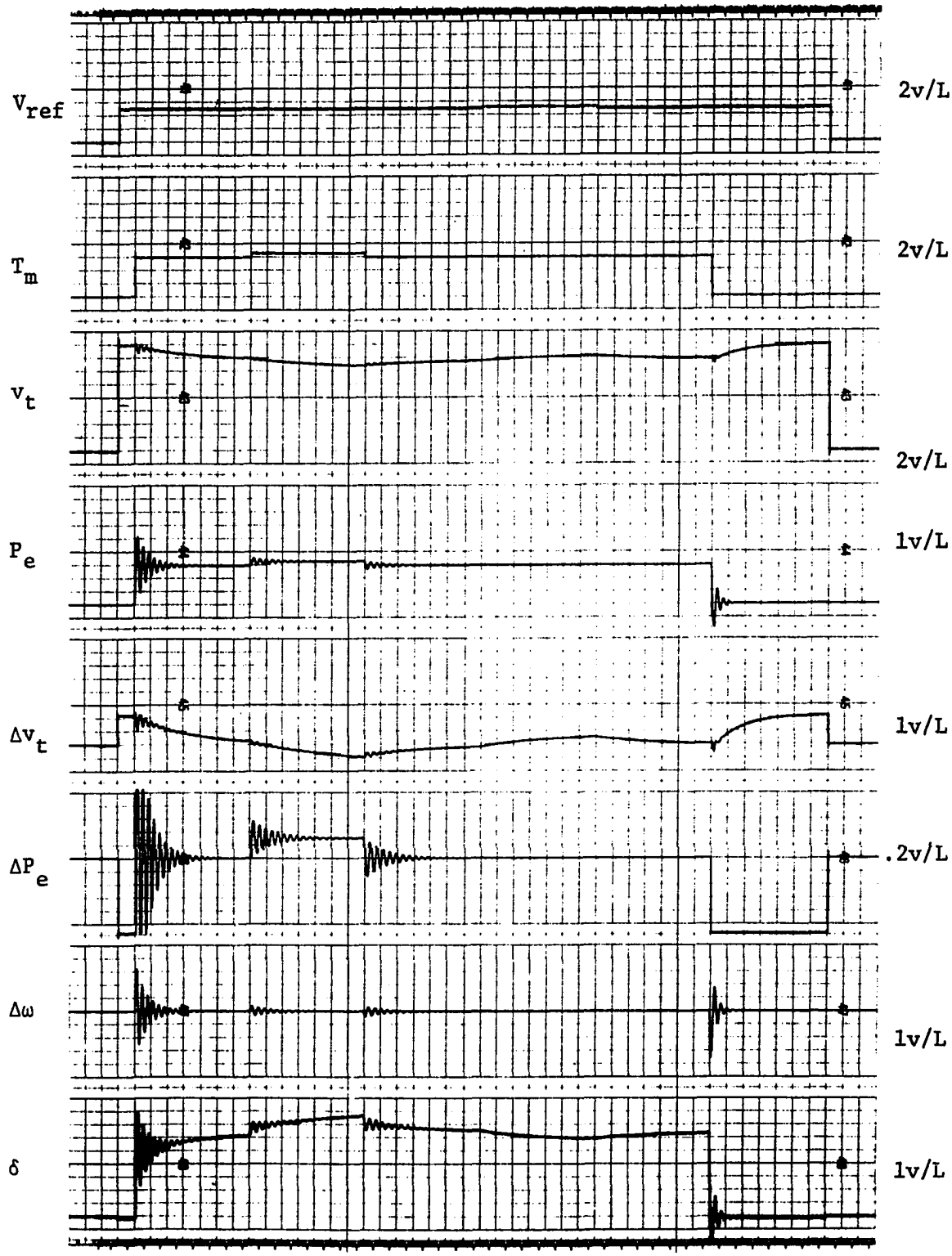

Figure 88. Synchronous machine dynamic operation

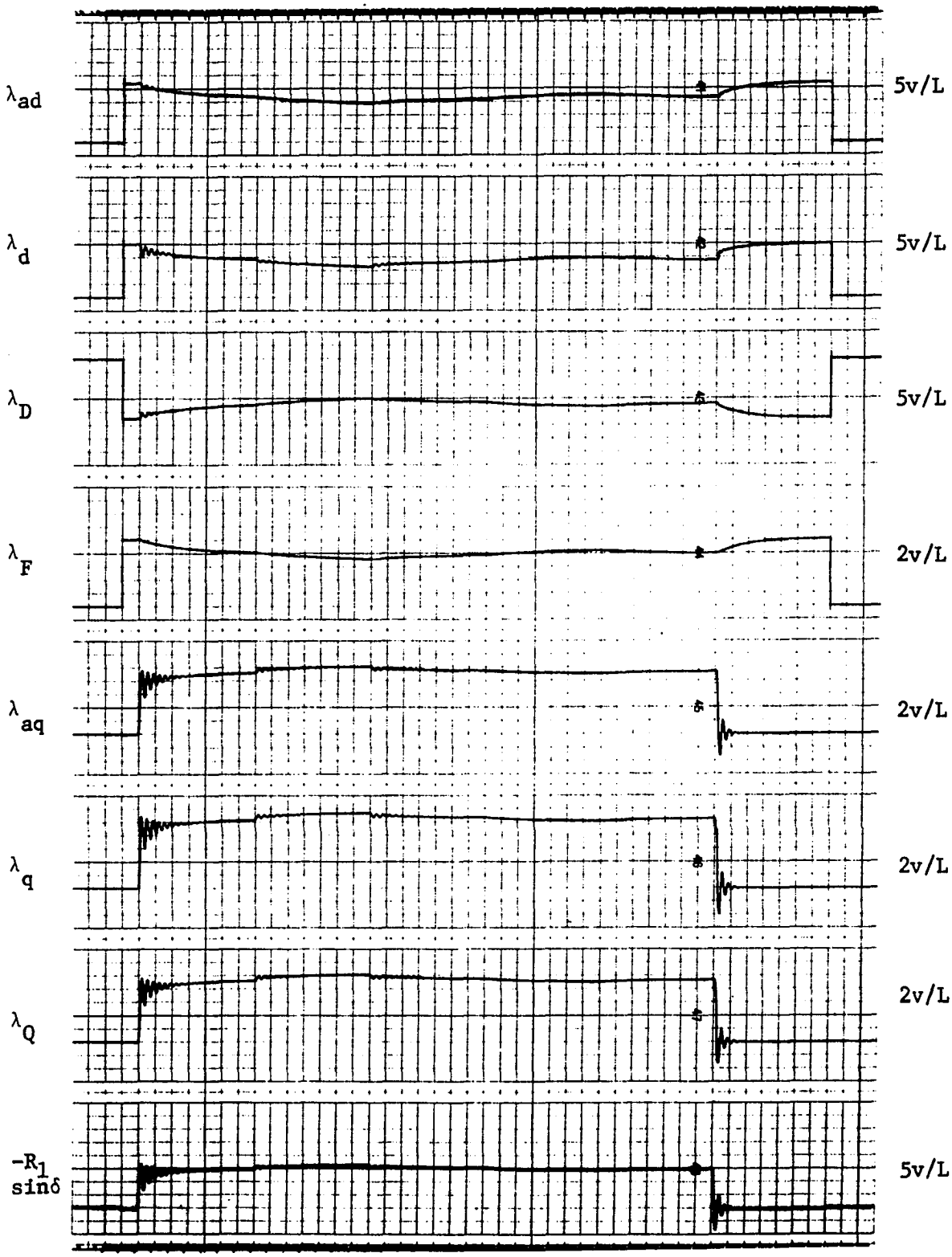

Figure 89. Synchronous machine dynamic operation

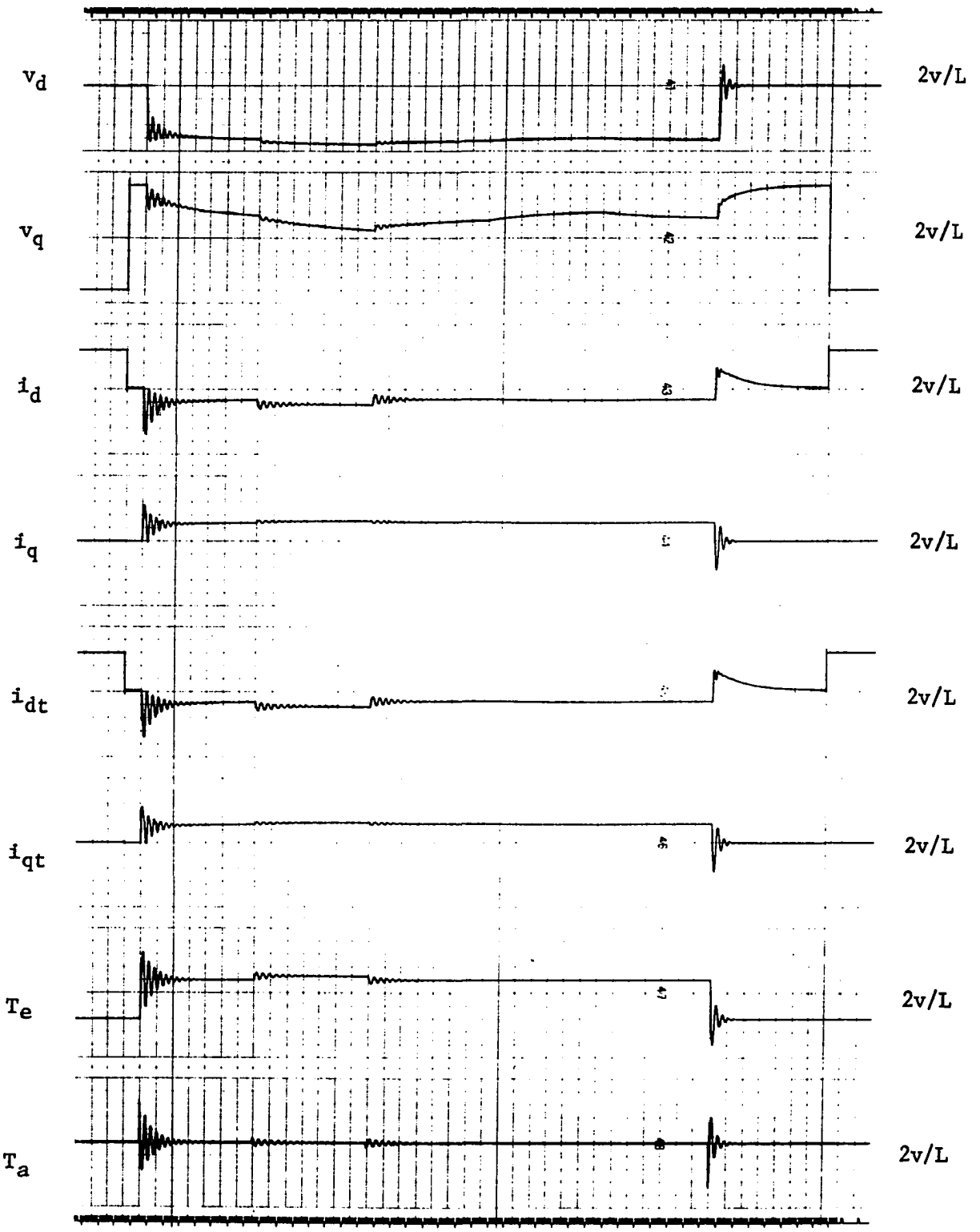

Figure 90. Synchronous machine dynamic operation

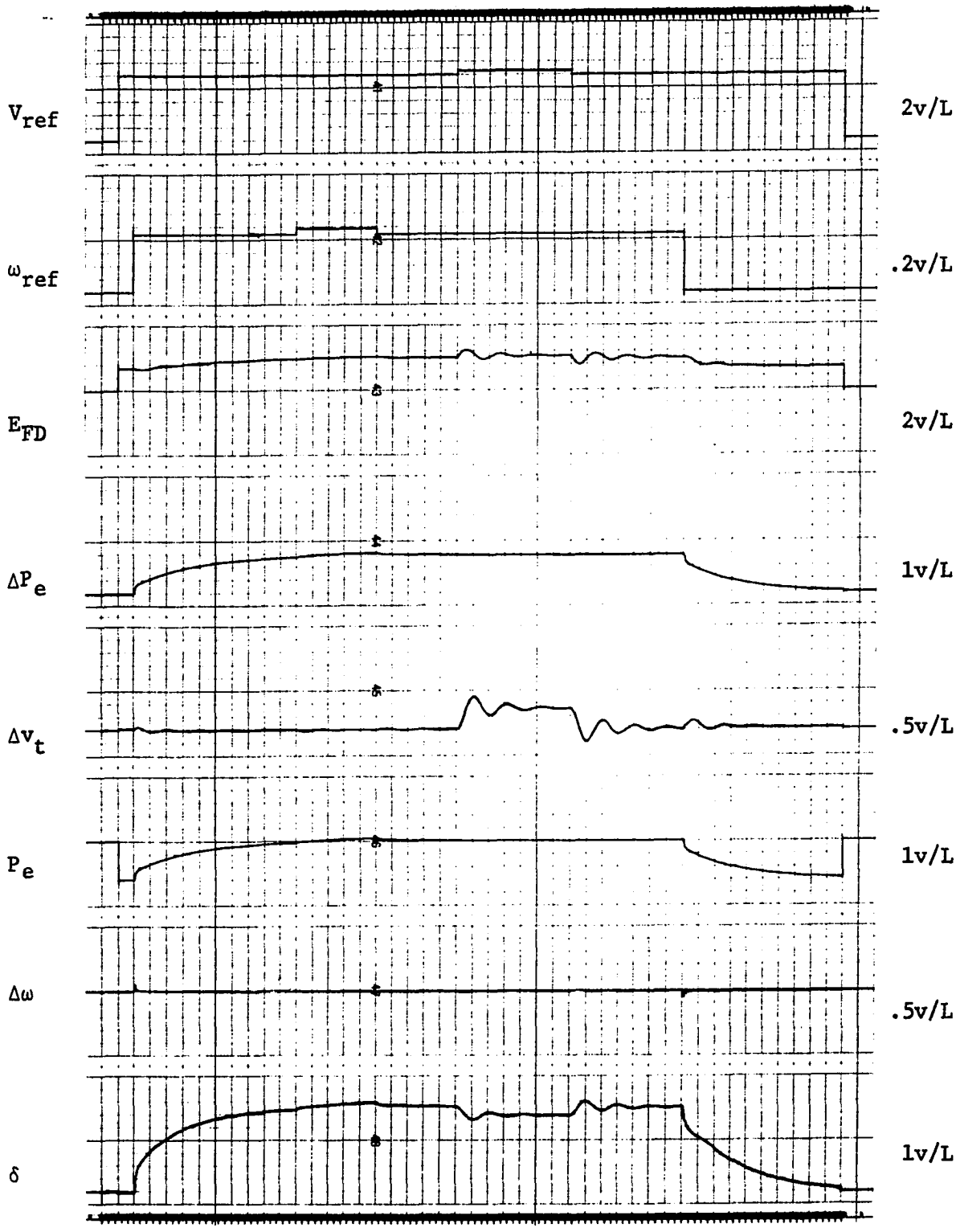

Figure 91. Synchronous machine with exciter and governor

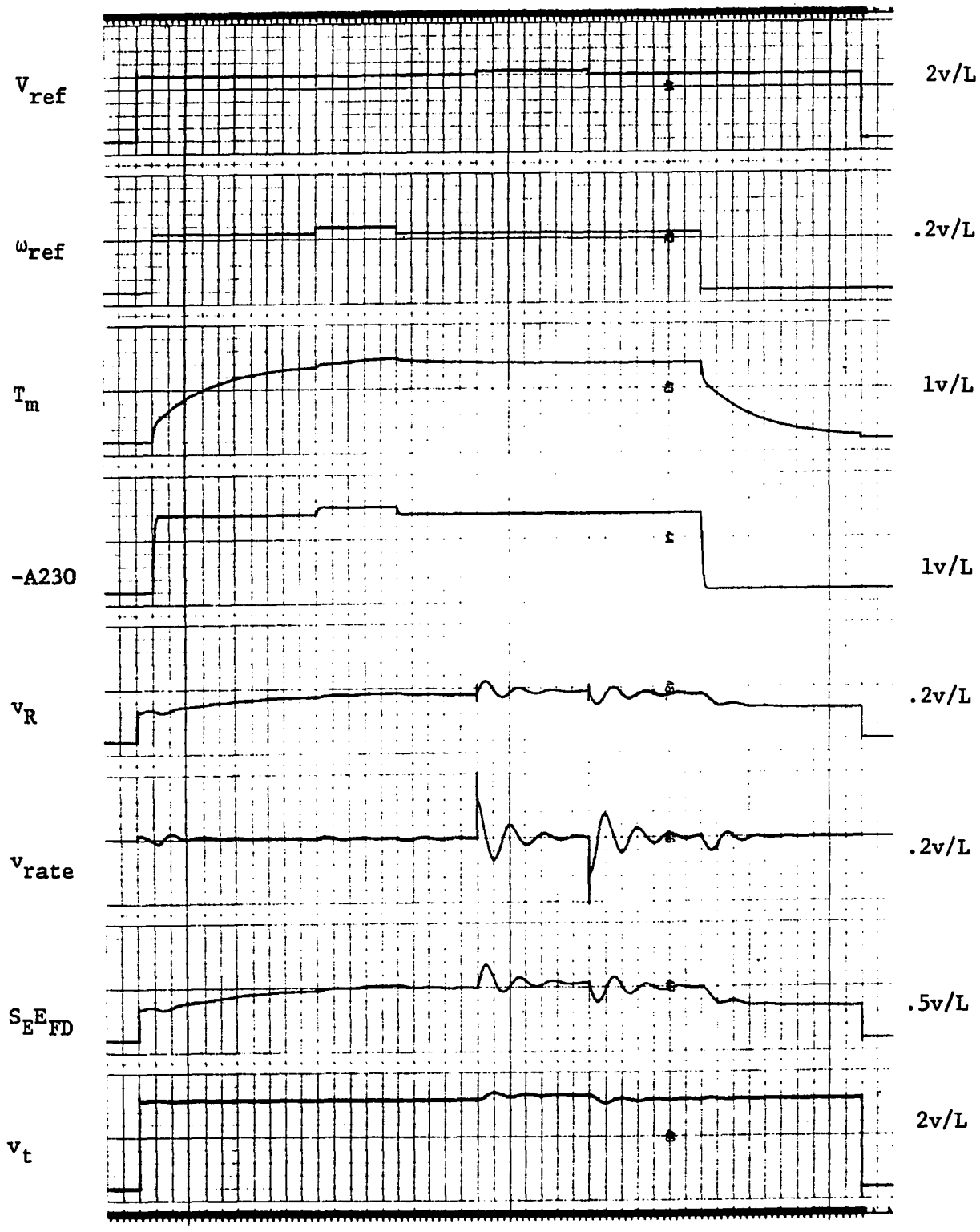

Figure 92. Synchronous machine with exciter and governor

was unstable. The voltage reference was adjusted to a value corresponding to Base Case 1. The speed reference was initially adjusted to produce a zero load on the machine.

The strip chart recordings show the result of changing the speed reference from the initial setting to one producing full load on the machine, then increasing and decreasing the speed reference to change the machine load by ± 10% of full load. Next the voltage reference was increased and decreased by 5%, and finally the speed reference was returned to a value producing zero machine loading.

The various reference levels were again switched at the same relative times resulting in a strip chart recording which is effectively 16 channels wide. Note that due to the long settling time of excitation rate feedback the strip chart recorder was operated at a slower chart speed. The distance between two downward timing marks still represents one second of synchronous machine operation.

The phase relationships for a signal propagating through the machine were also recorded. Figure 93 shows the signal in various parts of the simulation with the two-stage lead-lag network in the exciter forward loop, the bridged-T in the regulator loop and speed feedback through a gain. The machine was operated under conditions of Base Case 1 and the output of the oscillator used to modulate the infinite bus voltage was fed into amplifier 200.

Figure 94 shows similar results for the uncompensated system. The above compensation networks were originally in the circuit. The simulation was then started and a steady-state condition corresponding to Base Case 1 was established. All compensation was then removed. This

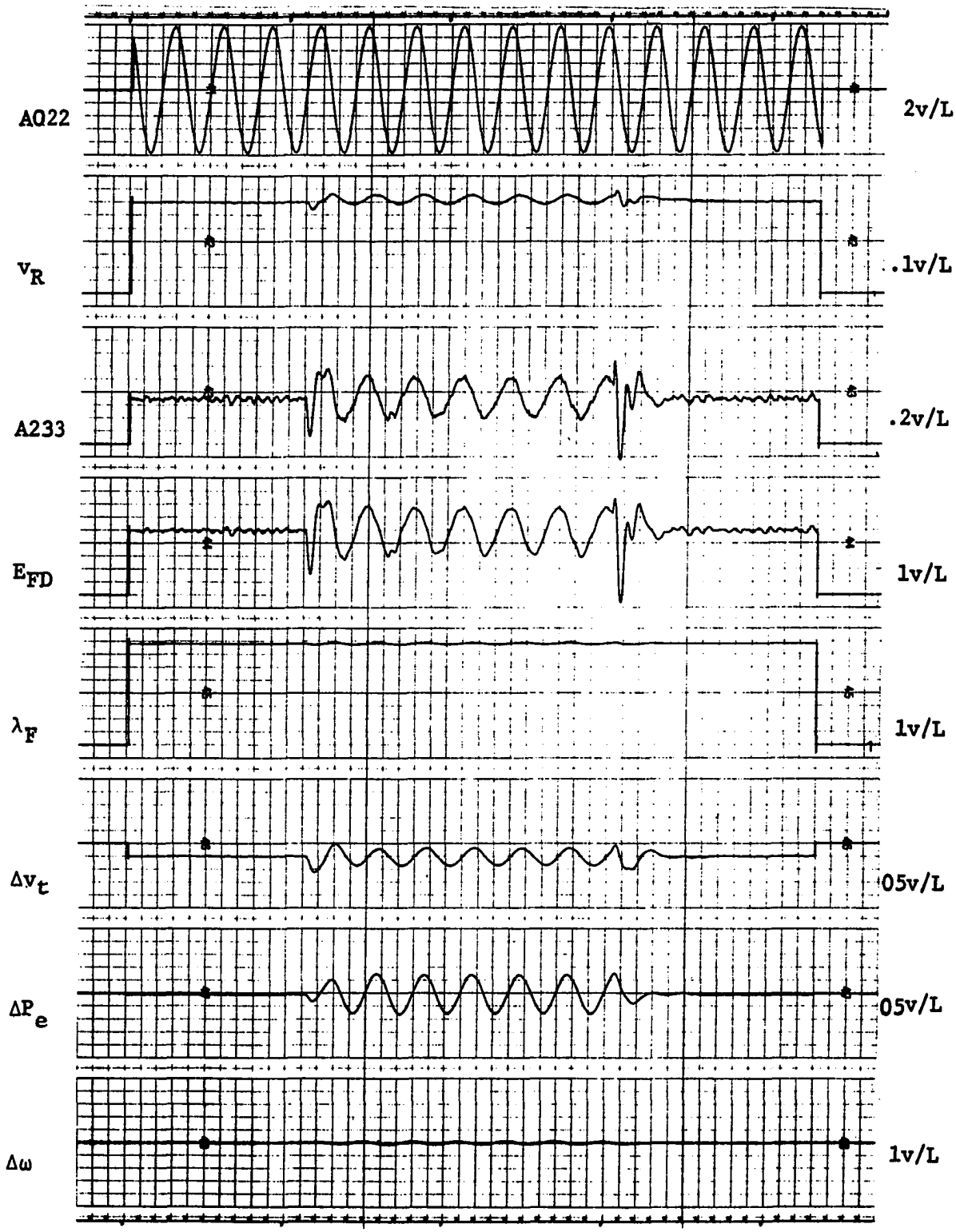

Figure 93. Phase relationships after lead-lag, bridged-T and speed compensation

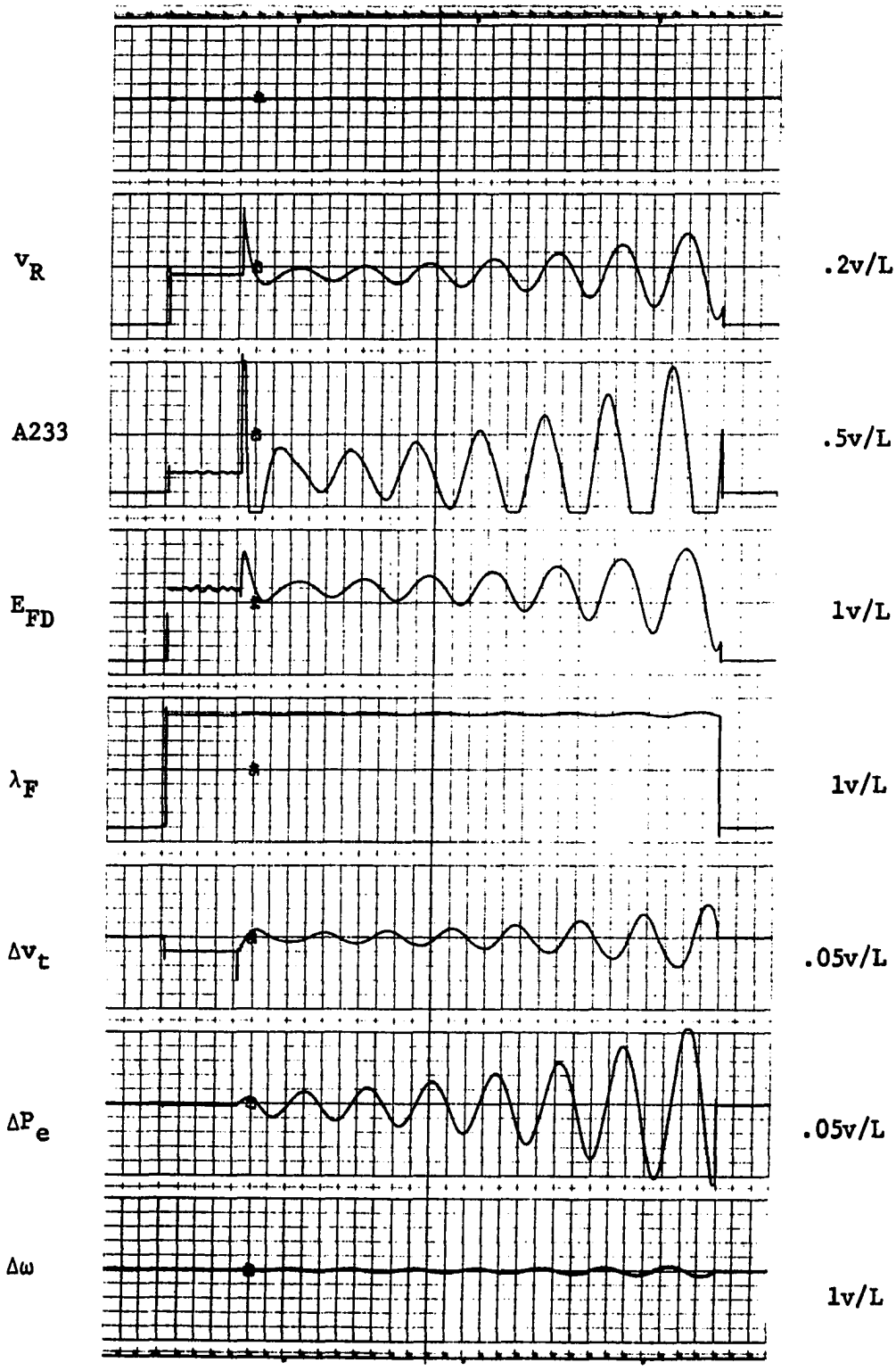

Figure 94. Phase relationships in uncompensated synchronous machine and exciter

particular loading condition with no compensation was unstable so the oscillator used above was not needed. Note the change in strip chart recorder speed. The downward timing marks again represent one second of synchronous machine operation.